THE UNIVERSITY
of EDINBURGH

Short telomeres in embryonic stem cells affect stable differentiation

Fabio Pucci

Thesis presented for the degree of Doctor of Philosophy

University of Edinburgh

2013

DECLARATION

I declare that this thesis has been composed by myself and the work presented herein is my own, except where stated otherwise. This research has not been submitted for any other degree except as specified.

Fabio Pucci

Edinburgh

October, 2013

Abstract

Murine embryonic stem cells (ESCs) are self-renewing, pluripotent cells able to differentiate into cells of all three germ layers. Pluripotency and self-renewal are maintained primarily by the core transcriptional factors Nanog, Oct4 and Sox2, but require the cooperation of other factors and coregulators and an efficient telomere maintenance mechanism. In mammals, telomere maintenance is achieved via a telomerase reverse transcriptase (Tert) that acts together with an RNA component (Terc). Maintenance of functional telomeres is essential to allow ESC proliferation, nevertheless if and how it is involved in the achievement and preservation of cell differentiation is still unknown. Here, we used *Tert* deficient mouse ESCs to elucidate the role of telomere length in differentiation. We found that *Tert*$^{-/-}$ ESCs with critically short telomeres are delayed, but still capable, to achieve differentiation after leukemia inhibitory factor (LIF) withdrawal and all-trans retinoic acid (ATRA) treatment, but failed to maintain it after LIF re-introduction to the growth medium. Telomere shortening effect on differentiation was accompanied by pluripotency gene dysregulation (e.g. Nanog overexpression), DNA hypomethylation and epigenetic disorders. This phenotype of metastable differentiation could be rescued by telomere lengthening via re-introduction of *Tert*, depletion of Nanog via short hairpin RNA, or via enforced expression of the *de novo* DNA methyltransferase 3b. These results reveal an unanticipated role of telomeres in the epigenetic regulation of gene expression and cell fate determination during physiological or pathological processes.

Acknowledgments

There are many people I would like to thank for their help and support during my Ph.D.

My supervisor, Lea Harrington, a true person of science, for her irreplaceable advices and suggestions, and for always being enthusiastic and supportive, even and above all, when things were not going well. Thank you for helping me to strength my weakness and develop my virtues both as scientist and as person.

Thank you to my Ph.D. committee members: Kei and Irina, and to Adrian for their feedback and imput.

Many sincere thanks to the Wellcome Trust for funding.

I would also like to thank former and current lab members, particularly Laura, Elisa, Sveta, Asia for their support and the fun work environment, and above all Emilie, for making my last month in Edinburgh so joyful.

A big thank you to all my friends here in Edinburgh, to Agata and Rad, Robert, Marta, Diana, Julio, Laura, Lisi, Giuseppe, Nuno, Nadine, Roberta, Dima, Nick, Vanessa, Manuel and Martina. Thank you for four unforgettable years. Thank you for making me feel like at home.

A particular thank to Cristina for always been present and reliable. Thank you for being one of the best people I know.

Alla mia famiglia, agli zii ed ai cugini, ed in particolare a mio padre, mia madre e mio fratello, ed ovviamente a Zoe, un grazie di cuore per essere sempre stati al mio fianco, pur essendo lontani.

Abbreviations

Bp base pair

BSA bovine serum albumin

cDNA complementary DNA

CMV cytomegalovirus

Da Dalton

DAPI 4'.6'-diamidino-2-phenylindole

DNA deoxyribonucleic acid

dNTP deoxynucleotide triphosphate

EDTA ethylenediaminetetraacetic acid

EGFP enhanced green fluorescent protein

GFP green fluorescent protein

H histone

h hour(s)

IRES internal ribosome entry sequence

K lysine

Kb kilobase

Min minutes

N number

PBS phosphate buffered saline

PCR polymerase chain reaction

pH -log10(aH+)

QRTPCR quantitative revere transcriptase PCR

RNA ribonucleic acid

RNAi RNA interference

SDS sodium-dodecyl sulfate

siRNA short interfering RNA

shRNA short hairpin RNA

WB western blot

Wt wild type

RIPA radio immunoprecipitation assay

List of figures

Table of Contents

Chapter 1

Introduction

1.1 Embryonic stem cells

Stem cells are characterized by two major traits: A) They are able to extensively, in some case unlimitedly, self-renew without entering senescence, B) they also possess the ability, called potency, to differentiate into one or more cell types (Hirai et al., 2011; Nichols and Smith, 2009). In mouse, an arbitrary distinction of the different kinds of stem cells can be performed according to the extent of their potency. In this hierarchical model the totipotent stem cells, cells from the early morula, occupy the top position. Zygote undergoes a cleavage division stage that, eventually, leads to the formation of the morula, which is formed by 8-16 cells called blastomeres. Blastomeres ultimately compact together, and the outside cells begin to form the trophoblast. Until compaction, blastomeres are symmetric (each cell has the same features and potency of the others), unresponsive to extrinsic signals, and able to differentiate into any kind of both embryonic and extra-embryonic cell (Hillman et al., 1972; Nichols and Smith, 2009; Selwood and Johnson, 2006).

Pluripotent, or embryonic, stem cells (ESC) arise soon after totipotent ones in terms of potency. Compacted blastomeres give raise to a structure called a blastocyst, formed by the trophoblast and the inner cell mass (ICM). ICM produces both embryonic (epiblast) and extra-embryonic (hypoblast) lineages. ESCs are derived from the epiblast of the inner cell mass of pre-implanted blastocysts (Fig1) (Friel et al., 2005; Nichols and Smith, 2009; Nichols et al., 1998). They are able to give raise to any embryonic (but not extra-embryonic) cell and to form teratomas. In addition, a single pre-implantation epiblast cell, when injected into another blastocyst, can contribute to all cell lineages. Epigenetically, female ESCs are characterized by reactivation of the paternal X chromosome resulting in two active X chromosomes (Friel et al., 2005; Gardner and Beddington, 1988; Nichols and Smith, 2009).

Epiblast stem cells (EpiSCs), derived from post-implantation epiblast, share many features with ESCs, like expression of key pluripotency genes, the ability to form, in *vitro*, cells from the three germ layers, and to form teratomas. However, EpiSCs are incapable to contribute to chimerism when injected into blastocysts, and female cells show random inactivation of one of the two X chromosomes (Heard, 2004; Mak et al., 2004; Nichols and Smith, 2009).

Multipotent, or adult, stem cells are able to differentiate only into cells of a specific organ or tissue or system. They locate into different tissues in the adult organism and their role is to replace mature cells after damage or disease-induced stress (Friel et al., 2005).

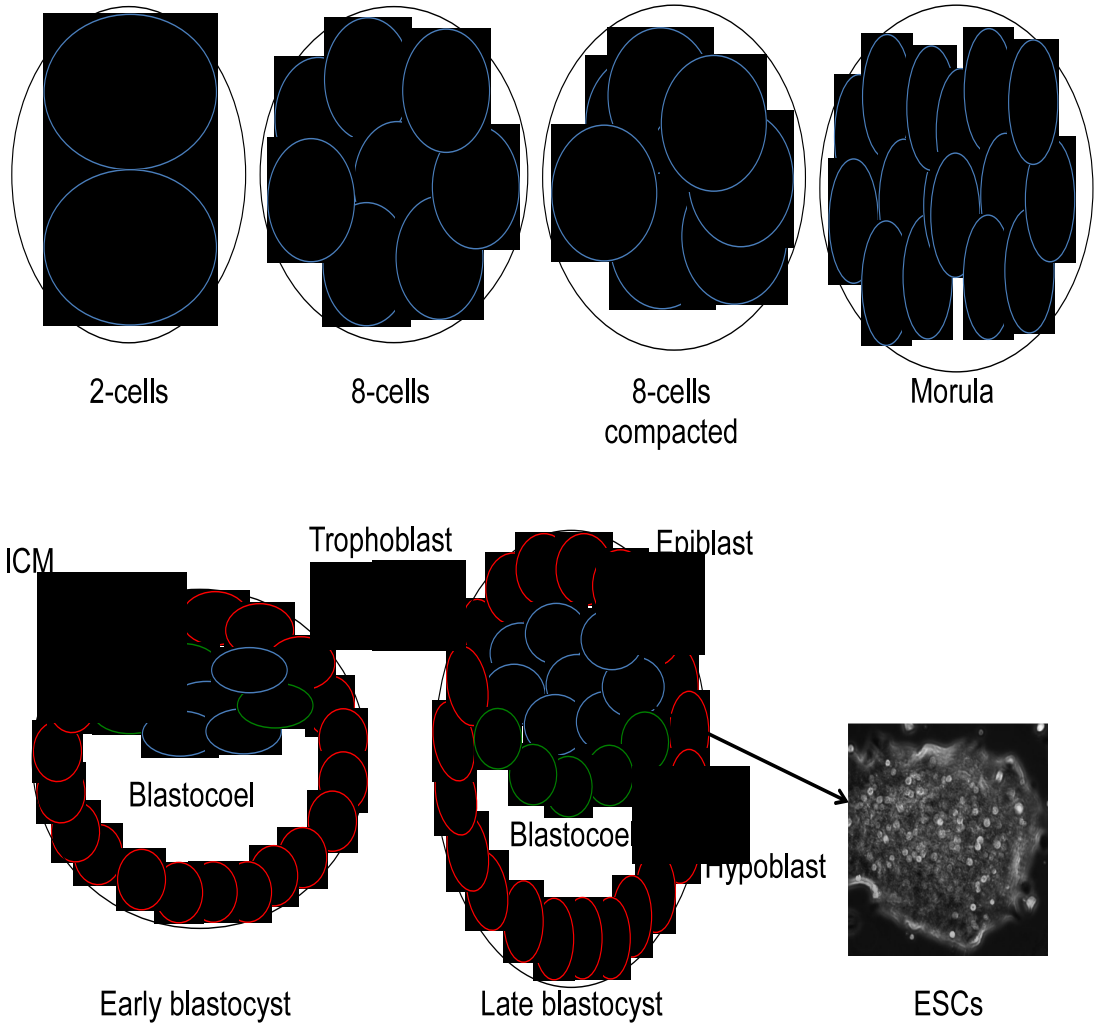

Figure 1. Schematic representation of early mouse embryo development. Zygote undergoes multi cell division to origin the morula, which compacts and gives raise to the early blastocyst (bottom left). Blastocyst is formed by the trophoblast (in red), which will generate extra-embryonic tissues (e. g. placenta), a fluid-filled space called blastocoel, and the ICM. In the late blastocyst, the ICM is re-organized into epiblast (in blue), which will differentiate into the three embryonic germ layers: endoderm, mesoderm and ectoderm, and hypoblast (in green), which lies beneath the epiblast and generates extra-embryonic primitive endoderm tissues (e.g. yolk sac). ESCs are derived form the epiblast of pre-implantation blastocyst. Figure adapted from (Nichols and Smith, 2009).

The origin of ESC studies in culture can be traced to findings from the 1950's on teratomas, a particular kind of tumour containing cells from the three germ layers: endoderm, mesoderm and ectoderm, and undifferentiated cells called embryonic carcinoma (EC) cells. EC cells, grown on mitotically inactivated fibroblasts, could be expanded in culture for years and were capable of multi-lineage differentiation (Martin and Evans, 1975). EC cells usage for pluripotency studies was severely limited by their tumour-related genetic instability, however they built the basis for future pluripotency studies (Friel et al., 2005; Martin, 1980).

Murine embryonic stem cells from the ICM were first isolated in 1981 by Evans and Kaufman in Cambridge, and Gail Martin at University of California, San Francisco. ESCs cultured either on feeder cells (typically irradiated mouse embryonic fibroblasts) or on gelatin-coated dishes can be kept in culture for many passages and still maintain the ability to contribute to chimerism after blastocyst injection (Evans and Kaufman, 1981; Hirai et al., 2011; Martin, 1981).

1.2 Pluripotency and self-renewal master regulators

The ability to differentiate into cells of the three germ layers and to replicate without entering senescence are the key characteristics of ESCs both in the embryo and *in vitro*. Pluripotency and self-renewal are mainly maintained by the core transcription factors Nanog, Oct4 and Sox2 (Chambers et al., 2003; Nichols and Smith, 2009; Nichols et al., 1998; Yuan et al., 1995). Their targets encompass both transcribed and inactive genes, some of which are involved in the maintenance of ESC self-renewal and pluripotency, whereas others execute critical developmental activities including differentiation into cells of the three germ layers (Loh et al., 2006; Niwa, 2007; Silva

and Smith, 2008). It is worth noting that many of the genes involved in the maintenance of ESC self-renewal and pluripotency are co-occupied by at least two of the core transcription factors, including the Sox2, Oct4, and Nanog promoter themselves (Ivanova et al., 2006; Li, 2010; Silva and Smith, 2008; Tsumura et al., 2006).

Oct4, encoded by the Pou5f1 gene, is a transcription factor that binds to the octameric sequence: ATGCAAAT. During mouse embryo development, Oct4 is expressed at the four-cell stage, and is subsequently restricted to the cells of the ICM of the blastocyst (Yeom et al., 1996). Oct4 expression has to be tightly regulated; as it has been shown that depletion of this factor leads to trophectoderm lineage, whereas its increase over two-fold leads toward endoderm and mesoderm differentiation (Niwa et al., 2000). However, it has been reported recently that heterozygosity for Oct4, and subsequent reduced expression, leads to a strong maintenance of pluripotent undifferentiated state. *Oct4*$^{+/-}$ ESCs present an enrichment of Oct4 and Nanog at pluripotency-associated enhancers, a more uniform expression of pluripotency factors, and a delayed differentiation compared to *Oct4*$^{+/+}$ ESCs (Karwacki-Neisius et al., 2013).

Sox2 has been identified as target of Oct4 and, just like Oct4, it is expressed in all the cells at the four-cell stage whereas it is restricted to the ICM in the blastocyst (Avilion et al., 2003; Grinnell et al., 2007). Sox2 is able to form a complex with Oct4 to induce transcription of pluripotency genes, and both its depletion and its increase over two-fold lead to differentiation (Kopp et al., 2008; Nakatake et al., 2006; Rodda et al., 2005).

Nanog is the third component of the core pluripotency factors. During mouse development, it first appears in the morula, whereas its expression in the blastocyst is limited to the epiblast cells of the ICM (Chambers et al., 2007; Silva et al., 2009). Differently from Oct4 and Sox2, Nanog has a negative feedback on its own transcription, and its overexpression does not result in cell differentiation, but maintains cells in an undifferentiated state (Chambers et al., 2007; Fidalgo et al., 2011). In addition, although Nanog is dispensable in the maintenance of pluripotency, it is crucial to acquire it both during embryogenesis and during reprogramming. In fact, *Nanog*$^{-/-}$ zygotes are unable to form epiblasts, and Nanog presence is fundamental to generate truly pluripotent induce pluripotent stem (iPS) cells, despite the fact that Nanog is unnecessary for the onset of reprogramming, as it is not one of the original Yamanaka factors (Oct4, Sox2, c-Myc and Klf4). Furthermore, forced expression of Nanog alone is able to convert EpiSCs into ESCs. (Chambers et al., 2007; Fidalgo et al., 2011; Li, 2010; Silva et al., 2009; Takahashi and Yamanaka, 2006).

Although these three core factors locate are at the nexus of the pluripotency regulatory network and reciprocally influence their expression, in order to maintain pluripotency and self-renewal capacity they still need the collaboration of other factors and coregulators (Heng et al., 2010; Li, 2010). Factors like: Essrb, Klf2, Klf4, Tbx3, Tcf3, Sal4, Rex1, Zfp281 and many others have all been shown to regulate and/or be-regulated by the three core factors (Festuccia et al., 2012; Fidalgo et al., 2011; Ivanova et al., 2006; Li, 2010; Navarro et al., 2012). However, although each of the described factors is important to maintain an undifferentiated state, none, apart

from Sox2 and Oct4, not even Nanog, is essential provided that the other pluripotency factors are present and functional (Martello et al., 2012)(Fig. 2).

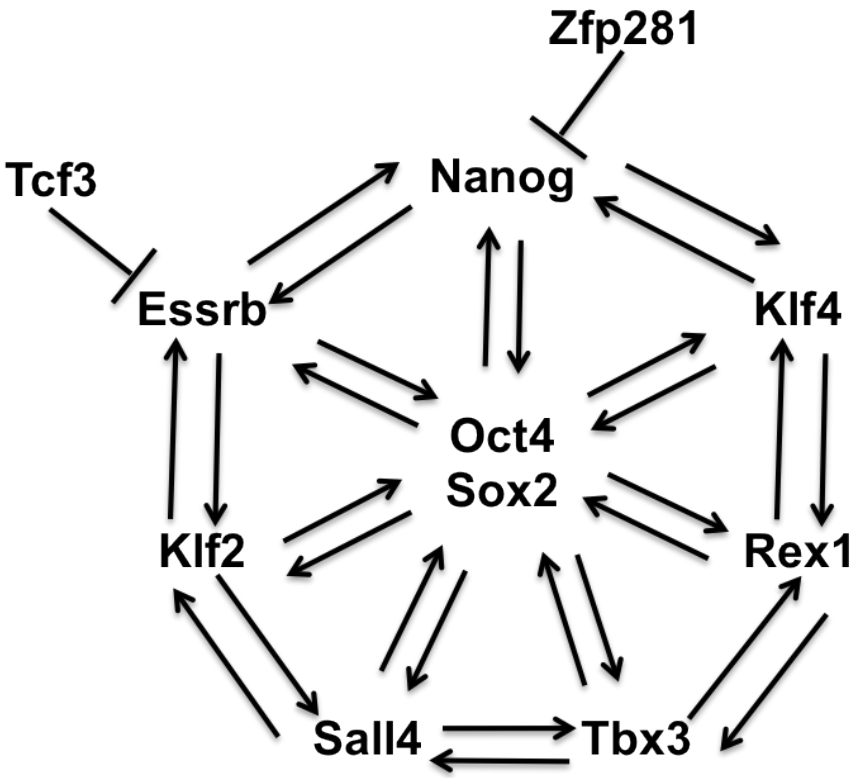

Figure 2: Schematic representation of pluripotency regulatory circuit. Oct4 and Sox2, which presence is essential for maintaining pluripotency and self-renewal, form the core of the circuit. Adapted from (Fidalgo et al., 2011; Martello et al., 2012).

1.3 Signalling pathways in pluripotency maintenance

There are many different pathways involved in the regulation and maintenance of pluripotency and self-renewal in embryonic stem cells. One of the main pathways involved in the regulation of pluripotency is the Wnt/β-catenin signalling network (MacDonald et al., 2009). This network is also targeted, by inhibition of GSK3-β, via the 2-inhibitors (2i) method (together with the inhibition of FGF4-MAPK) for ESC

maintenance (Blair et al., 2011). β-catenin has a pivotal role in the canonical Wnt signalling network, where its stability is controlled by a protein complex composed of adenomatous polyposis coli (APC), casein kinase 1 (CK1), Axin, and glycogen synthase kinase-3β (GSK3-β). In absence of binding between Wnt and its receptors, β-catenin is bound by APC and Axin and phosphorylated by CK1 and GSK3-β. Phosphorylated β-catenin recruits E3 ubiquitin ligase, which targets β-catenin for proteosomal degradation. The binding of Wnt to its receptors causes a phosphorylation-mediated GSK3-β inhibition with subsequent release of β-catenin, which migrates into the nucleus where it interacts with the Tcf3/Lef complex, and suppresses its transcription repression activity (Fig. 3) (Atcha et al., 2007; Sansom et al., 2005).

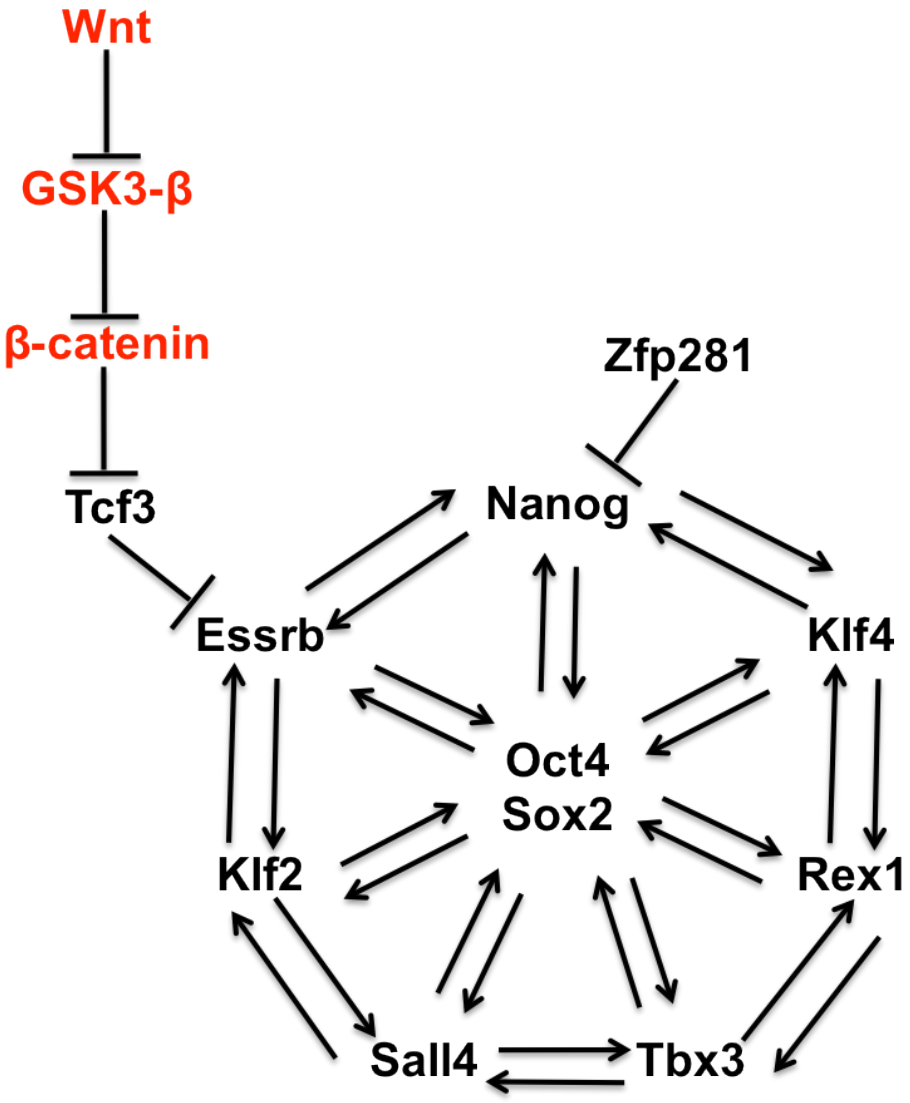

Figure 3. Role of the Wnt canonical signalling network in ESC pluripotency and self-renewal. Wnt interaction with its receptors causes phosphorylation and subsequent inhibition of GSK3-β, which in turn causes nuclear accumulation of β-catenin. In the nucleolus, β-catenin replaces histone de-acetylase 1 (HDAC1) in the Tcf3/Lef complex, suppressing its negative transcriptional regulation of Wnt responsive genes. Adapted from (Atcha et al., 2007; Blair et al., 2011; Martello et al., 2012).

Independently of (or in combination with) the 2i method, it is possible to maintain mouse ESCs in a pluripotent and self-renewing state in culture by addition of the

cytokine LIF (leukemia inhibitory factor) to the culture media (Tomida et al., 1984). LIF belongs to the interleukin-6 cytokine family and, when it interacts with its receptor (LIFR), LIF acts on the maintenance of self-renewal and pluripotency through, at least, two signalling pathways: LIF/JAK/STAT3 and LIF/PI3K/AKT (Hirai et al., 2011; Tomida et al., 1984).

The LIF/JAK/STAT3 signalling pathway is triggered by the binding of LIF to its receptor, and consequent dimerization of LIFR and gp130. This dimerization leads to activation of Janus kinases (JAKs) and subsequent recruitment of STAT3 to the receptor complex and its phosphorylation by JAKs. Phosphorylated STAT3 dimerizes and migrates into the nucleus where it activates transcription of target genes (e.g. Klf4) (Fig. 4) (Hirai et al., 2011; Li, 2010; Martello et al., 2012; Matsuda et al., 1999; Nishinakamura et al., 1999).

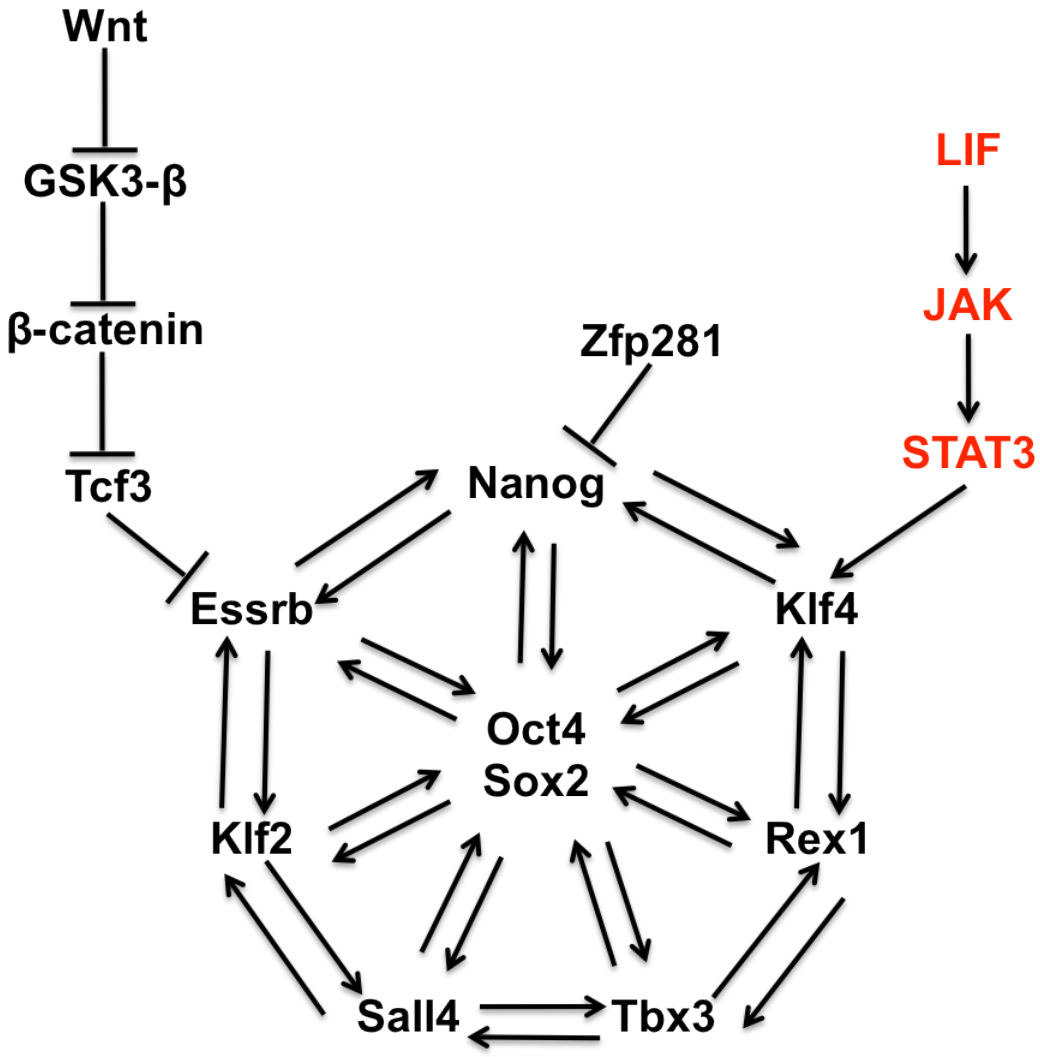

Figure 4. The role of LIF/JAK/STAT3 in ESC pluripotency and self-renewal. LIF interaction with its receptors leads to hetero-dimerization of LIFR and gp130, with consequent JAK auto-phosphorylation and STAT3 recruitment and phosphorylation. Phosphorylated STAT3 dimerizes and migrates into the nucleus where it activates target gene transcription. Adapted from (Hirai et al., 2011; Martello et al., 2012).

In the LIF/PI3K/AKT cascade, JAKs phosphorylate PI3K, which, in turn, activates AKT (Migone et al., 1998). There are numerous downstream targets of AKT, which positively regulates factors involved in maintenance of self-renewal and pluripotency (e.g. Tbx3, mTOR), and inhibits pro-differentiation agents like GSK3-β, that is able

to repress pluripotency genes also independently by restraining β –catenin activity (Fig. 5) (Hirai et al., 2011; Niwa et al., 2009).

Although both LIF/PI3K/AKT and the canonical Wnt signalling networks target GSK3-β, these two networks can act independently of each other. In fact, it has been shown that even high-dosage treatment of mouse ESCs with LIF, as well as forced AKT activation, are incapable of altering β-catenin phosphorylation and nuclear levels (Paling et al., 2004; Watanabe et al., 2006).

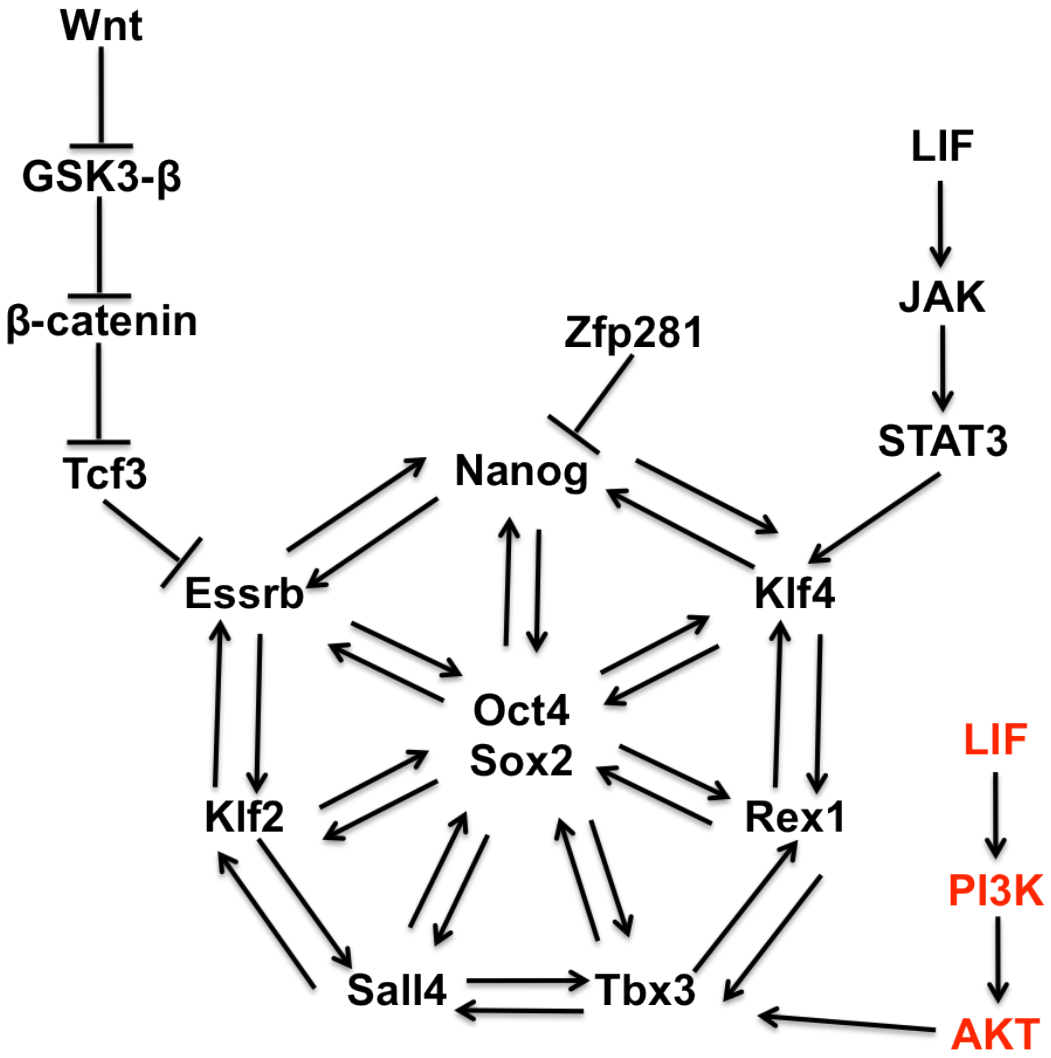

Figure 5. Role of LIF/PIK3/AKT pathway in ESC pluripotency and self-renewal. LIF interaction with its receptors causes JAK-dependent PIK3 phosphorylation. Phosphorylated

PIK3 phosphorylates and activates AKT, which can modulate many positive and negative pluripotency regulators (e.g. Tbx3). Adapted from (Hirai et al., 2011; Martello et al., 2012).

However, LIF alone is incapable to maintain cells in a fully pluripotent state. ES cells also require the activation of inhibitor of differentiation (*ID*) genes. ID proteins are negative regulators of basic helix loop helix (bHLH) transcriptional factors, which comprise many pro-differentiation factors (e.g. MyoD, Neurogenin 1, etc.) (Benezra et al., 1990; Ying et al., 2003). In foetal calf serum (FCS)-supplemented growth medium, *ID* genes are activated by multiple pathways (e.g. fibronectin-mediated integrin activation). In serum-free medium, transcription of *ID* genes can be stimulated by bone morphogenic protein 4 (BMP4). BMP4 binding to its receptors, which are heterodimers of serine/threonine kinases, leads to recruitment and phosphorylation of Smad1, 5 and 8 proteins. Phosphorylated Smads can dimerize with Smad4 and migrate into the nucleus where they induce the transcription of target genes (e.g. *ID* genes) and consequent inhibition of bHLH factors (Fig. 6) (Ying et al., 2003).

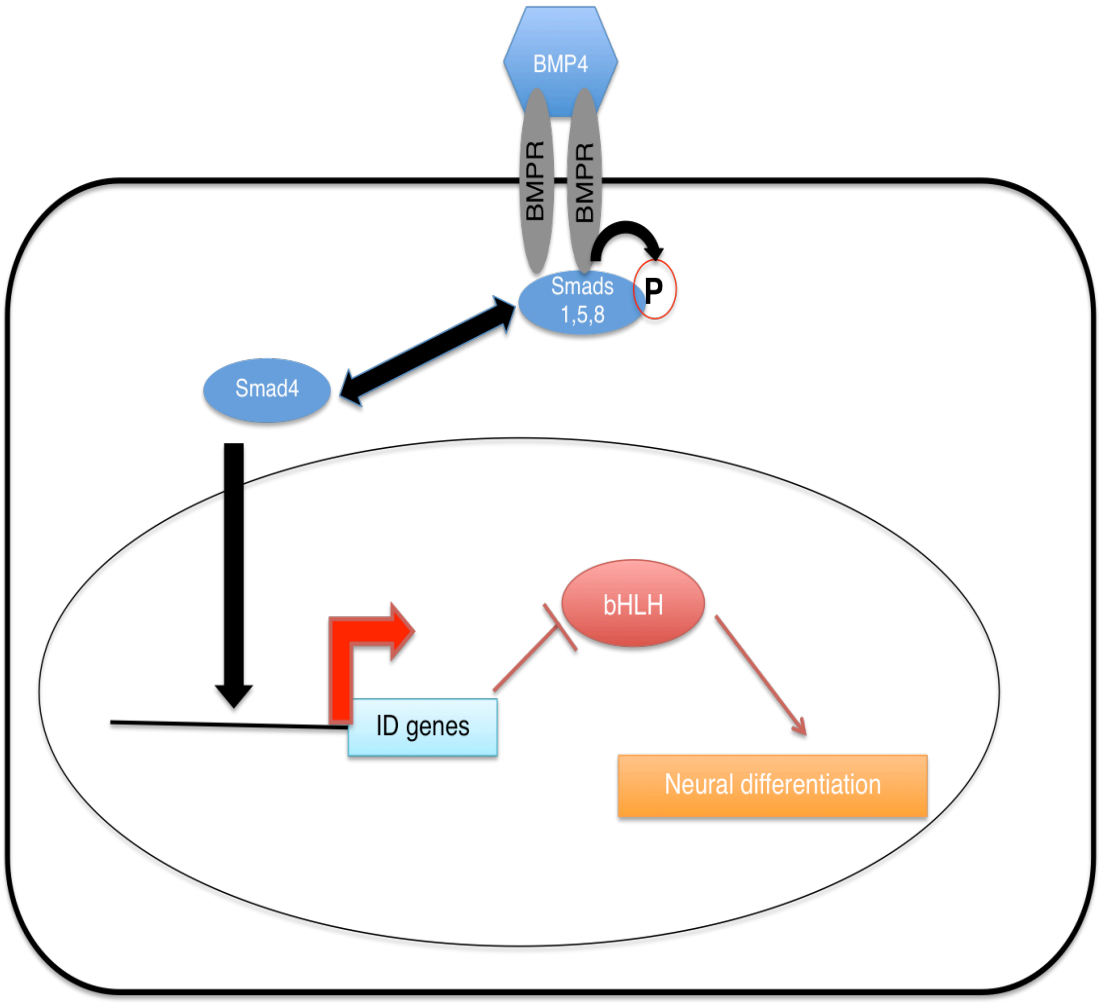

Figure 6. Schematic representation of Smad-mediated BMP4 inhibition of differentiation. BMP4 binds to its serine-threonine kinase receptors on the cell membrane. This ligand-receptor interaction causes recruitment of Smad1, 5 and 8 proteins to the receptor complex and subsequent phosphorylation. Phosphorylated Smads dimerize with Smad4 and migrate into the nucleus where they mediate certain transcriptional gene targets, such as *ID* genes. ID proteins bind to bHLH transcriptional factors, which are involved in differentiation processes (e.g. neural differentiation), thus preventing their binding to DNA. Adapted from (Ying et al., 2003).

In order to be defined as pluripotent, ESCs need to be able to respond to differentiation signals. In fact, the pluripotency factors Oct4 and Sox2 not only act to maintain ESCs self-renewal, but they also induce the transcription of fibroblast

growth factor 4 (FGF4), which renders ESCs responsive to differentiation cues (Kunath et al., 2007; Silva and Smith, 2008). FGF4 is a secreted factor and, when it binds to its tyrosine kinase receptors, it induces receptor trans-phosphorylation with subsequent activation of the mitogen-activated protein kinase (MAPK) signalling cascade through the MEK-Erk1/2 pathway. Once activated by phosphorylation, Erk1/2 can activate downstream transcriptional factors, which ultimately render the cells susceptible to lineage commitment stimuli (Fig. 7) (Kunath et al., 2007).

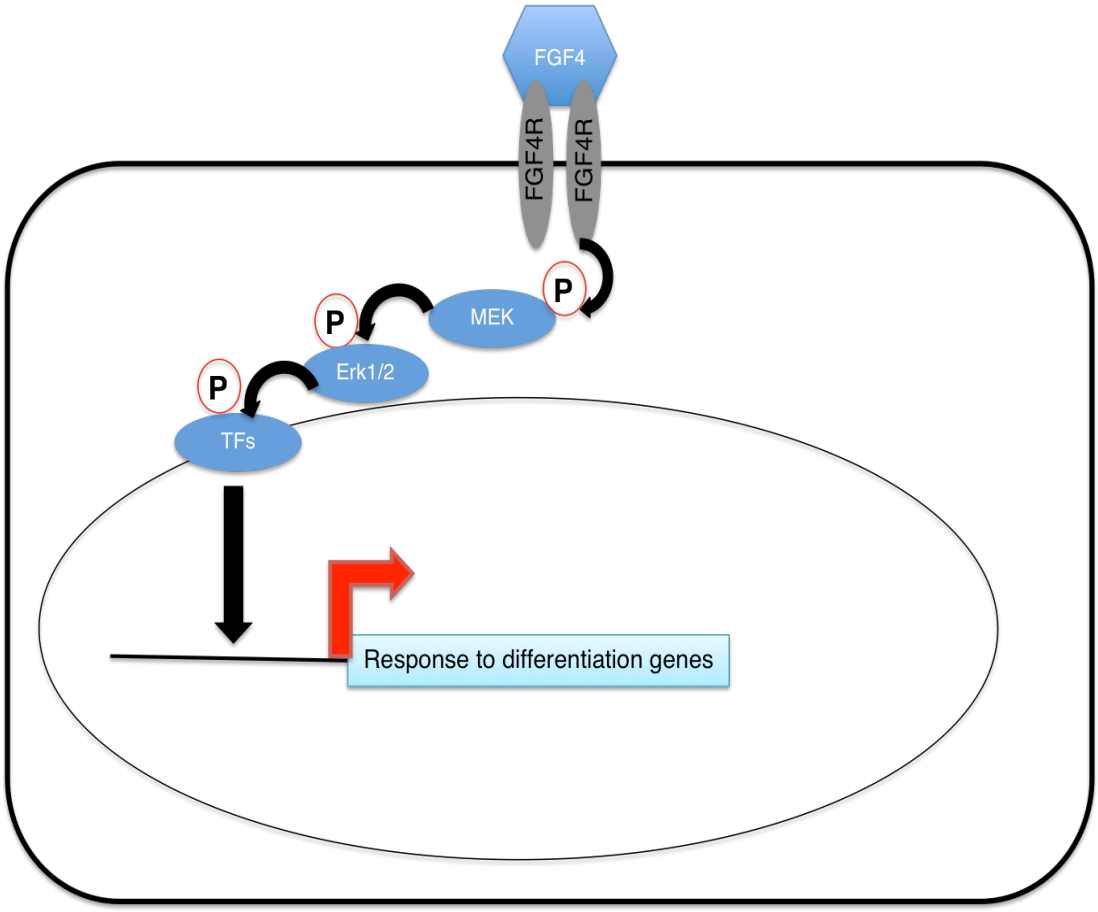

Figure 7. Schematic representation of the FGF4 signaling network. FGF4 binds to its tyrosine kinase receptors (TKR) on the cell membrane. This ligand-receptor interaction causes receptor activation by trans-phosphorylation. Activated TKRs cause phosphorylation and subsequent activation of MEK, which in turn leads to phosphorylation of Erk1/2 and Erk1/2 downstream target transcriptional factors (TF). Activated TFs migrate into the nucleus where they mediate

the transcription of target genes involved in response to differentiation clues. Adapted from (Kunath et al., 2007).

1.4 Induced pluripotent stem cells

Stem cell research, and above all human embryonic stem cell research, has been the center of deep public debate. Ethical issues were raised about the generation and use of human embryonic material for research. In 2006 Kazutoshi Takahashi and Shinya Yamanaka offered a potential solution to this debate. They found that differentiated cells could be reprogrammed to become embryonic stem cells by the introduction of four factors: Oct4, c-Myc, Sox2 and Klf4. These induced pluripotent stem (iPS) cells exhibited the self-renewal potential and morphology of ESCs, reactivated the silenced X-chromosome, and expressed ESC marker genes (Takahashi and Yamanaka, 2006). In addition, subcutaneous transplantation of iPS cells into nude mice resulted in the formation of teratomas. Furthermore, iPS cells that were injected into blastocysts contributed to mouse embryonic development (Takahashi and Yamanaka, 2006).

It has become evident that reprogramming cannot happen without massive chromatin reorganization. In fact, already early in reprogramming, during the first 72h post transfection, there is a widespread histone modification activity. Changes in DNA methylation happen, instead, in later stages during de-differentiation (Fig. 8) (Koche et al., 2011; Mikkelsen et al., 2008).

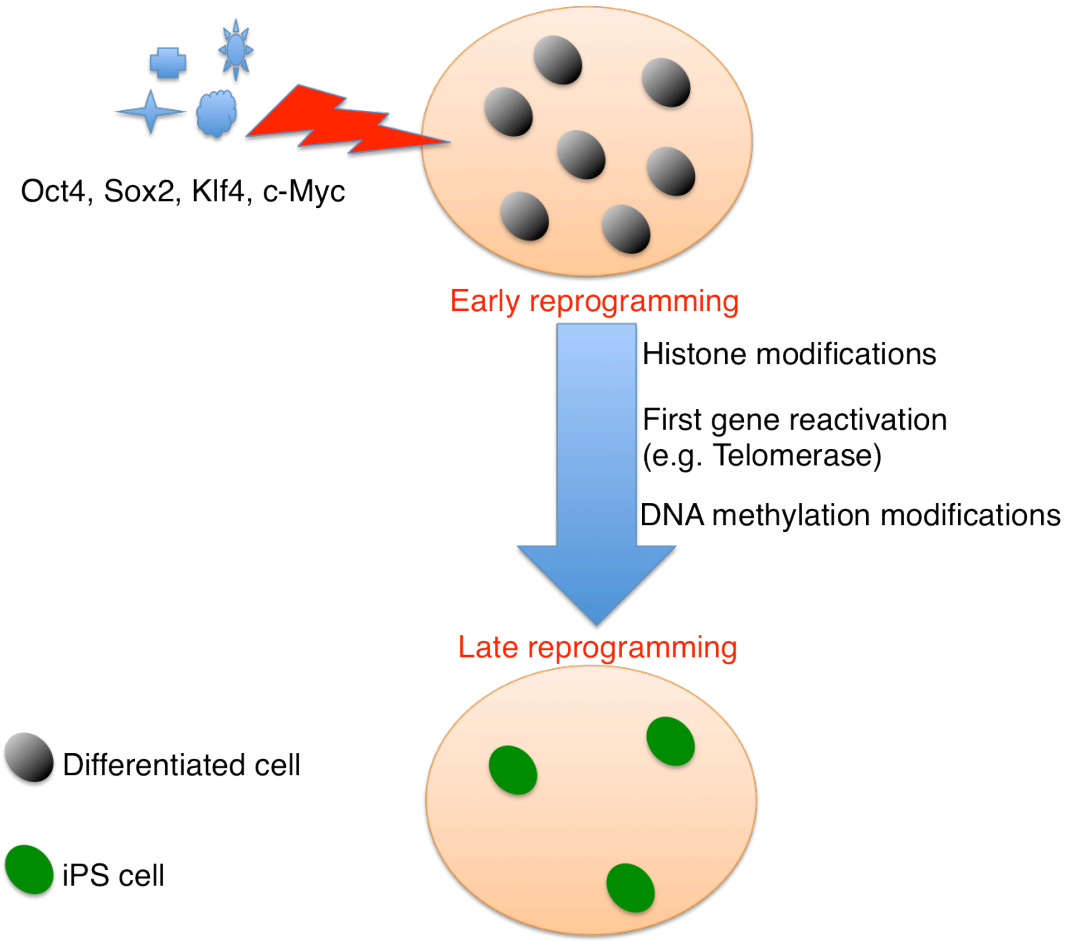

Figure 8. Schematic representation of iPS cell reprogramming mediated by the four Yamanaka factors. Differentiated cells infected with retroviral vectors encoding Oct4, Sox2, Klf4 and c-Myc exhibit, soon after infection, widespread histone modifications. Later on during the reprogramming process, genes involved in pluripotency (but not silenced by DNA methylation) are reactivated. DNA demethylation of pluripotency promoter genes happens only in late stages of reprogramming. Figure adapted from (Koche et al., 2011; Mikkelsen et al., 2008).

1.5 Chromatin and epigenetic modifications

Chromatin condensation is regulated by DNA methylation and by a wide range of histone post-transcriptional modifications. In mammals, DNA methylation at cytosine residues tends to essentially occur at CpG sites (Ramsahoye et al., 2000;

Ziller et al., 2011). In the genome, CpG can cluster into so-called CpG islands, which are regions of DNA, approximately 1000 bp long, characterised by elevated CpG composition and usually unmethylated (Bird et al., 1985; Cross et al., 1994; Deaton and Bird, 2011). Approximately 70% of annotated gene promoters are associated with CpG islands, which usually define transcriptional permissive promoters (Deaton and Bird, 2011; Saxonov et al., 2006).

CpG methylation at CpG island promoters acts to silence gene expression by recruiting chromatin-condensing factors and by direct, methylated-DNA based, transcription factors binding inhibition (Klose and Bird, 2006). CpG promoters can also be silenced by histone modifications mediated by Polycomb complex proteins (see section 1.6).

Among histone modifications, acetylation was the first to be identified (Phillips, 1963). Acetylation neutralises histone positive charges (due to lysine residues, where acetylation occurs) weakening the opposite charge attraction between histone and nucleosomal DNA, and leading to a more relaxed chromatin state that is accessible to transcriptional factors (Zentner and Henikoff, 2013). Lysine acetylation and deacetylation processes are mediated by histone acetyl transferases (HATs) and histone deacetylase (HDAC) enzymes, which are key regulators of chromatin condensation (Allis et al., 2007; Wang et al., 2009). Distinct from other histone modifications, lysine acetylation executes its functions by cumulative charge neutralization more than by lysine-specific acetylation effects (Martin et al., 2004; Zentner and Henikoff, 2013).

Histone lysines can also be mono, bi or tri-methylated and, in contrast to lysine acetylation, histone methylation on specific lysine residues defines very different

activities, like activation or repression of transcription (Zentner and Henikoff, 2013), Histone methylation also plays a central role in defining the chromatin state of ESCs (see section 1.6).

Finally, histones also undergo phosphorylation. This modification is triggered by many cellular processes, such as ATM-dependent serine phosphorylation of γ-H2A.X in response to DNA double strand breaks (Paull et al., 2000). In response to DNA damage, histones can also be ADP-ribosylated, and this modification leads to a more relaxed chromatin state that is accessible to the DNA repair machinery (Messner and Hottiger, 2011).

1.6 Chromatin state in ESCs

The chromatin state of ESCs is different from both progenitor and fully differentiated cells. ESCs show less heterochromatic regions, which results in a more transcriptionally permissive chromatin state compared with differentiated cells. In addition, ESCs are characterized, typically on lineage regulatory gene promoters, by chromatin bivalency (Fig. 9) (Fisher and Fisher, 2011). Bivalent domains consist of regions marked by histone 3 lysine 27 trimethylation (H3K27me3) and histone 3 lysine 4 trimethylation (H3K4me3). H3K4me3 is a mark of transcriptionally active chromatin, whereas H3K27me3 is a mark of transcriptional repressed promoters (Deaton and Bird, 2011; Smith and Meissner, 2013).

H3K4me3 and H3K27me3 are deposited by Trithorax (Trx)/mixed lineage leukemia (Mll) and Polycomb proteins, respectively. In mammals, there are two Polycomb repressive complexes (PRC): PRC1 and PRC2. PRC2, via its catalytic subunit Ezh2, is responsible for H3K27 trimethylation, whereas PRC1 recognise H3K27me3 and

mediates chromatin compaction and transcription silencing (Fisher and Fisher, 2011; Stock et al., 2007).

It has been proposed that the coexistence of active and repressive marks on lineage regulatory gene promoters may keep genes repressed when under pluripotency conditions, but poises them to become activated in response to differentiation clues (Fisher and Fisher, 2011; Margueron and Reinberg, 2011; Mendenhall et al., 2010; Vastenhouw and Schier, 2012).

Bivalency at gene regulatory regions is resolved either by loss of H3K27me3 and subsequent switch to fully transcription active gene, or by DNA methylation at cytosine residues and subsequent stable gene silencing. Bivalent DNA regions in ESCs are unmethylated and ESCs show an overall decrease in DNA methylation at CpG islands compared to more differentiated cells, although DNA methylation at non CpG islands is increased (Fig.9) (Fisher and Fisher, 2011; Ramsahoye et al., 2000). During differentiation, cells opt for stable silencing of some genes and switch from bivalent chromatin to cytosine methylation. In mammals, four DNA methyl transferase (Dnmt) enzymes are assigned to establish DNA methylation: Dnmt1, 3a, 3b and 3L. Dnmt1 is responsible for DNA methylation maintenance, but it has low affinity for unmethylated DNA regions and this limits its *de novo* methylation activity. Dnmt3a, Dnmt3b and Dnmt3L are deputed to *de novo* DNA methylation, although they are also important for methylation maintenance as evidenced by severe hypomethylation in Dnmt3a/3b null cells (Li et al., 1992; Okano et al., 1999; Smith and Meissner, 2013; Tsumura et al., 2006). Dnmt3a/3b act in complex with other chromatin compacting factors, such as histone methyltransferases and deacetylases,

to establish permanent gene suppression, whereas Dnmt3L does not have an enzymatic activity *per se*, but it interacts with, and stimulates the activity of Dnmt3a and 3b (Hata et al., 2002).

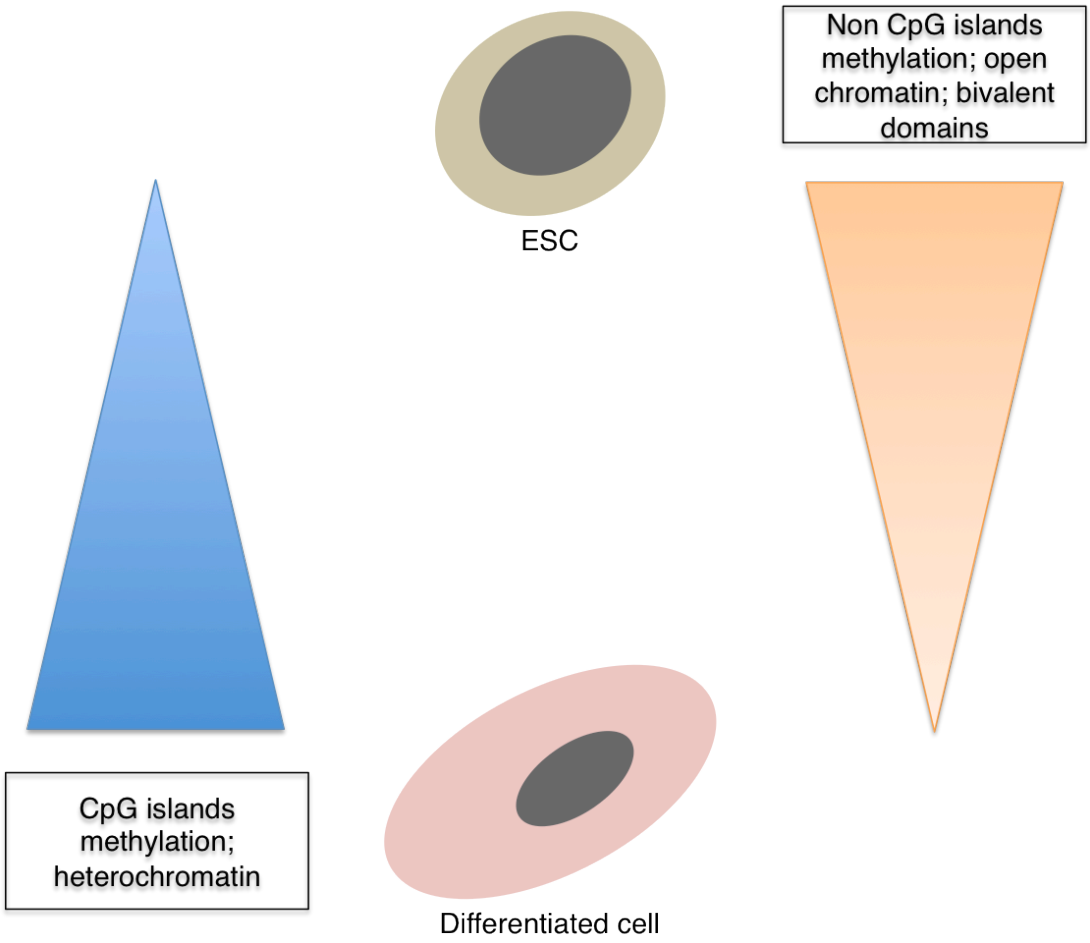

Figure 9. Schematic representation of chromatin conformation evolution during ESC differentiation. In comparison with more differentiated cells, ESCs exhibit less extensive heterochromatin regions, an increase in non-CpG islands methylation and a decrease in CpG islands one. Furthermore, ESC chromatin is also characterized by bivalent domains. Chromatin bivalency is phased out during differentiation. Figure adapted from (Fisher and Fisher, 2011).

Improper DNA methylation at specific *loci*, such as pluripotency gene promoters, can affect maintenance of an undifferentiated state in ESCs. The enzymes deputed to demethylate cytosine residues are the ten-eleven translocation (TET) methyl-cytosine hydroxylase proteins: TET1, 2, 3. TET proteins can, through three subsequent reactions, convert 5-methyl cytosine into 5-hydroxymethylcytosine, then 5-formylcytosine, and finally into 5-carboxylcytosine (Wu and Zhang, 2011).

TET1, in particular, is important to maintain ESCs in an undifferentiated and self-renewing state, thus preserving the *Nanog* promoter as active and unmethylated. Evidence in support of its crucial role in this process is that *TET1*$^{-/-}$ ESCs undergo spontaneous differentiation (Ito et al., 2010). Furthermore, TET1 is also important to establish ICM lineage specification, and in the reprogramming of differentiated cells into iPS cells. Specifically, it has been shown that TET1 interacts with Nanog, which can tether it to its target regions (e.g. the *Oct4* and *Esrrb* promoters) (Costa et al., 2013; Gao et al., 2013; Ito et al., 2010; Wu and Zhang, 2011).

However neither DNA methylation nor bivalent domains are crucial to maintain pluripotency, although they are important for achieving and maintaining differentiation. In fact, although lack of H3K27me3 in ESCs leads to increase expression in some lineage commitment genes, cells remain undifferentiated. In addition, ESCs are also able to support global DNA hypomethylation, as evidenced by the ability of cells null for all three Dnmts to persist without defects in self-renewal capacity and/or genomic instability (Schoeftner et al., 2006; Silva and Smith, 2008; Smith and Meissner, 2013; Tsumura et al., 2006).

1.7 Telomere function and biology

Telomeres are specialized DNA-protein complexes that protect chromosome ends from inappropriately timed DNA repair activities such as homologous recombination and non-homologous end joining that can lead to genomic instability. Their average length changes during aging and is highly heterogeneous among different species, different individuals and even among different tissues and compartments in the same organism (Kipling and Cooke, 1990; Luke and Lingner, 2009; Palm and de Lange, 2008; Smogorzewska and de Lange, 2002). In *mus musculus*, which possesses telomeres up to 100k bp (where the average human length at birth is 10k bp), a seven-protein complex (six in humans), named shelterin, associates specifically with telomeres and protects chromosome ends from a DNA damage response. Four shelterin proteins (three in humans, which have only one isoform of Pot1), TRF1, TRF2, POT1a and POT1b, are responsible for the direct recognition of telomeric sequence. They interact with TIN2, TPP1, and Rap1 to form the complete Shelterin complex (Chiodi et al., 2013; Hockemeyer et al., 2006; Palm and de Lange, 2008).

Because telomeres become shorten with each cell cycle in somatic tissues that do not express telomerase, telomere length can regulate cellular lifespan in some cellular contexts. Telomere shortening, in fact, it has been associated with the famous experiments performed in 1961 by Leonard Hayflick, which showed how human cells in culture could proliferate only a certain number of times (Hayflick limit) before entering senescence. Therefore, cells need an efficient telomere maintenance system to prevent the attrition of their ends and consequent cellular senescence (Blackburn, 2001; Hayflick and Moorhead, 1961).

In the vast majority of cases, telomeres are elongated by telomerase. Carol Greider and Elizabeth Blackburn discovered this reverse transcriptase in 1984 while working with the ciliate Tetrahymena. Telomerase is composed of a catalytic subunit (Tert, telomerase reverse transcriptase) and an RNA component that serves as template (Terc, telomerase RNA). In mammals, telomeres bear the repeating sequence 5'-TTAGGG-3'. Telomerase compensates for telomere erosion by adding TTAGGG repeats onto chromosome ends (Fig.10) (Geserick and Blasco, 2006; Greider and Blackburn, 1985).

Telomerase is constitutively expressed in many unicellular eukaryotes. During mouse development, telomerase activity appears first in blastocyst. Telomerase is, in fact, a stemness hallmark; expression of telomerase in embryonic stem cells is sufficient to fully maintain telomere length (Liu et al., 2007; Shay and Wright, 2010). During differentiation, its activity is largely (but not exclusively) limited to tissues characterized by a highly proliferative grade such as progenitor cell compartments (Liu et al., 2007). It also presents a dynamic regulation, as shown by variable and inducible levels during lymphocyte T maturation and activation (Weng et al., 1996). However, mouse somatic cells present a less strict suppression of telomerase activity compared to human somatic cells (Geserick and Blasco, 2006; Prowse and Greider, 1995).

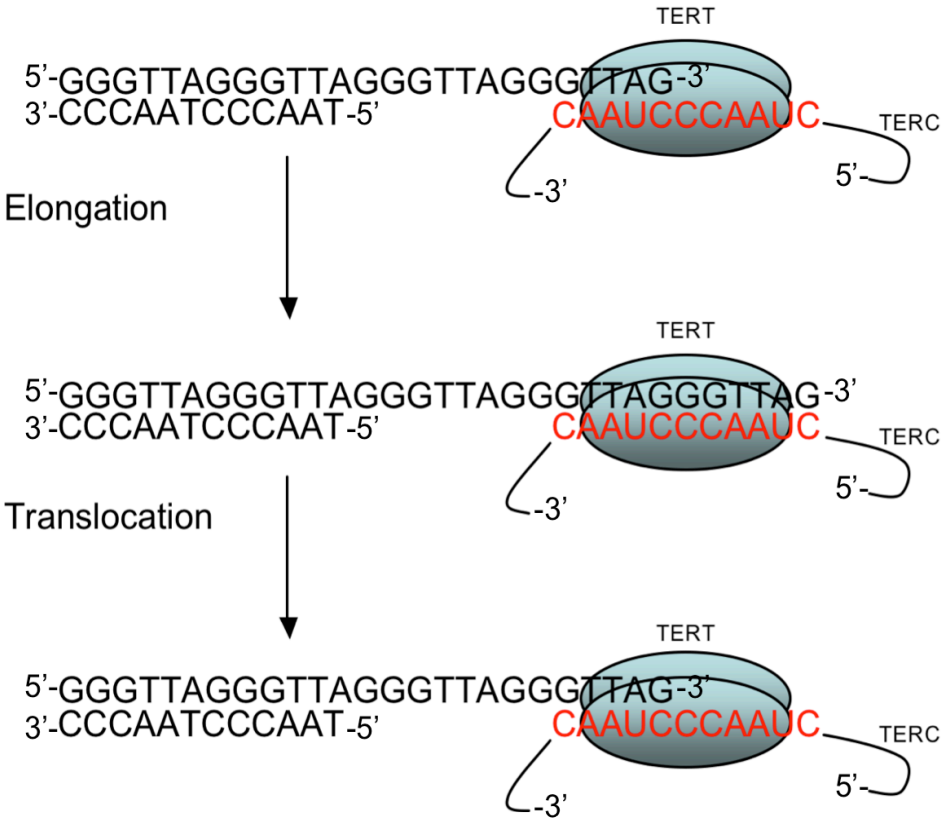

Figure 10. Telomere elongation by telomerase in mammals. Telomerase binds chromosome ends by the annealing of Tert to telomere DNA. Using Terc as template for reverse transcription, Tert elongates telomeres by adding a repeating nucleotide sequence (TTAGGG). Adapted from (Granger et al., 2002).

1.8 Tert: telomere commitment vs moonlight activities

Apart from well-characterized, telomere-related, functions, Tert has been associated with several non-canonical activities. In 2008, Lee's group reported that Tert overexpression in mouse neurons had an anti-apoptotic effect on N-mehtyl-D-aspartic Acid (NDMA)-induced receptor mediated toxicity by entering the mitochondria and increasing calcium mobilization (Lee et al., 2008).

In addition, Steven Artandi and collaborators observed that Tert overexpression might lead, independently from telomere elongation, to mouse epidermal stem cell proliferation, self-renewal and migration by stimulating Wnt3a and c-Myc. Also, they noticed Wnt-associated development defects in *Tert*$^{-/-}$ mice (Choi et al., 2008; Park et al., 2009; Sarin et al., 2005).

However, the hypothesis that Tert possesses non-canonical functions, when expressed at physiological levels, is still unclear. As one example, recent work from Carol Greider and colleagues focused on the analysis of *Tert*$^{+/-}$ and *Tert*$^{-/-}$ mice. In this study they looked for Wnt pathway alteration and Wnt-dependent differentiation impairment, but they did not observe any difference between *Tert*$^{-/-}$ and wild-type animals (Strong et al., 2011).

1.9 The role of telomere length in the regulation of telomere chromatin

Mammalian telomeres and subtelomeric regions exhibit a highly compact chromatin conformation. In particular, both telomeric and subtelomeric regions are characterized by trimethylation of lysine 9 on histone H3 (H3K9me3) and trimethylation of lysine 20 on histone H4 (H3K20me3). In addition, subtelomeric DNA is also heavily methylated (Benetti et al., 2007; Gonzalo and Blasco, 2005).

Telomere shortening and the presence of uncapped telomeres affect heterochromatin conformation at both telomeric and subtelomeric regions. Specifically, it has been observed, in mouse embryonic fibroblasts (MEFs) from late generation (G4) *Terc*$^{-/-}$ mice compared to Wt and G1 *Terc*$^{-/-}$ MEFs, that cytosine methylation is lost at

subtelomeric regions. At telomeric and subtelomeric regions in *Terc*$^{-/-}$ MEFs compared to Wt and G1 *Terc*$^{-/-}$ cells, the heterochromatin marks H3K9me3 and H4K20me3 are replaced with marks that are diagnostic of open chromatin, e.g. acetyl-H3K9 and acetyl-H4 (Benetti et al., 2007).

These results indicate that telomere shortening and/or uncapped telomeres can trigger chromatin modifications, at least at within telomeric and subtelomeric regions.

1.10 Alternative lengthening of telomeres and the role of telomere chromatin in the regulation of telomere length

Besides telomerase, alternative telomere maintenance mechanisms exist. Although these 'alternative lengthening of telomeres' (ALT) mechanisms are not completely understood, they are typically associated with long and heterogeneous telomeres, extra-chromosomal telomeric DNA (both circular and linear), and ALT-associated promyelocytic bodies (APBs) which contain telomere binding proteins and proteins involved in DNA recombination and replication (Lafferty-Whyte et al., 2009; Royle et al., 2008a). ALT cells are also often characterized by loss of function mutation in the chromatin H3.3 assembling complex ATRX/DAXX (Bower et al., 2012). However, it is worth to mention that these characteristics are not only confined to telomerase-inactive cells. It is in fact been reported that both t-circles and telomere recombination can happen in normal cells harboring long telomeres (Neumann et al., 2013; Pickett et al., 2009; Pickett et al., 2011).

ALT mechanisms can occur in both pathological (tumour) and physiological (embryogenesis) contexts. Most human cancers (85%) gain unlimited replicative

potential through the reactivation of telomerase. In the remaining 15% of tumours, telomere maintenance occurs through the activation of ALT (Bryan et al., 1995; Kim et al., 1994).

During embryogenesis, telomerase is absent or present at low levels in cleavage-stage embryos, and becomes strongly activated in blastocysts. Interestingly, despite the lack of telomerase, telomeres are elongated considerably during the cleavage stage by an ALT-like mechanism characterized by long telomeres and extensive telomere sister-chromatid exchange (T-SCE) (Liu et al., 2007).

In this regard, a recent study identified Zscan4c as a candidate protein involved in telomerase-independent telomere lengthening during embryogenesis (Zalzman et al., 2010). However, role and mechanism of action of this protein at telomeres are still being elucidated.

Furthermore, it has been shown that despite mouse embryonic stem cells shorten their telomeres from generation to generation of *Terc*$^{-/-}$ mice, ESCs from late generation (G4) *Terc*$^{-/-}$ mice maintain (without lengthening it though) the same telomere length of the previous generation (G3) (Huang et al., 2011).

Although the mechanisms of the ALT pathway(s) are still undefined, previous studies have shown that ALT requires telomere-telomere recombination (i.e. T-SCE) (Dunham et al., 2000; Jiang et al., 2007; Murnane et al., 1994; Royle et al., 2008a).

Recent studies in DNA methyl transferase-knockout mouse cells (*Dnmts*$^{-/-}$) (Benetti et al., 2008; Gonzalo et al., 2006a), and in human cells treated with demethylating agents (Vera et al., 2008), showed that hypomethylation of subtelomeric regions leads to increased T-SCE. On the other hand, the relationship between subtelomeric

hypomethylation and ALT does not seem to always hold in human cells (Tilman et al., 2009).

.

The discovery that telomeres are transcribed into long non-coding RNAs that remain associated with telomeric chromatin may offer new insight into the regulation of telomere length and the structure of telomeric chromatin (Azzalin et al., 2007). In fact, it has been proposed that this telomeric repeat-containing RNA (TERRA) may not only inhibit telomerase activity by pairing with the RNA component of telomerase (Terc) (Luke and Lingner, 2009), but could also play a role in the maintenance of telomere heterochromatin through the recruitment of heterochromatic factors such as DNA methyl transferase 3b (Dnmt3b) and Heterochromatin Protein(s) (HP1) (Fig. 11) (Schoeftner and Blasco, 2010).

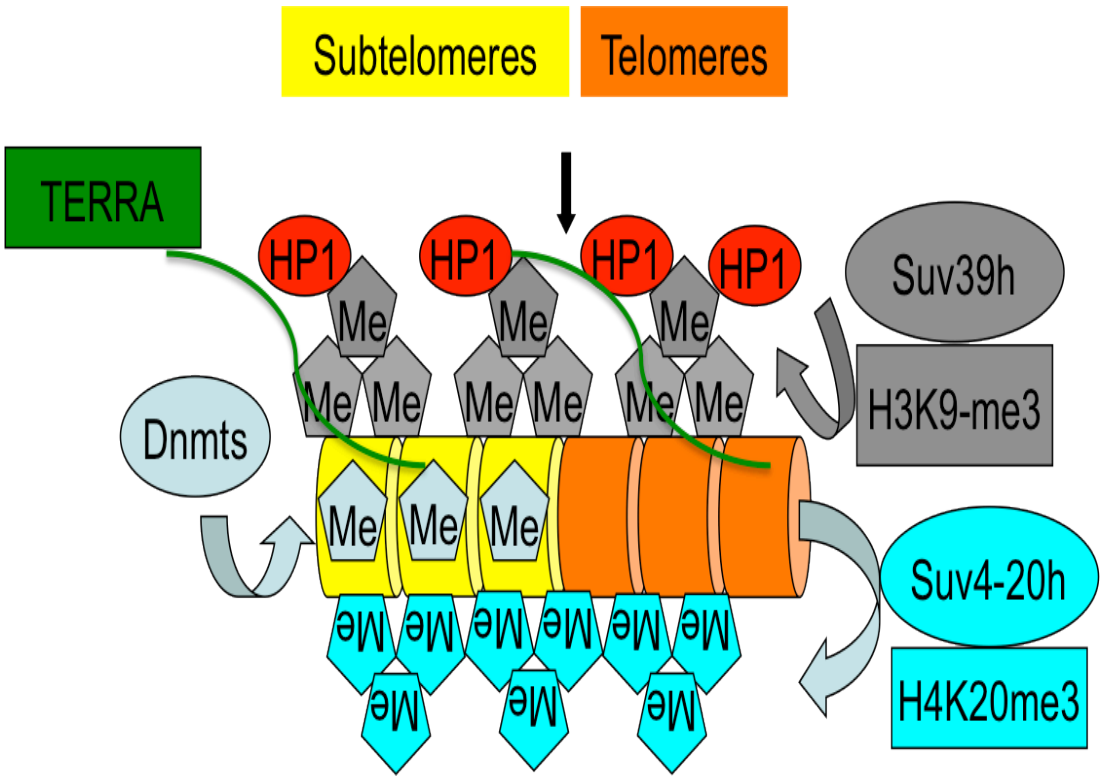

Figure 11. Schematic model for the formation of heterochromatin on mammalian telomeric and subtelomeric regions. Methylation of H3K9, on both telomeric and subtelomeric regions, generates a high-affinity site for HP1 (also recruited by TERRA), which in turn can recruit histone methyl-transferase (such as Suv4-20h) causing tri-methylation of H3K9 and H4K20. In parallel, DNA methylation by Dnmts, on subtelomeric regions, also contributes to heterochromatin formation. Adapted from (Schoeftner and Blasco, 2010).

1.11 Telomeres and telomerase in embryonic stem cells

Recently, few telomere-related proteins have been associated to ESC identity. In 2010 for example, Minoru Ko and colleagues identified in the zinc finger and SCAN domain containing 4c (Zscan4c) one of the candidate factors involved in telomerase-independent telomere elongation in cleavage stage of embryo development. In addition they found that in an ESC culture, Zscan4c localized at telomeres and was

transiently expressed by every cell, small proportion of cells per time, and its expression was associated to telomere recombination and elongation (Zalzman et al., 2010).

The Rap1 interacting factor 1 (Rif1), which is recruited on telomeres by the Shelterin protein Rap1, was instead identified as an important factor to maintain pluripotency in an RNAi screening study. Although its mechanism of action is still unclear, it was shown that Rif1 depletion led to ESC differentiation (Loh et al., 2006).

Rap1 itself, instead, has never been linked to ESC functions, so far, but lately it has been shown to possess gene regulation activities apart from telomere protection ones (Martinez et al., 2010).

A further proof of the importance of telomerase and telomere regulation in ESCs is that during reprogramming of somatic cells to embryonic stem cells, telomerase is reactivated and telomeres acquire characteristics of ES cell telomeres (Marion et al., 2009b). Notably, cellular reprogramming is impaired when cells have very short telomeres (G3-G4 *Terc*$^{-/-}$ MEFs) and telomerase is absent or non-functional (i.e. when it cannot elongate telomeres). Furthermore, all attempts to produce chimeric mice from telomerase-negative iPS cells (derived from G1, G2 or G3 *Terc*$^{-/-}$ MEFs) have failed (Marion et al., 2009b).

In addition, it has been shown that ESCs from late generation (G3-G4) *Terc*$^{-/-}$ mice had an impaired ability to form teratoma and to contribute to chimeric animal formation after blastocyst injections (Huang et al., 2011).

The role of telomerase in the ability of ESCs to proliferate indefinitely, the putative telomere-unrelated Tert activities on stem cell biology, and the emerging functions of

telomere-related factors in gene expression and/or ESC identity, strongly pointed toward a major role of telomere biology in stem cell regulation.

Furthermore, the importance of telomere length in iPS cell reprogramming, contribution to teratoma formation and animal chimerism upon blastocyst injections suggested a possible role of telomeres not only in preserving the replicative potential of the cell, but also in undergoing differentiation.

In this study, we decided to question whether absence of Tert and/or telomere shortening and uncapped telomeres could affect also ESC differentiation processes.

Chapter 2

Materials and Methods

2.1 Cell culture and transfection

Cells employed in this study consisted of a wild type, paternal cell line of E14 ESCs (derived from R129J strain), and two separately generated *Tert*-/- ESC lines, produced by electroporating E14 ESCs with a targeting construct replacing five exons of mouse *Tert* with the neomycin resistance gene (Liu et al., 2000). After selection with G418 (0.3 mg/mL), homologous recombinants were identified and confirmed by southern blot and PCR (Liu et al., 2000). ESC lines were cultured on gelatin-covered dishes and maintained in Glasgow's modified Eagle medium (GMEM; GIBCO) supplemented with 15% v/v fetal bovine serum (FBS), 0.055 mM b-mercaptoethanol (Sigma), 2 mM L-glutamine, 0.1 mM MEM nonessential amino acids, 5,000 units/ml penicillin/streptomycin, 1,000 units/ml LIF and doxycycline 1 µg/ml, and maintained at 37°C with 5% v/v CO_2. To restore Tert expression to $Tert^{-/-S}$ ESCs, cells at passage 70 were co-transfected with pTRE-Bi-*Tert*-IRES-EGFP-Hygro (or a similar vector lacking *Tert*) and CAG-rtTA advanced (pTET-ON advanced vector, Clontech). For constitutive expression of Tert, $Tert^{-/-S}$ ESCs were transfected with CAG-*mTert*-IRES-Puro or CAG-IRES-Puro. For expression of Dnmt3b, $Tert^{-/-S}$ ESCs were transfected with CAG-*Dnmt3b*-IRES-Puro or CAG-IRES-Puro. All transfections employed Fugene6 (Roche) in a 3:1 ratio to DNA

according to the manufacturer's instructions. For *Tert* rescue or *Dnmt3b* reintroduction, cells were propagated for 4 passages under selection with hygromycin (500 μg/ml) or puromycin (5 μg/ml), and individual colonies were isolated. For Nanog shRNA transduction, cells were infected with commercially available lentiviral particles (Santa Cruz), and selected with puromycin (5 μg/ml). Cell transduction with Oct4 promoter-GFP was performed by infection with commercially available lentiviral particles (System Biosciences). All lentiviral infections were performed in presence of Polybrene (5 μg/ml) (Santa Cruz). All experiments were performed with more than one clonal isolate.

2.2 Differentiation assay

Cell populations of the indicated genotype (1 x 10^5) were plated in non gelatin-covered dishes in LIF-free media containing 5 μM ATRA (Sigma) for the indicated amount of time, with ATRA-media replaced every 3 days. At the indicated time point, cells were re-plated in gelatin-covered dishes containing LIF-supplemented media. For the single colony formation assay, a set of serial dilutions was performed and the number of viable ES cell colonies assessed with alkaline phosphatase (Millipore).

2.3 Quantitative fluorescence in situ hybridization (Q-FISH)

The Q-FISH protocol was carried out as described (Liu et al., 2000). Briefly, cells were treated with 0.2 μg/mL colcemid for 6 hours, harvested and resuspended in 0.5 mL warm 75 mM KCl at 37 °C for 12 min with gentle stirring to prevent

precipitation. Cells were spun at 128.7 x *g* for 5 min. The supernatant was discarded and cells were resuspended in 100 µL 75 mM KCl. One mL of 3:1 ice-cold methanol-acetic acid was added drop-by-drop to the cells, which were then incubated for 30 min at room temperature. Cells were spun as above, resuspended in an adequate volume of fixative and stored at -20°C for at least 6 hours before being dropped onto slides and left to air-dry overnight. The next day, cells were fixed in 4% v/v paraformaldehyde (PFA), digested with 100 mg/mL pepsin for 10 min at 37°C and dehydrated in ethanol (5 min in each of 70% v/v, 90% v/v and 100% v/v ethanol). Slides were air-dried and hybridized in the dark with a Tel-Cy3 PNA probe (Panagene) in hybridization solution (70% v/v formamide, 0.25% v/v blocking solution (Roche), 10 mM Tris-HCl pH 7.4, 0.5 µg/ml Tel-Cy3 PNA probe, 5% v/v $MgCl_2$). Slides were then denatured at 80°C for 3 min, left in the dark for at least 2 hours, then washed. DAPI was subsequently added. Metaphase spreads were captured using Metafer 4 software and analyzed using Isis software. Statistical analysis of telomere intensity distribution was performed using Welch's unpaired t-test. The incidence of telomere-signal free ends was defined as the number of chromosome ends possessing a telomere signal (in arbitrary units) between 0 and 600, and statistical significance was assessed using Fisher's exact test (Instat3, GraphPad).

2.4 QRT-PCR

Total RNA was isolated from cells using Triazol (Invitrogen) according to manufacturer's instructions. Reverse transcription was carried out using 0.5 µg of

template RNA, random hexamer primers and smart MMLV reverse transcriptase (Clontech). Diluted cDNA (20 times) was subjected to real-time PCR analysis using a SYBR Green Mastermix (Roche) on a LightCycler480 system (Roche). Background values (no reverse transcriptase added) were subtracted, and values were normalized to *GAPDH* (n>3). Oligos employed are listed in Table 1. Statistical analysis was performed by ANOVA and related Dunnett's test comparing every group with Wt values.

2.5 Chromatin immunoprecipitation (ChIP)

ChIP experiments were performed as described (Bergmann et al., 2011), except phenol-chloroform was replaced with a Chelex-100 resin-based DNA isolation method described in (Nelson et al., 2006). Briefly: at day 0, protein-A covered magnetic beads (Thermo scientific) were aliquoted in 1.5 mL tubes (1 tube per IP, 20 µL per tube). Beads were magnetically precipitated and incubated with 0.5 mL of 0.5% v/v PBS/BSA for 30 min during rotation at 4°C. The supernatant was aspirated and beads were resuspended in 0.5 mL of RIPA-BSA (50 mM Tris-HCl pH 7.4, 1% v/v NP-40, 0.25% w/v Na-deoxycholate, 150 mM NaCl, 1 mM EDTA, 1 mM PMSF, 1 µg/ml each of aprotinin, leupeptin and pepstatin, 1 mM Na_3VO_4, 1 mM NaF, BSA 0.5% v/v). 5 µg of Ab were added to the resuspended beads and incubated for at least 6h on rotation at 4°C.

Cells (at least 5 x 10^6 per sample, including 4 test samples + IgG control) were harvested and spun at 1000 x *g* for 5 min. The cell pellet was then resuspended in PBS 1X (1 mL of PBS per million of cells). Formaldehyde was added to cells for

crosslinking at a final concentration of 1% v/v, and cells were incubated on a rocking plate for 10 min. Formaldehyde was then quenched by adding glycine at a final concentration of 125 mM and incubating cells on a rocking plate for 5 min. Cells were then centrifuged at 3000 x *g* for 3 min at 4°C. Afterwards, cells were resuspended in TBS (1 mL per million cells) and aliquoted in 1.5 mL tubes (1 mL each) and precipitated at 3000 x *g* for 3 min at 4°C. After quick removal of supernatant, cells were resuspended in 1 mL of freshly prepared lysis buffer (10 mM Tris-HCl pH 7.4, 10 mM NaCl, 0.5% v/v NP-40, PMSF 1 mM, 1 nM aprotinin, 25 mM pepstatin, 25 mM antipain, 25 mM chymostatin) and incubated for 10 min on ice. After lysis, cells were spun at 1000 x *g* for 3 min at 4°C and resuspended in 0.5 mL of lysis buffer. 300 µL of dilution buffer 1 (50 mM Tris-HCl pH 7.4, 0.2 mM EDTA, 0.2% v/v SDS, 130 mM NaCl, 0.8% v/v triton-x 100, 0.1% v/v sodium deoxycholate, PMSF 1 mM, 1 nM aprotinin, 25 mM pepstatin, 25 mM antipain, 25 mM chymostatin) were added to each sample. Samples were incubated on ice for 5 min. Ice-cold samples were then sonicated for 50 cycles of 30 seconds, and precipitated at 20,800 x *g* for 10 min at 4°C. Three hundred µL of supernatant from each sample was then collected in a new tube and mixed with 1.2 mL of a buffer composed of 1/6 dilution buffer 1, 2.5/6 of RIPA buffer, and 2.5/6 of dilution buffer 2 (50 mM Tris-HCl pH 7.4, 130 mM NaCl, 0.8% v/v triton-x 100, 0.1% v/v sodium deoxycholate). Ten percent (150 µL) of the resulting input sample was collected and frozen at -80°C.

Meanwhile, dynabeads were magnetically isolated and washed twice with RIPA/BSA buffer. The supernatant was then removed and the beads incubated with

450 µL of the remaining input sample. Samples were incubated during rotation for 16h at 4°C.

At day 2, beads were magnetically isolated, supernatant was removed, and beads were washed twice with 1 mL of RIPA buffer, twice with 1 mL of RIPA-500 buffer (50 mM Tris-HCl pH 7.4, 1% v/v NP-40, 0.25% w/v Na-deoxycholate, 500 mM NaCl, 1 mM EDTA, 1 mM PMSF, 1 µg/ml each of aprotinin, leupeptin and pepstatin, 1 mM Na_3VO_4, 1 mM NaF) and once with 1 mL of Tris-EDTA. The supernatant was then removed and 0.1 mL of 10% w/v Chelex-100 resin (Bio-Rad) was added to each sample. In parallel, 10 µL of stored input for each sample was incubated together with 0.1 mL of 10% w/v Chelex-100.

Samples were boiled at 95°C for 12 min to de-crosslink samples and then treated with 2.5 µL of 10 mg/mL RNase A for 30 min at 37°C. Samples were then treated with 2.5 µL of 10 mg/mL proteinase K for 1h at 55°C. To inactivate the proteinase K, samples were boiled at 95°C for 10 min. Finally, samples were quickly precipitated and the supernatant was stored at -20°C.

DNA recovered from at least three biological replicates was analyzed by QRT-PCR as described above. For each pair of primers, triplicate measurements were taken, and normalized to input DNA and the amount of DNA recovered from the *GAPDH* promoter (n>3). Antibodies employed were: rabbit anti-Nanog (Bethyl labs); mouse anti-H3K27me3, anti-H3K4me3, anti-acH4, acH3K9 (Abcam) and anti-methyl cytosine (Millipore); and, as control, murine IgG (Sigma). Oligos employed are listed in Table 1. Statistical analysis was performed by ANOVA and related Dunnett's test comparing every group with Wt values. In each experiment, the signal

present after immunoprecipitation with IgG was defined as background and subtracted prior to normalization to input DNA and GAPDH.

2.6 Methylation assay

Relative genomic DNA methylation was assessed using the ELISA-based imprint methylated DNA quantification kit (Sigma) according to manufacturer's instructions and using 100ng of genomic DNA per sample (n>3).

2.7 Bisulphite sequencing analysis

DNA bisulphite conversion was performed as described (Clouaire et al., 2010). After bisulphite conversion of unmethylated cytosines to uracil, samples were resuspended in 1×Tris–EDTA for PCR amplification. PCR products were cloned into pcDNA3.1 (Invitrogen) vector, and colony PCR was performed. Clones (at least ten per sample) of the correct molecular mass were sequenced and results analyzed with BiQ Analyzer (http://biq-analyzer.bioinf.mpi-inf.mpg.de). Primers employed are listed in Table 1. Statistical analysis of samples employed Fisher's exact test (two-sided) using GraphPad Instat3 (www.graphpad.com).

2.8 Telomerase activity assay

The telomere repeat amplification protocol, TRAP, was conducted with the TRAPeze Telomerase Detection Kit, Chemicon International, according to manufacturer's instructions.

2.9. Plasmid construction

The plasmid pTRE-Bi-*Tert*-IRES-EGFP-Hygro was constructed by amplification of *Tert* cDNA by PCR and cloning it into pTRE-Tight-Bi (Clontech) following digestion with EcoRI and SalI. IRES-EGFP sequence was obtained from pCAGMKOSiE (from K.Kaji) and inserted into pTRE-Tight-Bi (following digestion with SalI and EcorV) using SalI and HpaI sites and then inserted into pTRE-Bi-*Tert* using NotI sites. Finally, the hygromycin-resistance gene was cloned by PCR into the XbaI restriction site of pTRE-Tight-Bi and pTRE-Bi-*Tert*-IRES-EGFP vectors to create pTRE-Bi-EGFP-Hygro and pTRE-Bi-*Tert*-IRES-EGFP-Hygro. The pCAG-rtTA-advanced vector was constructed by removal of the MKOS ORFs from CAGMKOSiE with EcoRI and BamHI and replacement with the advanced tetracycline reverse transactivator sequence (Clontech). The plasmid pCAG-*Dnmt3b*-IRES-puromycin vector was constructed by removal of the MKOS ORFs from CAGMKOSiE with EcoRI. *Dnmt3b* was subcloned from a *Dnmt3b* expression vector (Thermo scientific) and inserted pCAG-IRES-EGFP following digestion EcoRI and SalI. IRES-EGFP was replaced with IRES-Puro (from pIRESPuro2, Clontech) after

digestion with PmlI and PvuII. *Dnm3b* was also subcloned in pTRE-Bi-Hygro using EcoRI and SalI sites.

2.10 Fluorescence-activated cell sorting (FACS)

Hoechst stain (5µg/ml) was added to the cell culture and incubated for 30 minutes. Cells were harvested and resuspended in 0.5 ml of 1X PBS and analyzed for cell cycle distribution using a Becton Dickinson Fluorescence Activated Cell Sorter. After gating on the appropriate channels, the percentage of cells in G1, S, or G2/M were calculated. For FACS analysis of Nanog expression, cells were fixed and stained as indicated (Festuccia and Chambers, 2011). Cell sorting after transduction with Oct4 promoter-GFP was carried out as described in (Zheng and Hu, 2012).

2.11 Protein extraction and western blot analysis

Histones were acid-extracted as follows: Cells were harvested and washed twice with ice cold 1X PBS. Cells were resuspended (10^7 cells/ml) in TEB buffer (PBS 1X, 0.5% v/v Triton X-100, 2 mM PMSF, 0.02% v/v NaN_3) and left on ice for 10 minutes with gentle stirring to enhance lysis. Cells were spun at 800 x *g* for 10 minutes at 4°C, washed in TEB buffer, and pelleted as above. Cells were resuspended in 0.2 N HCl (4 x10^7 cells/ml) and incubated overnight at 4°C. Cells were pelleted as above, and the supernatant was recovered and stored at -80°C. Protein extracts were resolved on 15% w/v SDS-PAGE, transferred to nitrocellulose and blocked overnight with 3% w/v BSA in 1X PBS. Rabbit anti-histone H3 (Abcam) and mouse anti H3K27me3 (Abcam) were used as primary antibodies.

For non-histone protein extraction, cells were resuspended in Radio Immunoprecipitation Assay (RIPA) buffer (50 mM Tris-HCl pH 7.4, 1% v/v NP-40, 0.25% w/v Na-deoxycholate, 0.1% v/v SDS, 150 mM NaCl, 1 mM EDTA, 1 mM PMSF, 1 μg/ml each of aprotinin, leupeptin and pepstatin, 1 mM Na_3VO_4, 1 mM NaF) and lysed for 30 minutes on ice. Cells were then quickly sonicated (10 cycles 30 sec. On and 30 sec. Off), and put back on ice. RIPA buffer allows extraction of all cellular proteins, including membrane-bound ones, due to the combined use of ionic (SDS, Na-deoxycholate) and non-ionic (NP-40) denaturing agents, which disrupt protein-protein interactions, both at cell and nuclear membranes. Cells were then pelleted at 20,800 x *g* for 10 min at at 4°C. The supernatant was recovered and stored at -80°C. Protein extracts were resolved on 10% w/v SDS PAGE, transferred to nitrocellulose and blocked overnight with 5% w/v non-fat dry milk in 1X PBS. Rabbit anti-Nanog (Bethyl labs), anti-Dnmt3b (Abcam) and Dnmt1 (Abcam), goat anti-Oct4 (Santa Cruz) and mouse anti- β-Tubulin (Sigma) were used as primary antibodies. Anti mouse and anti rabbit peroxidase-conjugated were used as secondary antibodies followed by detection with ECL Plus luminescent reagent (Amersham Biosciences) or with LI-COR in which instance the secondary antibodies employed were donkey anti-rabbit IRDye 800CW (green) and donkey anti-mouse IRDye680 (red) (Odyssey). All experiments were repeated at least three times.

2.12 Immunofluorescence

Cells were fixed in 4% v/v paraformaldehyde (PFA)/PBS according to manufacturer's instructions (Abcam). Rabbit anti-Nanog (Bethyl labs) and Alexa

fluor® Goat anti-rabbit-488 were used as primary and secondary antibodies. Rhodamine-phalloidin (Sigma) was used to detect actin. DNA was stained with DAPI. ImageJ software was employed to define the relative fluorescence intensities of single cells (for channels 488), with DAPI fluorescence as internal control. Individual values were used for quantitative analysis of Nanog expression levels among genotypes as described (Savarese et al., 2009). Statistical analysis was performed using Welch's unpaired t-test.

2.13 3D Analysis of Cell Nuclei

Cells were fixed in 4% v/v paraformaldehyde (PFA)/PBS for 15 min, then treated as described for Q-FISH analysis of telomere fluorescence. At least 25 interphase nuclei were analyzed for Wt, *Tert*$^{-/-S}$ and *Tert*$^{-/-L}$. Images were acquired using a Nikon TE-2000 microscope equipped with a 1.45 numerical aperture 100× objective, PIFOC Z-axis focus drive (Physik Instruments), Sedat quad filter set, and CoolSnapHQ High Speed Monochrome charge-coupled device camera (Photometrics). Images were deconvolved from 0.2-μm sections using AutoquantX. Deconvolved images were analyzed for chromosome and telomere distribution using a macro described in (Korfali et al., 2010).

2.14 Inhibition of p53 transcriptional activity

Pifithrin-α (Sigma) was dissolved in DMSO at working concentration of 30 mM.

Cells were treated with 15-30 μM of Pifithrin-α (and equivalent volume of DMSO in control cells) and incubated 16h at 37 °C. After incubation cells were harvested, RNA extracted and analysed for Q-RT-PCR.

ChiP	Fw	Rv
GAPDH^{F}	5'-AAGCTCATGAGGCACAGAATGGTC-3'	5'TGGGTACATGGTGACTTTCCTAGGC-3'
Gata6^{F}	5'-TGACCCAGGAGGGGGCGAGT-3'	5'-CCGCCACCCAGGGCAGAAGA-3'
Nanog^{F}	5'-ACTCCAAGGCTAGCGATTCA-3'	5'-AATAGGGAGGAGGGCGTCTA-3'
Oct4^{D}	5'-CTGTAAGGACAGGCCGAGAG-3'	5'-CAGGAGGCCTTCATTTTCAA-3'
Sub. Telo. Chr. 16^{B}	5'-GATGGGATTTGGAAGGGTATT-3'	5'-ACTCCCTAATTAACTACAACCCATC-3'
QRT-PCR	**Fw**	**Rv**
Cdx2^{I}	5'-CCTGCGACAAGGGCTTGTTTAG-3'	5'-TCCCGACTTCCCTTCACCATAC-3'
Dnmt1	5'-TGGGCTGATGCAGGAGAAAAT-3'	5'-GCGCTTCATGGCATTCTCCTT-3'
Dnmt3a2^{S}	5'-AGGGGCTGCACCTGGCCTT-3'	5'-TCCCCCACACCAGCTCTCC-3'
Dnmt3b^{Si}	5'-TGGGATCGAGGGCCTCAAAC-3'	5'-TTCCACAGGACAAACAGCGG-3'
Esrrb^{I}	5'-CAGGCAAGGATGACAGACG-3'	5'-GAGACAGCACGAAGGACTGC-3'
GAPDH^{F}	5'-CCATCACCATCTTCCAGG-3'	5'-CCTGCTTCACCACCTTCTTG-3'
Gata4^{F}	5'-CTGTCATCTCACTATGGGCA-3'	5'-CCAAGTCCGAGCAGGAATTT-3'
Gata6^{F}	5'-TTGCTCCGGTAACAGCAGTG-3'	5'-GTGGTCGCTTGTGTAGAAGGA-3'

Klf4^{T}	5'-AGTGTGACAGGGCCTTTCCAGGT-3'	5'-AAGCTGACTTGCTGGGAACTTGAC C-3'
Nanog^{F}	5'-AGGGTCTGCTACTGAGATGCTCT G-3'	5'-CAACCACTGGTTTTTCTGCCACC G-3'
Oct4^{Si}	5'-GGCGTTCGCTTTGGAAAGGTGTT C-3'	5'-CTCGAACCACATCCTTCTCT-3'
Rex-1^{T}	5'-CACCGACAACATGAATGAACAAAA A-3'	5'-CAATCTGTCTCCACCTTCAGCATT T-3'
Sox2^{T}	5'-TAGAGCTAGACTCCGGGCGATG A-3'	5'-TTGCCTTAAACAAGACCACGAA A-3'
Lin28^{F}	5'-CGAAGCCTCAAGGAGGGTGA-3'	5'-TGCATTCCTTGGCATGATGG-3'
INSR^{So}	5'-GACTTACAGATGGTTGGGCA-3'	5'-AAGACCAACTGTCCTGCCAC-3'
IRS2^{So}	5'-TCCGCGGCTGGAGTACTACGAG-3'	5'-ACAGCAGTCGAGCGCGATCAC-3'
Tbx3^{F}	5'-TCTCCATCGTGGGGACAT-3'	5'-TTGTCGCGGCCTGGCTCCTCG-3'
Tert^{J}	5'-TTCTAGACTTGCAGGTGAACAGCC-3'	5'-TTCCTAACACGCTGGTCAAAGGG A-3'
Zfp281^{F}	5'-TGAGCCCAGGCACCCA-3'	5'-TGGAGAGGTGAAGACAAGCTGA C-3'
Bisulphite	**Fw**	**Rv**
Nanog^{T}	5'-GATTTTGTAGGTGGGATTAATTGTG AATTT-3'	5'-ACCAAAAAAACCCACACTCATATC AATATA-3'
Oct4^{Si}	5'-AGGATTTTGAAGGTTGAAAATGAA GG-3'	5'-TCCCTCCCCAATCCCACCCTC-3'

Table 1. List of oligos employed in this study. Superscripts indicate first author initial (Benetti et al., 2007; Dahl et al., 2010; Fidalgo et al., 2011; Ivanova et al., 2006; Jia et al., 2011; Sinkkonen et al., 2008; Softic et al., 2012; Takahashi and Yamanaka, 2006). Fw, forward primer; Rv, reverse primer.

Chapter 3

Results

ESCs with short telomeres show dysregulation of pluripotency genes

One of the most influential findings of the modern molecular biology era is the discovery that cells need to maintain a minimal telomere length to be able to maintain their proliferative capacity, which was established through the introduction of Tert into primary fibroblasts and their subsequent ability to completely and indefinitely bypass the Hayflick limit (Bodnar et al., 1998; Shay and Wright, 2010; Vaziri and Benchimol, 1998). Although telomerase is the primary factor responsible for telomere elongation and maintenance, other telomerase-independent lengthening mechanisms have been described both in physiological and pathological conditions (Liu et al., 2007; Royle et al., 2008b). In addition, it has also been shown that ESCs derived from late generation (G4) mice deficient for the telomerase RNA component, *Terc,* maintain a telomere length similar to the previous generation (Huang et al., 2011). Finally, another factor to be considered is that Tert may have telomere-unrelated functions that affect gene expression (Choi et al., 2008; Park et al., 2009).

This chapter aimed to test the effect of Tert deficiency and telomere shortening on ESC self-renewal and pluripotency gene expression using a wide range of biochemical and microscopy methodologies. Importantly, we took advantage of specific genetic backgrounds: parental E14 ESCs (Wt); ESCs with disrupted *Tert* gene at late passage, and then with short telomeres ($Tert^{-/-S}$); ESCs with disrupted *Tert* gene at earlier passage, and then with longer telomeres ($Tert^{-/-L}$); and eventually $Tert^{-/-S}$ ESCs where *Tert* cDNA had been re-introduced ($Tert^{-/-R}$). We hypothesized that the combination of these different genotypes would have enabled us to distinguish the impact of telomere integrity versus telomerase status on the phenotypes we queried.

3.1 Critically short telomeres lead to increased Nanog both at mRNA and protein levels

First, we decided to investigate the effect of *Tert* deficiency on self-renewal. Initially, we characterized late passage (p70) *Tert*$^{-/-}$ ESCs (*Tert*$^{-/-S}$) (Liu et al., 2000). These cells were negative for telomerase enzymatic activity (Fig. 12A) and exhibited telomere length shortening and a significant accumulation of uncapped (signal-free ends) telomeres relative to Wt cells at same passage. (Fig. 12B, p<0.0001, Fisher's exact test).

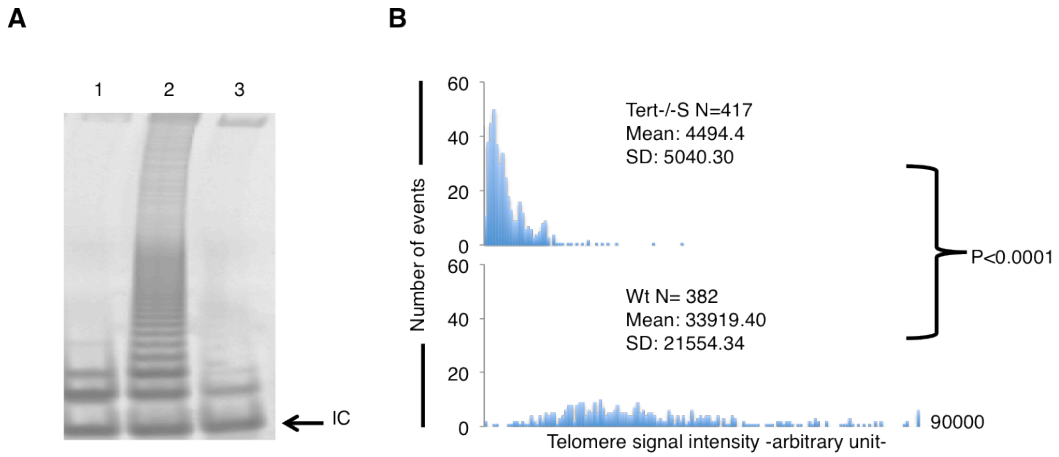

Figure 12. Characterisation of telomerase activity and telomere length in Tert-/- ESCs. A) Telomere repeat assay protocol (TRAP) performed on protein extracts (the equivalent of 5 x 10^4 cells) from *Tert*$^{-/-}$ ESCs (lane 1), Wt ESCs untreated (lane 2) or after digestion with ribonuclease A (lane 3). IC = internal PCR control. B) Q-FISH analysis of indicated genotypes; statistical significance was analysed by Welch's unpaired t-test; S = short telomeres (passage 70); The difference in the incidence of signal-free ends relative to total ends between Tert$^{-/-S}$ (49/417) and Wt (2/382) was statistically significant (p<0.00001 for each comparison, Fisher's exact test). N = number of chromosome ends; y-axis, number of events; x-axis, telomere signal intensity in arbitrary units. The experiment in panel A was performed by Dr. Laura Gardano.

Despite telomere shortening and lack of telomerase activity, *Tert*$^{-/-S}$ did not show altered cell morphology or cell cycle distribution compared to Wt ESCs (Fig. 13A, 13B)

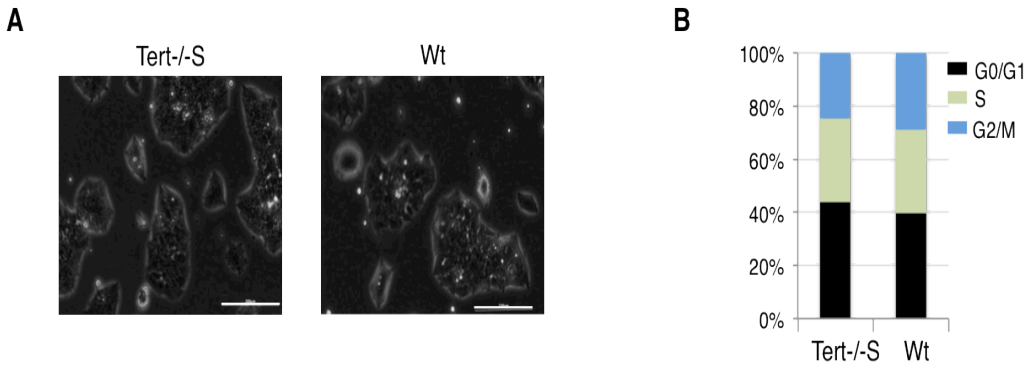

Figure 13. Characterisation of cell morphology and cell cycle distribution of Tert-/- ESCs. A) Bright field image of Wt and Tert-/-S cells. Micrograph bars indicate 200 μm. B) Cell cycle profile of the same samples as in (A).

We then investigated whether the observed telomere shortening and/or the absence of Tert might affect pluripotency gene expression. We used Q-RT-PCR to examine the mRNA levels of the pluripotency core transcriptional factors: *Nanog, Oct4 and Sox2*. Among these three genes, only *Nanog* resulted altered (an ≈ 4-fold increase) in *Tert*$^{-/-S}$ compared to Wt cells (Fig. 14).

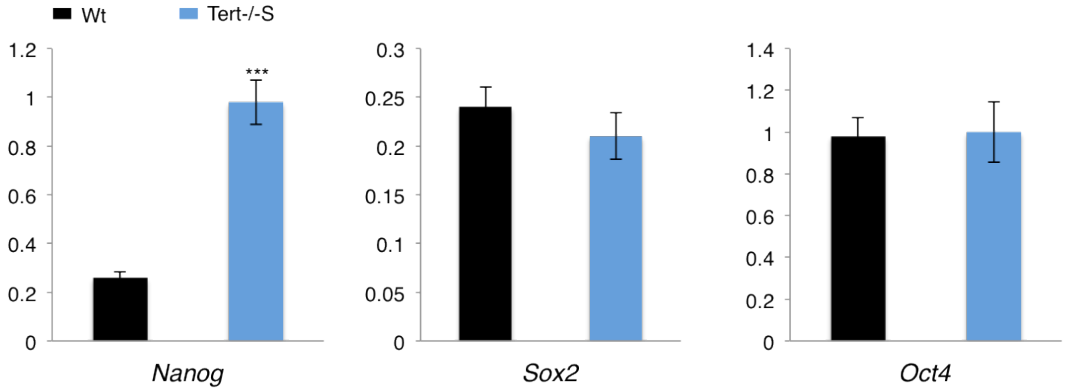

Figure 14. Relative gene expression of Wt and *Tert*$^{-/-S}$ ESCs analysed by QRT-PCR. Data are represented as mean ± SD. *** = p<0.0001. Background values (no reverse transcriptase added) were subtracted, and values were normalized to *GAPDH* (n>3). Statistical analysis was performed by unpaired t-test.

In order to confirm that the increased *Nanog* levels were Tert and/or telomere-length-dependent, we reintroduced *Tert* into *Tert*$^{-/-S}$ cells using an expression vector under the control of the CMV early enhancer/chicken β actin (CAG) promoter (Fig. 15A). Transfected cells (*Tert*$^{-/-R}$) exhibited the expected re-acquisition of telomerase enzymatic activity (Fig. 15B) and, after propagation for 4 passages in culture, also exhibited telomere lengthening and a significant reduction of uncapped telomeres (Fig. 15C, 15D).

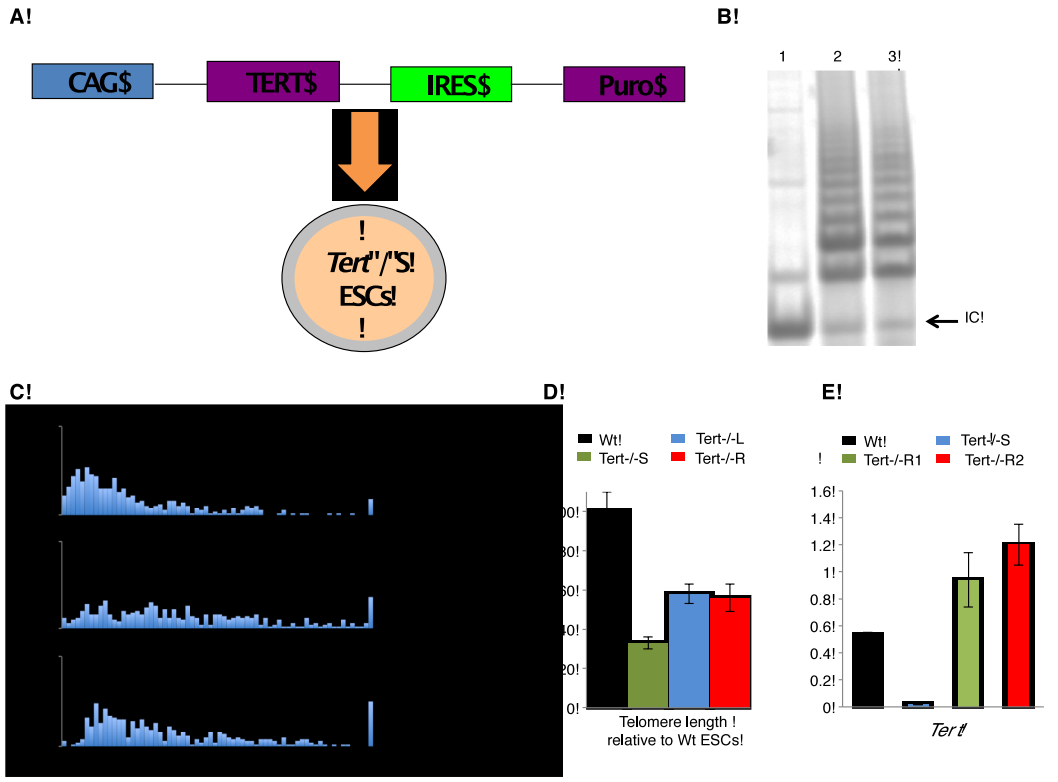

Figure 15. Effect of *Tert* reintroduction into *Tert*$^{-/-S}$ ESCs on telomere length. A) Schematic representation of *Tert* expression vector. 1 x 10^5 Tert-/-S ESCs were transfected with *Tert* expression vector or empty vector and selected for puromycin resistance. B) TRAP assay performed on protein extracts (the equivalent of 5 x 10^4 cells) from *Tert*$^{-/-R}$ ESCs after digestion with ribonuclease A (lane 1), untreated *Tert*$^{-/-R}$ ESCs (lane 2), and untreated Wt ESCs (lane 3). IC = internal PCR control. B) Q-FISH analysis of indicated genotypes; statistical significance was analysed by Welch's unpaired t-test; The difference in the incidence of signal free ends among *Tert*$^{-/-S}$ (49/417) and *Tert*$^{-/-L}$ (14/416) or *Tert*$^{-/-R}$ (4/417) was statistically significant ($p<0.00001$ for each comparison, Fisher's exact test). L = long telomeres (passage 30); S = short telomeres (passage 70); R = *Tert*-/-S cells after reintroduction of *Tert* (passage 74, including 4 passages under puromycin selection). N = number of chromosome ends; y-axis, number of events; x-axis, telomere signal intensity in arbitrary units. D) Average of mean telomere signal intensity relative to Wt. Data are represented as mean ± SD (n=3); Number of chromosomes per sample ≥ 350. E) Relative gene expression of *Tert* in Wt, *Tert*$^{-/-S}$, *Tert*$^{-/-R}$ (colony 1, indicated as *Tert*$^{-/-R1}$) and *Tert*$^{-/-R}$ (colony 2, indicated as *Tert*$^{-/-R2}$) ESCs analysed by QRT-PCR. Data are

represented as mean ± SD. Background values (no reverse transcriptase added) were subtracted, and values were normalized to *GAPDH* (n>2). The experiment in panel B was performed by Dr. Laura Gardano.

In parallel, in order to distinguish whether putative effects on *Nanog* expression in *Tert*$^{-/-R}$ cells were due to non canonical Tert activities or to telomere lengthening, we examined *Nanog* mRNA levels in *Tert*$^{-/-}$ cells at earlier passage (p28) (*Tert*$^{-/-L}$). We observed, both in *Tert*$^{-/-R}$ and in *Tert*$^{-/-L}$ a restoration of *Nanog* mRNA levels comparable to Wt ESCs (Fig. 16). This result suggested that Nanog dysregulation was telomerase-independent and determined by critically short telomeres.

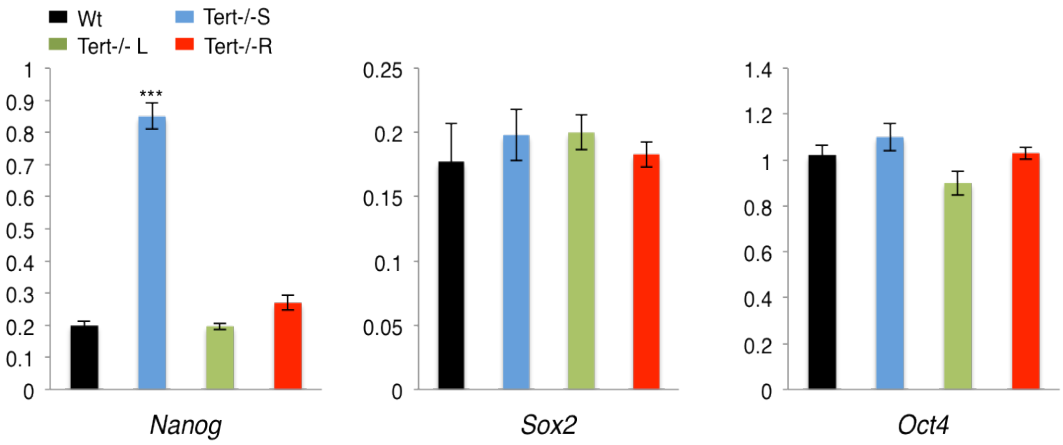

Figure 16. Relative gene expression of Wt, *Tert*$^{-/-S}$, *Tert*$^{-/-L}$ and *Tert*$^{-/-R}$ ESCs analysed by QRT-PCR. Data are represented as mean ± SD. * = p<0.005 ** = p<0.001 *** = p<0.0001. Background values (no reverse transcriptase added) were subtracted, and values were normalized to *GAPDH* (n>3). Statistical analysis was performed by ANOVA and related Dunnett's test comparing every group with Wt values.

We then tested if Nanog was altered at the protein level. The results were consistent with Q-RT-PCR, and an increase in Nanog protein levels was observed in *Tert*$^{-/-S}$ compared to *Tert*$^{-/-L}$, *Tert*$^{-/-R}$, and Wt cells (Fig. 17A, 17B). Oct4 results were also consistent with Q-RT-PCR showing no significant alteration among genotypes (Fig. 17B). Finally, *Tert*$^{-/-S}$ cells were transfected with CAG-*Tert*-IRES-*Egfp* or control vectors for 72 hours, an interval of time insufficient to elicit telomere extension, and sorted for EGFP by FACS. No difference in Nanog levels was observed between *Tert* transfected and control cells. These results further confirmed that the Nanog increase in *Tert*$^{-/-S}$ cells is independent from non-canonical Tert activities (Fig 17C).

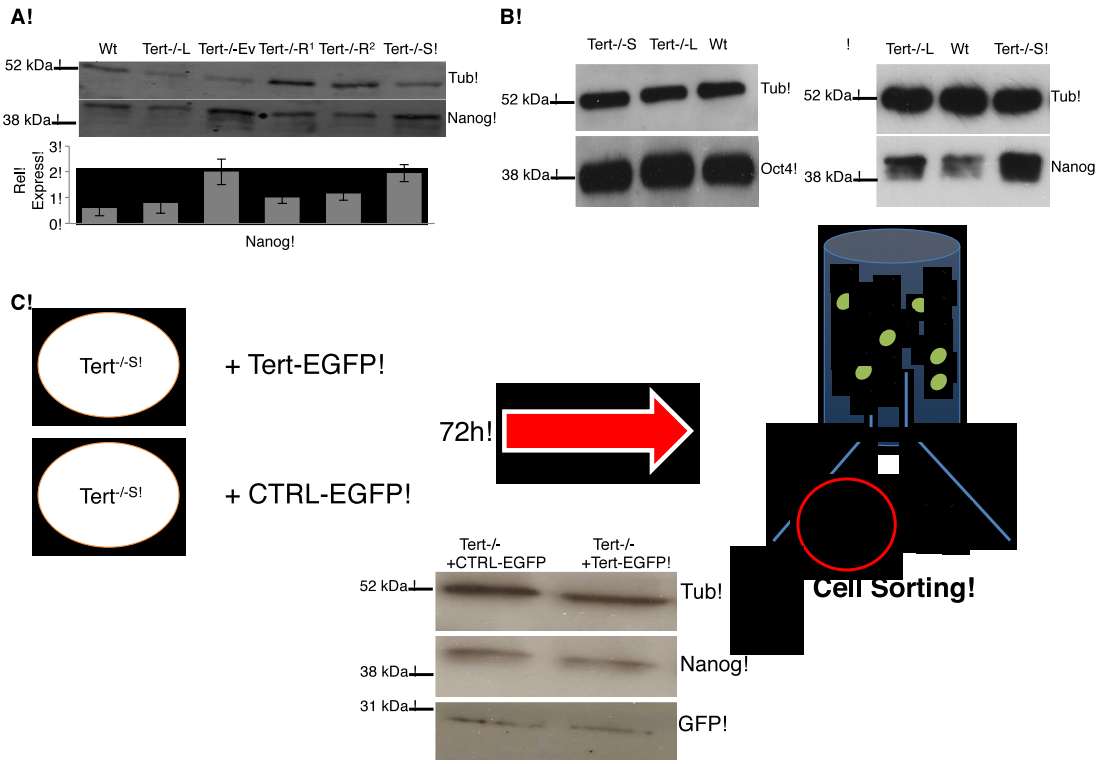

Figure 17. Effects of telomere shortening on Nanog protein expression. A) Nanog protein expression, with Li-Cor quantification (n=3). Error bar indicates SD; L = long telomeres (passage 30); S = short telomeres (passage 70); R = Tert rescue (70 passages, followed by clonal selection and a further 4 passages after *Tert* re-introduction). The numeric superscripts 1 and 2

indicate two independently generated *Tert*$^{-/-}$R colonies. EV = empty vector. B) Oct 4 and Nanog protein detection by western blot. β-Tubulin was used as an internal control (Tub). L = long telomeres (passage 70); S = short telomeres (passage 30); n=3 for Oct4 blot, n=10 for Nanog blot. C) Nanog expression in *Tert*$^{-/-S}$ ESCs 72h post-transfection with CAG-*Tert*-IRES-*EGFP* or CAG-IRES-*EGFP* vectors and cell sorting for EGFP-positive cells.

3.2 *Tert*$^{-/-}$ cells exhibit an altered Nanog-High/Nanog-Low population distribution and pluripotency gene regulation

The ability of ESCs to maintain self-renewal and respond to differentiation signals has been correlated with heterogeneity in the expression of particular pluripotency transcription factors such as Nanog. In particular, cells expressing high levels of this factor are prone to self-renew, whereas cells expressing low levels of this protein tend to differentiate (Chambers et al., 2007; Savarese et al., 2009).

To assess whether Nanog upregulation in *Tert*$^{-/-S}$ ESCs was reflected in an altered heterogeneity of protein expression, we performed FACS analysis on Wt, *Tert*$^{-/-S}$ and *Tert*$^{-/-R}$ ESCs Wt and *Tert*$^{-/-R}$ ESCs showed a lower percentage of Nanog-high expressing cells, and a higher percentage of Nanog-low expressing cells compared to *Tert*$^{-/-S}$ cells (Fig. 18).

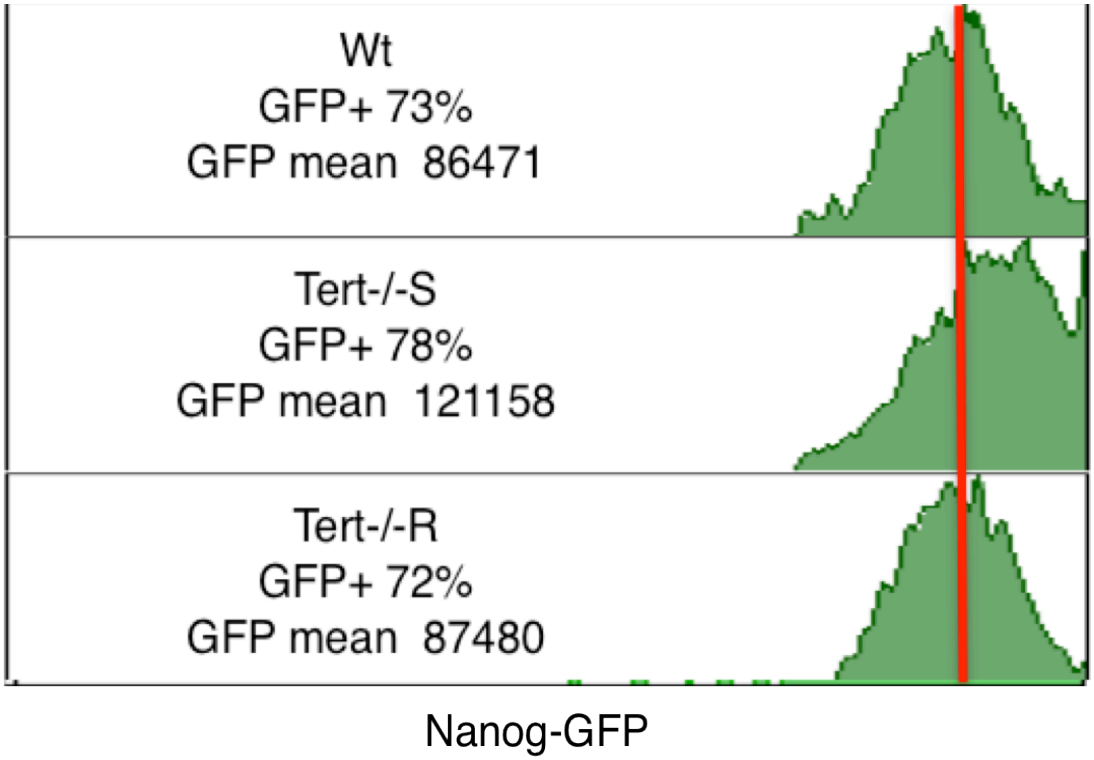

Figure 18. FACS analysis of Nanog expression in Wt, *TERT*$^{-/-S}$ and *Tert*$^{-/-R}$. Note the rightward shift and increase in average Nanog signal intensity in *Tert*$^{-/-}$S ESCs. The red line indicates the mean value of Nanog expression in Wt ESCs.

We also examined the level of expression of other genes involved in the Nanog regulatory network (*Tbx3, Esrrb and Rex1*) (Festuccia et al., 2012; Ivanova et al., 2006; Shi et al., 2006), comprising factors that have a negative impact on Nanog expression (i.e. *Zfp281)* (Fidalgo et al., 2011), and markers of lineage differentiation such as *Cdx2* and the directly negatively regulated by Nanog endoderm markers *Gata6* and *Gata4* (Singh et al., 2007). As expected, the mRNA levels of *Rex1, Esrrb and Tbx3* increased in *Tert*$^{-/-S}$ ESCs, where *Zpf281* and *Cdx2* levels remained unaltered (Fig. 16). However, the levels of *Gata6* and *Gata4* were also increased (Fig. 19).

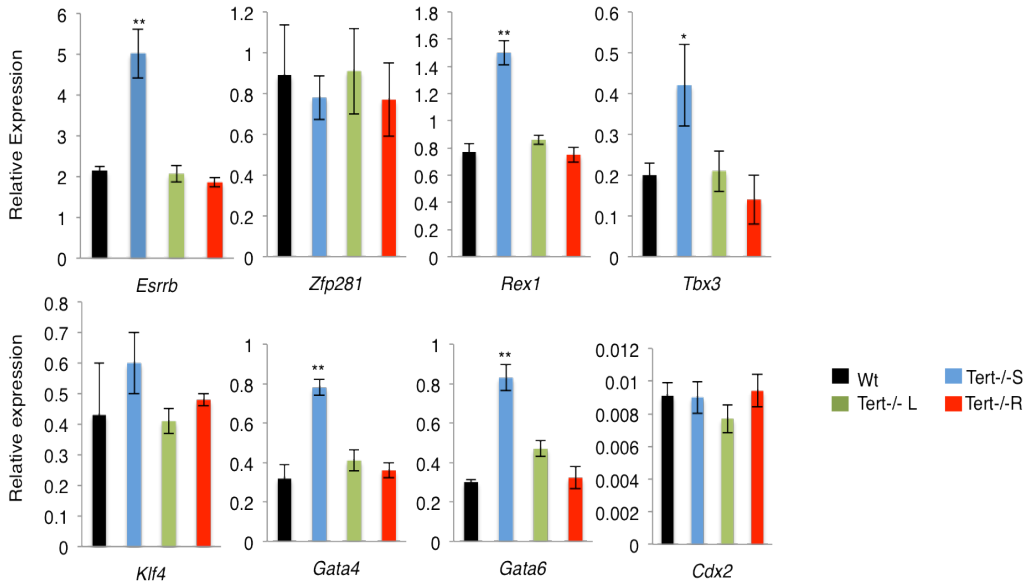

Figure 19. Relative gene expression in Wt, *Tert*$^{-/-S}$, *Tert*$^{-/-L}$ and *Tert*$^{-/-R}$ ESCs analysed by QRT-PCR. Data are represented as mean ± SD. * = p<0.005 ** = p<0.001. Background values (no reverse transcriptase added) were subtracted, and values were normalized to *GAPDH* (n>3). Statistical analysis was performed by ANOVA and related Dunnett's test comparing every group with Wt values.

3.3 *Tert*$^{-/-}$ cells show impaired Nanog repression capability

The increased expression in *Tert*$^{-/-S}$ ESCs of negatively regulated targets of Nanog induced us to investigate the capacity of Nanog to occupy specific promoters. Consistent with our previous observations, chromatin immunoprecipitation (ChIP) analysis revealed lower levels of Nanog occupancy on the *Gata6* promoter (Fig. 20). Nevertheless, Nanog recruitment on its own promoter, which represses its own expression (Fidalgo et al., 2011), increased in *Tert*$^{-/-S}$ ESCs (Fig. 20). Thus, the increased expression of *Nanog* is not the consequence of impaired occupancy of Nanog on its own promoter.

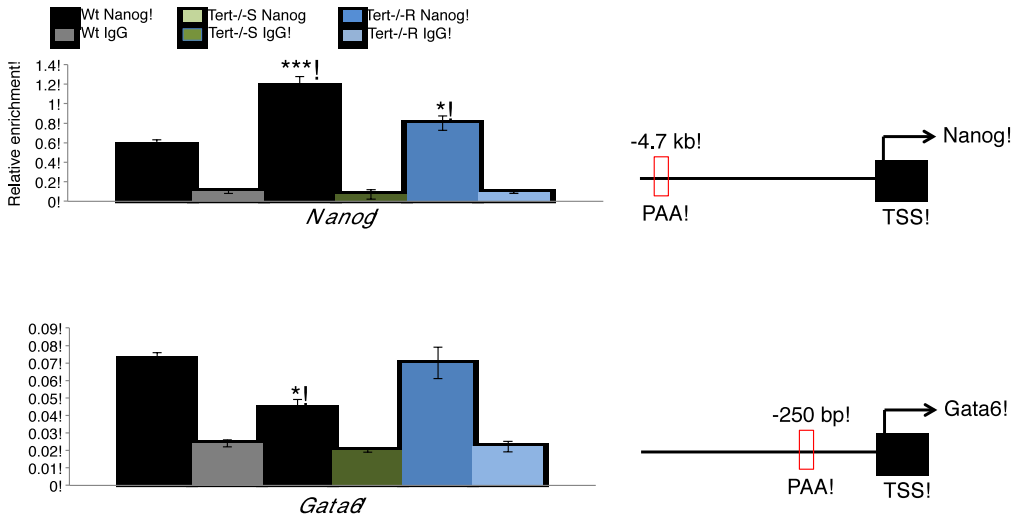

Figure 20. (Left) ChIP analysis using an antibody to Nanog in Wt, Tert-/-S and Tert-/-R cells. Relative enrichment was quantified using region specific qPCR primers for Nanog (top) and Gata6 (bottom) promoters. Generic IgG was used as a control (n=3). Statistical analysis was performed by ANOVA and related Dunnett's test comparing every group with Wt values Error bars indicate SD. * = p<0.05; *** = p<0.0001. (Right) Map of DNA region amplified by QRTPCR after chromatin immunoprecipitation. The red box indicates the position of primer annealing region (PAA) relative to the transcriptional starting site (TSS).

3.4 Summary of chapter 3

In this chapter we characterized *Tert* deficient ESCs with short telomeres for cell cycle distribution, cell morphology and pluripotency gene expression. We found that, although *Tert*$^{-/-S}$ cells maintained similar morphological characteristics and and a cell cycle profile comparable to Wt ESCs, they presented altered expression of genes

involved both in pluripotency (e.g. *Nanog*, *Esrrb,* etc.) and differentiation (e.g. *Gata6,* etc.). We showed that *Tert*$^{-/-S}$ ESCs possess an increased population of Nanog-high cells, and that, in these cells, Nanog repression capability seems to be impaired. Finally, we confirmed that the above-mentioned effects are due to critically short telomeres and are not dictated by telomerase expression alone.

Chapter 4

Results

Tert$^{-/-S}$ ESCs display epigenetic alterations at telomere proximal and distal *loci*

The results in chapter 3 led us to investigate whether epigenetic, transcriptionally active and repressive marks (i.e. H3K4me3 and H3K27me3) were also affected by telomere shortening. It has been reported that telomere shortening may induce loss of heterochromatin marks and DNA methylation at subtelomeric regions (Benetti et al., 2007). In addition, it is known that low levels of trimethylation on H3K27me3 lead to increase number of Nanog-high expressing cells, as well as to promote *Gata6* expression (Lu et al., 2011; Shen et al., 2008; Villasante et al., 2011). Thereby, using western blot and ChIP, we investigated these aspects of epigenetic regulation in *Tert*$^{-/-S}$ cells.

4.1 Alteration of histone marks in *Tert*$^{-/-S}$ cells

First, we decided to analyse the enrichment of "open" chromatin marks at subtelomeric regions. Subtelomeric regions are segments of DNA placed just before telomeres. They are characterized by repetitive sequences of DNA, mostly (TTAGGG)-like sequences, and tend to be heavily heterochromatic (Gonzalo et al., 2006b). We focused on the subtelomeric region of the q arm of the chromosome 16, since it has been reported that this region is widely heterochromatic in physiological conditions and that telomere shortening leads to an increased enrichment of acetyl-histone 4 (acH4) and acetyl-histone-3-lysine 9 (acH3K9) on it (Benetti et al., 2007; Gonzalo et al., 2006b). As expected, we found a higher enrichment of these epigenetic marks in the in *Tert*$^{-/-S}$ cells compared to *Tert*$^{-/-R}$ and Wt ESCs (Fig. 21). These results confirmed the hypothesis that chromatin conformation at region proximal to telomeres is affected by telomere length.

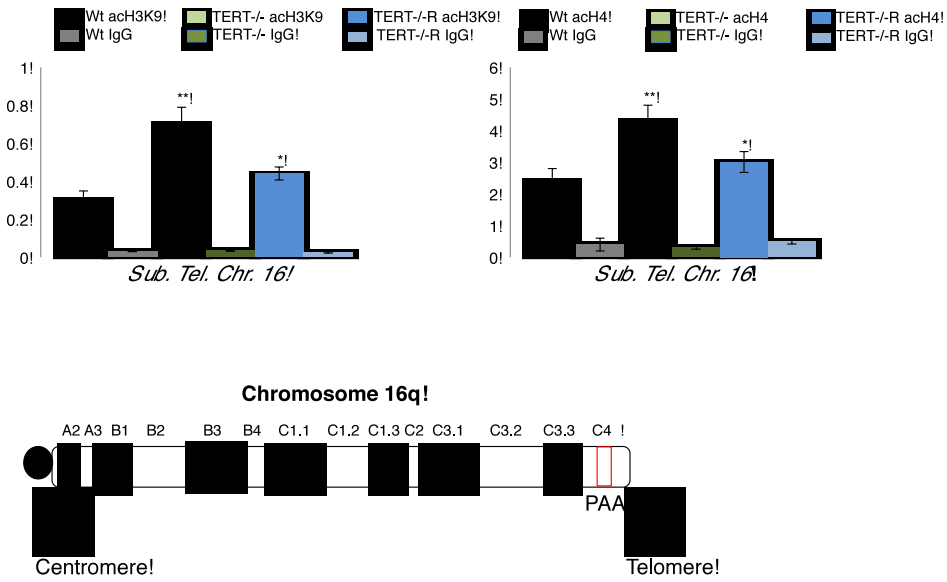

Figure 21. (Top) ChIP analysis using antibodies to acetyl H3K9 (left) and acetyl H4 (right) in Wt, *Tert*$^{-/-S}$ and *Tert*$^{-/-R}$ ESCs. Relative enrichment was quantified using region specific qPCR primers for chromosome 16, subtelomeric region. Generic IgG was used as a control (n=3). Statistical analysis was performed by ANOVA and related Dunnett's test comparing every group with Wt values Error bars indicate SD. * = p<0.05; ** = p<0.01. (Bottom) Map of DNA region amplified by QRTPCR after chromatin immunoprecipitation. The red box indicates the position of primer annealing region (PAA) relative to the *loci* on chromosome 16q.

We then aimed to investigate whether chromatin conformation at telomere distal *loci* was also perturbed by critically short telomeres. For that purpose, we tested the levels of H3K4me3 for *Nanog* and *Oct4* promoters and H3K27me3 for the promoter regions of *Nanog, Oct4 and Gata6*. We observed that, although the total level of H3K27me3 is slightly higher in *Tert* null cells, its enrichment on both *Gata6* and *Nanog* promoters is lower compared to Wt and *Tert* rescue cells (Fig. 22A, 22D). We

could not detect H3K27me3 enrichment on the *Oct4* promoter (Fig. 22A). H3K4me3 levels were unaffected by telomere shortening in both *loci* (Fig 22B). These data implied that telomere length could affect chromatin conformation also at loci distal to telomeres.

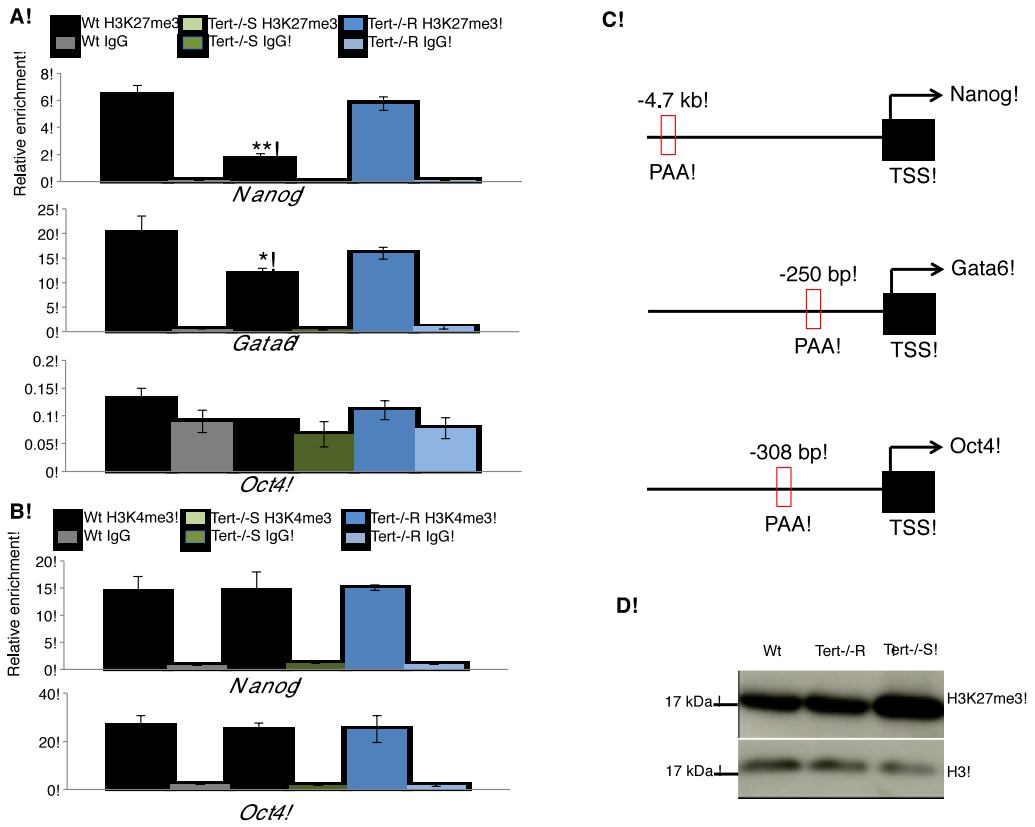

Figure 22. ChIP analysis using antibodies to acetyl H3K4me3 and H3K27me3. A) H3K27me3 relative enrichment on *Nanog*, *Gata6* and *Oct4* promoters in Wt, *Tert*$^{-/-S}$ and *Tert*$^{-/-R}$ ESCs. B) H3K4me3 relative enrichment on *Nanog* and *Oct4* promoters in Wt, *Tert*$^{-/-S}$ and *Tert*$^{-/-R}$ ESCs. Generic IgG was used as a control (n=3). Statistical analysis was performed by ANOVA and related Dunnett's test comparing every group with Wt values Error bars indicate SD. ** = p<0.01. C) Map of DNA region amplified by QRTPCR after chromatin immunoprecipitation. The red box indicates the position of primer annealing region (PAA) relative to the transcriptional starting site (TSS). D) Detection of H3K27me3 and total histone H3 (as a control) by western blot (n=3).

It is known that chromatin conformation may affect chromosome localization (Dostie and Bickmore, 2012). Considering the alteration in the enrichment of chromatin marks in ESCs with short telomeres, we decided to investigate whether this could lead to a re-localization of chromosomes into the nucleus. In order to address this question, we performed a FISH-based 3D analysis of cell nuclei. We then analysed

chromatin distribution (assessed by DAPI intensity) and telomere distribution (assessed Cy3 telomeric probe) of Wt and Tert ESCs with long or short telomeres (Fig. 23). However, we did not observe any difference in either chromatin or telomere distribution among genotypes.

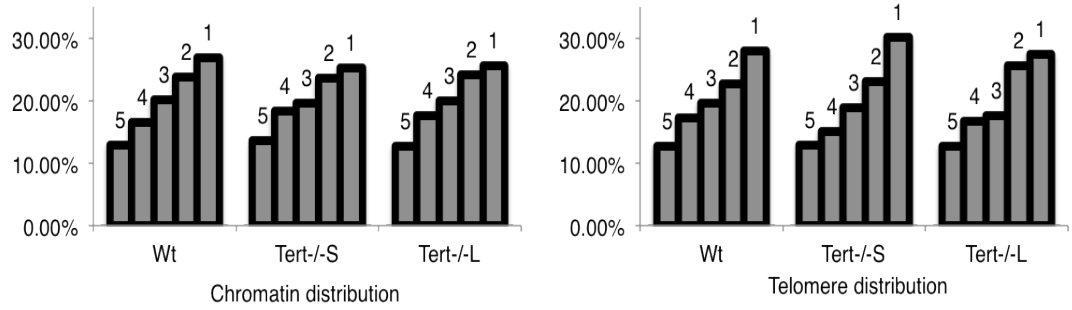

Figure 23. 3D-analysis of cell nuclei. DAPI and Cy3 telomeric probe FISH-stained nuclear images were analysed for chromatin and telomere distribution using a macro described in (Korfali et al., 2010), which divided the nuclear area in 5 equal concentric zones, where 1 is the inner one and 5 the most peripheral zone. Y-axis indicates the percentage of signal in each zone.

4.2 Telomere shortening leads to DNA hypomethylation induced by *de novo* DNA methyltransferase downregulation

Given the long-range effects of short telomeres on gene expression and histone post-translation modifications, we analysed whether DNA methylation was also affected in cells with critically short telomeres. As a starting point, since is known that telomere length can affect DNA methylation at subtelomeric regions (Benetti et al., 2007) we used ChiP to examine the enrichment of methyl-cytosine at subtelomeric regions of chromosome 16. Accordingly to what was previously described, we found

a loss of DNA methylation in ESCs with short telomeres (Fig. 24A) (Benetti et al., 2007). We next asked whether *Tert*$^{-/-S}$ ESCs might also possess an altered global genomic DNA methylation profile. Contrary to other cell types, ESCs can tolerate severe hypomethylation and retain proliferative capacity, although it leads to impaired differentiation and differentiation maintenance capability (Feldman et al., 2006; Jackson et al., 2004; Sinkkonen et al., 2008; Tsumura et al., 2006). We performed an ELISA-based assay to obtain a relative quantification of genomic DNA of Wt, *Tert*$^{-/-S}$ and rescue ESCs. We observed a significant decrease in DNA methylation in *Tert*$^{-/-S}$ cells compared to Wt (approximately 70%) and *Tert*$^{-/-R}$ cells (approximately 50%), (Fig. 24B). This result suggested that telomere length has an impact not only on subtelomeric methylation, but also upon global DNA methylation.

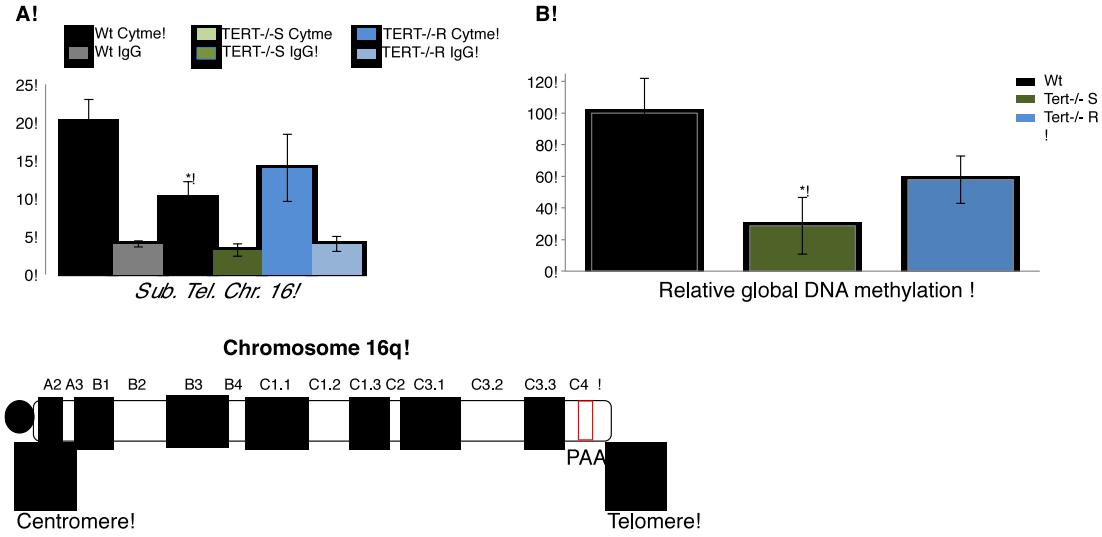

Figure 24. DNA methylation analysis in Wt, *Tert*$^{-/-S}$ and *Tert*$^{-/-R}$ ESCs. A) (Top) Methyl cytosine (Cytme) relative enrichment, analysed by ChIP, on chromosome 16 subtelomeric region. Relative enrichment on *Nanog*, *Gata6* and *Oct4* promoters. Generic IgG was used as a control (n=3). Statistical analysis was performed by ANOVA and related Dunnett's test comparing every group with Wt values. (Bottom) Map of DNA region amplified by QRTPCR after chromatin immunoprecipitation. The red box indicates the position of primer annealing region (PAA) relative to the *loci* of chromosome 16q. B) Relative quantification of global DNA methylation (n=3). Analysis performed by an ELISA-based assay for methyl cytosine. Error bars indicate SD. * = p<0.05

One possible mechanism for the observed DNA hypomethylation in *Tert*$^{-/-S}$ cells might be an alteration in the expression of enzymes responsible for CpG methylation. In mammals, genomic DNA methylation is principally regulated by three CpG DNA methyl transferases (Dnmts): Dnmt1 (responsible for DNA

methylation maintenance), and the *de novo* methyl transferases Dnmt3a and Dnmt3b (Li et al., 1992; Okano et al., 1999; Tsumura et al., 2006). We therefore tested Wt, *Tert*$^{-/-S}$ and *Tert*$^{-/-R}$ ESCs for altered expression of Dnmts. We did not notice any difference in Dnmt1 expression among the different cell lines (Fig. 25A). However, we observed a strongly reduced expression of the *de novo* Dnmt3a2 (predominant isoform in ESCs) and Dnmt3b both at RNA and protein level in *Tert*$^{-/-S}$ cells compared to Wt and Tert-rescued cells (Fig. 25A, 25B).

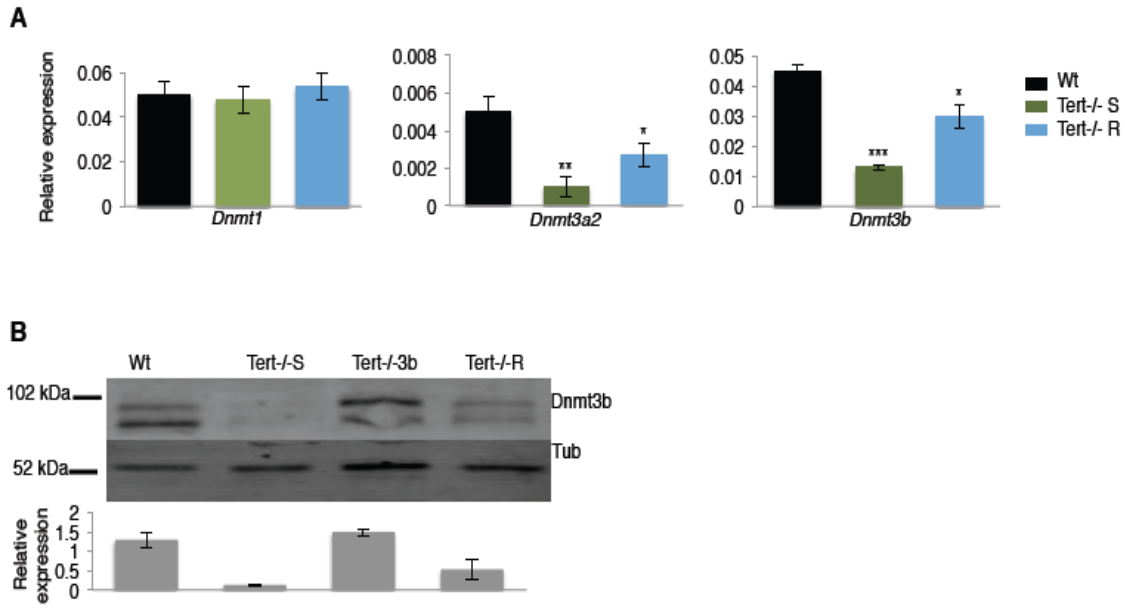

Figure 25. Dnmt expression analysis in Wt, *Tert*$^{-/-S}$ and *Tert*$^{-/-R}$. A) Relative gene expression of *Dnmt1*, *Dnmt3b* and *Dnmt3a2* analysed by QRT-PCR. Values were normalized to *GAPDH* (n=4). Error bars indicate SD. Statistical analysis was performed by ANOVA and related Dunnett's test comparing every group with Wt values. * = p<0.05, ** = p<0.01, *** = p<0.0001. B) (Top) Dnmt3b protein detection by western blot and (bottom) following Li-Cor quantification (n=3). Lane 3 indicates *Tert*$^{-/-S}$ ESCs transfected with Dnmt3b and propagated for 60 days (see chapter 4.3). Error bars indicate SD.

4.3 Enforced expression of *Dnmt3b* in *Tert*$^{-/-S}$ cells restores Nanog to levels comparable to Wt ESCs

While the decreased levels of Dnmt3a and 3b in *Tert* null ESCs could explain the mechanism for DNA hypomethylation in ESCs with short telomeres, these perturbations may also be the indirect result of changes in gene expression induced by critically short telomeres. To distinguish between these possibilities, we tested whether the enforced re-expression of Dnmt3b was sufficient to elicit a change in global DNA methylation or H3K27 enrichment at the *Nanog* promoter. It is in fact been shown how severe DNA hypomethylation may lead to redistribution of H3K27me3, with an increase on usually methylated DNA regions and a decrease on typically unmethylated ones (e. g. pluripotency gene promoters) (Brinkman et al., 2012). We selected for ESCs that expressed the Dnmt3b cDNA under the CAG promoter in *Tert* null ESCs (*Tert*$^{-/-3b}$) (Fig. 25B). Dnmt3b detection by western blot results in two bands of the approximate molecular weight of 100 kDa (the expected migration size of Dnmt3b). This may suggest the detection, by the antibody, of an unspecific band. However, although it is not possible to completely exclude this theory without further experiments (i.e. to add a peptide tag to the protein), the fact that exogenous expression of *Dnmt3b* cDNA leads to an increase of both bands seems to dismiss this hypothesis. The *Dnmt3b* cDNA exogenous expression rather suggests a situation where either A) Dnmt3b undergoes post-transcriptional modifications detectable by western blot, or B) the two bands belong to two isoforms and the exogenous expression of *Dnmt3b* cDNA positively modulates the expression

of the endogenous gene, or the stability of the endogenous isoforms, resulting in an increased expression of both these isoforms.

After 60 days post transfection, ESCs with critically short telomeres that expressed Dnmt3b comparable to Wt ESCs exhibited a partial restoration of global DNA methylation and H3K27 enrichment on Nanog promoter and reduced the level of Nanog expression closer to Wt (Fig. 26A, 26B, 26C). Therefore, it appears that reduced Dnmt3b expression (possibly in cooperation with Dnmt3a or Dnmt3L—see Discussion on session 7.2) is directly linked to the defect in DNA methylation observed in *Tert* null ESCs with short telomeres.

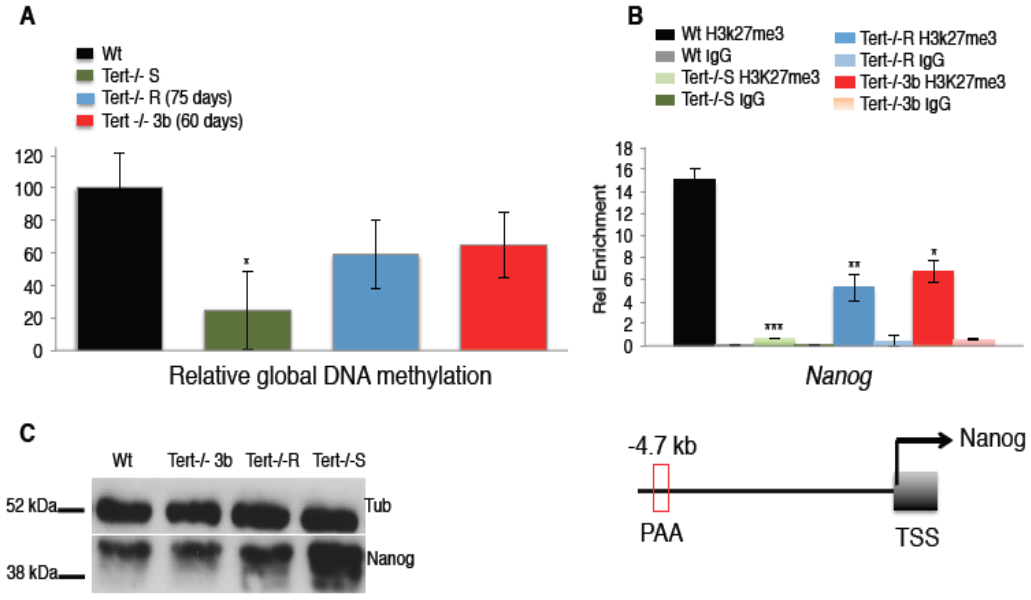

Figure 26. Effects of enforced Dnmt3b expression in *Tert*$^{-/-S}$ ESCs on global methylation and *Nanog* expression. A) Relative quantification of global DNA methylation (n=3). Analysis

performed by an ELISA-based assay for methyl cytosine. B) (Top) H3K27me3 relative enrichment in Wt, *Tert*$^{-/-S}$, *Tert*$^{-/-R}$ and *Tert*$^{-/-3b}$, analysed by ChIP, on Nanog promoter region. Generic IgG was used as a control (n=3). Statistical analysis was performed by ANOVA and related Dunnett's test comparing every group with Wt values. (Bottom) Map of DNA region amplified by QRTPCR after chromatin immunoprecipitation. The red box indicates the position of primer annealing region (PAA) relative to the transcription starting site (TSS). C) Detection of Nanog and tubulin (as a control) by western blot (n=3). Error bars indicate SD. * = p<0.05, * *= p<0.01, *** = p<0.0001

4.4 Summary of chapter 4

In this chapter we assessed the epigenetic regulation of DNA methylation and histone post-translational modification in *Tert* null ESCs with critically short telomeres. We found, as already reported, a gain of open chromatin marks (e.g. acH4, etc.) and a loss of DNA methylation at subtelomeric regions (Benetti et al., 2007). Interestingly though, we also found epigenetic alteration at *loci* distant form telomeres in *Tert*$^{-/-S}$ cells. We found that in ESCs with critically short telomeres, despite a global H3K27me3 increase, the promoter regions of *Nanog* and *Gata6* exhibited a reduced enrichment of this transcriptional repressive mark. Finally, we revealed how DNA hypomethylation is not confined to subtelomeric regions, but affects the whole genome. These effects were ameliorated via the restoration of Dnmt3b expression in *Tert* null ESCs with short telomeres. Altogether these results indicate that telomere shortening can affect chromatin conformation even at *loci* distant from telomeres.

Chapter 5

Results

Delayed and metastable differentiation of ESCs with critically short telomeres

Our observations that ESCs with short telomeres exhibited an increased proportion of Nanog-high cells, a displacement of chromatin repressive marks, and a decrease in *de novo* Dnmt expression led us to speculate that differentiation could be affected stem cells with critically short telomeres. In this chapter, we tested the kinetics and stability of lineage commitment and differentiation in *Tert*$^{-/-S}$ ESCs compared to Wt ESCs and *Tert*$^{-/-S}$ ESCs in which *Tert* or *Dnmt3b* were ectopically expressed.

5.1 Delayed response to ATRA treatment and re-gain of pluripotency after LIF

To test if pluripotency gene dysregulation in *Tert*$^{-/-S}$ ESCs affected the response to differentiation signals, we treated Wt, *Tert*$^{-/-S}$ and *Tert*$^{-/-R}$ ESCs with 5 μM all-trans retinoic acid (ATRA) for 6 days in a LIF-free media, followed by removal of ATRA and re-addition of LIF to the media. Contrary to Wt and *Tert*$^{-/-R}$ ESCs, after ATRA removal *Tert*$^{-/-S}$ ESCs exhibited a delayed acquisition of properties consistent with a differentiated state, and were prone to reacquire a stem cell-like morphology when cultured again in media containing LIF (Fig. 27).

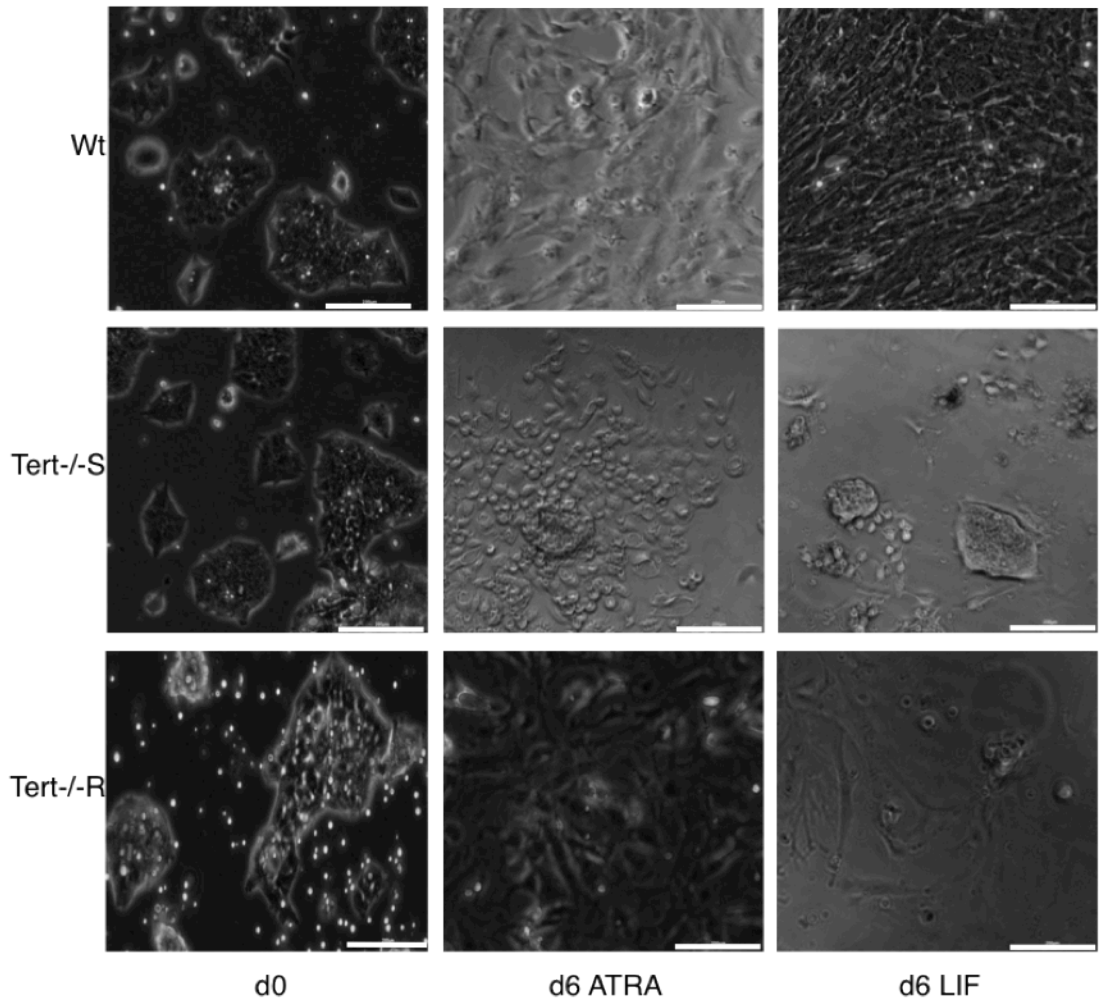

Figure 27. Bright field images of Wt, *TERT*$^{-/-S}$ and *TERT*$^{-/-R}$ ESC populations at day 0 and 6 in media containing 5 μ M all-trans retinoic acid (ATRA) and, following ATRA removal, a further 6 days in LIF-containing media. Micrograph bar indicates 200 μ m.

Differentiated cells cannot spontaneously de-differentiate by simple addition of LIF, and 6 days of 5μM ATRA treatment have been shown to be sufficient to irreversibly differentiate ESCs (Sinkkonen et al., 2008; Takahashi and Yamanaka, 2006). Consistently with literature, Wt ESCs treated for 6 days with ATRA, and re-placed for additional 6 days in LIF-containing medium, maintained repression of pluripotency genes (i.e. Nanog). In contrast, immunofluorescence and western blot

analysis revealed that *Tert*$^{-/-S}$ cells were unable to sustain Nanog repression when LIF was re-added to the media after ATRA treatment (Fig. 28).

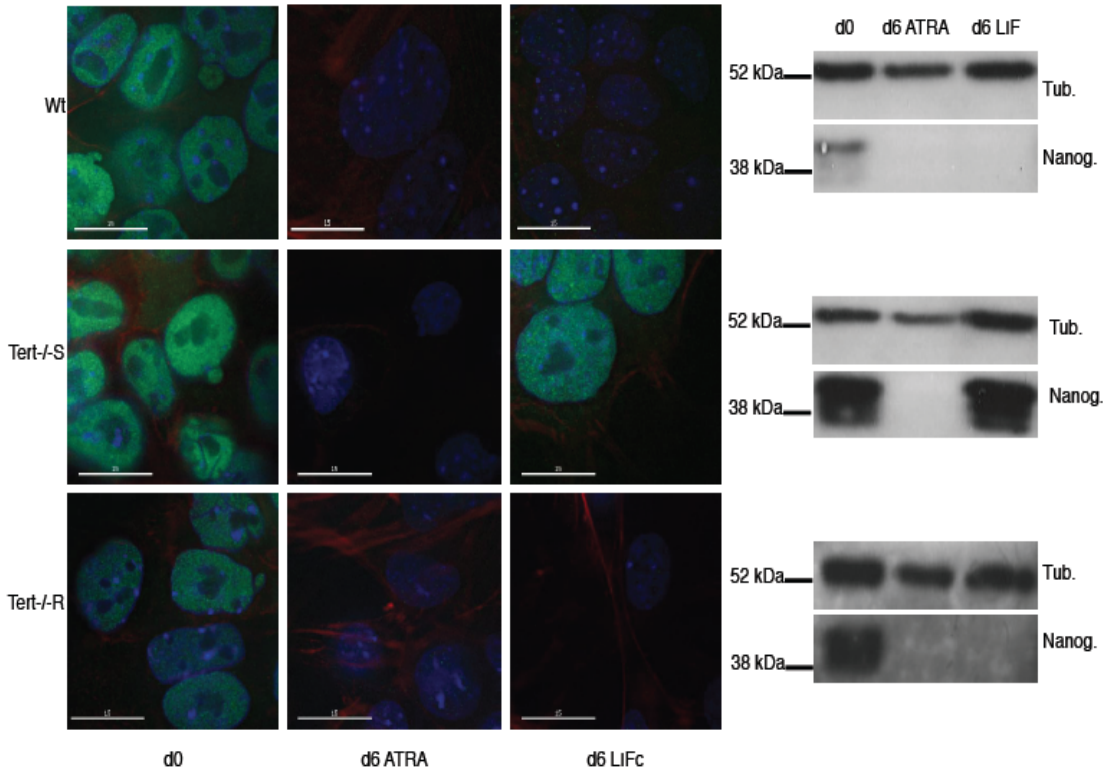

Figure 28. Nanog detection in Wt, *Tert*$^{-/-S}$ and *Tert*$^{-/-R}$ ESCs treated for 6 days with all trans retinoic acid and for 6 days with LIF. (Left), Nanog immunofluorescence analysis (green = Nanog; Red = Actin). (Right), Nanog protein detection by western blot. Tub= β -tubulin (n=3).

We asked whether the impaired differentiation of *Tert*$^{-/-S}$ ESCs might be due to inadequate downregulation of transcriptional factors involved in the maintenance of pluripotency and self-renewal. QRT-PCR analysis revealed that *Nanog*, *Oct4* and *Sox2* mRNA levels were elevated in *Tert*$^{-/-S}$ ESCs compared to Wt and *Tert* rescue cells after ATRA treatment, and were further up-regulated upon re-addition of LIF (Fig. 30). Perhaps not surprisingly, mRNA expression was a more sensitive read-out of the stability of the differentiated state, since Nanog protein levels were

undetectable after ATRA treatment (Fig 25A, 25B). These results suggest that short telomere ESCs were able to execute only an incomplete, transitory repression of pluripotency genes under differentiation conditions.

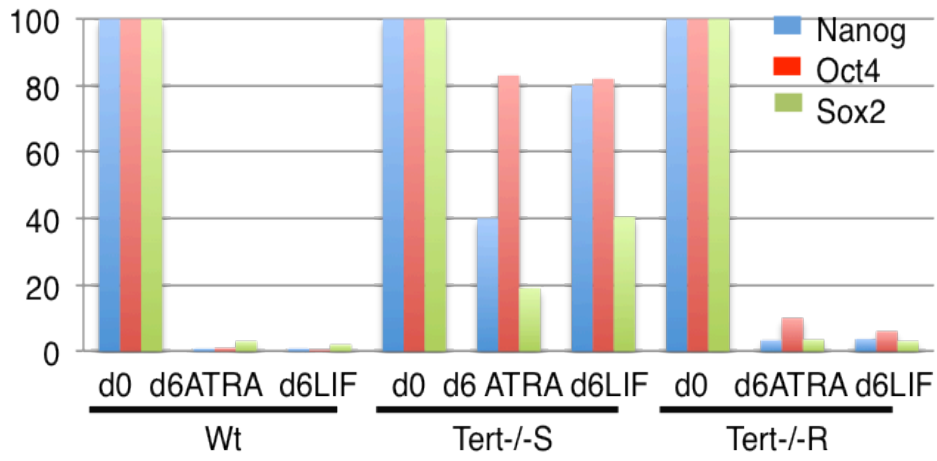

Figure 30. QRT-PCR analysis of pluripotency genes after ATRA-induced differentiation. Gene expression at day 0 was arbitrarily set as 100 and the expression through the time course was normalized to mRNA levels at day 0. Values were expressed as a ratio to *GAPDH*. N=3.

Next, we performed a single colony formation assay to assess the percentage of cells that were able to form ES colonies when cultured in LIF-containing media after ATRA treatment. As expected, no ES colony was observed in Wt and *Tert*$^{-/-L}$ ESCs after ATRA removal and LIF re-addition, which indicates the population had become differentiated (Fig. 31). However, Tert null ESCs with short telomeres exhibited a significant colony growth potential after 12 days in LIF-containing media (Fig. 31). This phenotype was rescued upon telomere elongation after re-introduction of *Tert*, which suggests that critically short telomeres impeded the ability of cells to remain differentiated after ATRA treatment (Fig. 31).

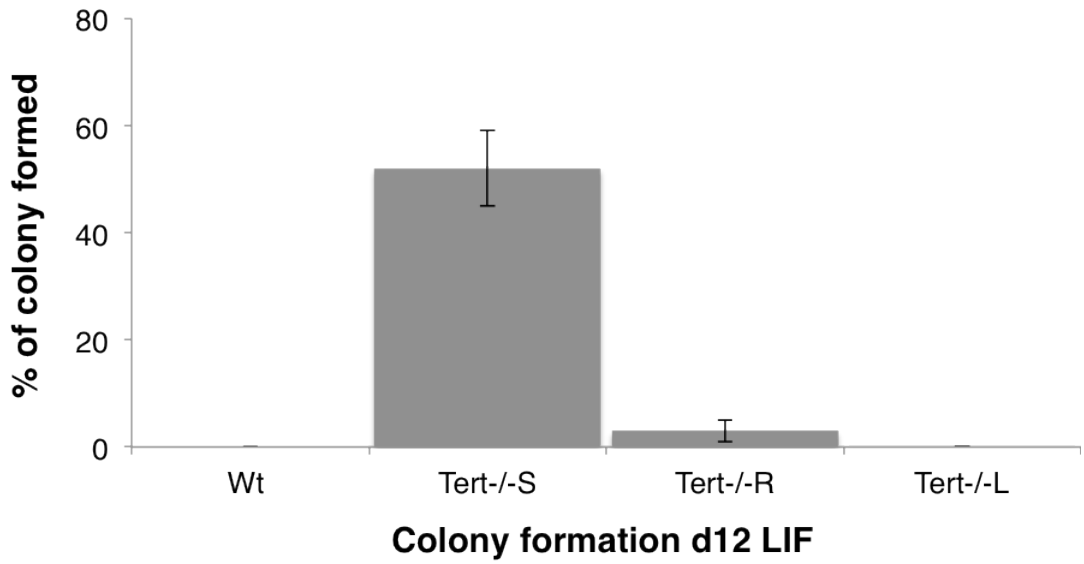

Figure 31. Single colony formation assay after ATRA treatment (6 days) and LIF-containing media (6 days) (n=3). A set of serial dilutions was performed and the percentage (n≥300) of viable ES cell colonies assessed with alkaline phosphatase assay. The difference in the incidence of colony formation between *Tert*$^{-/-S}$ and all the other genotypes was statistically significant ($p<0.0001$; ANOVA and related Dunnett's test comparing every group with *Tert*$^{-/-S}$ values). Error bars indicate SD. N=3. Wt= Wild type (parental ESC population); Tert-/-S = Tert deficient ESCs with short telomeres; Tert-/-R = Tert deficient ESCs with short telomeres, where *Tert* cDNA has been reintroduced; Tert-/-L = Tert deficient ESCs with long telomeres.

We further confirmed the link between telomere length and ability to maintain stable differentiation by testing the response to ATRA, and subsequent LIF re-addition, on *Tert*$^{-/-}$ ESCs with long telomeres. *Tert*$^{-/-L}$ cells were able to maintain suppression of pluripotency genes, and were unable to form ES colonies after ATRA treatment and LIF re-addition (Fig. 32A, 32B).

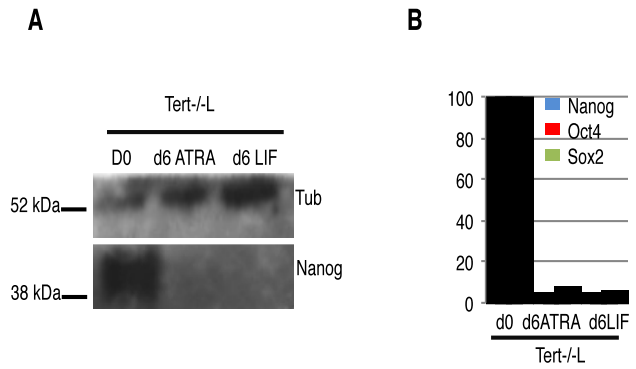

Figure 32. The response of *Tert*$^{-/-L}$ ESCs to ATRA and subsequent LIF treatment. A) Nanog protein detection by western blot. Tub= β -tubulin (n=3). B) QRT-PCR analysis of pluripotency genes after ATRA-induced differentiation. Gene expression at day 0 was arbitrarily set as 100 and the expression through the time course was normalized to mRNA levels at day 0. Values were expressed as a ratio to *GAPDH*.

We took into consideration the possibility that telomere deficiency and the existence of short telomeres might select against development of differentiation events, and thus inhibit the appearance of differentiated cells. To further examine this point, we performed a longer time course of ATRA treatment (Fig. 33). Indeed, *Tert*$^{-/-S}$ ESCs require a longer time to suppress pluripotency gene transcription.

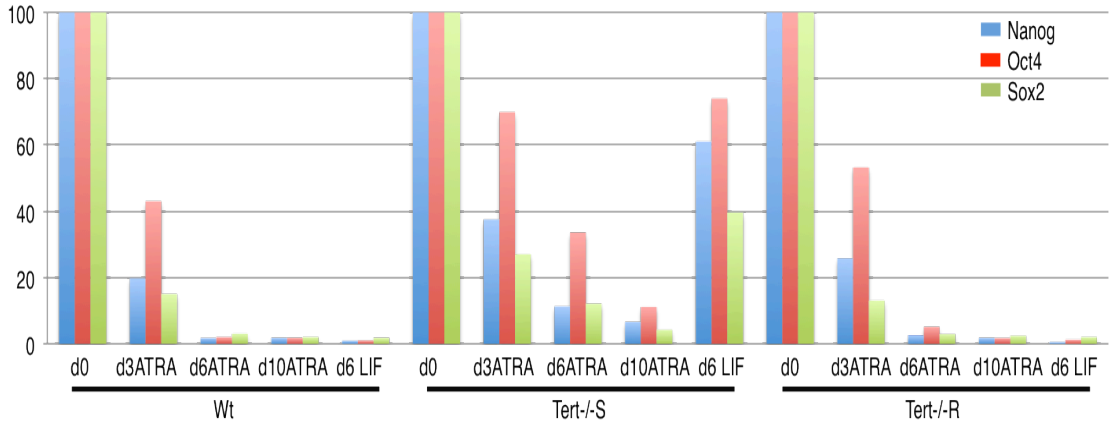

Figure 33. QRT-PCR analysis of pluripotency genes after ATRA-induced differentiation. Gene expression at day 0 was arbitrarily set as 100 and the expression through the time course was normalized to mRNA levels at day 0. Values were expressed as a ratio to *GAPDH*.

To assess to what extent ATRA-treated cells were able to support colony formation (without re-addition of LIF-containing media), we plated *Tert*$^{-/-S}$ ESCs after 6 days of ATRA treatment followed by 6 days in LIF-free media, and observed a very reduced colony formation capacity, compared with cells growth in LIF-containing media (Fig. 34).

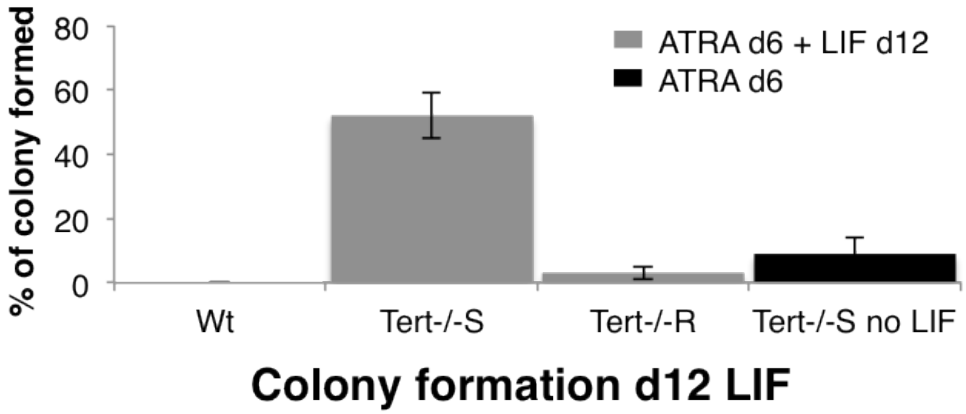

Figure 34. Single colony formation assay after ATRA treatment (6 days) and, where indicated, of LIF-containing media (6 days) (n=3). A set of serial dilutions was performed and the percentage (n≥300) of viable ES cell colonies assessed with alkaline phosphatase assay. The difference in the incidence of colony formation between *Tert*$^{-/-S}$ (after LIF re-addition) and all the other genotypes (and *Tert*$^{-/-S}$ without LIF re-addition) was statistically significant ($p<0.0001$; ANOVA and related Dunnett's test comparing every group with *Tert*$^{-/-S}$ values). Error bars indicate SD. N=3.

We sought to independently verify this result by transducing lentiviral particles containing *GFP* under control of the *Oct4* promoter into *Tert*$^{-/-S}$ and Wt cells. After selection, cells were treated with ATRA for 12 days and then sorted for GFP-negative cells by FACS. GFP-negative cells (after sorting) were re-plated in LIF-containing media and analysed again for GFP expression (by microscopic analysis) 10 days later. The results showed clearly that, apart from a small percentage, *Tert*$^{-/-S}$ cells were competent to suppress GFP after ATRA treatment. However, they also showed that GFP-negative selected *Tert*$^{-/-S}$ cells were able to reacquire significant levels of GFP expression after cultured in LIF-containing media and thus could not stably maintain differentiation (Fig. 35).

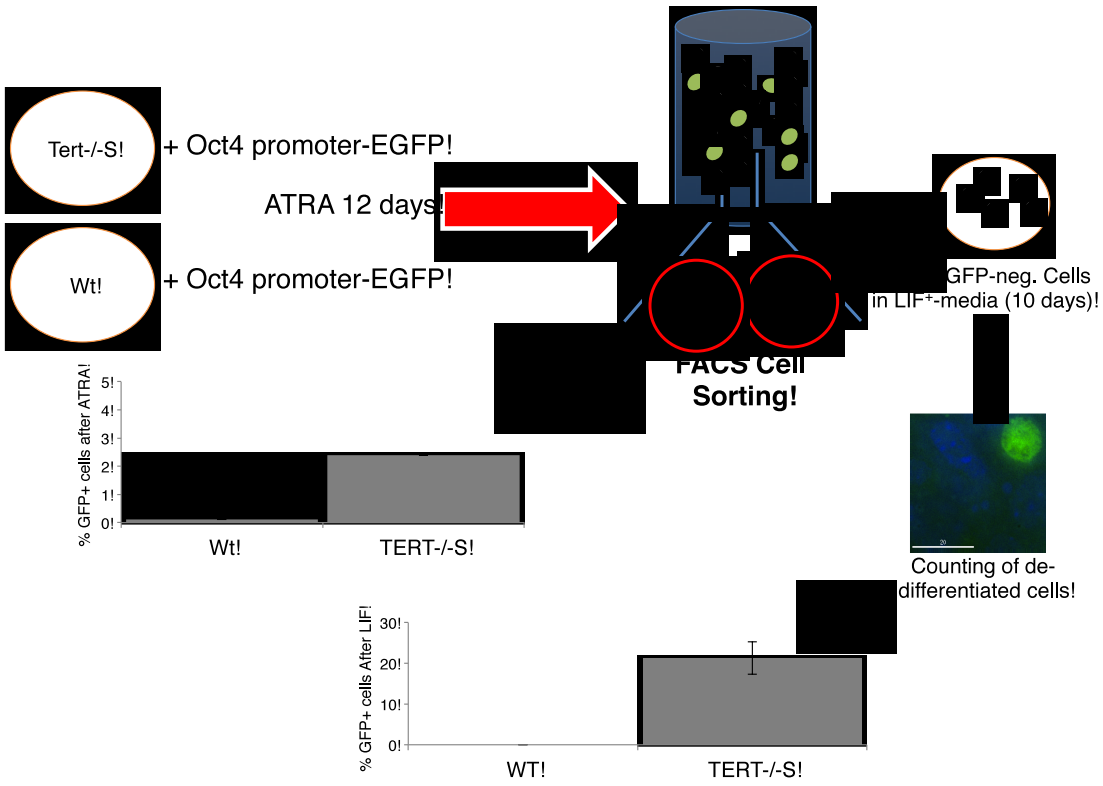

Figure 35. Oct4-promoter-driven GFP expression analysis of Wt and Tert−/−S ESCs post-ATRA treatment and after cell sorting for GFP-negative cells. Wt and Tert−/−S ESCs were transduced with a vector expressing GFP under the control of Oct4 promoter. Cells were treated with ATRA for 12 days and then sorted by FACS between GFP-positive 9 (green dots) and GFP-negative (black dots) cells. The upper graph shows the percentage of GFP-positive cells determined by FACS after 12 days of ATRA treatment. The lower chart shows the percentage of GFP-positive cells derived from sorted GFP-negative cells plated in LIF-containing media for 10 days. The difference in the incidence of GFP-positive cells, between Tert−/−S and Wt cells, was statistically significant ($p < 0.0001$; Welch's unpaired t test). Data are represented as mean ± SD.

5.2 Impairment of pluripotency gene promoter methylation after retinoic acid stimulation, and Dnmt3b-induced differentiation rescue

Methylation of CpG islands of pluripotency gene promoters is a key step in differentiation process (Altun et al., 2010). We used DNA bisulphite sequencing to test whether short telomere cells would exhibit an altered methylation profile of *Nanog* and *Oct4* promoters. In undifferentiated conditions, the promoters of all cell genotypes were entirely or almost entirely unmethylated. However, when treated with ATRA, *Tert*$^{-/-S}$ cells showed a much weaker increase in promoter methylation compared to Wt and *Tert*$^{-/-R}$ cells. In addition, once we re-plated cells in LIF-containing media, after ATRA treatment, *Tert*$^{-/-S}$ cells showed a loss of cytosine methylation on *Nanog* and *Oct4* promoters (Fig. 36).

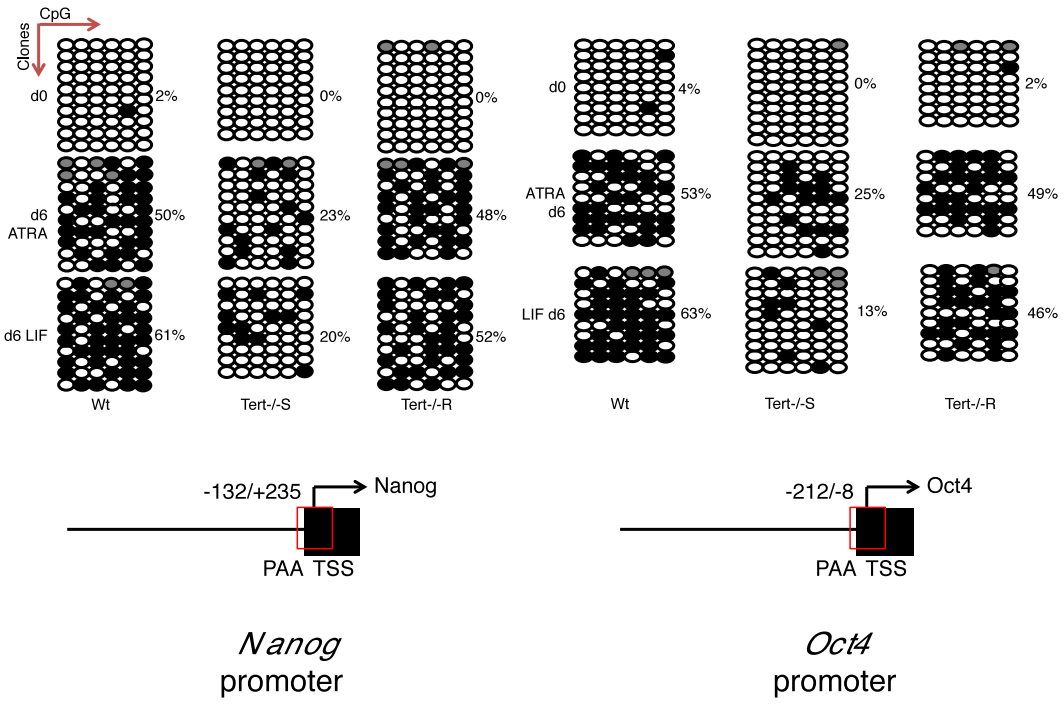

Figure 36. (TOP) CpG methylation analysis of the *Oct4* and *Nanog* promoters, by bisulphite sequencing, in Wt, *Tert*$^{-/-S}$ and *Tert*$^{-/-R}$ ESCs, during ATRA treatment followed by culture in LIF-conditioned media. Each row represents CpGs in a sequenced clone. Full dots symbolize methylated CpGs, empty dots symbolize unmethylated CpGs, and grey dots indicate an uncertain methylation status or an undefined sequence. Percentage values indicate the proportion of methylated cytosines relative to total cytosine residues (n≥8). (Bottom) Map of DNA region amplified and sequenced by bisulphite sequencing. The red box indicates the position of primer annealing region (PAA) relative to the transcription starting site (TSS).

To further confirm the importance of Dnmt down-regulation in the maintenance of differentiation of ESCs with critically short telomeres, we evaluated the ability *Tert*$^{-/-3b}$ to suppress and maintain suppress pluripotency genes. We found that, although not completely, Dnmt3b expression rescued the ability of *Tert*$^{-/-}$ ESCs to differentiate as assessed by the ability to suppress *Nanog*, *Oct4* and *Sox2* during ATRA treatment (Fig. 37A, 37B, 37C) and to maintain differentiation (Fig. 37C).

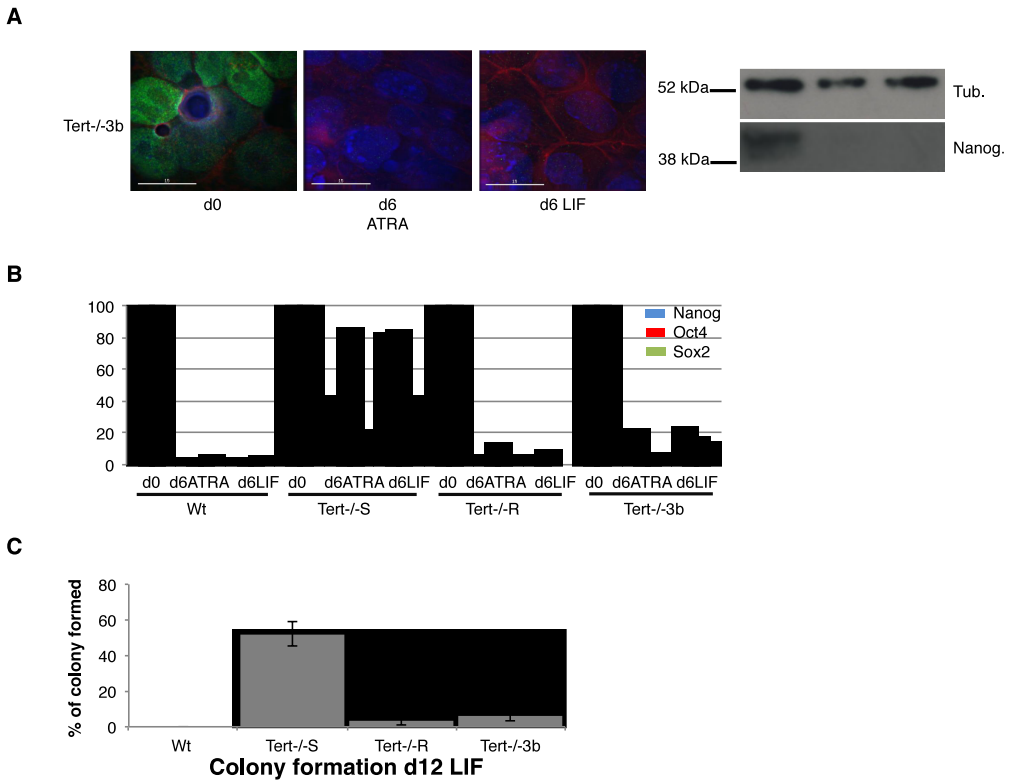

Figure 37. The response of *Tert*$^{-/-3b}$ ESCs to ATRA and subsequent LIF treatment A) (Left), Nanog immunofluorescence analysis (green = Nanog; Red = Actin). (Right), Nanog protein detection by western blot. Tub= β -tubulin. B) QRT-PCR analysis of pluripotency genes after ATRA-induced differentiation). (Wt, *Tert*$^{-/-S}$ and *Tert*$^{-/-R}$ same as in figure 25, samples analysed together). Gene expression at day 0 was arbitrarily set as 100 and the expression through the time course was normalized to mRNA levels at day 0. Values were expressed as a ratio to *GAPDH*. C) Single colony formation assay after ATRA treatment (6 days) and LIF-containing media (6 days) (n=3). (First 3 columns same as in figure 34, samples analysed together). A set of serial dilutions was performed and the percentage (n≥300) of viable ES cell colonies assessed with alkaline phosphatase assay. Error bar= SD. Wt= Wild type (parental ESC population); Tert-/-S = Tert deficient ESCs with short telomeres; Tert-/-R = Tert deficient ESCs with short telomeres, where *Tert* cDNA has been reintroduced. Tert-/-3b = Tert deficient ESCs with short telomeres ectopically expressing Dnmt3b.

This result suggested that both Nanog upregulation and reduced repressive ability of pluripotency genes upon ATRA treatment, and the ineffective ability to maintain differentiation of *Tert* null cells could be, at least in part, explained by impaired *de novo* methylation caused by downregulation of *de novo* Dnmt expression

5.3 Nanog depletion in *Tert*$^{-/-}$ ESCs induces spontaneous differentiation and differentiation maintenance

Finally, we decided to test whether we could bypass the impact of critically short telomeres and *de novo* Dnmts downregulation-induced impaired differentiation of *Tert*$^{-/-S}$ ESCs by depleting Nanog. We then transduced *Tert*$^{-/-S}$ cells with a lentiviral vector expression short hairpin RNA (shRNA) for *Nanog*.

Nanog depletion (Fig. 38A, 38B) induced loss of ESC morphology and a decrease in pluripotency gene expression (38B, 38C). In addition, *Tert*$^{-/-S}$ cells transduced with shRNA targeting Nanog also exhibited in the ability to maintain differentiation (38D). These data implied that, although *Tert*$^{-/-S}$ ESCs presented both increase in some pluripotency genes and defect in differentiation, they were still responsive to alterations to the core pluripotency regulatory network.

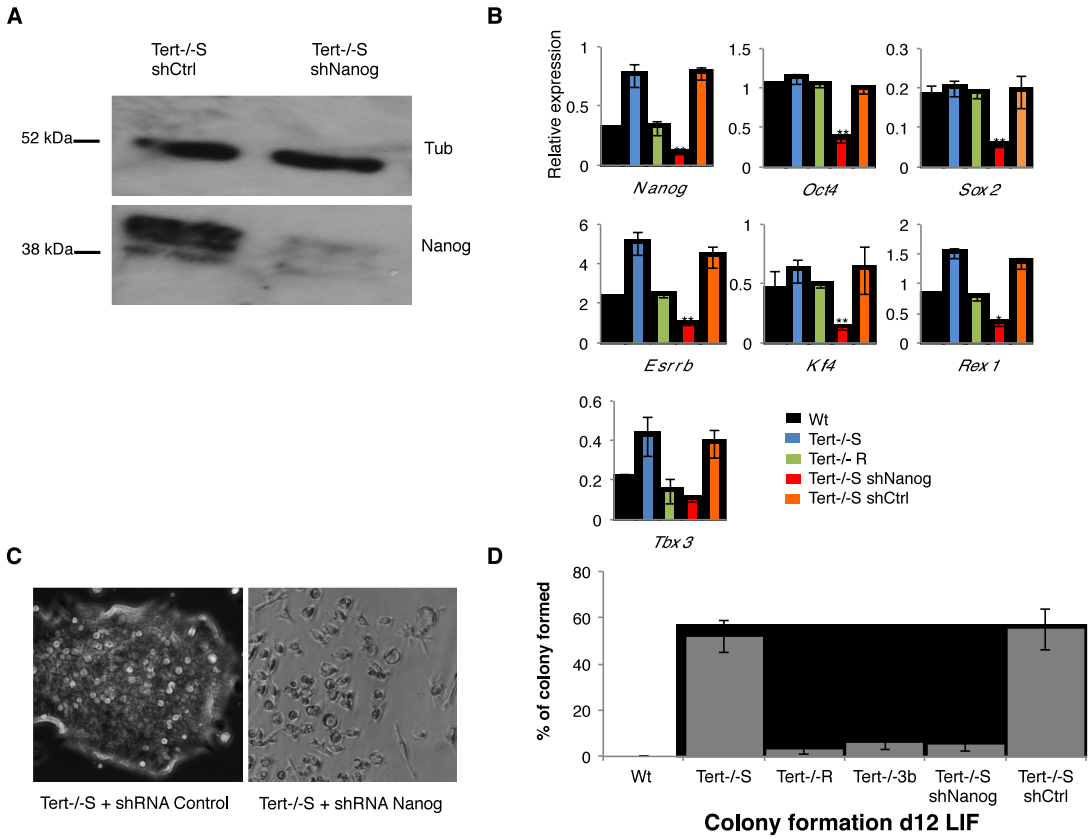

Figure 38. *Tert*$^{-/-S}$ ESCs response to Nanog depletion. A) Nanog protein detection by western blot. Tub= β -tubulin. B) Relative gene expression in Wt, *Tert*$^{-/-S}$, *Tert*$^{-/-L}$, *Tert*$^{-/-R}$, *Tert*$^{-/-S}$ shNanog, *Tert*$^{-/-S}$ shCtrl ESCs analysed by QRT-PCR. Data are represented as mean ± SD. ** = p<0.001. Background values (no reverse transcriptase added) were subtracted, and values were normalized to *GAPDH* (n>3). Statistical analysis was performed by ANOVA and related Dunnett's test comparing every group with Wt values. C) Bright field images of *Tert*$^{-/-S}$ ESCs transduced with shNanog and shCtrl. Micrograph bar indicates 200 μm. D) Single colony formation assay after ATRA treatment (6 days) and LIF-containing media (6 days) (n=3). (First 4 columns same as in figure 37, samples analysed together). A set of serial dilutions was performed and the percentage (n≥300) of viable ES cell colonies assessed with alkaline phosphatase assay. Error bar= SD.

5.4 Summary of chapter 5

In this chapter we tested the impact of critically short telomeres in mouse ESCs and observed a delay in the kinetics of differentiation upon ATRA treatment. This delay was associated with a metastable differentiation state where *Tert*$^{-/-S}$ cells were able to re-express, under LIF stimulation, pluripotency genes suppressed under ATRA-induced differentiation.

We showed how this phenotype could be, at least partially, rescued by enforced expression of Dnmt3b, independent of telomere length. In this regard, we noticed how methylation of pluripotency gene promoters, under ATRA-induced differentiation was impaired in *Tert*$^{-/-S}$ cells.

Finally, we demonstrated how this metastable differentiation phenotype could also be rescued independently of telomere length via Nanog depletion, thus underscoring the importance of this factor in maintaining *Tert*$^{-/-S}$ cells in an undifferentiated state and impeding their responsiveness to differentiation stimuli.

Chapter 6

Results

Tert$^{-/-S}$ ESCs show differential response to p53 inhibition, and altered regulation of insulin-responsive genes

The results illustrated in chapter 3, 4 and 5 presented a picture where *Tert*$^{-/-S}$ ESCs exhibited a tendency to undergo dysregulation of pluripotency gene expression and impairment in achieving and maintaining differentiation. In this chapter, we show preliminary data indicating that ESCs possessing critically short telomeres may also exhibit alterations of in p53 and insulin signalling networks.

6.1 Altered Nanog regulation in *Tert*$^{-/-S}$ cells upon inhibition of p53 transcriptional activity

It is well known that uncapped telomeres lead to p53 activation (Chin et al., 1999). In addition, p53, which is highly abundant in mouse ESCs (Sabapathy et al., 1997), may serve an emerging, and controversial, role in regulation of self-renewal, pluripotency and iPS reprogramming (Abdelalim and Tooyama, 2012; Kawamura et al., 2009; Lee et al., 2010; Lin et al., 2005; Marion et al., 2009a). Despite the fact that the role of p53 role in the inhibition of reprogramming has been widely established (Kawamura et al., 2009; Marion et al., 2009a), its role in ESC self-renewal and differentiation is much less clear with studies attributing it both pro-differentiation (Lin et al., 2005; Qin et al., 2007) and anti-differentiation activities (Abdelalim and Tooyama, 2012; Lee et al., 2010).

We decided to assess *Nanog* and *Oct4* expression on Wt and *Tert*$^{-/-S}$ ESCs upon treatment with pifithrin-α (PFT-α), a chemical inhibitor of p53 (Komarov et al., 1999). Although Oct4 levels were unchanged after 16h of treatment, Wt and *Tert*$^{-/-S}$ cells showed an inverse regulation of *Nanog* expression (Fig. 39).

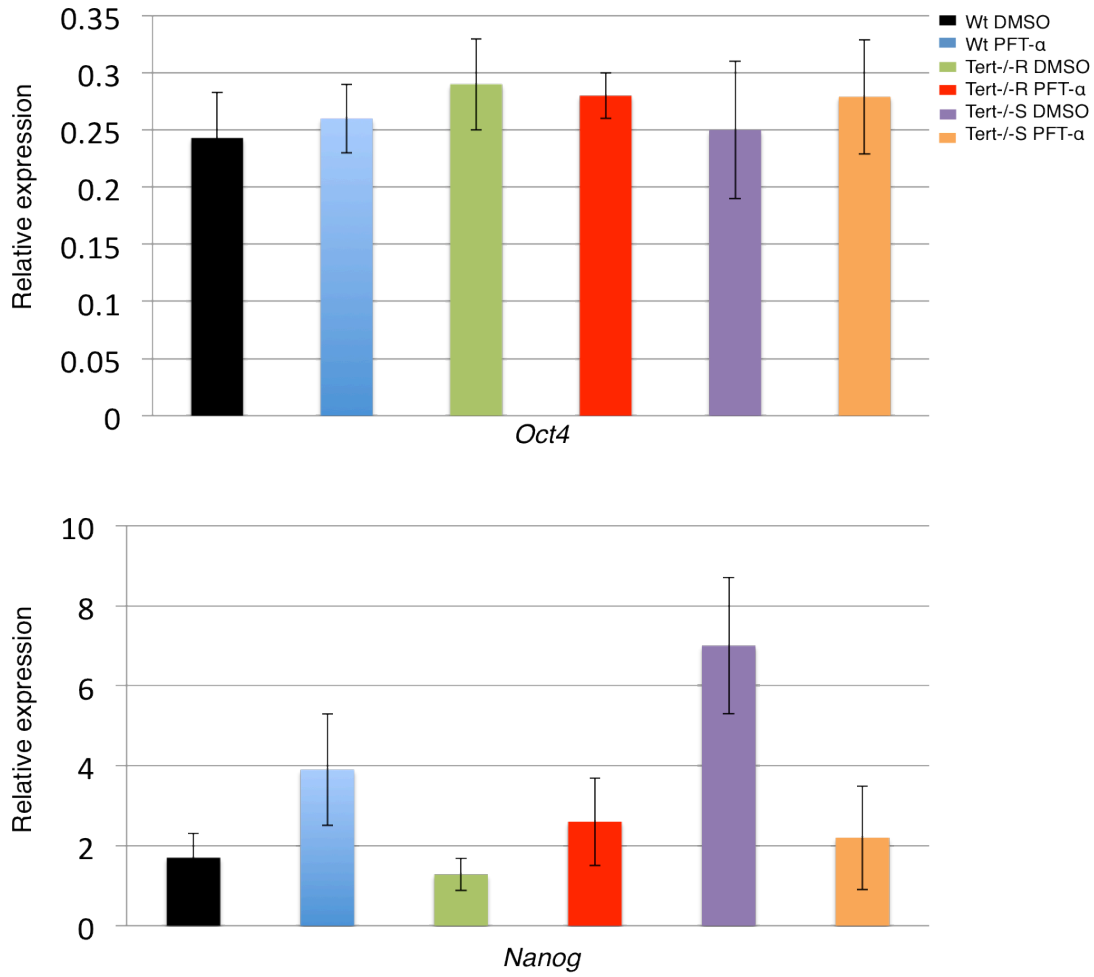

Figure 39. Relative gene expression in Wt, *Tert*$^{-/-S}$ and *Tert*$^{-/-R}$ ESCs treated with DMSO or 20µM of PTF-α analysed by QRT-PCR. Data are represented as mean ± SD. Background values (no reverse transcriptase added) were subtracted, and values were normalized to *GAPDH* N=2.

6.2 Upregulation of insulin-pathway genes in *Tert*$^{-/-S}$ ESCs

One of the characteristics of highly proliferative cells, included ESCs, is an increased ratio of anaerobic glycolysis over oxidative phosphorylation metabolism (Folmes et al., 2012). We then decided to investigate whether insulin –responsive genes were differentially regulated in *Tert*$^{-/-S}$ ESCs. We found that both insulin receptor (*INSR*) and insulin receptor substrate 2 (*IRS2*) mRNA were higher in *Tert*$^{-/-S}$ compared to Wt

and *Tert*$^{-/-R}$ cells (Fig. 40), suggesting that glucose metabolism might be altered in these cells.

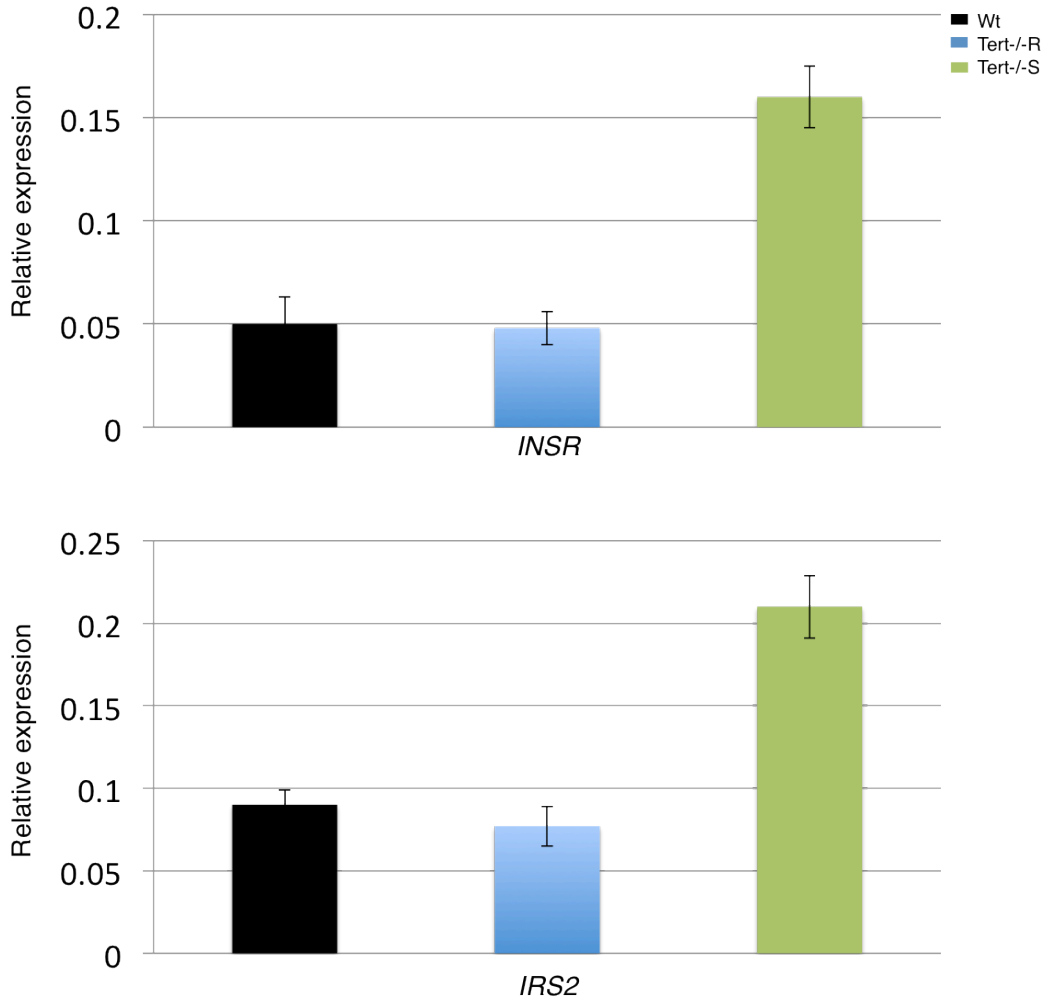

Figure 40. Relative gene expression in Wt, *Tert*$^{-/-S}$ and *Tert*$^{-/-R}$ ESCs analysed by QRT-PCR. Data are represented as mean ± SD. Background values (no reverse transcriptase added) were subtracted, and values were normalized to *GAPDH* N=2.

Finally, we decided to analyse the levels of Lin28 in Wt and *Tert*$^{-/-S}$ cells. Lin28, a RNA-binding protein (Ambros and Horvitz, 1984), is not only important for iPS reprogramming and for maintaining pluripotency (Moss and Tang, 2003; Yu et al., 2007), but it has also a role in glucose metabolism via its positive regulation of the

insulin-responsive genes *INSR* and *IRS2* (through suppression of *let-7* microRNA family, a Lin28 target) (Zhu et al., 2011). Quite surprisingly however, we found that *Lin28* was downregulate in *Tert*$^{-/-S}$ compared to Wt and *Tert*$^{-/-R}$ cells (Fig. 41). This result indicates not only that Lin28 is the only pluripotency factor found downregulated in *Tert*$^{-/-S}$ compared to Wt, but also that the increase in the mRNA of insulin-pathway genes, in *Tert*$^{-/-S}$ cells, is independent of Lin28 overexpression.

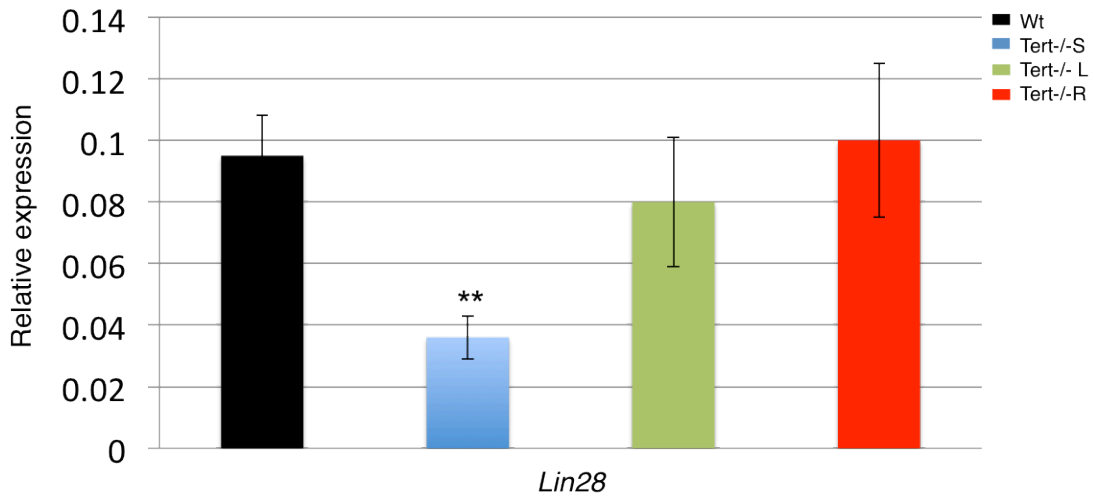

Figure 41. Relative gene expression in Wt, *Tert*$^{-/-S}$, *Tert*$^{-/-L}$, *Tert*$^{-/-R}$ ESCs analysed by QRT-PCR. Data are represented as mean ± SD. ** = p<0.001. Background values (no reverse transcriptase added) were subtracted, and values were normalized to *GAPDH*. N=5.

6.3 Summary of chapter 6

In this chapter, we tested the impact of critically short telomeres on other signalling networks known to influence cell pluripotency, and obtained preliminary evidence of the involvement of p53,in pluripotency gene dysregulation and, by inference, in impaired differentiation of *Tert*$^{-/-S}$ cells.

We also observed that *Tert*$^{-/-S}$ cells exhibit altered glucose metabolism. Surprisingly though, we found the Lin28, a hypothesized main candidate for increased insulin-pathway gene levels, was downregulated in *Tert*$^{-/-S}$ compared to *Tert*$^{-/-R}$ and Wt ESCs.

Chapter 7

Discussion and Perspectives

7.1 Telomeres and epigenetic

The connection between telomere length and chromatin compaction has been already established, at least at telomeric and subtelomeric regions, by the work of Maria Blasco and collaborators (Benetti et al., 2007). In this study, we uncovered a role of critically short telomeres in chromatin conformation both at telomeric and subtelomeric *loci,* and globally through the genome. In particular, we found that *Terc*$^{-/-S}$ exhibited widespread cytosine hypomethylation compared to Wt and *Terc*$^{-/-R}$ ESCs. Furthermore, we also noticed, in *Terc*$^{-/-S}$ ESC, an increase of open chromatin marks acH4 and acH3K9 at subtelomeric regions as predicted by (Benetti et al., 2007), and an overall increase, including a site-specific (e.g. *Nanog* promoter) displacement, of the repressive histone mark H3K27me3.

PRC2 mediates trimethylation of H3K27, which, although dispensable for maintaining an undifferentiated and self-renewing state, characterises ESC identity (Shen et al., 2008). H3K27me3 is one of the main histone repression marks, and its reduction, in ESCs, on *Nanog* and *Gata6* promoters has been connected to an increased expression of these genes (Lu et al., 2011; Shen et al., 2008; Villasante et al., 2011). Despite the overall increase of H3K27me3 in *Terc*$^{-/-S}$ ESCs, consistent with recent works that link H3K27me3 enrichment to unmethylated CpG contents

(Lynch et al., 2012; Mendenhall et al., 2010), its enrichment on the promoters of *Nanog* and *Gata6* was diminished. These results are in keeping with the observation that CpG loss of methylation leads to a redistribution, and overall increase, of H3K27me3 on regions which are normally methylated, but a reduction of H3K27me3 on regions that are ordinarily unmethylated (Brinkman et al., 2012). Our results suggest a working model (Fig.42) whereby uncapped-telomere induced Dnmt3a and Dnmt3b downregulation results into subtelomeric and global DNA hypomethylation and displacement of H3K27me3 at gene promoters. Reduced H3K27me3 at gene control elements, in turn, affects the ability of the cell to repress pluripotency factors, which is a key step to achieve stable differentiation.

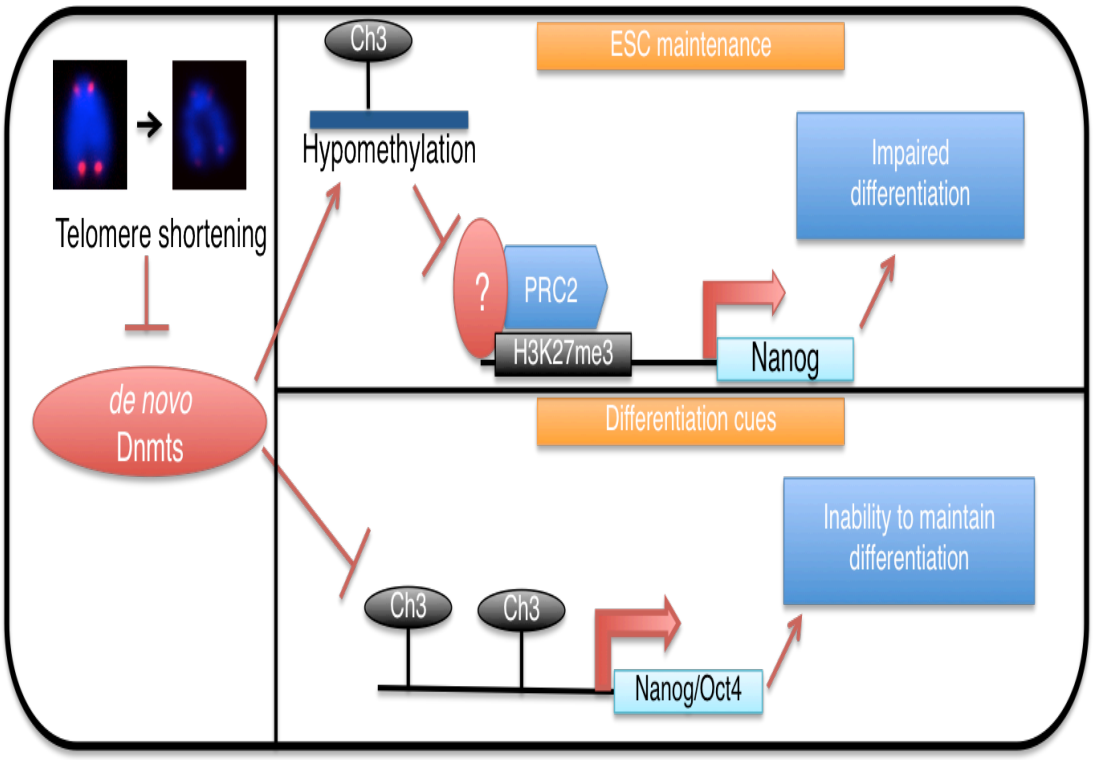

Figure 42. Schematic model: telomere shortening impairs expression of Dnmt3 isoforms, leading to genome-wide DNA hypomethylation, which in turn affects H3K27me3 enrichment on specific

loci (e.g. *Nanog*), thus impairing the ability to sustain pluripotency factor repression after differentiation and growth re-stimulation.

Notably, due to the impossibility, for unclear reasons, to generate *Tert*$^{-/-}$ embryos from our *Tert*$^{+/-}$ mice (Liu et al., 2000), and lack of time to perform *Tert* gene targeting on early passage ESCs, we had to use previously generated *Tert*$^{-/-}$ ESCs (Liu et al., 2000). This approach has many disadvantages compared to using new *ex-vivo* isolated ESCs. First of all, it implies that, in order to generate short telomere *Tert*$^{-/-}$ ESCs, we had to maintain *Tert*$^{-/-}$ ESCs in culture for many passages (70 or more passages). The extended growth of cells in culture may lead to accumulation of DNA mutations, or to a selection of cells with a higher preference to grow in culture than to differentiate. However, the observation of similar defects in differentiation in two independently generated *Tert*$^{-/-}$ ESCs (Liu et al., 2000) compared to parental ESCs, and the rescue phenotype after reintroduction of *Tert* in late passages *Tert*$^{-/-}$ ESCs rather suggested a telomere-based effect. Nevertheless we cannot completely exclude the possibility that secondary mutation(s) accumulated, over passages, in *Tert*$^{-/-S}$ ESCs and played a role in the described effects.

In any case, assuming the observed effects are indeed due to a telomere shortening, many questions still remain to be addressed: What is the molecular link between critically short telomeres and *de novo* Dnmts downregulation? Can these data suggest a different way to look at (some) kinds of tumours? What is the connection among short telomeres, downregulation of Lin28 and altered glucose metabolism?

7.2 *De novo* Dnmt downregulation and uncapped-telomere caused inhibition of differentiation activity (UCCIA)

In chapters 4 and 5, we showed that *Tert*$^{-/-S}$ ESCs exhibit a reduced expression of *de novo* Dnmts compared to Wt and *Tert*$^{-/-R}$ ESCs, and demonstrated that this downregulation led to improper pluripotency promoter methylation and unstable differentiation. We also showed that enforced expression of Dnmt3b was able to almost completely rescue proper differentiation in *Tert*$^{-/-S}$ cells, independently of telomere length. Lack of complete rescue could be due to fact that *Dnmt3b* was reintroduced, but not *Dnmt3a* (which was also found downregulated in *Tert*$^{-/-S}$) and *Dnmt3L* (whose expression levels were not tested).

The concept that reduced *de novo* methylation may lead to a metastable state of differentiation is not, *per se*, surprising, having been already established in the literature (Feldman et al., 2006; Jackson et al., 2004; Sinkkonen et al., 2008). What we found unexpected and fascinating was that critically short telomeres could trigger this mechanism. However, a few points should be considered regarding the apparent reversibility into ESCs of *Tert*$^{-/-S}$ cells which lost the expression of pluripotency markers. First, simply taking the loss of expression of pluripotency genes as the sole indicator of differentiation, without monitoring the appearance of differentiation markers, may hide a situation where some *Tert*$^{-/-S}$ cells strongly reduce, but do not suppress, the expression of pluripotency genes under ATRA treatment and re-express them after re-introduction of LIF into the culture medium. Second, even if the loss of expression of pluripotency factors, such as Oct4, was a sufficient indicator of differentiation, it would not be possible to exclude that a small percentage of *Tert*$^{-/-S}$

cells, resistant to differentiation, persisted in the population of properly differentiated cells and expanded after re-addition of LIF into the culture medium.

Nevertheless, whether *Tert*$^{-/-S}$ cells undergo a full (from completely differentiated cells) or partial (from incompletely differentiated cells) de-differentiation event or whether a sub-population of cells insensitive to differentiation clues can expand, it remains to be determined how telomere shortening affects Dnmt expression. A possible hypothesis could be that this uncapped-telomere caused inhibition of differentiation activity (UCCIA) is triggered by a DNA damage response originating from unprotected telomeres. We have, in fact, already seen in chapter 6 how the inhibition of p53 in *Tert*$^{-/-S}$ ESCs can restore *Nanog* expression to levels closer to Wt ESCs. So, it would be interesting to test whether inhibiting a telomere-dependent DNA damage response could rescue Dnmt expression. However, it should be noticed that Nanog downregulation in *Tert*$^{-/-S}$ treated with PFT-α is hardly due to a putative effect on Dnmt expression. In fact, even in the presence of a rescue of Dnmt expression, an incubation of 16h would have not been sufficient to restore genomic DNA methylation. This result suggests that dysregulation of pluripotency genes in *Tert*$^{-/-S}$ may be due to more than one mechanism (Fig. 43A, 43B).

Another hypothesis, which should be tested, is whether UCCIA may be caused by genomic mislocalization of telomeric factors such as Rap1 or Rif1 following telomere shortening (Fig. 43C).

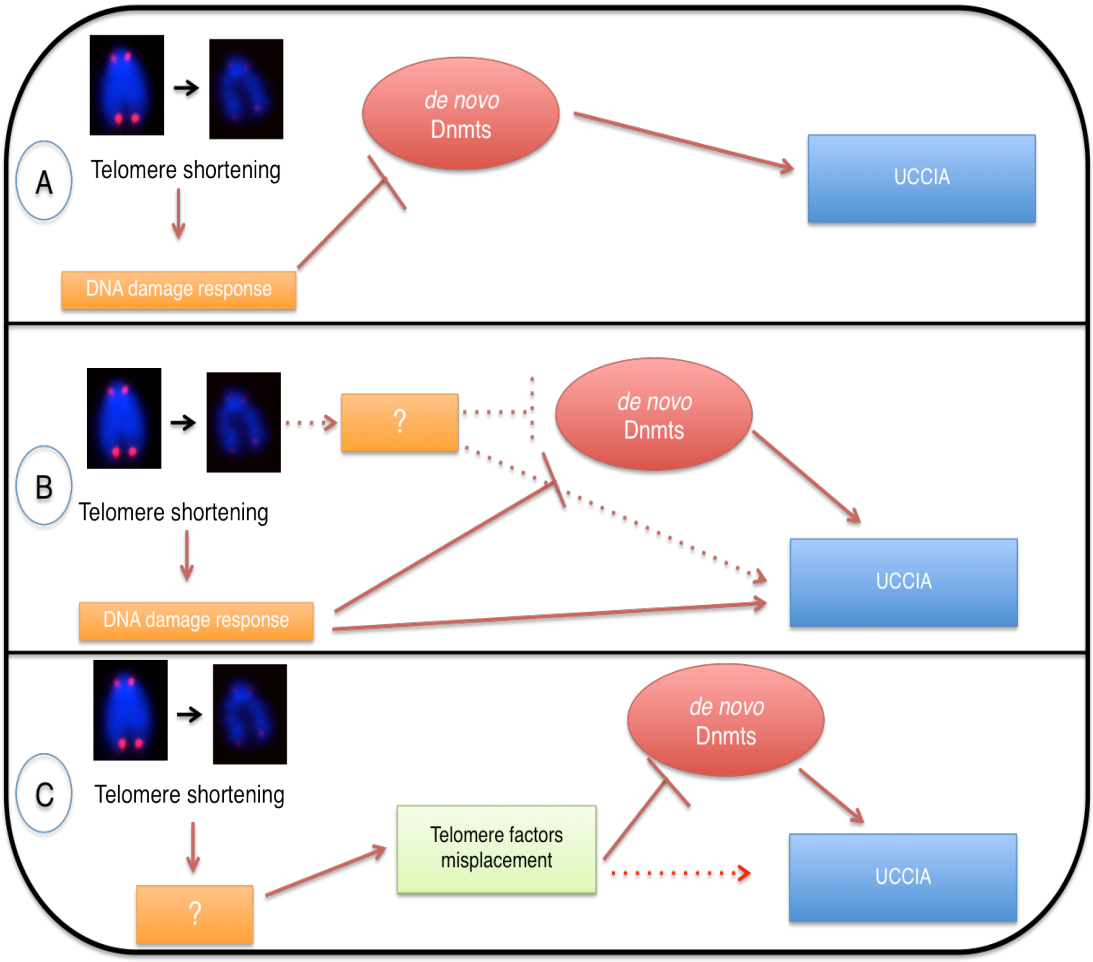

Figure 43. Schematic representation of putative models connecting telomere shortening to *de novo* Dnmt downregulation and UCCIA. A) Uncapped telomeres trigger a DNA damage response, which mediates *de novo* Dnmt downregulation. B) Uncapped telomeres trigger DNA damage response and/or unknown mechanisms to downregulate Dnmts. In parallel DNA damage response may have Dnmt-independent effects upon UCCIA. C) Telomere shortening leads to misplacement of telomeric factors involved in gene regulation and pluripotency maintenance, with subsequent induction of UCCIA.

7.3 Necessity to examine some cancer therapies from a different angle?

Cancer cells are highly proliferative and they require an appropriate maintenance of telomere length to safeguard their replicative potential. In approximately 85% of cases telomeres are preserved by re-activation of telomerase (Matsuo et al., 2009). When telomerase is inhibited or deleted in culture, telomerase-positive cancer cells shorten their telomeres with each cell division and eventually enter senescence (Hahn et al., 1999; Taboski et al., 2012; Zhang et al., 1999). In the other 15% of cases, instead, cancer cell telomeres undergo ALT-mechanisms (Cesare and Reddel, 2010). Thus, an obvious rationale is to target the inhibition of telomerase and/or telomere maintenance as a putative cancer therapy (Biffi et al., 2013; Folini et al., 2011; Roth et al., 2010).

The regulation of many factors involved in pluripotency and differentiation has not only effects on physiological development, but is also important in human disease. For example, it is known that some pluripotency factors (e.g. Nanog, Oct4) tend to be highly abundant in undifferentiated cancer cells and putative cancer stem cells (Tysnes, 2010). Furthermore, treatment of some kind of tumours (e.g. promyelocytic leukemia) requires the usage of pro-differentiating chemicals such as retinoic acid. (Petrie et al., 2009).

A question that rises spontaneously is whether critically short telomeres affect the response of cancer cells to pro-differentiating agents, and in this case whether a

telomere/telomerase targeting strategy may have, in such a situation, the undesirable effect to impede cell differentiation. Speculating further, one may propose that, in particular cases of undifferentiated tumours, a telomere-elongation approach, in combination with other treatments, could improve the response to the therapy (Fig. 44). In support of this hypothesis, it is worth mentioning a very recent work from Hiroyuki Seimiya and colleagues, which have shown how lengthening telomeres of human prostatic cancer cells with short telomeres led to differentiation of tumour cells (Hirashima et al., 2013).

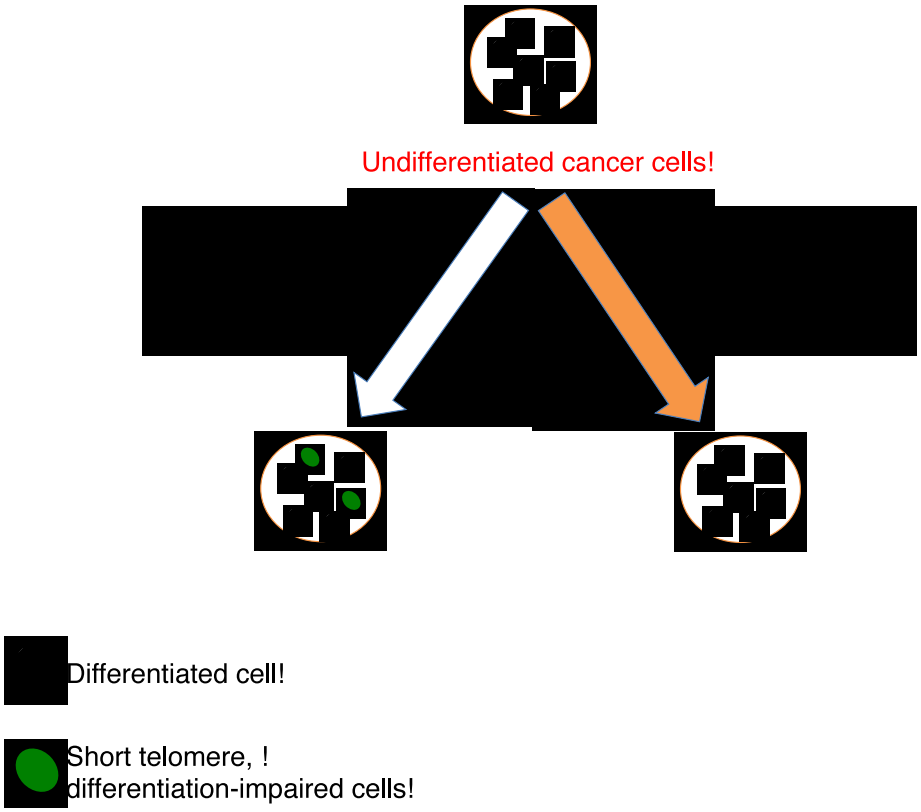

Figure 44. Schematic representation of speculative impact of contrasting telomere shortening in particular cases of cancer therapy.

7.4 Affecting glucose uptake

Tert$^{-/-S}$ ESCs appear to have higher levels of mRNA of the insulin-pathway genes *INSR* and *IRS2* compared to Wt ESCs, suggesting that these cells might have enhanced glucose uptake and glycolysis. This result itself may not be surprising, considering that ESCs have an increased anaerobic over aerobic metabolism ratio compared to differentiated cells (Folmes et al., 2012), and that *Tert*$^{-/-S}$ showed an overall increase in pluripotency and self-renewing genes compared to Wt and *Tert*$^{-/-R}$ ESCs. In fact the increase in IRS2 and INSR could simply reflect the upregulation of pluripotency genes such as *Nanog* and *Essrb* in *Tert*$^{-/-S}$ cells. However, the fact that *Lin28*, one of the main positive regulators of insulin-pathway genes (Zhu et al., 2011), has been found as the only pluripotency factor that is repressed in *Tert*$^{-/-S}$, (among those tested), is somewhat puzzling. In addition, both *Lin28* downregulation and telomere shortening have been connected, separately, to Diabetes mellitus type 2, a disease characterised by insulin resistance (Guo et al., 2011; Zhu et al., 2011).

Our data demonstrate a decrease in *Lin28* expression in ESCs with critically short telomeres, and thus may offer a possible molecular link between the two phenotypes. In *Tert*$^{-/-S}$ cells, insulin-pathway genes could be upregulated, regardless of *Lin28* downregulation, due to the overexpression of other pluripotency genes. It would be very interesting to assess whether, in differentiated cells with critically short telomeres, Lin28 and insulin pathway genes are downregulated, and whether telomere elongation can rescue their expression (Fig. 45).

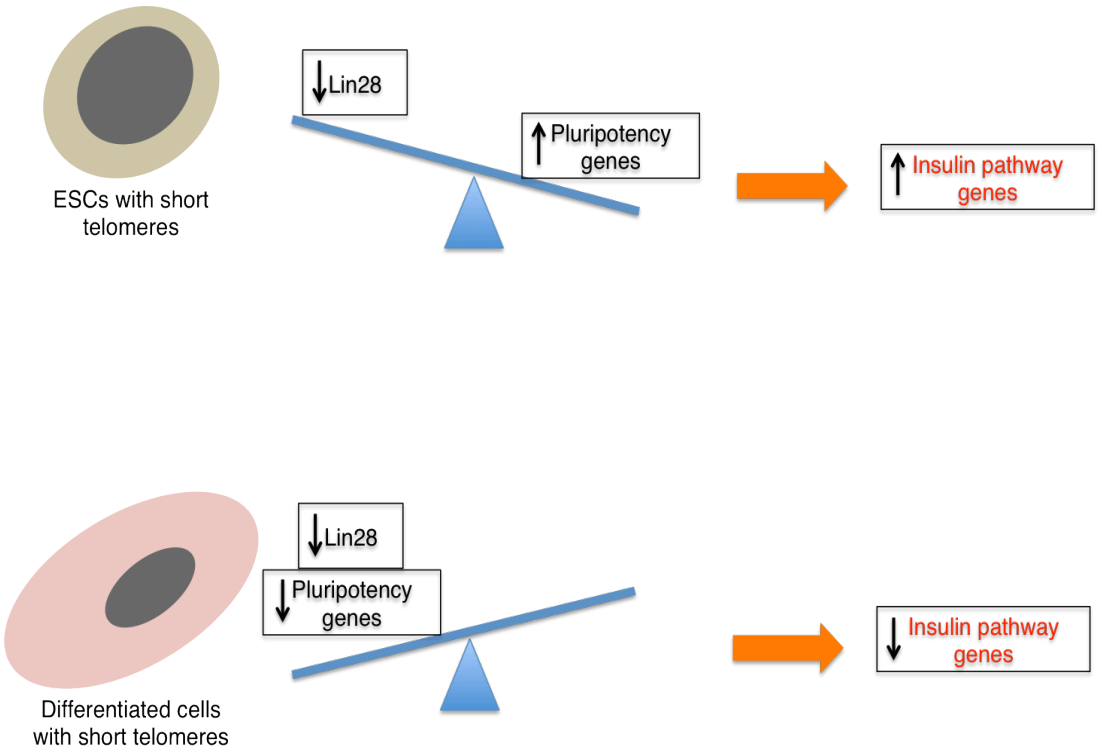

Figure 45. Schematic representation of hypothetical mechanism of insulin pathway gene control. ***Tert***$^{-/-S}$ **ESCs show increase in insulin pathway genes, despite reduced Lin28, perhaps as a response to an overall increase in pluripotency gene expression. In differentiated cells, short telomeres lead to Lin28 downregulation and subsequent repression of insulin pathway genes.**

7.5 Final remarks

The results presented in this work provided conceptual advances in the field of telomere biology and its effects on chromatin and gene expression, and in the field of pluripotency maintenance in ESCs. Having found that critically short telomeres affect chromatin compaction even at a global genomic level, this work completes a picture initiated by other studies (Benetti et al., 2007), which observed telomere-shortening effects on chromatin only at regions proximal to telomeres.

As for the discovery of uncapped telomeres impacting on pluripotency gene regulation, this study provides us with new information about the complex network of factors and mechanisms necessary to regulate the pluripotent state of embryonic stem cells.

Finally, our discovery of the role of critically short telomeres in regulating the kinetics and stability of ESC differentiation opens new perspectives on the functions of telomeres in the cell.

The fact that telomere regulation seems to be a sophisticated process, which not only provides the cell with replicative potential, but that also affects cell fate decisions is intriguing, and clearly demands further studies to investigate its role in different contexts (e.g. progenitor cells, cancer cells, etc.) in order to gain a complete picture of the intricate interplay between these processes.

Bibliography

Abdelalim, E.M., and Tooyama, I. (2012). The p53 inhibitor, pifithrin-alpha, suppresses self-renewal of embryonic stem cells. Biochem Biophys Res Commun *420*, 605-610.

Allis, C.D., Berger, S.L., Cote, J., Dent, S., Jenuwien, T., Kouzarides, T., Pillus, L., Reinberg, D., Shi, Y., Shiekhattar, R., *et al.* (2007). New nomenclature for chromatin-modifying enzymes. Cell *131*, 633-636.

Altun, G., Loring, J.F., and Laurent, L.C. (2010). DNA methylation in embryonic stem cells. J Cell Biochem *109*, 1-6.

Ambros, V., and Horvitz, H.R. (1984). Heterochronic mutants of the nematode Caenorhabditis elegans. Science *226*, 409-416.

Atcha, F.A., Syed, A., Wu, B., Hoverter, N.P., Yokoyama, N.N., Ting, J.H., Munguia, J.E., Mangalam, H.J., Marsh, J.L., and Waterman, M.L. (2007). A unique DNA binding domain converts T-cell factors into strong Wnt effectors. Mol Cell Biol *27*, 8352-8363.

Avilion, A.A., Nicolis, S.K., Pevny, L.H., Perez, L., Vivian, N., and Lovell-Badge, R. (2003). Multipotent cell lineages in early mouse development depend on SOX2 function. Genes Dev *17*, 126-140.

Azzalin, C.M., Reichenbach, P., Khoriauli, L., Giulotto, E., and Lingner, J. (2007). Telomeric repeat containing RNA and RNA surveillance factors at mammalian chromosome ends. Science *318*, 798-801.

Benetti, R., Garcia-Cao, M., and Blasco, M.A. (2007). Telomere length regulates the epigenetic status of mammalian telomeres and subtelomeres. Nat Genet *39*, 243-250.

Benetti, R., Gonzalo, S., Jaco, I., Munoz, P., Gonzalez, S., Schoeftner, S., Murchison, E., Andl, T., Chen, T., Klatt, P.*, et al.* (2008). A mammalian microRNA cluster controls DNA methylation and telomere recombination via Rbl2-dependent regulation of DNA methyltransferases. Nat Struct Mol Biol *15*, 998.

Benezra, R., Davis, R.L., Lockshon, D., Turner, D.L., and Weintraub, H. (1990). The protein Id: a negative regulator of helix-loop-helix DNA binding proteins. Cell *61*, 49-59.

Bergmann, J.H., Rodriguez, M.G., Martins, N.M., Kimura, H., Kelly, D.A., Masumoto, H., Larionov, V., Jansen, L.E., and Earnshaw, W.C. (2011). Epigenetic engineering shows H3K4me2 is required for HJURP targeting and CENP-A assembly on a synthetic human kinetochore. Embo J *30*, 328-340.

Biffi, G., Tannahill, D., McCafferty, J., and Balasubramanian, S. (2013). Quantitative visualization of DNA G-quadruplex structures in human cells. Nat Chem *5*, 182-186.

Bird, A., Taggart, M., Frommer, M., Miller, O.J., and Macleod, D. (1985). A fraction of the mouse genome that is derived from islands of nonmethylated, CpG-rich DNA. Cell *40*, 91-99.

Blackburn, E.H. (2001). Switching and signaling at the telomere. Cell *106*, 661-673.

Blair, K., Wray, J., and Smith, A. (2011). The liberation of embryonic stem cells. PLoS Genet *7*, e1002019.

Bodnar, A.G., Ouellette, M., Frolkis, M., Holt, S.E., Chiu, C.P., Morin, G.B., Harley, C.B., Shay, J.W., Lichtsteiner, S., and Wright, W.E. (1998). Extension of life-span by introduction of telomerase into normal human cells. Science *279*, 349-352.

Bower, K., Napier, C.E., Cole, S.L., Dagg, R.A., Lau, L.M., Duncan, E.L., Moy, E.L., and Reddel, R.R. (2012). Loss of wild-type ATRX expression in somatic cell hybrids segregates with activation of Alternative Lengthening of Telomeres. PLoS One *7*, e50062.

Brinkman, A.B., Gu, H., Bartels, S.J., Zhang, Y., Matarese, F., Simmer, F., Marks, H., Bock, C., Gnirke, A., Meissner, A.*, et al.* (2012). Sequential ChIP-bisulfite sequencing enables direct genome-scale investigation of chromatin and DNA methylation cross-talk. Genome Res.

Bryan, T.M., Englezou, A., Gupta, J., Bacchetti, S., and Reddel, R.R. (1995). Telomere elongation in immortal human cells without detectable telomerase activity. Embo J *14*, 4240-4248.

Cesare, A.J., and Reddel, R.R. (2010). Alternative lengthening of telomeres: models, mechanisms and implications. Nat Rev Genet *11*, 319-330.

Chambers, I., Colby, D., Robertson, M., Nichols, J., Lee, S., Tweedie, S., and Smith, A. (2003). Functional expression cloning of Nanog, a pluripotency sustaining factor in embryonic stem cells. Cell *113*, 643-655.

Chambers, I., Silva, J., Colby, D., Nichols, J., Nijmeijer, B., Robertson, M., Vrana, J., Jones, K., Grotewold, L., and Smith, A. (2007). Nanog safeguards pluripotency and mediates germline development. Nature *450*, 1230-1234.

Chin, L., Artandi, S.E., Shen, Q., Tam, A., Lee, S.L., Gottlieb, G.J., Greider, C.W., and DePinho, R.A. (1999). p53 deficiency rescues the adverse effects of telomere loss and cooperates with telomere dysfunction to accelerate carcinogenesis. Cell *97*, 527-538.

Chiodi, I., Belgiovine, C., Zongaro, S., Ricotti, R., Horard, B., Lossani, A., Focher, F., Gilson, E., Giulotto, E., and Mondello, C. (2013). Super-telomeres in transformed human fibroblasts. Biochim Biophys Acta.

Choi, J., Southworth, L.K., Sarin, K.Y., Venteicher, A.S., Ma, W., Chang, W., Cheung, P., Jun, S., Artandi, M.K., Shah, N.*, et al.* (2008). TERT promotes epithelial proliferation through transcriptional control of a Myc- and Wnt-related developmental program. PLoS Genet *4*, e10.

Clouaire, T., de Las Heras, J.I., Merusi, C., and Stancheva, I. (2010). Recruitment of MBD1 to target genes requires sequence-specific interaction of the MBD domain with methylated DNA. Nucleic Acids Res *38*, 4620-4634.

Costa, Y., Ding, J., Theunissen, T.W., Faiola, F., Hore, T.A., Shliaha, P.V., Fidalgo, M., Saunders, A., Lawrence, M., Dietmann, S.*, et al.* (2013). NANOG-dependent function of TET1 and TET2 in establishment of pluripotency. Nature *495*, 370-374.

Cross, S.H., Charlton, J.A., Nan, X., and Bird, A.P. (1994). Purification of CpG islands using a methylated DNA binding column. Nat Genet *6*, 236-244.

Dahl, J.A., Reiner, A.H., Klungland, A., Wakayama, T., and Collas, P. (2010). Histone H3 lysine 27 methylation asymmetry on developmentally-regulated promoters distinguish the first two lineages in mouse preimplantation embryos. PLoS One *5*, e9150.

Deaton, A.M., and Bird, A. (2011). CpG islands and the regulation of transcription. Genes Dev *25*, 1010-1022.

Dostie, J., and Bickmore, W.A. (2012). Chromosome organization in the nucleus - charting new territory across the Hi-Cs. Curr Opin Genet Dev *22*, 125-131.

Dunham, M.A., Neumann, A.A., Fasching, C.L., and Reddel, R.R. (2000). Telomere maintenance by recombination in human cells. Nat Genet *26*, 447-450.

Evans, M.J., and Kaufman, M.H. (1981). Establishment in culture of pluripotential cells from mouse embryos. Nature *292*, 154-156.

Feldman, N., Gerson, A., Fang, J., Li, E., Zhang, Y., Shinkai, Y., Cedar, H., and Bergman, Y. (2006). G9a-mediated irreversible epigenetic inactivation of Oct-3/4 during early embryogenesis. Nat Cell Biol *8*, 188-194.

Festuccia, N., and Chambers, I. (2011). Quantification of pluripotency transcription factor levels in embryonic stem cells by flow cytometry. Curr Protoc Stem Cell Biol *Chapter 1*, Unit 1B 9.

Festuccia, N., Osorno, R., Halbritter, F., Karwacki-Neisius, V., Navarro, P., Colby, D., Wong, F., Yates, A., Tomlinson, S.R., and Chambers, I. (2012). Esrrb is a direct Nanog target gene that can substitute for Nanog function in pluripotent cells. Cell Stem Cell *11*, 477-490.

Fidalgo, M., Shekar, P.C., Ang, Y.S., Fujiwara, Y., Orkin, S.H., and Wang, J. (2011). Zfp281 functions as a transcriptional repressor for pluripotency of mouse embryonic stem cells. Stem Cells *29*, 1705-1716.

Fisher, C.L., and Fisher, A.G. (2011). Chromatin states in pluripotent, differentiated, and reprogrammed cells. Curr Opin Genet Dev *21*, 140-146.

Folini, M., Venturini, L., Cimino-Reale, G., and Zaffaroni, N. (2011). Telomeres as targets for anticancer therapies. Expert Opin Ther Targets *15*, 579-593.

Folmes, C.D., Dzeja, P.P., Nelson, T.J., and Terzic, A. (2012). Metabolic plasticity in stem cell homeostasis and differentiation. Cell Stem Cell *11*, 596-606.

Friel, R., van der Sar, S., and Mee, P.J. (2005). Embryonic stem cells: understanding their history, cell biology and signalling. Adv Drug Deliv Rev *57*, 1894-1903.

Gao, Y., Chen, J., Li, K., Wu, T., Huang, B., Liu, W., Kou, X., Zhang, Y., Huang, H., Jiang, Y.*, et al.* (2013). Replacement of Oct4 by Tet1 during iPSC induction

reveals an important role of DNA methylation and hydroxymethylation in reprogramming. Cell Stem Cell *12*, 453-469.

Gardner, R.L., and Beddington, R.S. (1988). Multi-lineage 'stem' cells in the mammalian embryo. J Cell Sci Suppl *10*, 11-27.

Geserick, C., and Blasco, M.A. (2006). Novel roles for telomerase in aging. Mech Ageing Dev *127*, 579-583.

Gonzalo, S., and Blasco, M.A. (2005). Role of Rb family in the epigenetic definition of chromatin. Cell Cycle *4*, 752-755.

Gonzalo, S., Jaco, I., Fraga, M.F., Chen, T., Li, E., Esteller, M., and Blasco, M.A. (2006). DNA methyltransferases control telomere length and telomere recombination in mammalian cells. Nat Cell Biol *8*, 416-424.

Granger, M.P., Wright, W.E., and Shay, J.W. (2002). Telomerase in cancer and aging. Crit Rev Oncol Hematol *41*, 29-40.

Greider, C.W., and Blackburn, E.H. (1985). Identification of a specific telomere terminal transferase activity in Tetrahymena extracts. Cell *43*, 405-413.

Grinnell, K.L., Yang, B., Eckert, R.L., and Bickenbach, J.R. (2007). De-differentiation of mouse interfollicular keratinocytes by the embryonic transcription factor Oct-4. J Invest Dermatol *127*, 372-380.

Guo, N., Parry, E.M., Li, L.S., Kembou, F., Lauder, N., Hussain, M.A., Berggren, P.O., and Armanios, M. (2011). Short telomeres compromise beta-cell signaling and survival. PLoS One *6*, e17858.

Hahn, W.C., Stewart, S.A., Brooks, M.W., York, S.G., Eaton, E., Kurachi, A., Beijersbergen, R.L., Knoll, J.H., Meyerson, M., and Weinberg, R.A. (1999). Inhibition of telomerase limits the growth of human cancer cells. Nat Med *5*, 1164-1170.

Hata, K., Okano, M., Lei, H., and Li, E. (2002). Dnmt3L cooperates with the Dnmt3 family of de novo DNA methyltransferases to establish maternal imprints in mice. Development *129*, 1983-1993.

Hayflick, L., and Moorhead, P.S. (1961). The serial cultivation of human diploid cell strains. Exp Cell Res *25*, 585-621.

Heard, E. (2004). Recent advances in X-chromosome inactivation. Curr Opin Cell Biol *16*, 247-255.

Heng, J.C., Orlov, Y.L., and Ng, H.H. (2010). Transcription factors for the modulation of pluripotency and reprogramming. Cold Spring Harb Symp Quant Biol *75*, 237-244.

Hillman, N., Sherman, M.I., and Graham, C. (1972). The effect of spatial arrangement on cell determination during mouse development. J Embryol Exp Morphol *28*, 263-278.

Hirai, H., Karian, P., and Kikyo, N. (2011). Regulation of embryonic stem cell self-renewal and pluripotency by leukaemia inhibitory factor. Biochem J *438*, 11-23.

Hirashima, K., Migita, T., Sato, S., Muramatsu, Y., Ishikawa, Y., and Seimiya, H. (2013). Telomere length influences cancer cell differentiation in vivo. Mol Cell Biol.

Hockemeyer, D., Daniels, J.P., Takai, H., and de Lange, T. (2006). Recent expansion of the telomeric complex in rodents: Two distinct POT1 proteins protect mouse telomeres. Cell *126*, 63-77.

Huang, J., Wang, F., Okuka, M., Liu, N., Ji, G., Ye, X., Zuo, B., Li, M., Liang, P., Ge, W.W.*, et al.* (2011). Association of telomere length with authentic pluripotency of ES/iPS cells. Cell research *21*, 779-792.

Ito, S., D'Alessio, A.C., Taranova, O.V., Hong, K., Sowers, L.C., and Zhang, Y. (2010). Role of Tet proteins in 5mC to 5hmC conversion, ES-cell self-renewal and inner cell mass specification. Nature *466*, 1129-1133.

Ivanova, N., Dobrin, R., Lu, R., Kotenko, I., Levorse, J., DeCoste, C., Schafer, X., Lun, Y., and Lemischka, I.R. (2006). Dissecting self-renewal in stem cells with RNA interference. Nature *442*, 533-538.

Jackson, M., Krassowska, A., Gilbert, N., Chevassut, T., Forrester, L., Ansell, J., and Ramsahoye, B. (2004). Severe global DNA hypomethylation blocks differentiation and induces histone hyperacetylation in embryonic stem cells. Mol Cell Biol *24*, 8862-8871.

Jiang, H., Ju, Z., and Rudolph, K.L. (2007). Telomere shortening and ageing. Z Gerontol Geriatr *40*, 314-324.

Karwacki-Neisius, V., Goke, J., Osorno, R., Halbritter, F., Ng, J.H., Weisse, A.Y., Wong, F.C., Gagliardi, A., Mullin, N.P., Festuccia, N.*, et al.* (2013). Reduced oct4 expression directs a robust pluripotent state with distinct signaling activity and increased enhancer occupancy by oct4 and nanog. Cell Stem Cell *12*, 531-545.

Kawamura, T., Suzuki, J., Wang, Y.V., Menendez, S., Morera, L.B., Raya, A., Wahl, G.M., and Izpisua Belmonte, J.C. (2009). Linking the p53 tumour suppressor pathway to somatic cell reprogramming. Nature *460*, 1140-1144.

Kim, N.W., Piatyszek, M.A., Prowse, K.R., Harley, C.B., West, M.D., Ho, P.L., Coviello, G.M., Wright, W.E., Weinrich, S.L., and Shay, J.W. (1994). Specific association of human telomerase activity with immortal cells and cancer. Science *266*, 2011-2015.

Kipling, D., and Cooke, H.J. (1990). Hypervariable ultra-long telomeres in mice. Nature *347*, 400-402.

Klose, R.J., and Bird, A.P. (2006). Genomic DNA methylation: the mark and its mediators. Trends Biochem Sci *31*, 89-97.

Koche, R.P., Smith, Z.D., Adli, M., Gu, H., Ku, M., Gnirke, A., Bernstein, B.E., and Meissner, A. (2011). Reprogramming factor expression initiates widespread targeted chromatin remodeling. Cell Stem Cell *8*, 96-105.

Komarov, P.G., Komarova, E.A., Kondratov, R.V., Christov-Tselkov, K., Coon, J.S., Chernov, M.V., and Gudkov, A.V. (1999). A chemical inhibitor of p53 that protects mice from the side effects of cancer therapy. Science *285*, 1733-1737.

Kopp, J.L., Ormsbee, B.D., Desler, M., and Rizzino, A. (2008). Small increases in the level of Sox2 trigger the differentiation of mouse embryonic stem cells. Stem Cells *26*, 903-911.

Korfali, N., Wilkie, G.S., Swanson, S.K., Srsen, V., Batrakou, D.G., Fairley, E.A., Malik, P., Zuleger, N., Goncharevich, A., de Las Heras, J.*, et al.* (2010). The leukocyte nuclear envelope proteome varies with cell activation and contains novel transmembrane proteins that affect genome architecture. Mol Cell Proteomics *9*, 2571-2585.

Kunath, T., Saba-El-Leil, M.K., Almousailleakh, M., Wray, J., Meloche, S., and Smith, A. (2007). FGF stimulation of the Erk1/2 signalling cascade triggers transition of pluripotent embryonic stem cells from self-renewal to lineage commitment. Development *134*, 2895-2902.

Lafferty-Whyte, K., Cairney, C.J., Will, M.B., Serakinci, N., Daidone, M.G., Zaffaroni, N., Bilsland, A., and Keith, W.N. (2009). A gene expression signature classifying telomerase and ALT immortalization reveals an hTERT regulatory network and suggests a mesenchymal stem cell origin for ALT. Oncogene *28*, 3765-3774.

Lee, J., Sung, Y.H., Cheong, C., Choi, Y.S., Jeon, H.K., Sun, W., Hahn, W.C., Ishikawa, F., and Lee, H.W. (2008). TERT promotes cellular and organismal survival independently of telomerase activity. Oncogene *27*, 3754-3760.

Lee, K.H., Li, M., Michalowski, A.M., Zhang, X., Liao, H., Chen, L., Xu, Y., Wu, X., and Huang, J. (2010). A genomewide study identifies the Wnt signaling pathway as a major target of p53 in murine embryonic stem cells. Proc Natl Acad Sci U S A *107*, 69-74.

Li, E., Bestor, T.H., and Jaenisch, R. (1992). Targeted mutation of the DNA methyltransferase gene results in embryonic lethality. Cell *69*, 915-926.

Li, Y.Q. (2010). Master stem cell transcription factors and signaling regulation. Cellular reprogramming *12*, 3-13.

Lin, T., Chao, C., Saito, S., Mazur, S.J., Murphy, M.E., Appella, E., and Xu, Y. (2005). p53 induces differentiation of mouse embryonic stem cells by suppressing Nanog expression. Nat Cell Biol *7*, 165-171.

Liu, L., Bailey, S.M., Okuka, M., Munoz, P., Li, C., Zhou, L., Wu, C., Czerwiec, E., Sandler, L., Seyfang, A.*, et al.* (2007). Telomere lengthening early in development. Nat Cell Biol *9*, 1436-1441.

Liu, Y., Snow, B.E., Hande, M.P., Yeung, D., Erdmann, N.J., Wakeham, A., Itie, A., Siderovski, D.P., Lansdorp, P.M., Robinson, M.O.*, et al.* (2000). The telomerase reverse transcriptase is limiting and necessary for telomerase function in vivo. Curr Biol *10*, 1459-1462.

Loh, Y.H., Wu, Q., Chew, J.L., Vega, V.B., Zhang, W., Chen, X., Bourque, G., George, J., Leong, B., Liu, J.*, et al.* (2006). The Oct4 and Nanog transcription network regulates pluripotency in mouse embryonic stem cells. Nat Genet *38*, 431-440.

Lu, R., Yang, A., and Jin, Y. (2011). Dual functions of T-box 3 (Tbx3) in the control of self-renewal and extraembryonic endoderm differentiation in mouse embryonic stem cells. J Biol Chem *286*, 8425-8436.

Luke, B., and Lingner, J. (2009). TERRA: telomeric repeat-containing RNA. Embo J *28*, 2503-2510.

Lynch, M.D., Smith, A.J., De Gobbi, M., Flenley, M., Hughes, J.R., Vernimmen, D., Ayyub, H., Sharpe, J.A., Sloane-Stanley, J.A., Sutherland, L.*, et al.* (2012). An interspecies analysis reveals a key role for unmethylated CpG dinucleotides in vertebrate Polycomb complex recruitment. Embo J *31*, 317-329.

MacDonald, B.T., Tamai, K., and He, X. (2009). Wnt/beta-catenin signaling: components, mechanisms, and diseases. Dev Cell *17*, 9-26.

Mak, W., Nesterova, T.B., de Napoles, M., Appanah, R., Yamanaka, S., Otte, A.P., and Brockdorff, N. (2004). Reactivation of the paternal X chromosome in early mouse embryos. Science *303*, 666-669.

Margueron, R., and Reinberg, D. (2011). The Polycomb complex PRC2 and its mark in life. Nature *469*, 343-349.

Marion, R.M., Strati, K., Li, H., Murga, M., Blanco, R., Ortega, S., Fernandez-Capetillo, O., Serrano, M., and Blasco, M.A. (2009a). A p53-mediated DNA damage response limits reprogramming to ensure iPS cell genomic integrity. Nature *460*, 1149-1153.

Marion, R.M., Strati, K., Li, H., Tejera, A., Schoeftner, S., Ortega, S., Serrano, M., and Blasco, M.A. (2009b). Telomeres acquire embryonic stem cell characteristics in induced pluripotent stem cells. Cell Stem Cell *4*, 141-154.

Martello, G., Sugimoto, T., Diamanti, E., Joshi, A., Hannah, R., Ohtsuka, S., Gottgens, B., Niwa, H., and Smith, A. (2012). Esrrb is a pivotal target of the Gsk3/Tcf3 axis regulating embryonic stem cell self-renewal. Cell Stem Cell *11*, 491-504.

Martin, A.M., Pouchnik, D.J., Walker, J.L., and Wyrick, J.J. (2004). Redundant roles for histone H3 N-terminal lysine residues in subtelomeric gene repression in Saccharomyces cerevisiae. Genetics *167*, 1123-1132.

Martin, G.R. (1980). Teratocarcinomas and mammalian embryogenesis. Science *209*, 768-776.

Martin, G.R. (1981). Isolation of a pluripotent cell line from early mouse embryos cultured in medium conditioned by teratocarcinoma stem cells. Proc Natl Acad Sci U S A *78*, 7634-7638.

Martin, G.R., and Evans, M.J. (1975). Differentiation of clonal lines of teratocarcinoma cells: formation of embryoid bodies in vitro. Proc Natl Acad Sci U S A *72*, 1441-1445.

Martinez, P., Thanasoula, M., Carlos, A.R., Gomez-Lopez, G., Tejera, A.M., Schoeftner, S., Dominguez, O., Pisano, D.G., Tarsounas, M., and Blasco, M.A. (2010). Mammalian Rap1 controls telomere function and gene expression through binding to telomeric and extratelomeric sites. Nat Cell Biol *12*, 768-780.

Matsuda, T., Nakamura, T., Nakao, K., Arai, T., Katsuki, M., Heike, T., and Yokota, T. (1999). STAT3 activation is sufficient to maintain an undifferentiated state of mouse embryonic stem cells. Embo J *18*, 4261-4269.

Matsuo, T., Shimose, S., Kubo, T., Fujimori, J., Yasunaga, Y., and Ochi, M. (2009). Telomeres and telomerase in sarcomas. Anticancer Res *29*, 3833-3836.

Mendenhall, E.M., Koche, R.P., Truong, T., Zhou, V.W., Issac, B., Chi, A.S., Ku, M., and Bernstein, B.E. (2010). GC-rich sequence elements recruit PRC2 in mammalian ES cells. PLoS Genet *6*, e1001244.

Messner, S., and Hottiger, M.O. (2011). Histone ADP-ribosylation in DNA repair, replication and transcription. Trends Cell Biol *21*, 534-542.

Migone, T.S., Rodig, S., Cacalano, N.A., Berg, M., Schreiber, R.D., and Leonard, W.J. (1998). Functional cooperation of the interleukin-2 receptor beta chain and Jak1 in phosphatidylinositol 3-kinase recruitment and phosphorylation. Mol Cell Biol *18*, 6416-6422.

Mikkelsen, T.S., Hanna, J., Zhang, X., Ku, M., Wernig, M., Schorderet, P., Bernstein, B.E., Jaenisch, R., Lander, E.S., and Meissner, A. (2008). Dissecting direct reprogramming through integrative genomic analysis. Nature *454*, 49-55.

Moss, E.G., and Tang, L. (2003). Conservation of the heterochronic regulator Lin-28, its developmental expression and microRNA complementary sites. Dev Biol *258*, 432-442.

Murnane, J.P., Sabatier, L., Marder, B.A., and Morgan, W.F. (1994). Telomere dynamics in an immortal human cell line. Embo J *13*, 4953-4962.

Nakatake, Y., Fukui, N., Iwamatsu, Y., Masui, S., Takahashi, K., Yagi, R., Yagi, K., Miyazaki, J., Matoba, R., Ko, M.S.*, et al.* (2006). Klf4 cooperates with Oct3/4 and

Sox2 to activate the Lefty1 core promoter in embryonic stem cells. Mol Cell Biol *26*, 7772-7782.

Navarro, P., Festuccia, N., Colby, D., Gagliardi, A., Mullin, N.P., Zhang, W., Karwacki-Neisius, V., Osorno, R., Kelly, D., Robertson, M.*, et al.* (2012). OCT4/SOX2-independent Nanog autorepression modulates heterogeneous Nanog gene expression in mouse ES cells. Embo J.

Nelson, J.D., Denisenko, O., and Bomsztyk, K. (2006). Protocol for the fast chromatin immunoprecipitation (ChIP) method. Nature protocols *1*, 179-185.

Neumann, A.A., Watson, C.M., Noble, J.R., Pickett, H.A., Tam, P.P.L., and Reddel, R.R. (2013). Alternative lengthening of telomeres in normal mammalian somatic cells. Genes Dev *27*, 18-23.

Nichols, J., and Smith, A. (2009). Naive and primed pluripotent states. Cell Stem Cell *4*, 487-492.

Nichols, J., Zevnik, B., Anastassiadis, K., Niwa, H., Klewe-Nebenius, D., Chambers, I., Scholer, H., and Smith, A. (1998). Formation of pluripotent stem cells in the mammalian embryo depends on the POU transcription factor Oct4. Cell *95*, 379-391.

Nishinakamura, R., Matsumoto, Y., Matsuda, T., Ariizumi, T., Heike, T., Asashima, M., and Yokota, T. (1999). Activation of Stat3 by cytokine receptor gp130 ventralizes Xenopus embryos independent of BMP-4. Dev Biol *216*, 481-490.

Niwa, H. (2007). How is pluripotency determined and maintained? Development *134*, 635-646.

Niwa, H., Miyazaki, J., and Smith, A.G. (2000). Quantitative expression of Oct-3/4 defines differentiation, dedifferentiation or self-renewal of ES cells. Nat Genet *24*, 372-376.

Niwa, H., Ogawa, K., Shimosato, D., and Adachi, K. (2009). A parallel circuit of LIF signalling pathways maintains pluripotency of mouse ES cells. Nature *460*, 118-122.

Okano, M., Bell, D.W., Haber, D.A., and Li, E. (1999). DNA methyltransferases Dnmt3a and Dnmt3b are essential for de novo methylation and mammalian development. Cell *99*, 247-257.

Paling, N.R., Wheadon, H., Bone, H.K., and Welham, M.J. (2004). Regulation of embryonic stem cell self-renewal by phosphoinositide 3-kinase-dependent signaling. J Biol Chem *279*, 48063-48070.

Palm, W., and de Lange, T. (2008). How shelterin protects mammalian telomeres. Annual review of genetics *42*, 301-334.

Park, J.I., Venteicher, A.S., Hong, J.Y., Choi, J., Jun, S., Shkreli, M., Chang, W., Meng, Z., Cheung, P., Ji, H.*, et al.* (2009). Telomerase modulates Wnt signalling by association with target gene chromatin. Nature *460*, 66-72.

Paull, T.T., Rogakou, E.P., Yamazaki, V., Kirchgessner, C.U., Gellert, M., and Bonner, W.M. (2000). A critical role for histone H2AX in recruitment of repair factors to nuclear foci after DNA damage. Curr Biol *10*, 886-895.

Petrie, K., Zelent, A., and Waxman, S. (2009). Differentiation therapy of acute myeloid leukemia: past, present and future. Curr Opin Hematol *16*, 84-91.

Phillips, D.M. (1963). The presence of acetyl groups of histones. Biochem J *87*, 258-263.

Pickett, H.A., Cesare, A.J., Johnston, R.L., Neumann, A.A., and Reddel, R.R. (2009). Control of telomere length by a trimming mechanism that involves generation of t-circles. The EMBO journal *28*, 799-809.

Pickett, H.A., Henson, J.D., Au, A.Y., Neumann, A.A., and Reddel, R.R. (2011). Normal mammalian cells negatively regulate telomere length by telomere trimming. Hum Mol Genet *20*, 4684-4692.

Prowse, K.R., and Greider, C.W. (1995). Developmental and tissue-specific regulation of mouse telomerase and telomere length. Proc Natl Acad Sci U S A *92*, 4818-4822.

Qin, H., Yu, T., Qing, T., Liu, Y., Zhao, Y., Cai, J., Li, J., Song, Z., Qu, X., Zhou, P.*, et al.* (2007). Regulation of apoptosis and differentiation by p53 in human embryonic stem cells. J Biol Chem *282*, 5842-5852.

Ramsahoye, B.H., Biniszkiewicz, D., Lyko, F., Clark, V., Bird, A.P., and Jaenisch, R. (2000). Non-CpG methylation is prevalent in embryonic stem cells and may be mediated by DNA methyltransferase 3a. Proc Natl Acad Sci U S A *97*, 5237-5242.

Rodda, D.J., Chew, J.L., Lim, L.H., Loh, Y.H., Wang, B., Ng, H.H., and Robson, P. (2005). Transcriptional regulation of nanog by OCT4 and SOX2. J Biol Chem *280*, 24731-24737.

Roth, A., Harley, C.B., and Baerlocher, G.M. (2010). Imetelstat (GRN163L)--telomerase-based cancer therapy. Recent Results Cancer Res *184*, 221-234.

Royle, N.J., Foxon, J., Jeyapalan, J.N., Mendez-Bermudez, A., Novo, C.L., Williams, J., and Cotton, V.E. (2008a). Telomere length maintenance--an ALTernative mechanism. Cytogenet Genome Res *122*, 281-291.

Royle, N.J., Foxon, J., Jeyapalan, J.N., Mendez-Bermudez, A., Novo, C.L., Williams, J., and Cotton, V.E. (2008b). Telomere length maintenance--an ALTernative mechanism. Cytogenet Genome Res *122*, 281-291.

Sabapathy, K., Klemm, M., Jaenisch, R., and Wagner, E.F. (1997). Regulation of ES cell differentiation by functional and conformational modulation of p53. Embo J *16*, 6217-6229.

Sansom, O.J., Reed, K.R., van de Wetering, M., Muncan, V., Winton, D.J., Clevers, H., and Clarke, A.R. (2005). Cyclin D1 is not an immediate target of beta-catenin following Apc loss in the intestine. J Biol Chem *280*, 28463-28467.

Sarin, K.Y., Cheung, P., Gilison, D., Lee, E., Tennen, R.I., Wang, E., Artandi, M.K., Oro, A.E., and Artandi, S.E. (2005). Conditional telomerase induction causes proliferation of hair follicle stem cells. Nature *436*, 1048-1052.

Savarese, F., Davila, A., Nechanitzky, R., De La Rosa-Velazquez, I., Pereira, C.F., Engelke, R., Takahashi, K., Jenuwein, T., Kohwi-Shigematsu, T., Fisher, A.G.*, et al.* (2009). Satb1 and Satb2 regulate embryonic stem cell differentiation and Nanog expression. Genes Dev *23*, 2625-2638.

Saxonov, S., Berg, P., and Brutlag, D.L. (2006). A genome-wide analysis of CpG dinucleotides in the human genome distinguishes two distinct classes of promoters. Proc Natl Acad Sci U S A *103*, 1412-1417.

Schoeftner, S., and Blasco, M.A. (2010). Chromatin regulation and non-coding RNAs at mammalian telomeres. Semin Cell Dev Biol *21*, 186-193.

Schoeftner, S., Sengupta, A.K., Kubicek, S., Mechtler, K., Spahn, L., Koseki, H., Jenuwein, T., and Wutz, A. (2006). Recruitment of PRC1 function at the initiation of X inactivation independent of PRC2 and silencing. Embo J *25*, 3110-3122.

Selwood, L., and Johnson, M.H. (2006). Trophoblast and hypoblast in the monotreme, marsupial and eutherian mammal: evolution and origins. Bioessays *28*, 128-145.

Shay, J.W., and Wright, W.E. (2010). Telomeres and telomerase in normal and cancer stem cells. FEBS Lett *584*, 3819-3825.

Shen, X., Liu, Y., Hsu, Y.J., Fujiwara, Y., Kim, J., Mao, X., Yuan, G.C., and Orkin, S.H. (2008). EZH1 mediates methylation on histone H3 lysine 27 and complements EZH2 in maintaining stem cell identity and executing pluripotency. Molecular cell *32*, 491-502.

Shi, W., Wang, H., Pan, G., Geng, Y., Guo, Y., and Pei, D. (2006). Regulation of the pluripotency marker Rex-1 by Nanog and Sox2. J Biol Chem *281*, 23319-23325.

Silva, J., Nichols, J., Theunissen, T.W., Guo, G., van Oosten, A.L., Barrandon, O., Wray, J., Yamanaka, S., Chambers, I., and Smith, A. (2009). Nanog is the gateway to the pluripotent ground state. Cell *138*, 722-737.

Silva, J., and Smith, A. (2008). Capturing pluripotency. Cell *132*, 532-536.

Singh, A.M., Hamazaki, T., Hankowski, K.E., and Terada, N. (2007). A heterogeneous expression pattern for Nanog in embryonic stem cells. Stem Cells *25*, 2534-2542.

Sinkkonen, L., Hugenschmidt, T., Berninger, P., Gaidatzis, D., Mohn, F., Artus-Revel, C.G., Zavolan, M., Svoboda, P., and Filipowicz, W. (2008). MicroRNAs control de novo DNA methylation through regulation of transcriptional repressors in mouse embryonic stem cells. Nat Struct Mol Biol *15*, 259-267.

Smith, Z.D., and Meissner, A. (2013). DNA methylation: roles in mammalian development. Nat Rev Genet *14*, 204-220.

Smogorzewska, A., and de Lange, T. (2002). Different telomere damage signaling pathways in human and mouse cells. Embo J *21*, 4338-4348.

Softic, S., Kirby, M., Berger, N.G., Shroyer, N.F., Woods, S.C., and Kohli, R. (2012). Insulin concentration modulates hepatic lipid accumulation in mice in part via transcriptional regulation of fatty acid transport proteins. PLoS One *7*, e38952.

Stock, J.K., Giadrossi, S., Casanova, M., Brookes, E., Vidal, M., Koseki, H., Brockdorff, N., Fisher, A.G., and Pombo, A. (2007). Ring1-mediated ubiquitination

of H2A restrains poised RNA polymerase II at bivalent genes in mouse ES cells. Nat Cell Biol *9*, 1428-1435.

Strong, M.A., Vidal-Cardenas, S.L., Karim, B., Yu, H., Guo, N., and Greider, C.W. (2011). Phenotypes in mTERT(+)/(-) and mTERT(-)/(-) mice are due to short telomeres, not telomere-independent functions of telomerase reverse transcriptase. Mol Cell Biol *31*, 2369-2379.

Taboski, M.A.S., Sealey, D.C.F., Dorrens, J., Tayade, C., Betts, D.H., and Harrington, L. (2012). Long telomeres bypass the requirement for long telomeres in human tumorigenesis. Cell Reports *1*, 91-98.

Takahashi, K., and Yamanaka, S. (2006). Induction of pluripotent stem cells from mouse embryonic and adult fibroblast cultures by defined factors. Cell *126*, 663-676.

Tilman, G., Loriot, A., Van Beneden, A., Arnoult, N., Londono-Vallejo, J.A., De Smet, C., and Decottignies, A. (2009). Subtelomeric DNA hypomethylation is not required for telomeric sister chromatid exchanges in ALT cells. Oncogene *28*, 1682-1693.

Tomida, M., Yamamoto-Yamaguchi, Y., and Hozumi, M. (1984). Purification of a factor inducing differentiation of mouse myeloid leukemic M1 cells from conditioned medium of mouse fibroblast L929 cells. J Biol Chem *259*, 10978-10982.

Tsumura, A., Hayakawa, T., Kumaki, Y., Takebayashi, S., Sakaue, M., Matsuoka, C., Shimotohno, K., Ishikawa, F., Li, E., Ueda, H.R.*, et al.* (2006). Maintenance of self-renewal ability of mouse embryonic stem cells in the absence of DNA

methyltransferases Dnmt1, Dnmt3a and Dnmt3b. Genes to cells : devoted to molecular & cellular mechanisms *11*, 805-814.

Tysnes, B.B. (2010). Tumor-initiating and -propagating cells: cells that we would like to identify and control. Neoplasia *12*, 506-515.

Vastenhouw, N.L., and Schier, A.F. (2012). Bivalent histone modifications in early embryogenesis. Curr Opin Cell Biol *24*, 374-386.

Vaziri, H., and Benchimol, S. (1998). Reconstitution of telomerase activity in normal human cells leads to elongation of telomeres and extended replicative life span. Curr Biol *8*, 279-282.

Vera, E., Canela, A., Fraga, M.F., Esteller, M., and Blasco, M.A. (2008). Epigenetic regulation of telomeres in human cancer. Oncogene *27*, 6817-6833.

Villasante, A., Piazzolla, D., Li, H., Gomez-Lopez, G., Djabali, M., and Serrano, M. (2011). Epigenetic regulation of Nanog expression by Ezh2 in pluripotent stem cells. Cell cycle *10*, 1488-1498.

Wang, Z., Zang, C., Cui, K., Schones, D.E., Barski, A., Peng, W., and Zhao, K. (2009). Genome-wide mapping of HATs and HDACs reveals distinct functions in active and inactive genes. Cell *138*, 1019-1031.

Watanabe, S., Umehara, H., Murayama, K., Okabe, M., Kimura, T., and Nakano, T. (2006). Activation of Akt signaling is sufficient to maintain pluripotency in mouse and primate embryonic stem cells. Oncogene *25*, 2697-2707.

Weng, N.P., Levine, B.L., June, C.H., and Hodes, R.J. (1996). Regulated expression of telomerase activity in human T lymphocyte development and activation. J Exp Med *183*, 2471-2479.

Wu, H., and Zhang, Y. (2011). Mechanisms and functions of Tet protein-mediated 5-methylcytosine oxidation. Genes Dev *25*, 2436-2452.

Yeom, Y.I., Fuhrmann, G., Ovitt, C.E., Brehm, A., Ohbo, K., Gross, M., Hubner, K., and Scholer, H.R. (1996). Germline regulatory element of Oct-4 specific for the totipotent cycle of embryonal cells. Development *122*, 881-894.

Ying, Q.L., Nichols, J., Chambers, I., and Smith, A. (2003). BMP induction of Id proteins suppresses differentiation and sustains embryonic stem cell self-renewal in collaboration with STAT3. Cell *115*, 281-292.

Yu, J., Vodyanik, M.A., Smuga-Otto, K., Antosiewicz-Bourget, J., Frane, J.L., Tian, S., Nie, J., Jonsdottir, G.A., Ruotti, V., Stewart, R.*, et al.* (2007). Induced pluripotent stem cell lines derived from human somatic cells. Science *318*, 1917-1920.

Yuan, H., Corbi, N., Basilico, C., and Dailey, L. (1995). Developmental-specific activity of the FGF-4 enhancer requires the synergistic action of Sox2 and Oct-3. Genes Dev *9*, 2635-2645.

Zalzman, M., Falco, G., Sharova, L.V., Nishiyama, A., Thomas, M., Lee, S.L., Stagg, C.A., Hoang, H.G., Yang, H.T., Indig, F.E.*, et al.* (2010). Zscan4 regulates telomere elongation and genomic stability in ES cells. Nature *464*, 858-863.

Zentner, G.E., and Henikoff, S. (2013). Regulation of nucleosome dynamics by histone modifications. Nat Struct Mol Biol *20*, 259-266.

Zhang, X., Mar, V., Zhou, W., Harrington, L., and Robinson, M.O. (1999). Telomere shortening and apoptosis in telomerase-inhibited human tumor cells. Genes Dev *13*, 2388-2399.

Zheng, X., and Hu, G. (2012). Oct4GiP reporter assay to study genes that regulate mouse embryonic stem cell maintenance and self-renewal. J Vis Exp.

Zhu, H., Shyh-Chang, N., Segre, A.V., Shinoda, G., Shah, S.P., Einhorn, W.S., Takeuchi, A., Engreitz, J.M., Hagan, J.P., Kharas, M.G.*, et al.* (2011). The Lin28/let-7 axis regulates glucose metabolism. Cell *147*, 81-94.

Ziller, M.J., Muller, F., Liao, J., Zhang, Y., Gu, H., Bock, C., Boyle, P., Epstein, C.B., Bernstein, B.E., Lengauer, T.*, et al.* (2011). Genomic distribution and inter-sample variation of non-CpG methylation across human cell types. PLoS Genet *7*, e1002389.

Appendix A

I declare to have been allowed to reproduce the following contents from Elsevier.

License number: 3159540195836.

Cell Stem Cell
Short Article

Short Telomeres in ESCs Lead to Unstable Differentiation

Fabio Pucci,[1] Laura Gardano,[1] and Lea Harrington[1,2,*]
[1]Wellcome Trust Centre for Cell Biology and Institute of Cell Biology, School of Biological Sciences, Michael Swann Building, The University of Edinburgh, Edinburgh EH9 3JR, Scotland, UK
[2]Institut de Recherche en Immunologie et en Cancérologie, Université de Montréal, 2950 Chemin de Polytechnique, Pavillon Marcelle-Coutu, Montréal, Québec H3T 1J4, Canada
*Correspondence: lea.harrington@umontreal.ca
http://dx.doi.org/10.1016/j.stem.2013.01.018

SUMMARY

Functional telomeres are critical for stem cell proliferation; however, whether they are equally important for the stability of stem cell differentiation is not known. We found that mouse embryonic stem cells (ESCs) with critically short telomeres (*Tert*$^{-/-}$ ESCs) initiated normal differentiation after leukemia inhibitory factor (LIF) withdrawal but, unlike control ESCs, failed to maintain stable differentiation when LIF was reintroduced to the growth medium. *Tert*$^{-/-}$ ESCs expressed higher levels of Nanog and, overall, had decreased genomic CpG methylation levels, which included the promoters of *Oct4* and *Nanog*. This unstable differentiation phenotype could be rescued by telomere elongation via reintroduction of *Tert*, via suppression of Nanog by small hairpin RNA (shRNA) knockdown, or via enforced expression of the de novo DNA methyltransferase 3b. These results demonstrate an unexpected role of functional telomeres in the genome-wide epigenetic regulation of cell differentiation and suggest a potentially important role of telomere instability in cell fate during development or disease.

INTRODUCTION

Murine embryonic stem cells (ESCs) are self-renewing, pluripotent cells able to differentiate into cells of all three germ layers. Pluripotency and self-renewal are maintained primarily by the core transcriptional factors Nanog, Oct4, and Sox2 (Heng et al., 2010) but require both the cooperation of other factors and coregulators (Li, 2010) and an efficient telomere maintenance mechanism (Huang et al., 2011). In mammals, telomere maintenance is achieved via a telomerase reverse transcriptase (*Tert*) and an integral RNA component (*Terc*) that synthesize new telomeric DNA during cell proliferation. An appropriate telomere maintenance system is important for ESC replicative potential (Agarwal et al., 2010; Batista et al., 2011; Marion et al., 2009). During the reprogramming of differentiated cells into stem cells, an increase in telomerase activity leads to telomere elongation and the acquisition of epigenetic marks characteristic of longer telomeres (Marion et al., 2009). Notably, the teratoma-forming ability of ESCs derived from late generation (G3–G4) *Terc*$^{-/-}$ mice with critically short telomeres is greatly reduced (Huang et al., 2011).

RESULTS

Critically Short Telomeres in ESCs Lead to Elevated Basal Levels of Nanog

We sought to address the impact of telomere dysfunction not only upon the capacity for cell differentiation but also upon the maintenance of a differentiated state. Late-passage *Tert*$^{-/-}$ ESCs (*Tert*$^{-/-S}$) (Liu et al., 2000) that possessed shorter telomeres and a significant accumulation of telomere signal-free ends relative to wild-type (WT) ESCs or *Tert*$^{-/-}$ cells at earlier passages (*Tert*$^{-/-L}$) (Figures S1A–S1C available online; $p < 0.0001$; Fisher's exact test) were nonetheless proliferation-competent and did not exhibit an altered doubling time, cell morphology, or cell-cycle distribution (Figures S1D and S1E; data not shown). However, *Nanog* messenger RNA (mRNA) and protein levels were significantly elevated (Figures 1A–1C and S1F–S1G). No difference was observed in *Oct4*, *Sox2*, and *Klf4* expression (Figures 1C and S1F). To test whether the difference in Nanog expression was related to telomere dysfunction, we reintroduced WT *Tert* into late-passage *Tert*$^{-/-}$ ESCs (*Tert*$^{-/-R}$), and, after the propagation of clonal lines expressing *Tert*, we observed the reparation of telomere signal-free ends and a restoration of Nanog levels closer to the levels observed in WT ESCs and *Tert*$^{-/-}$ ESCs at early passage (Figures 1A–1D, S1A–S1C, S1F, and S1G). Transient expression of *Tert* for 72 hr, a period of time insufficient to permit telomere extension, failed to restore Nanog to levels comparable to WT ESCs (data not shown). These data suggest that the dysregulation of Nanog in *Tert*$^{-/-S}$ ESCs is a consequence of critically short telomeres.

ESCs that express high levels of Nanog tend to self-renew, whereas cells that express low levels of this factor tend to differentiate (Chambers et al., 2007; Savarese et al., 2009; Singh et al., 2007). Immunofluorescence analysis of *Tert*$^{-/-S}$ ESCs cultured on gelatin in leukemia inhibitory factor (LIF)-containing media revealed a significant increase in the percentage of Nanog^{high} cells in comparison to WT and *Tert*$^{-/-R}$ ESCs (Figures 1A and S1G) (Savarese et al., 2009). We confirmed elevated Nanog expression in *Tert*$^{-/-S}$ ESCs via fluorescence-activated cell sorting (FACS) analysis (Figure 1B). We also measured the

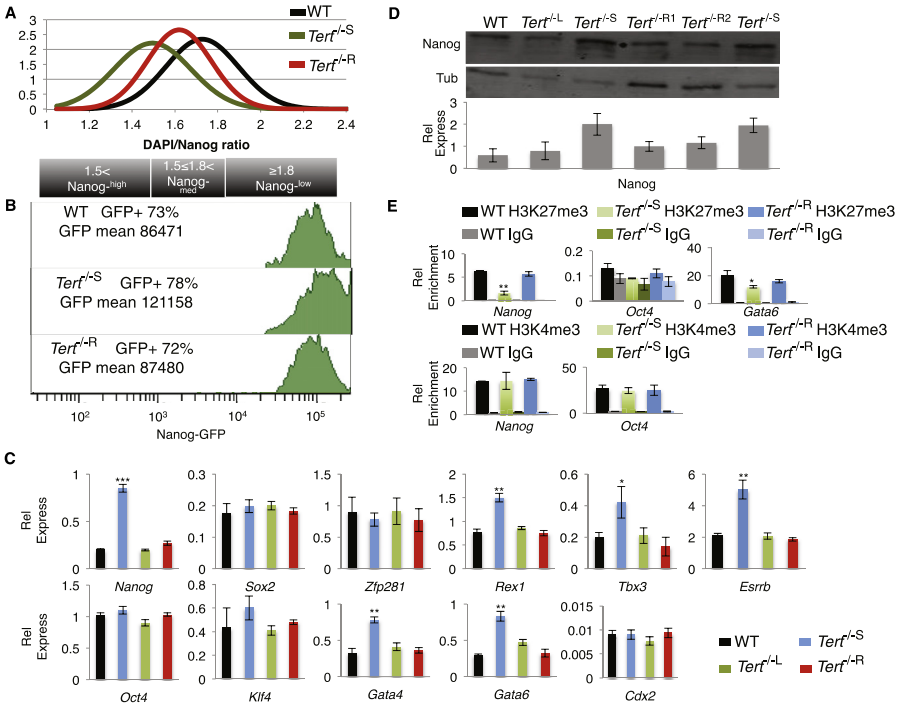

Figure 1. Analysis of Pluripotency Factors in WT and *Tert*$^{-/-}$ ESCs

(A) Quantification of Nanog levels normalized over DAPI (see Figure S1G for corresponding immunofluorescence images). Note a significant shift ($p < 0.0001$) from Nanog-low (DAPI to Nanog-488 ≥ 1.8) to Nanog-high (DAPI to Nanog-488 < 1.5) cells in *Tert*$^{-/-S}$ in comparison to WT and *Tert*$^{-/-R}$ ESCs ($n \geq 100$ per cell population).

(B) FACS analysis of the Nanog expression profile in the same genotypes as in (A). Note the rightward shift and increase in average Nanog signal intensity in *Tert*$^{-/-S}$ ESCs.

(C) Relative gene expression analyzed by qRT-PCR, normalized to *GAPDH* ($n = 4$). Data are represented as mean ± SD.

(D) (Top) Nanog protein expression with LI-COR quantification below ($n = 3$). Data are represented as mean ± SD; L, long telomeres (passage 30); S, short telomeres (passage 70); R, *Tert* rescue (70 passages, followed by clonal selection and an additional 4 passages after *Tert* reintroduction). The superscripts 1 and 2 indicate two independently generated *Tert*$^{-/-R}$ colonies.

(E) ChIP analysis using an antibody to H3K27me3 and H3K4me3. Relative enrichment was quantified with the use of region-specific qPCR primers for *Nanog*, *Oct4*, and *Gata6* promoters. Generic IgG was used as a control ($n = 3$). Data are represented as mean ± SD. *, $p < 0.05$; **, $p < 0.01$; ***, $p < 0.0001$.

See also Figure S1 and Table S1.

expression of other factors involved in the pluripotency regulatory network (*Rex1*, *Esrrb*, and *Tbx3*) (Festuccia et al., 2012; Ivanova et al., 2006; Shi et al., 2006), including pluripotency factors that negatively regulate Nanog expression (*Zfp281*) (Fidalgo et al., 2011) and lineage differentiation markers (*Cdx2*) and the endoderm markers (*Gata6* and *Gata4*) that are negatively regulated by Nanog (Singh et al., 2007). As anticipated, *Rex1*, *Esrrb*, and *Tbx3* mRNA levels were increased in *Tert*$^{-/-S}$ ESCs, whereas *Zpf281* and *Cdx2* levels were unaffected (Figure 1C).

However, *Gata6* and *Gata4* were also increased (Figure 1C). Consistent with these observations, chromatin immunoprecipitation (ChIP) analysis revealed lower levels of Nanog occupancy on the *Gata6* promoter (Figure S1I). Nevertheless, the recruitment of Nanog to its own promoter, which represses its own expression (Fidalgo et al., 2011), increased in *Tert*$^{-/-S}$ ESCs (Figure S1I). Thus, the increased expression of *Nanog* is not a consequence of the impaired occupancy of Nanog on its own promoter.

Perturbations in H3K27me3 Are Associated with Critically Short Telomeres

Telomere attrition is associated with the loss of certain heterochromatin markers and DNA hypomethylation at telomeric and subtelomeric regions (Benetti et al., 2007). We postulated that the increase in *Nanog* expression could be linked to a general dysregulation of epigenetic repression, given that low levels of trimethylation on histone H3 lysine 27 (H3K27me3) promote *Nanog* and *Gata6* expression (Lu et al., 2011; Shen et al., 2008; Villasante et al., 2011). H3K27me3 was reduced at *Nanog* and *Gata6* promoters in $Tert^{-/-S}$ ESCs, whereas H3K4me3 levels at the *Nanog* promoter were unaffected (Figure 1E). H3K27me3 and H3K4me3 enrichment on the *Oct4* promoter was unaffected (Figure 1E). These perturbations, including a slightly increased level of global H3K27me3 in $Tert^{-/-S}$ ESCs, were restored upon telomere elongation (Figures 1E and S1H). These changes were not accompanied by a significant alteration in the three-dimensional localization of telomere DNA or chromatin in interphase nuclei (Figure S1J). Thus, the altered expression of *Nanog* and *Gata6* reflects changes in heterochromatin at their respective promoters independent of Nanog occupancy. Moreover, these results demonstrate that critically short telomeres also affect chromatin organization at loci distal to telomeres.

Critically Short Telomeres Perturb the Ability of ESCs to Remain Stably Differentiated

The impact of Nanog misregulation upon differentiation was tested by treating ESCs with 5 μM all-*trans* retinoic acid (ATRA), which was followed by the removal of ATRA and the readdition of LIF-containing media (Figure 2). Although longer ATRA treatment times were required to achieve suppression of *Oct4*, *Nanog*, and *Sox2* mRNA and protein to levels comparable to WT or $Tert^{-/-}$ ESCs with longer telomeres (Figures 2A–2D and S2), $Tert^{-/-S}$ ESCs nevertheless exhibited a low proliferative capacity after ATRA treatment, which was consistent with a differentiated state (Figure 2E). However, after the readdition of LIF-containing media, $Tert^{-/-S}$ ESCs failed to maintain repression of Nanog and exhibited robust colony formation only 6 days after the readdition of LIF-containing media (Figures 2 and S2). As an independent marker of differentiation, WT and $Tert^{-/-S}$ cells were transduced with an *Oct4* promoter-driven green fluorescent protein (GFP) construct, treated with ATRA for 12 days, and then sorted to allow the selection of the GFP-negative population by FACS. Sorted GFP-negative cells were plated in the presence of LIF-containing media for 10 days, followed by an assessment of the percentage of GFP-positive cells. $Tert^{-/-S}$ cells exhibited a high percentage of GFP-positive cells after the readdition of LIF-containing media (Figure 2F). These results demonstrate that ESCs with telomere dysfunction were able to execute only an incomplete, transitory repression of pluripotency genes in response to differentiation cues.

ESCs with Short Telomeres Exhibit DNA Hypomethylation

Critically short telomeres are associated with DNA hypomethylation at subtelomeric DNA (Benetti et al., 2007). Given that we observed chromatin alterations at loci distal to telomeres, we tested whether $Tert^{-/-S}$ ESCs also exhibited altered DNA methylation throughout the genome. Bisulphite-sequencing analysis of the *Nanog* and *Oct4* promoters revealed a significant reduction in the acquisition of methylated cytosine in $Tert^{-/-S}$ ESCs treated with ATRA relative to WT or $Tert^{-/-R}$ ESCs ($p \leq 0.01$ and $p < 0.0001$, respectively; Fisher's exact test) (Figure 3A). Furthermore, $Tert^{-/-S}$ ESCs failed to maintain even this level of cytosine methylation after the readdition of the LIF-containing media ($p < 0.0001$ and $p = 0.03$, respectively). At both promoters, this impairment was rescued in $Tert^{-/-R}$ ESCs ($p > 0.05$; Figure 3A). Genome-wide methylation measured by an ELISA-based detection system against methylcytosine was also significantly reduced in $Tert^{-/-S}$ ESCs (Figure 3B). Nonspecific epigenetic drift appeared improbable, given that WT and $Tert^{-/-R}$ ESCs did not exhibit these changes after a similar propagation period. Although ESCs can tolerate DNA hypomethylation without impairment of cell proliferation (Tsumura et al., 2006), hypomethylation nonetheless impairs the capability of ESCs to achieve, and maintain a differentiated state (Feldman et al., 2006; Jackson et al., 2004; Sinkkonen et al., 2008). Thus, DNA hypomethylation in $Tert^{-/-S}$ ESCs arose in response to critically short telomeres and impeded their stable differentiation.

Restoration of Dnmt3b or Depletion of Nanog Rescue the Stable Differentiation of ESCs with Short Telomeres

We tested whether the restoration of DNA methylation might restore the differentiation capability of $Tert^{-/-S}$ ESCs. In mammals, genomic DNA methylation is principally regulated by three DNA methyltransferases (Dnmts): Dnmt1 (methylation maintenance) and the de novo methyltransferases Dnmt3a and Dnmt3b (Li et al., 1992; Okano et al., 1999). Although Dnmt1 expression was unaffected in $Tert^{-/-S}$ ESCs, the expression of de novo methylases was reduced (Figure 3C). Enforced expression of Dnmt3b in $Tert^{-/-S}$ ESCs restored repression of Nanog (Figures 3D, 3E, and S3(A) and restored the repression of *Nanog*, *Oct4*, and *Sox2* mRNA upon ATRA treatment (Figures 4A and 4B). Dnmt3b expression also led to a significant reduction in the colony formation of $Tert^{-/-S}$ ESCs after the readdition of LIF-containing media (Figure 4C). The level of H3K27me3 at the *Nanog* promoter was also partially rescued in $Tert^{-/-S}$ ESCs that expressed elevated Dnmt3b (Figure 4D). Consistent with a direct role of Nanog suppression in the maintenance of stable differentiation, Nanog depletion by small hairpin RNA (shRNA) was sufficient to overcome the inability of $Tert^{-/-S}$ ESCs to remain differentiated (Figure 4C), and all genotypes transduced with *Nanog* shRNA exhibited a decrease in pluripotency gene expression (Figure S4). These results demonstrate that the mechanism of impaired ability to maintain stable differentiation in $Tert^{-/-S}$ ESCs acts via the perturbation of de novo DNA methylation, which, in turn, influences chromatin organization and the ability to repress pluripotency factors such as *Nanog* under differentiation conditions.

DISCUSSION

Here, we report that critically short telomeres led to genome-wide DNA hypomethylation and that changes in H3K27 trimethylation occurred at loci distal to telomeres. The trimethylation of H3K27 is mediated by the polycomb repressive complex 2 (PRC2) and is associated with ESC identity (Shen et al., 2008). H3K27me3 is one of the principal histone repression markers,

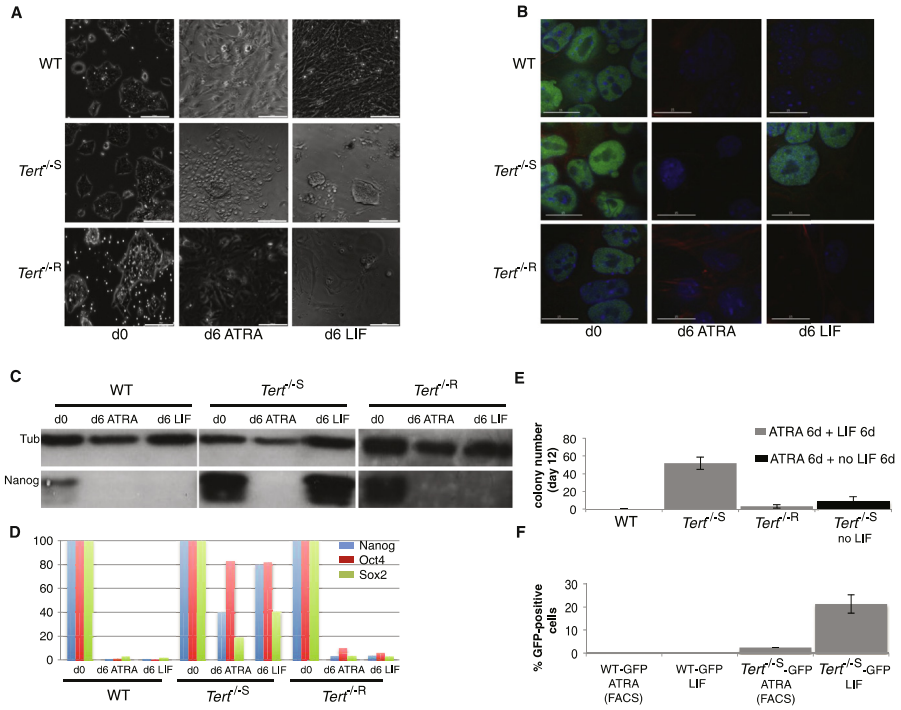

Figure 2. Differentiation Analysis of *Tert*$^{-/-}$ ESCs

(A) Bright field images of ESC populations at day 0 and day 6 in media containing 5 μM all-*trans* retinoic acid (ATRA) and, after ATRA removal, an additional 6 days in LIF-containing media. The micrograph bar indicates 200 μm for bright field images and15 μm for immunofluorescence images.

(B) Nanog immunofluorescence analysis (green, Nanog; red, Actin).

(C) Nanog protein detection by western blot. Tub, β-tubulin (n = 3).

(D) qRT-PCR analysis of pluripotency genes after ATRA-induced differentiation. Gene expression at day 0 was arbitrarily set as 100, and the expression through the time course was normalized to mRNA levels at day 0. Values were expressed as a ratio to *GAPDH*.

(E) Single-colony formation assay after ATRA treatment (6 days) is shown, and, where indicated, the readdition of LIF-containing media (6 days) (n = 3) is shown. The difference in the incidence of colony formation between *Tert*$^{-/-S}$ (after LIF readdition) and all the other genotypes (or *Tert*$^{-/-S}$ without LIF) was statistically significant ($p < 0.0001$; ANOVA and related Dunnett's test comparing every group with *Tert*$^{-/-S}$ values). The y axis indicates colony number. Data are represented as mean ± SD.

(F) *Oct4*-promoter-driven GFP expression analysis of WT and *Tert*$^{-/-S}$ ESCs post-ATRA treatment and after cell sorting for GFP-negative cells. The y axis indicates the percentage of GFP-positive WT, or *Tert*$^{-/-}$ cells after 12 days of ATRA treatment and FACS sorting (FACS; columns 1 and 3) and after the readdition of LIF-containing media to GFP-negative sorted cells (columns 2 and 4). The difference in the incidence of GFP-positive cells between *Tert*$^{-/-S}$ and WT cells was statistically significant ($p < 0.00001$; Welch's unpaired t test). Data are represented as mean ± SD.

See also Figure S2.

and its diminished enrichment on *Nanog* and *Gata6* promoters has been linked to the upregulation of these genes (Kim et al., 2008; Lu et al., 2011; Shen et al., 2008; Villasante et al., 2011). Although the global level of H3K27me3 increased in *Tert*$^{-/-S}$ ESCs similar to recent studies that associate H3K27me3 enrichment with unmethylated CpG islands, its presence at *Nanog* and *Gata6* promoters was reduced (Lynch et al., 2012; Mendenhall et al., 2010). These data support the observation that DNA hypomethylation leads to overall increased levels of H3K27me3 in normally methylated regions but decreased levels of H3K27me3 in ordinarily unmethylated regions (Brinkman et al., 2012). Our data suggest a model whereby telomere-shortening-induced de novo Dnmt downregulation leads to DNA hypomethylation and altered H3K27me3 enrichment at promoters, which, in turn, affects the ability to repress pluripotency factors critical to stable differentiation in ESCs (Figure 4E).

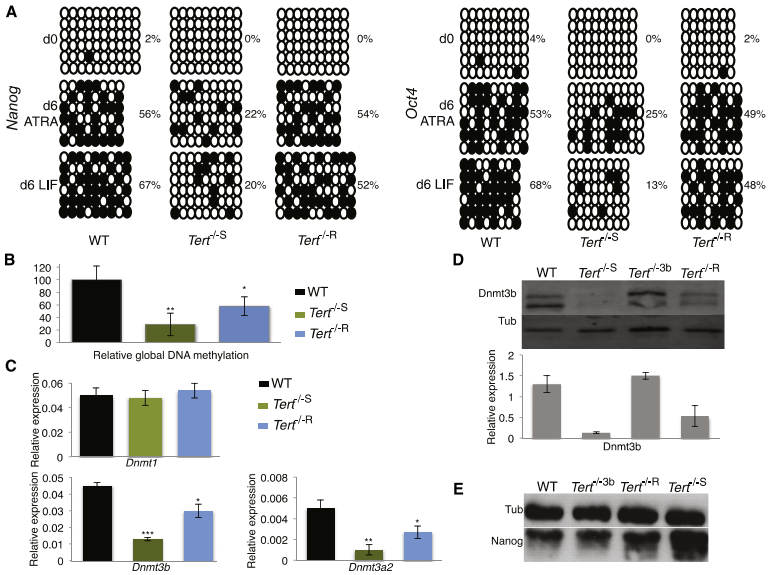

Figure 3. Expression of DNA Methyltransferases in ESCs Lacking *Tert*

(A) CpG methylation analysis of the *Oct4* and *Nanog* promoters during ATRA treatment, followed by culture in LIF-containing media. Each column represents CpGs in a sequenced clone. Full dots symbolize methylated CpGs, and empty dots symbolize unmethylated CpGs. Percentage values indicate the proportion of methylated cytosine relative to total cytosine residues (n = 10).

(B) Relative quantification of global DNA methylation (n = 3) is shown. Data are represented as mean ± SD.

(C) Relative gene expression of *Dnmt1*, *Dnmt3b*, and *Dnmt3a2* analyzed by qRT-PCR. Values were normalized to *GAPDH* (n = 4). Data are represented as mean ± SD.

(D) (Top) Dnmt3b protein detection by western blot and (bottom) after LI-COR quantification (n = 3). Data are represented as mean ± SD.

(E) Nanog protein detection by western blot. Tub, β-tubulin (n = 5); R, *Tert* rescue; 3b, *Dnmt3b* rescue. Passage numbers are as in Figure 1. *, $p < 0.05$; **, $p < 0.01$; ***, $p < 0.0001$.

See also Figure S3.

The regulation of factors that affect pluripotency and differentiation are important not only to development but also to disease. For example, pluripotency factors such as Nanog tend to be highly expressed in undifferentiated tumors and in putative cancer stem cells (Tysnes, 2010). In addition, some cancer therapies employ differentiation-inducing agents such as retinoic acid in the treatment of acute promyelocytic leukemia (Petrie et al., 2009). Thus, it will be important to test whether critically short telomeres also influence cell fate in human cancer cells, particularly in the case of telomerase-inhibition strategies designed to instigate telomere instability.

EXPERIMENTAL PROCEDURES

Cell Culture and Transfection

All experiments employed two separately generated ESC lines containing a disruption of endogenous *Tert*, as previously described (Liu et al., 2000). ESC lines were cultured on gelatin-covered dishes and maintained in Glasgow's Modified Eagle's Medium (GMEM; GIBCO) supplemented with 15% v/v fetal bovine serum (FBS), 0.055 mM β-mercaptoethanol (Sigma-Aldrich), 2 mM L-glutamine, 0.1 mM GMEM nonessential amino acids, 5,000 units/ml penicillin and streptomycin, 1,000 units/ml of recombinant LIF (Chemicon), and 1 μg/ml doxycycline and maintained at 37°C with 5% v/v CO_2. To restore *Tert* expression to $Tert^{-/-S}$ ESCs cells at passage, we cotransfected 70, ESCs with pTRE-Bi-*Tert*-IRES-EGFP-Hygro (or a similar vector lacking *Tert*) and CAG-rtTA advanced (pTET-ON advanced vector; Clontech). For constitutive expression of *Tert*, $Tert^{-/-S}$ ESCs were transfected with CAG-*mTert*-IRES-Puro or CAG-IRES-Puro. For expression of Dnmt3b, $Tert^{-/-S}$ ESCs were transfected with CAG-*Dnmt3b*-IRES-Puro or CAG-IRES-Puro. All transfections employed Fugene 6 (Roche) in a 3:1 ratio to DNA according to the manufacturer's instructions. For *Tert* rescue or *Dnmt3b* reintroduction, cells were propagated for four passages under selection with hygromycin (500 μg/ml) or puromycin (5 μg/ml), and individual colonies were isolated. For *Nanog* shRNA transduction, cells were infected with commercially available lentiviral particles (Santa Cruz Biotechnology) and selected with puromycin (5 μg/ml). Cell transduction with *Oct4*-promoter GFP was performed by infection with commercially available lentiviral particles (System Biosciences). All lentiviral infections were performed in the presence of Polybrene (5 μg/ml; Santa Cruz Biotechnology). All experiments were performed with more than one clonal isolate.

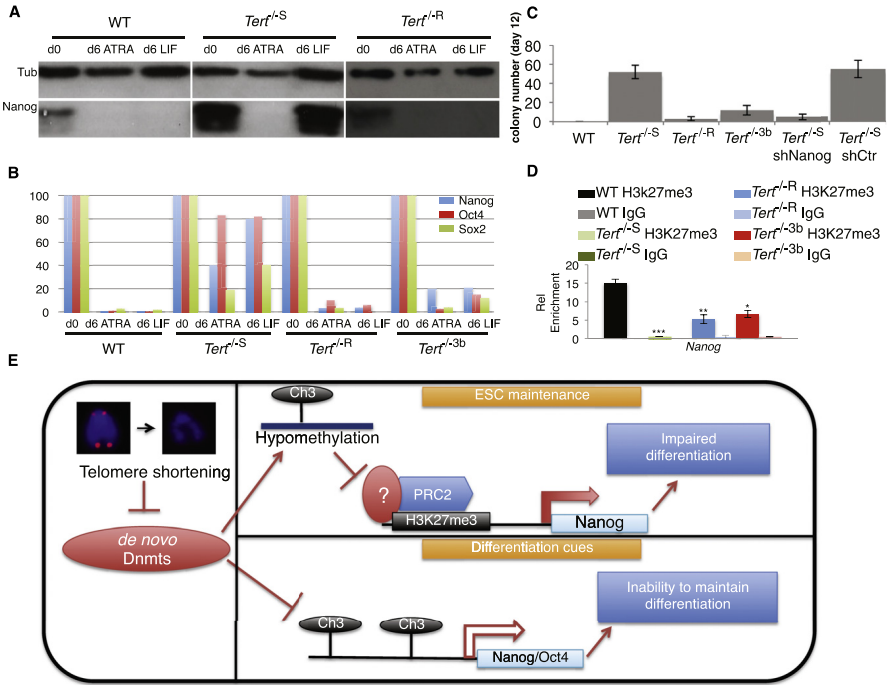

Figure 4. Differentiation Ability of *Tert*$^{-/-}$ ESCs after Enforced Expression of Dnmt3b

(A) Nanog protein detection by western blot. Tub, β-tubulin (n = 3). The first two panels on the left are reproduced from Figure 2C.

(B) qRT-PCR analysis of pluripotency genes upon ATRA-induced differentiation. Gene expression at day 0 was arbitrarily set as 100 and the expression through the time course was normalized to mRNA levels at day 0. Values were expressed as a ratio to GAPDH. The first two genotypes were reproduced from Figure 2D.

(C) Single-colony formation assay after the removal of ATRA and the readdition of LIF-containing media (n = 3). The difference in the incidence of colony formation between *Tert*$^{-/-S}$ and all the other genotypes, apart from short hairpin control-transduced *Tert*$^{-/-s}$ cells, was statistically significant ($p < 0.0001$; ANOVA and related Dunnett's test comparing every group with *Tert*$^{-/-S}$ values). The y axis indicates colony number. Data are represented as mean ± SD.

(D) Chromatin immunoprecipitation analysis of H3K27me3 enrichment at the *Nanog* promoter, as described in Supplemental Experimental Procedures. Data are represented as mean ± SD (n = 3). *, $p < 0.05$; **, $p < 0.01$; ***, $p < 0.0001$.

(E) A schematic showing that telomere shortening impairs the expression of Dnmt3 isoforms, leading to genome-wide DNA hypomethylation, which, in turn, affects H3K27me3 enrichment on specific loci (e.g., *Nanog*), thus impairing the ability of ESCs to sustain pluripotency factor repression after differentiation and growth restimulation.

See also Figure S4.

Differentiation Assay

Cell populations of the indicated genotype (1×10^5) were plated in non-gelatin-covered dishes in LIF-free media containing 5 μM ATRA (Sigma-Aldrich) for the indicated amount of time with ATRA-media replaced every 3 days. At the indicated time point, cells were replated in gelatin-covered dishes with LIF-containing media. For the single colony formation assay, a set of serial dilutions was performed, and the number of viable ES cell colonies was assessed with alkaline phosphatase (Millipore).

Quantitative Fluorescence In Situ Hybridization

The quantitative fluorescence in situ hybridization (Q-FISH) protocol was carried out as described previously (Liu et al., 2000). Metaphase spreads were captured with the use of Metafer 4 software and analyzed with Isis software. Statistical analysis of telomere intensity distribution was performed with Welch's unpaired t test. The incidence of telomere signal-free ends was defined as the number of chromosome ends possessing a telomere signal (in arbitrary units) between 0 and 600, and statistical significance was assessed with Fisher's exact test (InStat 3, GraphPad).

qRT-PCR

Total RNA was isolated from cells with the use of Triazol (Invitrogen) according to the manufacturer's instructions. Reverse transcription was carried out with the use of 0.5 μg of template RNA, random hexamer primers, and smart MMLV reverse transcriptase (Clontech). Diluted complementary DNA (20×) was subjected to real-time PCR analysis using a SYBR Green Master Mix (Roche) on a LightCycler 480 system (Roche). Background values (no reverse

transcriptase added) were subtracted and values were normalized to *glyceraldehyde 3-phosphate dehydrogenase* (*GAPDH*) (n > 3). The oligos employed are listed in Table S1. Statistical analysis was performed by ANOVA and a related Dunnett's test comparing every group with WT values.

ChIP Sequencing

ChIP experiments were performed as described in Bergmann et al., 2011, except phenol-chloroform was replaced with a Chelex, 100-based DNA isolation method described in Nelson et al., 2006. Recovered DNA was analyzed by qRT-PCR as described above. For each pair of primers, triplicate measurements were taken and normalized to input DNA and the amount of DNA recovered from the *GAPDH* promoter (n > 3). Antibodies employed were as follows: rabbit anti-Nanog (Bethyl Laboratories); mouse anti-H3K27me3 and anti-H3K4me3 (Abcam); and murine IgG (Sigma-Aldrich). Oligos employed are listed in Table S1. Statistical analysis was performed by ANOVA and a related Dunnett's test comparing every group with WT values. In each experiment, the signal present after immunoprecipitation with IgG was defined as background and subtracted prior to normalization to input DNA and *GAPDH*.

Methylation Assay

Relative genomic DNA methylation was assessed with the use of the ELISA-based Imprint Methylated DNA Quantification kit (Sigma-Aldrich) according to the manufacturer's instructions, with the use of 100 ng of genomic DNA per sample (n > 3).

Bisulphite Sequencing Analysis

DNA bisulphite conversion was performed as described previously (Clouaire et al., 2010). After bisulphite conversion of unmethylated cytosines to uracil, samples were resuspended in 1 × Tris–EDTA for PCR amplification. PCR products were cloned into pcDNA3.1 Directional TOPO Expression (Invitrogen) vector and colony PCR was performed. Clones (at least ten per sample) of the correct molecular mass were sequenced, and results were analyzed with BiQ Analyzer (http://biq-analyzer.bioinf.mpi-inf.mpg.de). Primers employed are listed in Table S1. Statistical analysis of samples employed Fisher's exact test (two-sided) using GraphPad InStat3 (www.graphpad.com).

SUPPLEMENTAL INFORMATION

Supplemental Information contains Supplemental Experimental Procedures, four figures, and one table and can be found with this article online at http://dx.doi.org/10.1016/j.stem.2013.01.018.

ACKNOWLEDGMENTS

We thank A. Bird, K. Kaji, I. Stancheva, and L.H. Wong for discussion and input; C. Furlan, S. Catania, D. Kelly, N. Martins, M. Robson, A. Termanis, M. Waterfall, and G. Vargiu for technical assistance; and K. Kaji for the pCAG-MKOSiE plasmid. This work was funded by Wellcome Trust grants 086580 and 084637 to L.H.

Received: September 10, 2012
Revised: December 24, 2012
Accepted: January 28, 2013
Published: April 4, 2013

REFERENCES

Agarwal, S., Loh, Y.H., McLoughlin, E.M., Huang, J., Park, I.H., Miller, J.D., Huo, H., Okuka, M., Dos Reis, R.M., Loewer, S., et al. (2010). Telomere elongation in induced pluripotent stem cells from dyskeratosis congenita patients. Nature *464*, 292–296.

Batista, L.F., Pech, M.F., Zhong, F.L., Nguyen, H.N., Xie, K.T., Zaug, A.J., Crary, S.M., Choi, J., Sebastiano, V., Cherry, A., et al. (2011). Telomere shortening and loss of self-renewal in dyskeratosis congenita induced pluripotent stem cells. Nature *474*, 399–402.

Benetti, R., García-Cao, M., and Blasco, M.A. (2007). Telomere length regulates the epigenetic status of mammalian telomeres and subtelomeres. Nat. Genet. *39*, 243–250.

Bergmann, J.H., Rodríguez, M.G., Martins, N.M., Kimura, H., Kelly, D.A., Masumoto, H., Larionov, V., Jansen, L.E., and Earnshaw, W.C. (2011). Epigenetic engineering shows H3K4me2 is required for HJURP targeting and CENP-A assembly on a synthetic human kinetochore. EMBO J. *30*, 328–340.

Brinkman, A.B., Gu, H., Bartels, S.J., Zhang, Y., Matarese, F., Simmer, F., Marks, H., Bock, C., Gnirke, A., Meissner, A., and Stunnenberg, H.G. (2012). Sequential ChIP-bisulfite sequencing enables direct genome-scale investigation of chromatin and DNA methylation cross-talk. Genome Res. *22*, 1128–1138.

Chambers, I., Silva, J., Colby, D., Nichols, J., Nijmeijer, B., Robertson, M., Vrana, J., Jones, K., Grotewold, L., and Smith, A. (2007). Nanog safeguards pluripotency and mediates germline development. Nature *450*, 1230–1234.

Clouaire, T., de Las Heras, J.I., Merusi, C., and Stancheva, I. (2010). Recruitment of MBD1 to target genes requires sequence-specific interaction of the MBD domain with methylated DNA. Nucleic Acids Res. *38*, 4620–4634.

Feldman, N., Gerson, A., Fang, J., Li, E., Zhang, Y., Shinkai, Y., Cedar, H., and Bergman, Y. (2006). G9a-mediated irreversible epigenetic inactivation of Oct-3/4 during early embryogenesis. Nat. Cell Biol. *8*, 188–194.

Festuccia, N., Osorno, R., Halbritter, F., Karwacki-Neisius, V., Navarro, P., Colby, D., Wong, F., Yates, A., Tomlinson, S.R., and Chambers, I. (2012). Esrrb is a direct Nanog target gene that can substitute for Nanog function in pluripotent cells. Cell Stem Cell *11*, 477–490.

Fidalgo, M., Shekar, P.C., Ang, Y.S., Fujiwara, Y., Orkin, S.H., and Wang, J. (2011). Zfp281 functions as a transcriptional repressor for pluripotency of mouse embryonic stem cells. Stem Cells *29*, 1705–1716.

Heng, J.C., Orlov, Y.L., and Ng, H.H. (2010). Transcription factors for the modulation of pluripotency and reprogramming. Cold Spring Harb. Symp. Quant. Biol. *75*, 237–244.

Huang, J., Wang, F., Okuka, M., Liu, N., Ji, G., Ye, X., Zuo, B., Li, M., Liang, P., Ge, W.W., et al. (2011). Association of telomere length with authentic pluripotency of ES/iPS cells. Cell Res. *21*, 779–792.

Ivanova, N., Dobrin, R., Lu, R., Kotenko, I., Levorse, J., DeCoste, C., Schafer, X., Lun, Y., and Lemischka, I.R. (2006). Dissecting self-renewal in stem cells with RNA interference. Nature *442*, 533–538.

Jackson, M., Krassowska, A., Gilbert, N., Chevassut, T., Forrester, L., Ansell, J., and Ramsahoye, B. (2004). Severe global DNA hypomethylation blocks differentiation and induces histone hyperacetylation in embryonic stem cells. Mol. Cell. Biol. *24*, 8862–8871.

Kim, J., Chu, J., Shen, X., Wang, J., and Orkin, S.H. (2008). An extended transcriptional network for pluripotency of embryonic stem cells. Cell *132*, 1049–1061.

Li, Y.Q. (2010). Master stem cell transcription factors and signaling regulation. Cell Reprogram *12*, 3–13.

Li, E., Bestor, T.H., and Jaenisch, R. (1992). Targeted mutation of the DNA methyltransferase gene results in embryonic lethality. Cell *69*, 915–926.

Liu, Y., Snow, B.E., Hande, M.P., Yeung, D., Erdmann, N.J., Wakeham, A., Itie, A., Siderovski, D.P., Lansdorp, P.M., Robinson, M.O., and Harrington, L. (2000). The telomerase reverse transcriptase is limiting and necessary for telomerase function in vivo. Curr. Biol. *10*, 1459–1462.

Lu, R., Yang, A., and Jin, Y. (2011). Dual functions of T-box 3 (Tbx3) in the control of self-renewal and extraembryonic endoderm differentiation in mouse embryonic stem cells. J. Biol. Chem. *286*, 8425–8436.

Lynch, M.D., Smith, A.J., De Gobbi, M., Flenley, M., Hughes, J.R., Vernimmen, D., Ayyub, H., Sharpe, J.A., Sloane-Stanley, J.A., Sutherland, L., et al. (2012). An interspecies analysis reveals a key role for unmethylated CpG dinucleotides in vertebrate Polycomb complex recruitment. EMBO J. *31*, 317–329.

Marion, R.M., Strati, K., Li, H., Tejera, A., Schoeftner, S., Ortega, S., Serrano, M., and Blasco, M.A. (2009). Telomeres acquire embryonic stem cell characteristics in induced pluripotent stem cells. Cell Stem Cell *4*, 141–154.

Mendenhall, E.M., Koche, R.P., Truong, T., Zhou, V.W., Issac, B., Chi, A.S., Ku, M., and Bernstein, B.E. (2010). GC-rich sequence elements recruit PRC2 in mammalian ES cells. PLoS Genet. *6*, e1001244.

Nelson, J.D., Denisenko, O., and Bomsztyk, K. (2006). Protocol for the fast chromatin immunoprecipitation (ChIP) method. Nat. Protoc. *1*, 179–185.

Okano, M., Bell, D.W., Haber, D.A., and Li, E. (1999). DNA methyltransferases Dnmt3a and Dnmt3b are essential for de novo methylation and mammalian development. Cell *99*, 247–257.

Petrie, K., Zelent, A., and Waxman, S. (2009). Differentiation therapy of acute myeloid leukemia: past, present and future. Curr. Opin. Hematol. *16*, 84–91.

Savarese, F., Dávila, A., Nechanitzky, R., De La Rosa-Velazquez, I., Pereira, C.F., Engelke, R., Takahashi, K., Jenuwein, T., Kohwi-Shigematsu, T., Fisher, A.G., and Grosschedl, R. (2009). Satb1 and Satb2 regulate embryonic stem cell differentiation and Nanog expression. Genes Dev. *23*, 2625–2638.

Shen, X., Liu, Y., Hsu, Y.J., Fujiwara, Y., Kim, J., Mao, X., Yuan, G.C., and Orkin, S.H. (2008). EZH1 mediates methylation on histone H3 lysine 27 and complements EZH2 in maintaining stem cell identity and executing pluripotency. Mol. Cell *32*, 491–502.

Shi, W., Wang, H., Pan, G., Geng, Y., Guo, Y., and Pei, D. (2006). Regulation of the pluripotency marker Rex-1 by Nanog and Sox2. J. Biol. Chem. *281*, 23319–23325.

Singh, A.M., Hamazaki, T., Hankowski, K.E., and Terada, N. (2007). A heterogeneous expression pattern for Nanog in embryonic stem cells. Stem Cells *25*, 2534–2542.

Sinkkonen, L., Hugenschmidt, T., Berninger, P., Gaidatzis, D., Mohn, F., Artus-Revel, C.G., Zavolan, M., Svoboda, P., and Filipowicz, W. (2008). MicroRNAs control de novo DNA methylation through regulation of transcriptional repressors in mouse embryonic stem cells. Nat. Struct. Mol. Biol. *15*, 259–267.

Tsumura, A., Hayakawa, T., Kumaki, Y., Takebayashi, S., Sakaue, M., Matsuoka, C., Shimotohno, K., Ishikawa, F., Li, E., Ueda, H.R., et al. (2006). Maintenance of self-renewal ability of mouse embryonic stem cells in the absence of DNA methyltransferases Dnmt1, Dnmt3a and Dnmt3b. Genes Cells *11*, 805–814.

Tysnes, B.B. (2010). Tumor-initiating and -propagating cells: cells that we would like to identify and control. Neoplasia *12*, 506–515.

Villasante, A., Piazzolla, D., Li, H., Gomez-Lopez, G., Djabali, M., and Serrano, M. (2011). Epigenetic regulation of Nanog expression by Ezh2 in pluripotent stem cells. Cell Cycle *10*, 1488–1498.

Supplementary Data:

Short Telomeres in ESCs Lead to Unstable Differentiation

Fabio Pucci, Laura Gardano, Lea Harrington

Supplemental Figures S1-S4

Supplemental Table S1

Supplemental Experimental Procedures

Supplemental References

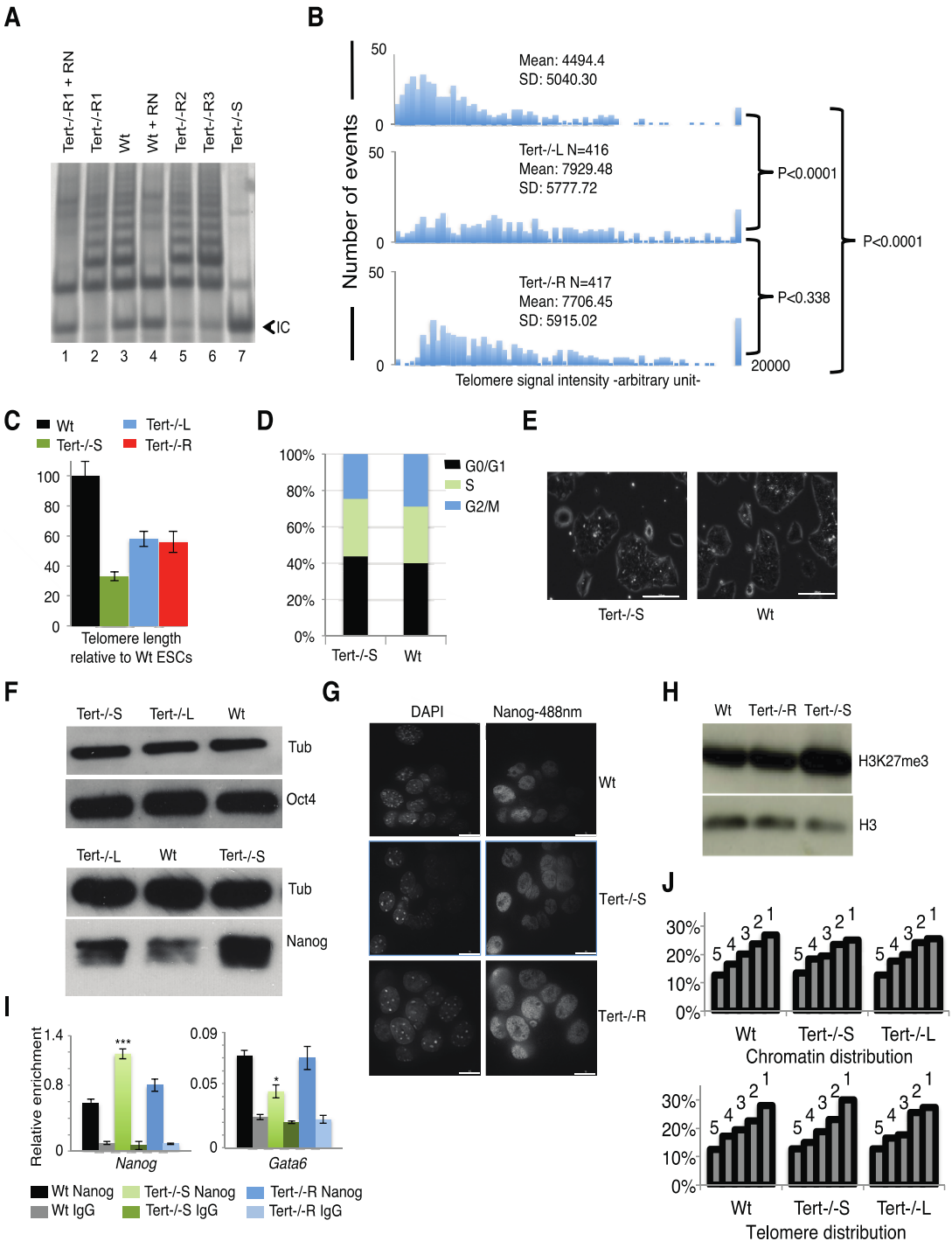

Figure S1 (related to Fig. 1). Characterization of telomerase activity, telomere length, cell cycle profile, morphology and pluripotency gene expression in *Tert*$^{-/-}$ ESCs. A) Telomere repeat assay protocol (TRAP) performed on protein extracts (the equivalent of 5 x 10^4 cells) from Wt ESCs (lanes 1, 2), *Tert*$^{-/-R}$ ESCs (3 independent

rescued clones; lanes 1, 2, 5, 6) untreated or after digestion with ribonuclease A (RN) and *Tert*$^{-/-S}$ ESCs (lane 7) (cells at between 67 and 74 passages); IC = internal PCR control. B) Q-FISH analysis of indicated genotypes; statistical significance was analyzed by Welch's unpaired t-test; L = long telomeres (passage 30); S = short telomeres (passage 70); R = *Tert*$^{-/-S}$ cells after reintroduction of *Tert* (passage 74, including 4 passages under hygromycin selection). The difference in the incidence of signal-free ends relative to total ends between *Tert*$^{-/-S}$ (49/417) and *Tert*$^{-/-L}$ (14/416) or *Tert*$^{-/-R}$ (4/417) was statistically significant ($p<0.00001$ for each comparison, Fisher's exact test). N = number of chromosome ends; y-axis, number of events; x-axis, telomere signal intensity in arbitrary units. C) Average of mean telomere signal intensity relative to Wt. Data are represented as mean ± SD (n=3); Number of chromosomes per sample ≥ 350 D) Cell cycle profile of Wt and *Tert*$^{-/-S}$ cells. E) Bright field image of the same samples as in (D), Micrograph bars indicate 200μm. F) Oct 4 and Nanog protein detection by western blot. β-Tubulin was used as an internal control (Tub). L = long telomeres (passage 70); S = short telomeres (passage 30); n=3 for Oct4 blot, n=10 for Nanog blot. G) Immunofluorescence analysis of Nanog expression in ESCs. Micrograph bar indicates 15μm. H) Detection of H3K27me3 and histone H3 (as a control) by western blot (n=3). I) ChIP analysis of Nanog occupancy on *Nanog* and *Gata6* promoters (see Supplementary Experimental Procedures for details). A murine IgG antibody was used as a negative control. Data are represented as mean ± SD (n=3). * = $p<0.05$; *** = $p<0.0001$. J) 3D-FISH analysis of chromatin (top) and telomere DNA distribution (bottom) in ESC nuclei (n=3). The nuclear area has been divided in 5 equal concentric zones, where 1 is the

inner and 5 the most peripheral zone. Y-axis indicates the percentage of signal in each zone. See Supplemental Experimental Procedures.

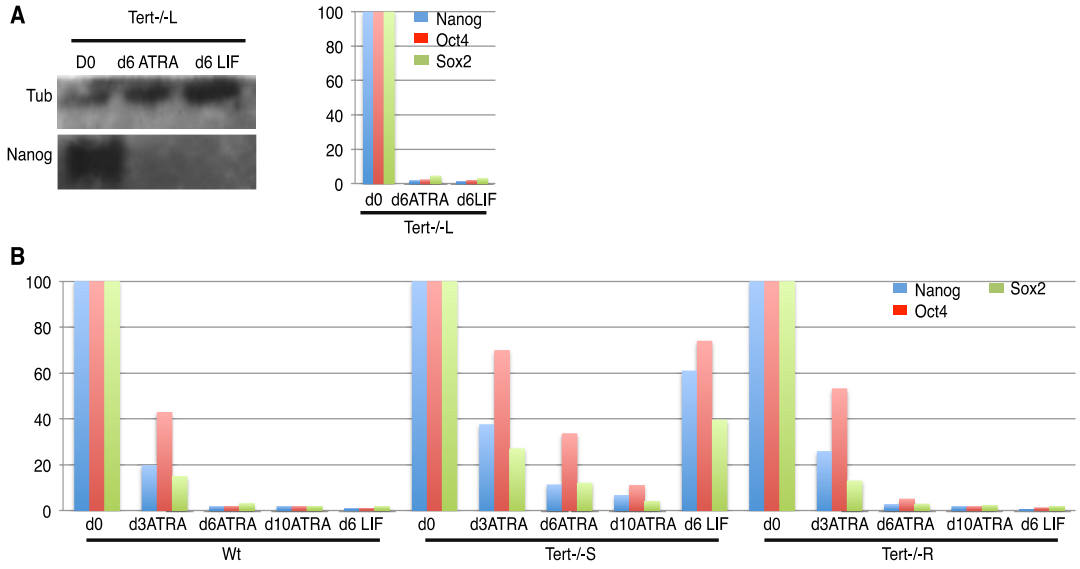

Figure S2 (related to Fig. 2). Analysis of *Nanog*, *Sox2*, and *Oct4* expression in response to all-trans retinoic acid and LIF. A) Pluripotency factor expression in *Tert*$^{-/-}$ ESC with long telomeres (*Tert*$^{-/-L}$). (Left) Detection of Nanog and β-tubulin by western blot (n=3); (Right) QRT-PCR analysis of pluripotency genes after ATRA-induced differentiation and LIF re-addition. Gene expression at day 0 was arbitrarily set as 100 and the expression through the time course was normalized to mRNA levels at day 0. Sample nomenclature as indicated in Figure 1. C) QRT-PCR analysis of pluripotency genes after ATRA-induced differentiation and LIF re-addition. Gene expression at day 0 was arbitrarily set as 100 and the expression through the time course was normalized to mRNA levels at day 0. Values were expressed as a ratio to *GAPDH*.

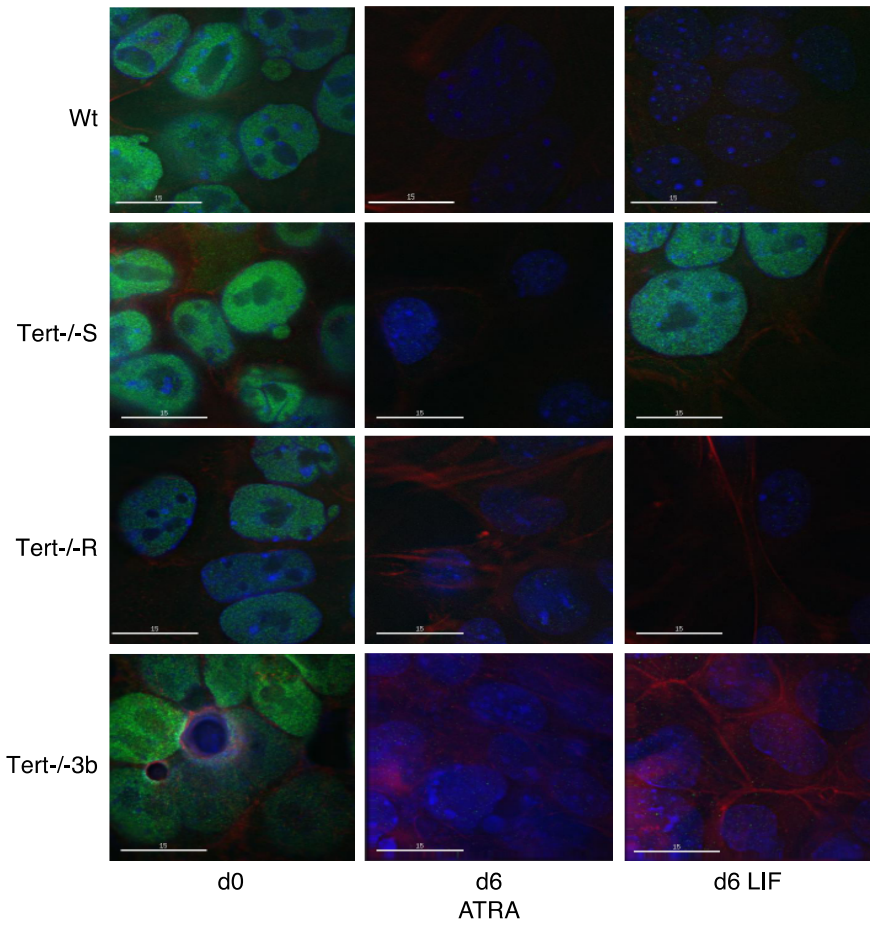

Figure S3 (related to Fig. 3). Nanog immunofluorescence analysis after ectopic expression of *Dnmt3b* in *Tert* null ESCs with short telomeres. Cells were analyzed for Nanog via immunofluorescence at d0, day 0; d6 ATRA, 6 days of treatment with ATRA; d6 LIF, a further 6 days after removal of ATRA and re-addition of LIF-conditioned media. Note that the top nine panels are identical to Figure 2B, but are reproduced here because all samples were analyzed contemporaneously (n= 3). Micrograph bars indicate 15μm (n= 3).

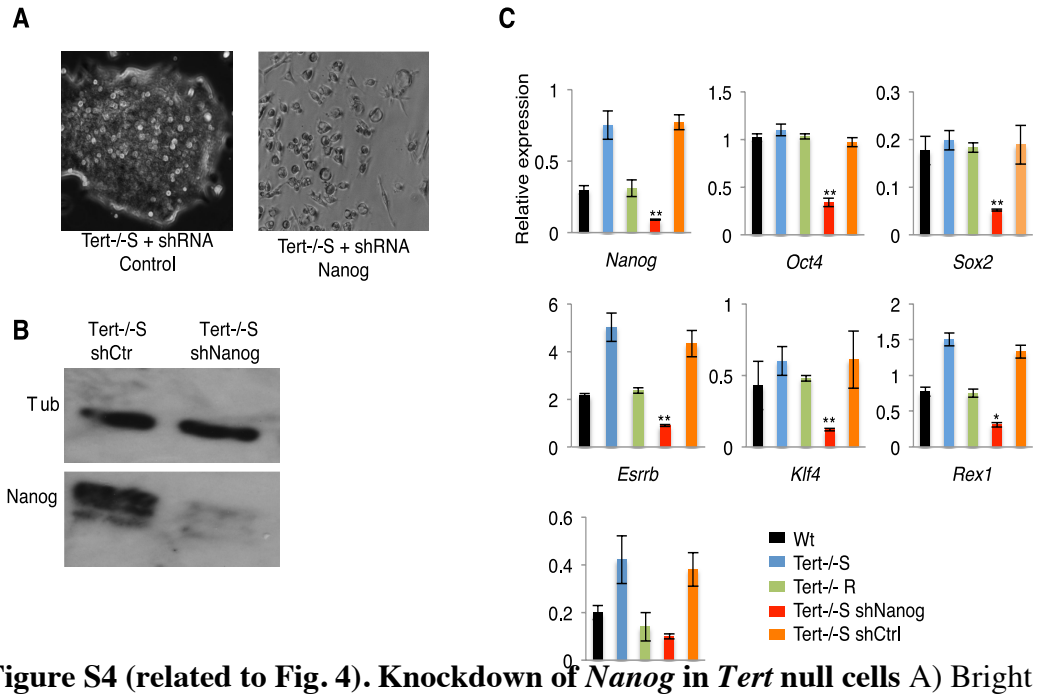

Figure S4 (related to Fig. 4). Knockdown of *Nanog* in *Tert* null cells A) Bright field image of shNanog and shControl transduced *Tert* null cells. B) Nanog protein detection by western blot. Tub= β-tubulin (n=3). C) Relative gene expression of shNanog and shControl transduced cells analyzed by QRT-PCR, normalized over GAPDH (n=3). Data are represented as mean ± SD. * = $p<0.05$; ** = $p<0.01$

Rex-1^{T}	5’-CACCGACAACATGAATGAACAAAA A-3’	5’-CAATCTGTCTCCACCTTCAGCATT T-3’
ChiP	Fw	Rv
Sox2^{T}	5’-TAGAGCTAGACTCCGGGCGATG A-3’	5’-TTGCCTTAAACAAGACCACGAA A-3’
GAPDH^{F}	5’-AAGCTCATGAGGCACAGAATGGT C-3’	5’-TGGGTACATGGTGACTTTCCTAGG C-3’
Tbx3^{F}	5’-TCTCCATCGTGGGGACAT-3’	5’-TTGTCGCGGCCTGGCTCCTCG-3’
Gata6^{F}	5’-TGACCCAGGAGGGGGCGAGT-3’	5’-CCGCCACCCAGGGCAGAAGA-3’
Zfp281^{F}	5’-TGAGCCCAGGCACCCA-3’	5’-TGGAGAGGTGAAGACAAGCTGA C-3’
Nanog^{F}	5’-ACTCCAAGGCTAGCGATTCA-3’	5’-AATAGGGAGGAGGGCGTCTA-3’
Bisulphite	**Fw**	**Rv**
Oct4^{H}	5’-CTGTAAGGACAGGCCGAGAG-3’	5’-CAGGAGGCCTTCATTTTCAA-3’
Nanog^{T}	5’-GATTTTGTAGGTGGGATTAATTGTG AATTT-3’	5’-ACCAAAAAAACCCACACTCATATC AATATA-3’
QRT-PCR	**Fw**	**Rv**
Cdx2^{Si}	5’-CCTGGGACATTGTTTAG-3’	5’-TCCCTCCCTCAATCCACCATC-3’
Oct4	5’-AGGATTTGAAGGTTGAAAATGAA GG-3’	5’-TCCCTCCCTCAATCCACCATC-3’
Dnmt1	5’-TGGGCTGATGCAGGAGAAAAT-3’	5’-GCGCTTCATGGCATTCTCCTT-3’
Dnmt3a2^{Si}	5’-AGGGGCTGCACCTGGCCTT-3’	5’-TCCCCCACACCAGCTCTCC-3’
Dnmt3b^{Si}	5’-TGGGATCGAGGGCCTCAAAC-3’	5’-TTCCACAGGACAAACAGCGG-3’
Esrrb^{I}	5’-CAGGCAAGGATGACAGACG-3’	5’-GAGACAGCACGAAGGACTGC-3’
GAPDH^{F}	5’-CCATCACCATCTTCCAGG-3’	5’-CCTGCTTCACCACCTTCTTG-3’
Gata4^{F}	5’-CTGTCATCTCACTATGGGCA-3’	5’-CCAAGTCCGAGCAGGAATTT-3’
Gata6^{F}	5’-TTGCTCCGGTAACAGCAGTG-3’	5’-GTGGTCGCTTGTGTAGAAGGA-3’
Klf4^{T}	5’-AGTGTGACAGGGCCTTTCCAGGT-3’	5’-AAGCTGACTTGCTGGGAACTTGAC C-3’
Nanog^{F}	5’-AGGGTCTGCTACTGAGATGCTCT G-3’	5’-CAACCACTGGTTTTTCTGCCACC G-3’
Oct4^{S}	5’-GGCGTTCGCTTTGGAAAGGTGTT C-3’	5’-CTCGAACCACATCCTTCTCT-3’
Rex-1^{T}	5’-CACCGACAACATGAATGAACAAAA A-3’	5’-CAATCTGTCTCCACCTTCAGCATT T-3’

Table S1 (related to Fig. 1). List of oligos employed in this study. Superscripts indicate first author initial (Dahl et al., 2010; Fidalgo et al., 2011; Ivanova et al., 2006; Sinkkonen et al., 2008; Takahashi and Yamanaka, 2006). Fw, forward primer; Rv, reverse primer.

Supplemental Experimental Procedures:

Telomerase activity assay. The telomere repeat amplification protocol, TRAP, was conducted with the TRAPeze Telomerase Detection Kit, Chemicon International, according to manufacturer's instructions.

Plasmid construction. The plasmid pTRE-Bi-*Tert*-IRES-EGFP-Hygro was constructed by amplification of *Tert* cDNA by PCR and cloning it into pTRE-Tight-Bi (Clontech) following digestion with EcoRI and SalI. IRES-EGFP sequence was obtained from pCAGMKOSiE (from K.Kaji) and inserted into pTRE-Tight-Bi (following digestion with SalI and EcorV) using SalI and HpaI sites and then inserted into pTRE-Bi-*Tert* using NotI sites. Finally, the hygromycin-resistance gene was cloned by PCR into the XbaI restriction site of pTRE-Tight-Bi and pTRE-Bi-*Tert*-IRES-EGFP vectors to create pTRE-Bi-EGFP-Hygro and pTRE-Bi-*Tert*-IRES-EGFP-Hygro. The pCAG-rtTA-advanced vector was constructed by removal of the MKOS ORFs from CAGMKOSiE with EcoRI and BamHI and replacement with the advanced tetracycline reverse transactivator sequence (Clontech). The plasmid pCAG-*Dnmt3b*-IRES-puromycin vector was constructed by removal of the MKOS ORFs from CAGMKOSiE with EcoRI. *Dnmt3b* was subcloned from a *Dnmt3b* expression vector (Thermo scientific) and inserted pCAG-IRES-EGFP following

digestion EcoRI and SalI. IRES-EGFP was replaced with IRES-Puro (from pIRESPuro2, Clontech) after digestion with PmlI and PvuII.

Fluorescence-activated cell sorting (FACS). Hoechst stain (5μg/ml) was added to the cell culture and incubated for 30 minutes. Cells were harvested and resuspended in 0.5 ml of 1X PBS and analyzed for cell cycle distribution using a Becton Dickinson Fluorescence Activated Cell Sorter. After gating on the appropriate channels, the percentage of cells in G1, S, or G2/M were calculated. For FACS analysis of Nanog expression, cells were fixed and stained as indicated (Festuccia and Chambers, 2011). Cell sorting after transduction with Oct4-GFP was carried out as described in Zheng and Hu, 2012.

Protein extraction and western blot analysis. Histones were acid-extracted as follows: Cells were harvested and washed twice with ice cold 1X PBS. Cells were resuspended (107 cells/ml) in TEB buffer (PBS 1X, 0.5% v/v Triton X-100, 2 mM PMSF, 0.02% v/v NaN_3) and left on ice for 10 minutes with gentle stirring to enhance lysis. Cells were spun at 800 x*g* for 10 minutes at 4°C, washed in TEB buffer, and pelleted as above. Cells were resuspended in 0.2 N HCl (4 $x10^7$ cells/ml) and incubated overnight at 4°C. Cells were pelleted as above, and the supernatant was recovered and stored at -80°C. Protein extracts were resolved on 15% w/v SDS-PAGE, transferred to nitrocellulose and blocked overnight with 3% w/v BSA in 1X PBS. Rabbit anti-histone H3 (Abcam) and mouse anti H3K27me3 (Abcam) were used as primary antibodies.

For non-histone protein extraction, cells were lysed for 30 minutes on ice in RIPA buffer (50 mM Tris-HCl pH 7.4, 1% v/v NP-40, 0.25% w/v Na-deoxycholate, 150 mM NaCl, 1 mM EDTA, 1 mM PMSF, 1 μg/ml each of aprotinin, leupeptin and

pepstatin, 1 mM Na_3VO_4, 1 mM NaF). Cells were pelleted at 20,800 x*g* for 10 min at at 4°C. The supernatant was recovered and stored at -80°C. Protein extracts were resolved on 10% w/v SDS PAGE, transferred to nitrocellulose and blocked overnight with 5% w/v non-fat dry milk in 1X PBS. Rabbit anti-Nanog (Bethyl labs), anti-Dnmt3b (Abcam) and Dnmt1 (Abcam), goat anti-Oct4 (Santa Cruz) and mouse anti-β-Tubulin (Sigma) were used as primary antibodies. Anti mouse and anti rabbit peroxidase-conjugated were used as secondary antibodies followed by detection with ECL Plus luminescent reagent (Amersham Biosciences) or with LI-COR in which instance the secondary antibodies employed were donkey anti-rabbit IRDye 800CW (green) and donkey anti-mouse IRDye680 (red) (Odyssey). All experiments were repeated at least three times.

Immunofluorescence. Cells were fixed in 4% v/v paraformaldehyde (PFA)/PBS according to manufacturer's instructions (Abcam). Rabbit anti-Nanog (Bethyl labs) and Alexa fluor® Goat anti-rabbit-488 were used as primary and secondary antibodies. Rhodamine-phalloidin (Sigma) was used to detect actin. DNA was stained with DAPI. ImageJ software was employed to define the relative fluorescence intensities of single cells (for channels 488), with DAPI fluorescence as internal control. Individual values were used for quantitative analysis of Nanog expression levels among genotypes as described (Savarese et al., 2009). Statistical analysis was performed using Welch's unpaired t-test.

3D Analysis of Cell Nuclei. Cells were fixed in in 4% v/v paraformaldehyde (PFA)/PBS for 15 min, then treated as described for Q-FISH analysis of telomere fluorescence. At least 25 interphase nuclei were analyzed for Wt, *Tert*$^{-/-S}$ and *Tert*$^{-/-L}$. Images were acquired using a Nikon TE-2000 microscope equipped with a 1.45

numerical aperture 100× objective, PIFOC Z-axis focus drive (Physik Instruments), Sedat quad filter set, and CoolSnapHQ High Speed Monochrome charge-coupled device camera (Photometrics). Images were deconvolved from 0.2-μm sections using AutoquantX.

Deconvolved images were analyzed for chromosome and telomere distribution using a macro described in (Korfali et al., 2010).

Supplemental References:

Abdelalim, E.M., and Tooyama, I. (2012). The p53 inhibitor, pifithrin-alpha, suppresses self-renewal of embryonic stem cells. Biochem Biophys Res Commun *420*, 605-610.

Allis, C.D., Berger, S.L., Cote, J., Dent, S., Jenuwien, T., Kouzarides, T., Pillus, L., Reinberg, D., Shi, Y., Shiekhattar, R.*, et al.* (2007). New nomenclature for chromatin-modifying enzymes. Cell *131*, 633-636.

Altun, G., Loring, J.F., and Laurent, L.C. (2010). DNA methylation in embryonic stem cells. J Cell Biochem *109*, 1-6.

Ambros, V., and Horvitz, H.R. (1984). Heterochronic mutants of the nematode Caenorhabditis elegans. Science *226*, 409-416.

Atcha, F.A., Syed, A., Wu, B., Hoverter, N.P., Yokoyama, N.N., Ting, J.H., Munguia, J.E., Mangalam, H.J., Marsh, J.L., and Waterman, M.L. (2007). A unique DNA binding domain converts T-cell factors into strong Wnt effectors. Mol Cell Biol *27*, 8352-8363.

Avilion, A.A., Nicolis, S.K., Pevny, L.H., Perez, L., Vivian, N., and Lovell-Badge, R. (2003). Multipotent cell lineages in early mouse development depend on SOX2 function. Genes Dev *17*, 126-140.

Azzalin, C.M., Reichenbach, P., Khoriauli, L., Giulotto, E., and Lingner, J. (2007). Telomeric repeat containing RNA and RNA surveillance factors at mammalian chromosome ends. Science *318*, 798-801.

Benetti, R., Garcia-Cao, M., and Blasco, M.A. (2007). Telomere length regulates the epigenetic status of mammalian telomeres and subtelomeres. Nat Genet *39*, 243-250.

Benetti, R., Gonzalo, S., Jaco, I., Munoz, P., Gonzalez, S., Schoeftner, S., Murchison, E., Andl, T., Chen, T., Klatt, P.*, et al.* (2008). A mammalian microRNA cluster controls DNA methylation and telomere recombination via Rbl2-dependent regulation of DNA methyltransferases. Nat Struct Mol Biol *15*, 998.

Benezra, R., Davis, R.L., Lockshon, D., Turner, D.L., and Weintraub, H. (1990). The protein Id: a negative regulator of helix-loop-helix DNA binding proteins. Cell *61*, 49-59.

Bergmann, J.H., Rodriguez, M.G., Martins, N.M., Kimura, H., Kelly, D.A., Masumoto, H., Larionov, V., Jansen, L.E., and Earnshaw, W.C. (2011). Epigenetic engineering shows H3K4me2 is required for HJURP targeting and CENP-A assembly on a synthetic human kinetochore. Embo J *30*, 328-340.

Biffi, G., Tannahill, D., McCafferty, J., and Balasubramanian, S. (2013). Quantitative visualization of DNA G-quadruplex structures in human cells. Nat Chem *5*, 182-186.

Bird, A., Taggart, M., Frommer, M., Miller, O.J., and Macleod, D. (1985). A fraction of the mouse genome that is derived from islands of nonmethylated, CpG-rich DNA. Cell *40*, 91-99.

Blackburn, E.H. (2001). Switching and signaling at the telomere. Cell *106*, 661-673.

Blair, K., Wray, J., and Smith, A. (2011). The liberation of embryonic stem cells. PLoS Genet *7*, e1002019.

Bodnar, A.G., Ouellette, M., Frolkis, M., Holt, S.E., Chiu, C.P., Morin, G.B., Harley, C.B., Shay, J.W., Lichtsteiner, S., and Wright, W.E. (1998). Extension of life-span by introduction of telomerase into normal human cells. Science *279*, 349-352.

Bower, K., Napier, C.E., Cole, S.L., Dagg, R.A., Lau, L.M., Duncan, E.L., Moy, E.L., and Reddel, R.R. (2012). Loss of wild-type ATRX expression in somatic cell hybrids segregates with activation of Alternative Lengthening of Telomeres. PLoS One *7*, e50062.

Brinkman, A.B., Gu, H., Bartels, S.J., Zhang, Y., Matarese, F., Simmer, F., Marks, H., Bock, C., Gnirke, A., Meissner, A.*, et al.* (2012). Sequential ChIP-bisulfite sequencing enables direct genome-scale investigation of chromatin and DNA methylation cross-talk. Genome Res.

Bryan, T.M., Englezou, A., Gupta, J., Bacchetti, S., and Reddel, R.R. (1995). Telomere elongation in immortal human cells without detectable telomerase activity. Embo J *14*, 4240-4248.

Cesare, A.J., and Reddel, R.R. (2010). Alternative lengthening of telomeres: models, mechanisms and implications. Nat Rev Genet *11*, 319-330.

Chambers, I., Colby, D., Robertson, M., Nichols, J., Lee, S., Tweedie, S., and Smith, A. (2003). Functional expression cloning of Nanog, a pluripotency sustaining factor in embryonic stem cells. Cell *113*, 643-655.

Chambers, I., Silva, J., Colby, D., Nichols, J., Nijmeijer, B., Robertson, M., Vrana, J., Jones, K., Grotewold, L., and Smith, A. (2007). Nanog safeguards pluripotency and mediates germline development. Nature *450*, 1230-1234.

Chin, L., Artandi, S.E., Shen, Q., Tam, A., Lee, S.L., Gottlieb, G.J., Greider, C.W., and DePinho, R.A. (1999). p53 deficiency rescues the adverse effects of telomere loss and cooperates with telomere dysfunction to accelerate carcinogenesis. Cell *97*, 527-538.

Chiodi, I., Belgiovine, C., Zongaro, S., Ricotti, R., Horard, B., Lossani, A., Focher, F., Gilson, E., Giulotto, E., and Mondello, C. (2013). Super-telomeres in transformed human fibroblasts. Biochim Biophys Acta.

Choi, J., Southworth, L.K., Sarin, K.Y., Venteicher, A.S., Ma, W., Chang, W., Cheung, P., Jun, S., Artandi, M.K., Shah, N.*, et al.* (2008). TERT promotes epithelial proliferation through transcriptional control of a Myc- and Wnt-related developmental program. PLoS Genet *4*, e10.

Clouaire, T., de Las Heras, J.I., Merusi, C., and Stancheva, I. (2010). Recruitment of MBD1 to target genes requires sequence-specific interaction of the MBD domain with methylated DNA. Nucleic Acids Res *38*, 4620-4634.

Costa, Y., Ding, J., Theunissen, T.W., Faiola, F., Hore, T.A., Shliaha, P.V., Fidalgo, M., Saunders, A., Lawrence, M., Dietmann, S.*, et al.* (2013). NANOG-dependent function of TET1 and TET2 in establishment of pluripotency. Nature *495*, 370-374.

Cross, S.H., Charlton, J.A., Nan, X., and Bird, A.P. (1994). Purification of CpG islands using a methylated DNA binding column. Nat Genet *6*, 236-244.

Dahl, J.A., Reiner, A.H., Klungland, A., Wakayama, T., and Collas, P. (2010). Histone H3 lysine 27 methylation asymmetry on developmentally-regulated promoters distinguish the first two lineages in mouse preimplantation embryos. PLoS One *5*, e9150.

Deaton, A.M., and Bird, A. (2011). CpG islands and the regulation of transcription. Genes Dev *25*, 1010-1022.

Dostie, J., and Bickmore, W.A. (2012). Chromosome organization in the nucleus - charting new territory across the Hi-Cs. Curr Opin Genet Dev *22*, 125-131.

Dunham, M.A., Neumann, A.A., Fasching, C.L., and Reddel, R.R. (2000). Telomere maintenance by recombination in human cells. Nat Genet *26*, 447-450.

Evans, M.J., and Kaufman, M.H. (1981). Establishment in culture of pluripotential cells from mouse embryos. Nature *292*, 154-156.

Feldman, N., Gerson, A., Fang, J., Li, E., Zhang, Y., Shinkai, Y., Cedar, H., and Bergman, Y. (2006). G9a-mediated irreversible epigenetic inactivation of Oct-3/4 during early embryogenesis. Nat Cell Biol *8*, 188-194.

Festuccia, N., and Chambers, I. (2011). Quantification of pluripotency transcription factor levels in embryonic stem cells by flow cytometry. Curr Protoc Stem Cell Biol *Chapter 1*, Unit 1B 9.

Festuccia, N., Osorno, R., Halbritter, F., Karwacki-Neisius, V., Navarro, P., Colby, D., Wong, F., Yates, A., Tomlinson, S.R., and Chambers, I. (2012). Esrrb is a direct Nanog target gene that can substitute for Nanog function in pluripotent cells. Cell Stem Cell *11*, 477-490.

Fidalgo, M., Shekar, P.C., Ang, Y.S., Fujiwara, Y., Orkin, S.H., and Wang, J. (2011). Zfp281 functions as a transcriptional repressor for pluripotency of mouse embryonic stem cells. Stem Cells *29*, 1705-1716.

Fisher, C.L., and Fisher, A.G. (2011). Chromatin states in pluripotent, differentiated, and reprogrammed cells. Curr Opin Genet Dev *21*, 140-146.

Folini, M., Venturini, L., Cimino-Reale, G., and Zaffaroni, N. (2011). Telomeres as targets for anticancer therapies. Expert Opin Ther Targets *15*, 579-593.

Folmes, C.D., Dzeja, P.P., Nelson, T.J., and Terzic, A. (2012). Metabolic plasticity in stem cell homeostasis and differentiation. Cell Stem Cell *11*, 596-606.

Friel, R., van der Sar, S., and Mee, P.J. (2005). Embryonic stem cells: understanding their history, cell biology and signalling. Adv Drug Deliv Rev *57*, 1894-1903.

Gao, Y., Chen, J., Li, K., Wu, T., Huang, B., Liu, W., Kou, X., Zhang, Y., Huang, H., Jiang, Y.*, et al.* (2013). Replacement of Oct4 by Tet1 during iPSC induction reveals an important role of DNA methylation and hydroxymethylation in reprogramming. Cell Stem Cell *12*, 453-469.

Gardner, R.L., and Beddington, R.S. (1988). Multi-lineage 'stem' cells in the mammalian embryo. J Cell Sci Suppl *10*, 11-27.

Geserick, C., and Blasco, M.A. (2006). Novel roles for telomerase in aging. Mech Ageing Dev *127*, 579-583.

Gonzalo, S., and Blasco, M.A. (2005). Role of Rb family in the epigenetic definition of chromatin. Cell Cycle *4*, 752-755.

Gonzalo, S., Jaco, I., Fraga, M.F., Chen, T., Li, E., Esteller, M., and Blasco, M.A. (2006a). DNA methyltransferases control telomere length and telomere recombination in mammalian cells. Nat Cell Biol *8*, 416-424.

Gonzalo, S., Jaco, I., Fraga, M.F., Chen, T., Li, E., Esteller, M., and Blasco, M.A. (2006b). DNA methyltransferases control telomere length and telomere recombination in mammalian cells. Nat Cell Biol *8*, 416-424.

Granger, M.P., Wright, W.E., and Shay, J.W. (2002). Telomerase in cancer and aging. Crit Rev Oncol Hematol *41*, 29-40.

Greider, C.W., and Blackburn, E.H. (1985). Identification of a specific telomere terminal transferase activity in Tetrahymena extracts. Cell *43*, 405-413.

Grinnell, K.L., Yang, B., Eckert, R.L., and Bickenbach, J.R. (2007). De-differentiation of mouse interfollicular keratinocytes by the embryonic transcription factor Oct-4. J Invest Dermatol *127*, 372-380.

Guo, N., Parry, E.M., Li, L.S., Kembou, F., Lauder, N., Hussain, M.A., Berggren, P.O., and Armanios, M. (2011). Short telomeres compromise beta-cell signaling and survival. PLoS One *6*, e17858.

Hahn, W.C., Stewart, S.A., Brooks, M.W., York, S.G., Eaton, E., Kurachi, A., Beijersbergen, R.L., Knoll, J.H., Meyerson, M., and Weinberg, R.A. (1999). Inhibition of telomerase limits the growth of human cancer cells. Nat Med *5*, 1164-1170.

Hata, K., Okano, M., Lei, H., and Li, E. (2002). Dnmt3L cooperates with the Dnmt3 family of de novo DNA methyltransferases to establish maternal imprints in mice. Development *129*, 1983-1993.

Hayflick, L., and Moorhead, P.S. (1961). The serial cultivation of human diploid cell strains. Exp Cell Res *25*, 585-621.

Heard, E. (2004). Recent advances in X-chromosome inactivation. Curr Opin Cell Biol *16*, 247-255.

Heng, J.C., Orlov, Y.L., and Ng, H.H. (2010). Transcription factors for the modulation of pluripotency and reprogramming. Cold Spring Harb Symp Quant Biol *75*, 237-244.

Hillman, N., Sherman, M.I., and Graham, C. (1972). The effect of spatial arrangement on cell determination during mouse development. J Embryol Exp Morphol *28*, 263-278.

Hirai, H., Karian, P., and Kikyo, N. (2011). Regulation of embryonic stem cell self-renewal and pluripotency by leukaemia inhibitory factor. Biochem J *438*, 11-23.

Hirashima, K., Migita, T., Sato, S., Muramatsu, Y., Ishikawa, Y., and Seimiya, H. (2013). Telomere length influences cancer cell differentiation in vivo. Mol Cell Biol.

Hockemeyer, D., Daniels, J.P., Takai, H., and de Lange, T. (2006). Recent expansion of the telomeric complex in rodents: Two distinct POT1 proteins protect mouse telomeres. Cell *126*, 63-77.

Huang, J., Wang, F., Okuka, M., Liu, N., Ji, G., Ye, X., Zuo, B., Li, M., Liang, P., Ge, W.W.*, et al.* (2011). Association of telomere length with authentic pluripotency of ES/iPS cells. Cell research *21*, 779-792.

Ito, S., D'Alessio, A.C., Taranova, O.V., Hong, K., Sowers, L.C., and Zhang, Y. (2010). Role of Tet proteins in 5mC to 5hmC conversion, ES-cell self-renewal and inner cell mass specification. Nature *466*, 1129-1133.

Ivanova, N., Dobrin, R., Lu, R., Kotenko, I., Levorse, J., DeCoste, C., Schafer, X., Lun, Y., and Lemischka, I.R. (2006). Dissecting self-renewal in stem cells with RNA interference. Nature *442*, 533-538.

Jackson, M., Krassowska, A., Gilbert, N., Chevassut, T., Forrester, L., Ansell, J., and Ramsahoye, B. (2004). Severe global DNA hypomethylation blocks differentiation and induces histone hyperacetylation in embryonic stem cells. Mol Cell Biol *24*, 8862-8871.

Jia, W., Wang, S., Horner, J.W., Wang, N., Wang, H., Gunther, E.J., DePinho, R.A., and Zhu, J. (2011). A BAC transgenic reporter recapitulates in vivo regulation of human telomerase reverse transcriptase in development and tumorigenesis. Faseb J *25*, 979-989.

Jiang, H., Ju, Z., and Rudolph, K.L. (2007). Telomere shortening and ageing. Z Gerontol Geriatr *40*, 314-324.

Karwacki-Neisius, V., Goke, J., Osorno, R., Halbritter, F., Ng, J.H., Weisse, A.Y., Wong, F.C., Gagliardi, A., Mullin, N.P., Festuccia, N.*, et al.* (2013). Reduced oct4 expression directs a robust pluripotent state with distinct signaling activity and increased enhancer occupancy by oct4 and nanog. Cell Stem Cell *12*, 531-545.

Kawamura, T., Suzuki, J., Wang, Y.V., Menendez, S., Morera, L.B., Raya, A., Wahl, G.M., and Izpisua Belmonte, J.C. (2009). Linking the p53 tumour suppressor pathway to somatic cell reprogramming. Nature *460*, 1140-1144.

Kim, N.W., Piatyszek, M.A., Prowse, K.R., Harley, C.B., West, M.D., Ho, P.L., Coviello, G.M., Wright, W.E., Weinrich, S.L., and Shay, J.W. (1994). Specific association of human telomerase activity with immortal cells and cancer. Science *266*, 2011-2015.

Kipling, D., and Cooke, H.J. (1990). Hypervariable ultra-long telomeres in mice. Nature *347*, 400-402.

Klose, R.J., and Bird, A.P. (2006). Genomic DNA methylation: the mark and its mediators. Trends Biochem Sci *31*, 89-97.

Koche, R.P., Smith, Z.D., Adli, M., Gu, H., Ku, M., Gnirke, A., Bernstein, B.E., and Meissner, A. (2011). Reprogramming factor expression initiates widespread targeted chromatin remodeling. Cell Stem Cell *8*, 96-105.

Komarov, P.G., Komarova, E.A., Kondratov, R.V., Christov-Tselkov, K., Coon, J.S., Chernov, M.V., and Gudkov, A.V. (1999). A chemical inhibitor of p53 that protects mice from the side effects of cancer therapy. Science *285*, 1733-1737.

Kopp, J.L., Ormsbee, B.D., Desler, M., and Rizzino, A. (2008). Small increases in the level of Sox2 trigger the differentiation of mouse embryonic stem cells. Stem Cells *26*, 903-911.

Korfali, N., Wilkie, G.S., Swanson, S.K., Srsen, V., Batrakou, D.G., Fairley, E.A., Malik, P., Zuleger, N., Goncharevich, A., de Las Heras, J.*, et al.* (2010). The leukocyte nuclear envelope proteome varies with cell activation and contains novel transmembrane proteins that affect genome architecture. Mol Cell Proteomics *9*, 2571-2585.

Kunath, T., Saba-El-Leil, M.K., Almousailleakh, M., Wray, J., Meloche, S., and Smith, A. (2007). FGF stimulation of the Erk1/2 signalling cascade triggers transition of pluripotent embryonic stem cells from self-renewal to lineage commitment. Development *134*, 2895-2902.

Lafferty-Whyte, K., Cairney, C.J., Will, M.B., Serakinci, N., Daidone, M.G., Zaffaroni, N., Bilsland, A., and Keith, W.N. (2009). A gene expression signature classifying telomerase and ALT immortalization reveals an hTERT regulatory network and suggests a mesenchymal stem cell origin for ALT. Oncogene *28*, 3765-3774.

Lee, J., Sung, Y.H., Cheong, C., Choi, Y.S., Jeon, H.K., Sun, W., Hahn, W.C., Ishikawa, F., and Lee, H.W. (2008). TERT promotes cellular and organismal survival independently of telomerase activity. Oncogene *27*, 3754-3760.

Lee, K.H., Li, M., Michalowski, A.M., Zhang, X., Liao, H., Chen, L., Xu, Y., Wu, X., and Huang, J. (2010). A genomewide study identifies the Wnt signaling pathway as a major target of p53 in murine embryonic stem cells. Proc Natl Acad Sci U S A *107*, 69-74.

Li, E., Bestor, T.H., and Jaenisch, R. (1992). Targeted mutation of the DNA methyltransferase gene results in embryonic lethality. Cell *69*, 915-926.

Li, Y.Q. (2010). Master stem cell transcription factors and signaling regulation. Cellular reprogramming *12*, 3-13.

Lin, T., Chao, C., Saito, S., Mazur, S.J., Murphy, M.E., Appella, E., and Xu, Y. (2005). p53 induces differentiation of mouse embryonic stem cells by suppressing Nanog expression. Nat Cell Biol *7*, 165-171.

Liu, L., Bailey, S.M., Okuka, M., Munoz, P., Li, C., Zhou, L., Wu, C., Czerwiec, E., Sandler, L., Seyfang, A.*, et al.* (2007). Telomere lengthening early in development. Nat Cell Biol *9*, 1436-1441.

Liu, Y., Snow, B.E., Hande, M.P., Yeung, D., Erdmann, N.J., Wakeham, A., Itie, A., Siderovski, D.P., Lansdorp, P.M., Robinson, M.O.*, et al.* (2000). The telomerase reverse transcriptase is limiting and necessary for telomerase function in vivo. Curr Biol *10*, 1459-1462.

Loh, Y.H., Wu, Q., Chew, J.L., Vega, V.B., Zhang, W., Chen, X., Bourque, G., George, J., Leong, B., Liu, J.*, et al.* (2006). The Oct4 and Nanog transcription network regulates pluripotency in mouse embryonic stem cells. Nat Genet *38*, 431-440.

Lu, R., Yang, A., and Jin, Y. (2011). Dual functions of T-box 3 (Tbx3) in the control of self-renewal and extraembryonic endoderm differentiation in mouse embryonic stem cells. J Biol Chem *286*, 8425-8436.

Luke, B., and Lingner, J. (2009). TERRA: telomeric repeat-containing RNA. Embo J *28*, 2503-2510.

Lynch, M.D., Smith, A.J., De Gobbi, M., Flenley, M., Hughes, J.R., Vernimmen, D., Ayyub, H., Sharpe, J.A., Sloane-Stanley, J.A., Sutherland, L.*, et al.* (2012). An interspecies analysis reveals a key role for unmethylated CpG dinucleotides in vertebrate Polycomb complex recruitment. Embo J *31*, 317-329.

MacDonald, B.T., Tamai, K., and He, X. (2009). Wnt/beta-catenin signaling: components, mechanisms, and diseases. Dev Cell *17*, 9-26.

Mak, W., Nesterova, T.B., de Napoles, M., Appanah, R., Yamanaka, S., Otte, A.P., and Brockdorff, N. (2004). Reactivation of the paternal X chromosome in early mouse embryos. Science *303*, 666-669.

Margueron, R., and Reinberg, D. (2011). The Polycomb complex PRC2 and its mark in life. Nature *469*, 343-349.

Marion, R.M., Strati, K., Li, H., Murga, M., Blanco, R., Ortega, S., Fernandez-Capetillo, O., Serrano, M., and Blasco, M.A. (2009a). A p53-mediated DNA damage response limits reprogramming to ensure iPS cell genomic integrity. Nature *460*, 1149-1153.

Marion, R.M., Strati, K., Li, H., Tejera, A., Schoeftner, S., Ortega, S., Serrano, M., and Blasco, M.A. (2009b). Telomeres acquire embryonic stem cell characteristics in induced pluripotent stem cells. Cell Stem Cell *4*, 141-154.

Martello, G., Sugimoto, T., Diamanti, E., Joshi, A., Hannah, R., Ohtsuka, S., Gottgens, B., Niwa, H., and Smith, A. (2012). Esrrb is a pivotal target of the Gsk3/Tcf3 axis regulating embryonic stem cell self-renewal. Cell Stem Cell *11*, 491-504.

Martin, A.M., Pouchnik, D.J., Walker, J.L., and Wyrick, J.J. (2004). Redundant roles for histone H3 N-terminal lysine residues in subtelomeric gene repression in Saccharomyces cerevisiae. Genetics *167*, 1123-1132.

Martin, G.R. (1980). Teratocarcinomas and mammalian embryogenesis. Science *209*, 768-776.

Martin, G.R. (1981). Isolation of a pluripotent cell line from early mouse embryos cultured in medium conditioned by teratocarcinoma stem cells. Proc Natl Acad Sci U S A *78*, 7634-7638.

Martin, G.R., and Evans, M.J. (1975). Differentiation of clonal lines of teratocarcinoma cells: formation of embryoid bodies in vitro. Proc Natl Acad Sci U S A *72*, 1441-1445.

Martinez, P., Thanasoula, M., Carlos, A.R., Gomez-Lopez, G., Tejera, A.M., Schoeftner, S., Dominguez, O., Pisano, D.G., Tarsounas, M., and Blasco, M.A. (2010). Mammalian Rap1 controls telomere function and gene expression through binding to telomeric and extratelomeric sites. Nat Cell Biol *12*, 768-780.

Matsuda, T., Nakamura, T., Nakao, K., Arai, T., Katsuki, M., Heike, T., and Yokota, T. (1999). STAT3 activation is sufficient to maintain an undifferentiated state of mouse embryonic stem cells. Embo J *18*, 4261-4269.

Matsuo, T., Shimose, S., Kubo, T., Fujimori, J., Yasunaga, Y., and Ochi, M. (2009). Telomeres and telomerase in sarcomas. Anticancer Res *29*, 3833-3836.

Mendenhall, E.M., Koche, R.P., Truong, T., Zhou, V.W., Issac, B., Chi, A.S., Ku, M., and Bernstein, B.E. (2010). GC-rich sequence elements recruit PRC2 in mammalian ES cells. PLoS Genet *6*, e1001244.

Messner, S., and Hottiger, M.O. (2011). Histone ADP-ribosylation in DNA repair, replication and transcription. Trends Cell Biol *21*, 534-542.

Migone, T.S., Rodig, S., Cacalano, N.A., Berg, M., Schreiber, R.D., and Leonard, W.J. (1998). Functional cooperation of the interleukin-2 receptor beta chain and Jak1 in phosphatidylinositol 3-kinase recruitment and phosphorylation. Mol Cell Biol *18*, 6416-6422.

Mikkelsen, T.S., Hanna, J., Zhang, X., Ku, M., Wernig, M., Schorderet, P., Bernstein, B.E., Jaenisch, R., Lander, E.S., and Meissner, A. (2008). Dissecting direct reprogramming through integrative genomic analysis. Nature *454*, 49-55.

Moss, E.G., and Tang, L. (2003). Conservation of the heterochronic regulator Lin-28, its developmental expression and microRNA complementary sites. Dev Biol *258*, 432-442.

Murnane, J.P., Sabatier, L., Marder, B.A., and Morgan, W.F. (1994). Telomere dynamics in an immortal human cell line. Embo J *13*, 4953-4962.

Nakatake, Y., Fukui, N., Iwamatsu, Y., Masui, S., Takahashi, K., Yagi, R., Yagi, K., Miyazaki, J., Matoba, R., Ko, M.S.*, et al.* (2006). Klf4 cooperates with Oct3/4 and Sox2 to activate the Lefty1 core promoter in embryonic stem cells. Mol Cell Biol *26*, 7772-7782.

Navarro, P., Festuccia, N., Colby, D., Gagliardi, A., Mullin, N.P., Zhang, W., Karwacki-Neisius, V., Osorno, R., Kelly, D., Robertson, M.*, et al.* (2012). OCT4/SOX2-independent Nanog autorepression modulates heterogeneous Nanog gene expression in mouse ES cells. Embo J.

Nelson, J.D., Denisenko, O., and Bomsztyk, K. (2006). Protocol for the fast chromatin immunoprecipitation (ChIP) method. Nature protocols *1*, 179-185.

Neumann, A.A., Watson, C.M., Noble, J.R., Pickett, H.A., Tam, P.P.L., and Reddel, R.R. (2013). Alternative lengthening of telomeres in normal mammalian somatic cells. Genes Dev *27*, 18-23.

Nichols, J., and Smith, A. (2009). Naive and primed pluripotent states. Cell Stem Cell *4*, 487-492.

Nichols, J., Zevnik, B., Anastassiadis, K., Niwa, H., Klewe-Nebenius, D., Chambers, I., Scholer, H., and Smith, A. (1998). Formation of pluripotent stem cells in the mammalian embryo depends on the POU transcription factor Oct4. Cell *95*, 379-391.

Nishinakamura, R., Matsumoto, Y., Matsuda, T., Ariizumi, T., Heike, T., Asashima, M., and Yokota, T. (1999). Activation of Stat3 by cytokine receptor gp130 ventralizes Xenopus embryos independent of BMP-4. Dev Biol *216*, 481-490.

Niwa, H. (2007). How is pluripotency determined and maintained? Development *134*, 635-646.

Niwa, H., Miyazaki, J., and Smith, A.G. (2000). Quantitative expression of Oct-3/4 defines differentiation, dedifferentiation or self-renewal of ES cells. Nat Genet *24*, 372-376.

Niwa, H., Ogawa, K., Shimosato, D., and Adachi, K. (2009). A parallel circuit of LIF signalling pathways maintains pluripotency of mouse ES cells. Nature *460*, 118-122.

Okano, M., Bell, D.W., Haber, D.A., and Li, E. (1999). DNA methyltransferases Dnmt3a and Dnmt3b are essential for de novo methylation and mammalian development. Cell *99*, 247-257.

Paling, N.R., Wheadon, H., Bone, H.K., and Welham, M.J. (2004). Regulation of embryonic stem cell self-renewal by phosphoinositide 3-kinase-dependent signaling. J Biol Chem *279*, 48063-48070.

Palm, W., and de Lange, T. (2008). How shelterin protects mammalian telomeres. Annual review of genetics *42*, 301-334.

Park, J.I., Venteicher, A.S., Hong, J.Y., Choi, J., Jun, S., Shkreli, M., Chang, W., Meng, Z., Cheung, P., Ji, H.*, et al.* (2009). Telomerase modulates Wnt signalling by association with target gene chromatin. Nature *460*, 66-72.

Paull, T.T., Rogakou, E.P., Yamazaki, V., Kirchgessner, C.U., Gellert, M., and Bonner, W.M. (2000). A critical role for histone H2AX in recruitment of repair factors to nuclear foci after DNA damage. Curr Biol *10*, 886-895.

Petrie, K., Zelent, A., and Waxman, S. (2009). Differentiation therapy of acute myeloid leukemia: past, present and future. Curr Opin Hematol *16*, 84-91.

Phillips, D.M. (1963). The presence of acetyl groups of histones. Biochem J *87*, 258-263.

Pickett, H.A., Cesare, A.J., Johnston, R.L., Neumann, A.A., and Reddel, R.R. (2009). Control of telomere length by a trimming mechanism that involves generation of t-circles. The EMBO journal *28*, 799-809.

Pickett, H.A., Henson, J.D., Au, A.Y., Neumann, A.A., and Reddel, R.R. (2011). Normal mammalian cells negatively regulate telomere length by telomere trimming. Hum Mol Genet *20*, 4684-4692.

Prowse, K.R., and Greider, C.W. (1995). Developmental and tissue-specific regulation of mouse telomerase and telomere length. Proc Natl Acad Sci U S A *92*, 4818-4822.

Qin, H., Yu, T., Qing, T., Liu, Y., Zhao, Y., Cai, J., Li, J., Song, Z., Qu, X., Zhou, P., *et al.* (2007). Regulation of apoptosis and differentiation by p53 in human embryonic stem cells. J Biol Chem *282*, 5842-5852.

Ramsahoye, B.H., Biniszkiewicz, D., Lyko, F., Clark, V., Bird, A.P., and Jaenisch, R. (2000). Non-CpG methylation is prevalent in embryonic stem cells and may be mediated by DNA methyltransferase 3a. Proc Natl Acad Sci U S A *97*, 5237-5242.

Rodda, D.J., Chew, J.L., Lim, L.H., Loh, Y.H., Wang, B., Ng, H.H., and Robson, P. (2005). Transcriptional regulation of nanog by OCT4 and SOX2. J Biol Chem *280*, 24731-24737.

Roth, A., Harley, C.B., and Baerlocher, G.M. (2010). Imetelstat (GRN163L)--telomerase-based cancer therapy. Recent Results Cancer Res *184*, 221-234.

Royle, N.J., Foxon, J., Jeyapalan, J.N., Mendez-Bermudez, A., Novo, C.L., Williams, J., and Cotton, V.E. (2008a). Telomere length maintenance--an ALTernative mechanism. Cytogenet Genome Res *122*, 281-291.

Royle, N.J., Foxon, J., Jeyapalan, J.N., Mendez-Bermudez, A., Novo, C.L., Williams, J., and Cotton, V.E. (2008b). Telomere length maintenance--an ALTernative mechanism. Cytogenet Genome Res *122*, 281-291.

Sabapathy, K., Klemm, M., Jaenisch, R., and Wagner, E.F. (1997). Regulation of ES cell differentiation by functional and conformational modulation of p53. Embo J *16*, 6217-6229.

Sansom, O.J., Reed, K.R., van de Wetering, M., Muncan, V., Winton, D.J., Clevers, H., and Clarke, A.R. (2005). Cyclin D1 is not an immediate target of beta-catenin following Apc loss in the intestine. J Biol Chem *280*, 28463-28467.

Sarin, K.Y., Cheung, P., Gilison, D., Lee, E., Tennen, R.I., Wang, E., Artandi, M.K., Oro, A.E., and Artandi, S.E. (2005). Conditional telomerase induction causes proliferation of hair follicle stem cells. Nature *436*, 1048-1052.

Savarese, F., Davila, A., Nechanitzky, R., De La Rosa-Velazquez, I., Pereira, C.F., Engelke, R., Takahashi, K., Jenuwein, T., Kohwi-Shigematsu, T., Fisher, A.G.*, et al.* (2009). Satb1 and Satb2 regulate embryonic stem cell differentiation and Nanog expression. Genes Dev *23*, 2625-2638.

Saxonov, S., Berg, P., and Brutlag, D.L. (2006). A genome-wide analysis of CpG dinucleotides in the human genome distinguishes two distinct classes of promoters. Proc Natl Acad Sci U S A *103*, 1412-1417.

Schoeftner, S., and Blasco, M.A. (2010). Chromatin regulation and non-coding RNAs at mammalian telomeres. Semin Cell Dev Biol *21*, 186-193.

Schoeftner, S., Sengupta, A.K., Kubicek, S., Mechtler, K., Spahn, L., Koseki, H., Jenuwein, T., and Wutz, A. (2006). Recruitment of PRC1 function at the initiation of X inactivation independent of PRC2 and silencing. Embo J *25*, 3110-3122.

Selwood, L., and Johnson, M.H. (2006). Trophoblast and hypoblast in the monotreme, marsupial and eutherian mammal: evolution and origins. Bioessays *28*, 128-145.

Shay, J.W., and Wright, W.E. (2010). Telomeres and telomerase in normal and cancer stem cells. FEBS Lett *584*, 3819-3825.

Shen, X., Liu, Y., Hsu, Y.J., Fujiwara, Y., Kim, J., Mao, X., Yuan, G.C., and Orkin, S.H. (2008). EZH1 mediates methylation on histone H3 lysine 27 and complements EZH2 in maintaining stem cell identity and executing pluripotency. Molecular cell *32*, 491-502.

Shi, W., Wang, H., Pan, G., Geng, Y., Guo, Y., and Pei, D. (2006). Regulation of the pluripotency marker Rex-1 by Nanog and Sox2. J Biol Chem *281*, 23319-23325.

Silva, J., Nichols, J., Theunissen, T.W., Guo, G., van Oosten, A.L., Barrandon, O., Wray, J., Yamanaka, S., Chambers, I., and Smith, A. (2009). Nanog is the gateway to the pluripotent ground state. Cell *138*, 722-737.

Silva, J., and Smith, A. (2008). Capturing pluripotency. Cell *132*, 532-536.

Singh, A.M., Hamazaki, T., Hankowski, K.E., and Terada, N. (2007). A heterogeneous expression pattern for Nanog in embryonic stem cells. Stem Cells *25*, 2534-2542.

Sinkkonen, L., Hugenschmidt, T., Berninger, P., Gaidatzis, D., Mohn, F., Artus-Revel, C.G., Zavolan, M., Svoboda, P., and Filipowicz, W. (2008). MicroRNAs control de novo DNA methylation through regulation of transcriptional repressors in mouse embryonic stem cells. Nat Struct Mol Biol *15*, 259-267.

Smith, Z.D., and Meissner, A. (2013). DNA methylation: roles in mammalian development. Nat Rev Genet *14*, 204-220.

Smogorzewska, A., and de Lange, T. (2002). Different telomere damage signaling pathways in human and mouse cells. Embo J *21*, 4338-4348.

Softic, S., Kirby, M., Berger, N.G., Shroyer, N.F., Woods, S.C., and Kohli, R. (2012). Insulin concentration modulates hepatic lipid accumulation in mice in part via transcriptional regulation of fatty acid transport proteins. PLoS One *7*, e38952.

Stock, J.K., Giadrossi, S., Casanova, M., Brookes, E., Vidal, M., Koseki, H., Brockdorff, N., Fisher, A.G., and Pombo, A. (2007). Ring1-mediated ubiquitination of H2A restrains poised RNA polymerase II at bivalent genes in mouse ES cells. Nat Cell Biol *9*, 1428-1435.

Strong, M.A., Vidal-Cardenas, S.L., Karim, B., Yu, H., Guo, N., and Greider, C.W. (2011). Phenotypes in mTERT(+)/(-) and mTERT(-)/(-) mice are due to short

telomeres, not telomere-independent functions of telomerase reverse transcriptase. Mol Cell Biol *31*, 2369-2379.

Taboski, M.A.S., Sealey, D.C.F., Dorrens, J., Tayade, C., Betts, D.H., and Harrington, L. (2012). Long telomeres bypass the requirement for long telomeres in human tumorigenesis. Cell Reports *1*, 91-98.

Takahashi, K., and Yamanaka, S. (2006). Induction of pluripotent stem cells from mouse embryonic and adult fibroblast cultures by defined factors. Cell *126*, 663-676.

Tilman, G., Loriot, A., Van Beneden, A., Arnoult, N., Londono-Vallejo, J.A., De Smet, C., and Decottignies, A. (2009). Subtelomeric DNA hypomethylation is not required for telomeric sister chromatid exchanges in ALT cells. Oncogene *28*, 1682-1693.

Tomida, M., Yamamoto-Yamaguchi, Y., and Hozumi, M. (1984). Purification of a factor inducing differentiation of mouse myeloid leukemic M1 cells from conditioned medium of mouse fibroblast L929 cells. J Biol Chem *259*, 10978-10982.

Tsumura, A., Hayakawa, T., Kumaki, Y., Takebayashi, S., Sakaue, M., Matsuoka, C., Shimotohno, K., Ishikawa, F., Li, E., Ueda, H.R.*, et al.* (2006). Maintenance of self-renewal ability of mouse embryonic stem cells in the absence of DNA methyltransferases Dnmt1, Dnmt3a and Dnmt3b. Genes to cells : devoted to molecular & cellular mechanisms *11*, 805-814.

Tysnes, B.B. (2010). Tumor-initiating and -propagating cells: cells that we would like to identify and control. Neoplasia *12*, 506-515.

Vastenhouw, N.L., and Schier, A.F. (2012). Bivalent histone modifications in early embryogenesis. Curr Opin Cell Biol *24*, 374-386.

Vaziri, H., and Benchimol, S. (1998). Reconstitution of telomerase activity in normal human cells leads to elongation of telomeres and extended replicative life span. Curr Biol *8*, 279-282.

Vera, E., Canela, A., Fraga, M.F., Esteller, M., and Blasco, M.A. (2008). Epigenetic regulation of telomeres in human cancer. Oncogene *27*, 6817-6833.

Villasante, A., Piazzolla, D., Li, H., Gomez-Lopez, G., Djabali, M., and Serrano, M. (2011). Epigenetic regulation of Nanog expression by Ezh2 in pluripotent stem cells. Cell cycle *10*, 1488-1498.

Wang, Z., Zang, C., Cui, K., Schones, D.E., Barski, A., Peng, W., and Zhao, K. (2009). Genome-wide mapping of HATs and HDACs reveals distinct functions in active and inactive genes. Cell *138*, 1019-1031.

Watanabe, S., Umehara, H., Murayama, K., Okabe, M., Kimura, T., and Nakano, T. (2006). Activation of Akt signaling is sufficient to maintain pluripotency in mouse and primate embryonic stem cells. Oncogene *25*, 2697-2707.

Weng, N.P., Levine, B.L., June, C.H., and Hodes, R.J. (1996). Regulated expression of telomerase activity in human T lymphocyte development and activation. J Exp Med *183*, 2471-2479.

Wu, H., and Zhang, Y. (2011). Mechanisms and functions of Tet protein-mediated 5-methylcytosine oxidation. Genes Dev *25*, 2436-2452.

Yeom, Y.I., Fuhrmann, G., Ovitt, C.E., Brehm, A., Ohbo, K., Gross, M., Hubner, K., and Scholer, H.R. (1996). Germline regulatory element of Oct-4 specific for the totipotent cycle of embryonal cells. Development *122*, 881-894.

Ying, Q.L., Nichols, J., Chambers, I., and Smith, A. (2003). BMP induction of Id proteins suppresses differentiation and sustains embryonic stem cell self-renewal in collaboration with STAT3. Cell *115*, 281-292.

Yu, J., Vodyanik, M.A., Smuga-Otto, K., Antosiewicz-Bourget, J., Frane, J.L., Tian, S., Nie, J., Jonsdottir, G.A., Ruotti, V., Stewart, R.*, et al.* (2007). Induced pluripotent stem cell lines derived from human somatic cells. Science *318*, 1917-1920.

Yuan, H., Corbi, N., Basilico, C., and Dailey, L. (1995). Developmental-specific activity of the FGF-4 enhancer requires the synergistic action of Sox2 and Oct-3. Genes Dev *9*, 2635-2645.

Zalzman, M., Falco, G., Sharova, L.V., Nishiyama, A., Thomas, M., Lee, S.L., Stagg, C.A., Hoang, H.G., Yang, H.T., Indig, F.E.*, et al.* (2010). Zscan4 regulates telomere elongation and genomic stability in ES cells. Nature *464*, 858-863.

Zentner, G.E., and Henikoff, S. (2013). Regulation of nucleosome dynamics by histone modifications. Nat Struct Mol Biol *20*, 259-266.

Zhang, X., Mar, V., Zhou, W., Harrington, L., and Robinson, M.O. (1999). Telomere shortening and apoptosis in telomerase-inhibited human tumor cells. Genes Dev *13*, 2388-2399.

Zheng, X., and Hu, G. (2012). Oct4GiP reporter assay to study genes that regulate mouse embryonic stem cell maintenance and self-renewal. J Vis Exp.

Zhu, H., Shyh-Chang, N., Segre, A.V., Shinoda, G., Shah, S.P., Einhorn, W.S., Takeuchi, A., Engreitz, J.M., Hagan, J.P., Kharas, M.G.*, et al.* (2011). The Lin28/let-7 axis regulates glucose metabolism. Cell *147*, 81-94.

Ziller, M.J., Muller, F., Liao, J., Zhang, Y., Gu, H., Bock, C., Boyle, P., Epstein, C.B., Bernstein, B.E., Lengauer, T.*, et al.* (2011). Genomic distribution and inter-sample variation of non-CpG methylation across human cell types. PLoS Genet *7*, e1002389.

Appendix B

Main contributions to the work: A) Performed Q-FISH experiments (as described in material and methods). B) Introduction, and selection for positive colonies, of mouse *Tert* cDNA into *Tert*$^{-/-}$ ESCs (as described in material and methods).

frontiers in ONCOLOGY

ORIGINAL RESEARCH ARTICLE
published: xx May 2013
doi: 10.3389/fonc.2013.00146

Telomeres, a busy platform for cell signaling

Q1 *Laura Gardano[1]*†, Fabio Pucci[1], Larissa Christian[1], Thierry Le Bihan[2] and Lea Harrington[1,3]**

[1] Wellcome Trust Centre for Cell Biology, University of Edinburgh, Edinburgh, UK
[2] Centre for Systems Biology, University of Edinburgh, Edinburgh, UK
[3] Institut de Recherche en Immunologie et Cancérologie, Université de Montréal, Montréal, QC, Canada

Edited by:
Claus M. Azzalin, ETH Zurich, Switzerland
Susan Bailey, Colorado State University, USA

Reviewed by:
Tara Lyn Beattie, University of Calgary, Canada
Michael Chang, European Research Institute for the Biology of Ageing, Netherlands

***Correspondence:**
Laura Gardano, INSERM U978, UFR SMBH, University Paris 13, 74 rue Marcel Cachin, 93017 Bobigny, France.
e-mail: laura.gardano@univ-paris13.fr; Lea Harrington, Institut de Recherche en Immunologie et en Cancérologie, Université de Montréal, Pavillon Marcelle-Coutu, 2950 Chemin de Polytechnique, Montréal, QC H3T 1J4, Canada.
e-mail: lea.harrington@umontreal.ca

† Present address:
Laura Gardano, INSERM U978, Université Paris 13, Bobigny, France.

Telomeres are the terminal structures at the ends of linear chromosomes that represent a solution to the end replication problem. Specific binding of the six-protein subunit complex shelterin to telomeric, repetitive TTAGGG DNA sequences contributes to the stable architecture and maintenance of telomeres. Proteins involved in the DNA damage response are also localized at telomeres, and play a role in the surveillance and maintenance of telomere integrity. The enzyme responsible for telomere extension is telomerase, a ribonucleoprotein with reverse transcriptase activity. In the absence of telomerase, telomeres shorten to a length threshold that triggers the DNA damage response and replicative senescence. Here, we will summarize the latest findings concerning vertebrate telomere structure and epigenetics, and we present data regarding the impact of short telomeres upon cell signaling. In particular, in murine embryonic stem cells lacking telomerase, we found that distribution of cytosolic/nuclear β-catenin, a key component of the Wnt signaling pathway, changes when telomeres become critically short. We discuss implications and future perspectives of the effect of epigenetic modifications and/or conformational changes of telomeres on cell metabolism and signaling networks. Such an analysis may unveil potential therapeutic targets for pathologies like cancer, where the integrity of telomeres is altered.

Keywords: telomere, telomerase, shelterin, Wnt signaling, β-catenin, APC

INTRODUCTION

TELOMERE STRUCTURE IN VERTEBRATES

Telomeres are the structures at the ends of chromosomes that protect them from end-to-end fusions and solve the problem of end replication, i.e., the loss of genetic material due to inherent limitations in the DNA replication process (Blackburn, 1991). Telomeres consists of a repeated six-nucleotide G-rich sequence, 5′-TTAGGG-3′, that is folded into a telomeric loop (t-loop) (Griffith et al., 1999). The telomere contains a double-stranded region and a single-stranded overhang, also referred to as the G-strand overhang, whose length is tightly regulated (Wright et al., 1997; Sfeir et al., 2005; Wu et al., 2012). Telomeres are protected and regulated by a specific hexaprotein complex, called shelterin (i.e., TRF1, TRF2, RAP1, TIN2, POT1, TPP1) (**Figure 1A**), and additional non-telomere specific proteins that are implicated in the cellular DNA damage response (de Lange, 2005; Longhese, 2008). Shelterin inhibits the ataxia telangiectasia mutated (ATM) and ATM and Rad3-related (ATR)-dependent DNA damage response, non-homologous end joining and homologous recombination DNA repair pathways, and resection by 5′-exonucleases (Sfeir and de Lange, 2012). Some of these activities are specific to shelterin whereas other activities that inhibit non-homologous end joining and resection are supported by other telomere-associated proteins such as Ku70/80 and 53BP1, respectively (Sfeir and de Lange, 2012). As the enzyme responsible for telomere extension, telomerase is a key factor that contributes to chromosome end protection (Blackburn et al., 1989). Telomerase is a reverse transcriptase that copies a stably associated RNA template into telomere DNA (Greider and Blackburn, 1987, 1989; Shippen-Lentz and Blackburn, 1990). In mice, the extension of telomeres occurs during S-phase and telomerase extends the shortest telomeres preferentially (Hemann and Greider, 1999; Samper et al., 2001; Stern and Bryan, 2008).

TELOMERE EPIGENETICS

Telomeric DNA contains nucleosomes, although the nature of telomeric chromatin is peculiar (Makarov et al., 1993) (**Figure 1B**). Simplistically, nucleosomes and shelterin compete with each other for the binding of telomeric DNA, hence it is not surprising that TRF2 influences the positioning of the nucleosomes, i.e., the nucleosome abundance at telomeres is inversely correlated with the amount of TRF2 (Benetti et al., 2008b; Galati et al., 2012). Nucleosome spacing by TRF2 occurs in S/G2 phase, which coincides with the end of DNA replication and telomere replication (Galati et al., 2012). Epigenetic marks, notably histone and DNA methylation, in sub-telomeric and telomeric regions contribute further to telomere maintenance and stability (Blasco, 2007) (**Figure 1B**). A high degree of DNA methylation guarantees a closed chromatin

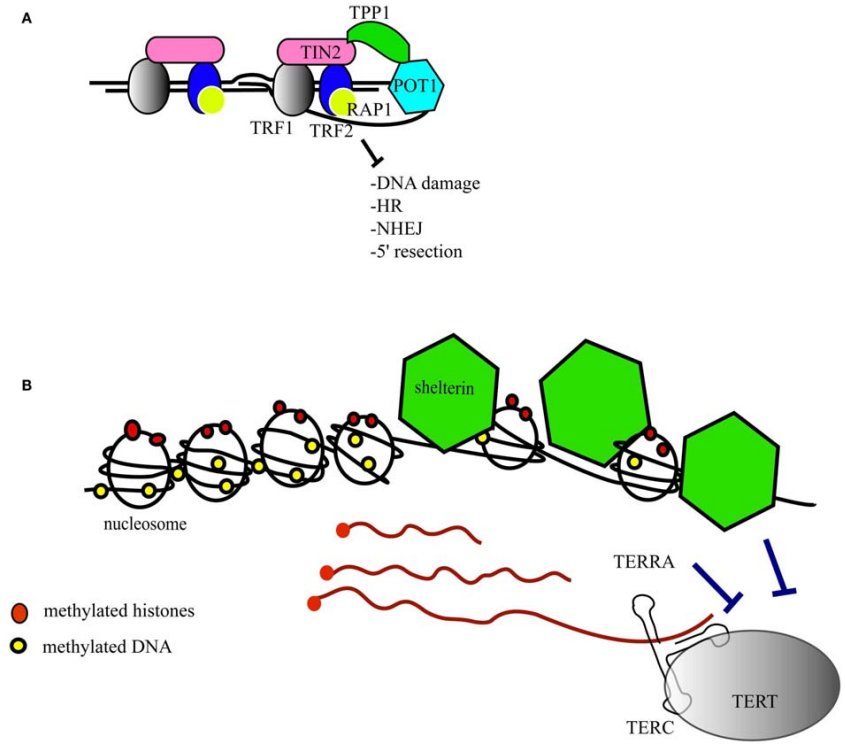

FIGURE 1 | Structure of the telomeres. (A) The telomere folds into a telomeric loop (t-loop) and binds the six-protein subunit complex shelterin. TRF1 (in gray) and TRF2 (in blue) bind double-stranded telomeric DNA. POT1 (in light blue) binds to single-stranded telomeric DNA. RAP1 (in yellow) is recruited to the telomere by an interaction with TRF2. TIN2 (in pink) serves as a scaffold to recruit TRF1, TRF2, and TPP1 (in green), which in turn interacts with POT1. The main functions are listed in the figure and further details are given in the text. HR, homologous recombination; NHEJ, non-homologous end joining. **(B)** Epigenetic marks at the telomere (red dots represent histone methylation and yellow dots represent DNA methylation). The shelterin complex (green) regulates nucleosome spacing. The telomeres are transcribed into TERRAs (red strings) that inhibit telomerase catalytic activity, and shelterin inhibits telomerase access. TERC, the RNA component of telomerase; TERT, the catalytic subunit of telomerase.

state that is associated with gene silencing in regions upstream of the telomeres. This phenomenon, first described in *Drosophila melanogaster* and yeast, is known as the telomere positioning effect or TPE (Levis et al., 1985; Gottschling et al., 1990; Nimmo et al., 1994). In humans, telomere length positively affects TPE through a change in the conformation of chromatin (Baur et al., 2001). Epigenetic defects at telomeres, such as those driven by the loss of DNA methyl transferases or histone methyl transferases, lead to telomere defects that result in aberrant telomere lengthening attributed partially to an increase in homologous recombination (Gonzalo et al., 2006; Benetti et al., 2007b, 2008a). In mice lacking the telomerase reverse transcriptase (*mTert*$^{-/-}$), short telomeres are associated with epigenetic changes at the telomeres, i.e., a decrease of tri-methylated histone 3 and histone 4 and an increase in histone acetylation (Benetti et al., 2007a). Thus, critically shortened telomeres show signs of an "open" chromatin state that favors recombination events (Benetti et al., 2008a). It is reasonable to postulate that epigenetic changes in telomeric DNA and histones affect the binding of shelterin and, in turn, affect telomere structure and the recruitment of telomerase (Blasco, 2007).

The complex regulation of telomeric structure, maintenance, and epigenetics has been underscored further by the discovery of the transcription of telomeres into a telomere repeat-containing RNA (TERRA) that contains UUAGGG repeats (Azzalin et al.,

2007; Schoeftner and Blasco, 2008) (**Figure 1B**). The length and amount of TERRAs are directly correlated with telomere length and vary with the cell cycle. The precise role of TERRAs has not yet been established fully, but TERRAs are proving to be an interesting regulator of telomere dynamics.

TELOMERES, TELOMERASE, AND THE WNT SIGNALING PATHWAY

Telomere dysfunction is also linked to perturbation of other cellular processes that include the Wnt/β-catenin signaling pathway. The Wnt/β-catenin signaling cascade controls many aspects of organism development, cell proliferation, and differentiation (Valenta et al., 2012). In the absence of Wnt, β-catenin is phosphorylated and rapidly degraded by a destruction complex containing Axin, APC, CK1, and GSK3β (Clevers and Nusse, 2012). However, in the presence of Wnt, β-catenin is stabilized and imported into the nucleus where, together with the transcription complex TCF/LEF, it regulates the transcription of Wnt target genes (Behrens et al., 1996; Molenaar et al., 1996). Cytoplasmic β-catenin localizes to the cell membrane through an interaction with E-cadherin and serves to stabilize cell adhesion (Ozawa et al., 1989).

The first link between telomerase and Wnt signaling was suggested from an analysis of transcription profiles of mouse and human cells expressing catalytically active or inactive Tert (Choi et al., 2008). Stem cells that express mTert, irrespective of its competence for catalytic activity, exhibit transcriptional activation of genes regulated by Wnt (Choi et al., 2008). In addition, mTert is localized to the promoters of genes regulated by Wnt3a and β-catenin (Park et al., 2009). In mESC over-expressing mTert, the activation of Wnt signaling by LiCl leads to the transcriptional activation of β-catenin (Park et al., 2009). However, another study compared the transcriptional profile of cells from *mTert*$^{-/-}$ mice with *mTerc*$^{-/-}$ mice, and observed no substantial difference in gene expression. In particular, the Wnt signaling network was unaffected, and the authors suggested that the link between telomerase and Wnt signaling might be a neomorph due to telomerase over-expression (Vidal-Cardenas and Greider, 2010). More recently, it has been found that β-catenin can regulate *mTert* transcription in mESC (Hoffmeyer et al., 2012). This regulation involves Klf4, one of the four transcription factors required to induce pluripotent stem cells. The control operated on *mTert* by β-catenin may be direct because β-catenin occupies the *mTert* promoter (Hoffmeyer et al., 2012). β-catenin also activates *TRF2* transcription (Diala et al., 2013). Finally, *c-myc*, which is also under the control of β-catenin/Wnt signaling, is a known regulator of *mTert* transcription (Wang et al., 1998), thus implying a very tight regulation of this gene and the involvement of multiple signaling networks (Greider, 2012).

Telomere attrition triggers activation of the DNA damage response and other changes that herald the onset of genome instability (Cimprich and Cortez, 2008; Schoeftner and Blasco, 2010). To dissect the complexity of such processes, it is important to distinguish between the impact of telomerase loss versus the impact on telomere length. In this regard, murine embryonic stem cells represent a valuable model system and in ESC lacking *mTert*, we show that critically short telomeres (and not telomerase presence *per se*) can impact cell signaling cascades even in the cytoplasm. We focused on β-catenin because of its known link to telomere function and because its dynamic phosphorylation-dependent regulation appeared a logical choice for a first examination of the impact of DNA damage signaling at the telomere in the cytoplasm. Our data suggest that alteration of telomere structure or epigenetic modifications elicited by telomere shortening impacts cell signaling in extra-nuclear locations, which in turn may affect cell adhesion, metabolism, and protein turnover.

RESULTS

SHORT TELOMERES AFFECT CELL ADHESION AND β-CATENIN DISTRIBUTION

Murine ESC lacking the telomerase reverse transcriptase were generated and characterized previously and show an accumulation of telomere signal-free ends at late passage (Liu et al., 2000; Erdmann et al., 2004). We queried whether the abundance of key signaling factors would be altered in the presence of short telomeres, and focused our investigation on β-catenin, a critical component of the Wnt signaling network that controls cell proliferation and differentiation (Clevers and Nusse, 2012). β-catenin distribution and post-translational modifications were compared in *mTert*$^{-/-}$ at late passage (>60 passages) and wild-type ESC at a similar passage number (**Figure 2A**). We observed that cytosolic β-catenin was significantly more abundant in *mTert*$^{-/-}$ ESC with critically short telomeres compared to wild-type cells (**Figure 2B**, Student's *t*-test $P = 0.003$) while the total content remained unchanged (**Figure 2B**, $P = 0.968$). Accordingly, higher levels of nuclear β-catenin were observed in wild-type cells (**Figure 2C**, $P = 0.027$). Taken together, these results indicate that the distribution of β-catenin differed between the two cell types.

β-Catenin is a target of the GSK3β kinase which phosphorylates the residues S33/37, and T41. The tri-phosphorylated form of β-catenin is rapidly degraded by the proteasome (Liu et al., 2002). We used an antibody specific for the triple-phosphorylated β-catenin (S33/37, T41) to assess the phosphorylation status of β-catenin in ESCs with or without short telomeres, and found no difference in the levels of phosphorylated, cytosolic β-catenin (**Figure 2E**). Since the degradation of phospho-β-catenin occurs very rapidly and may mask subtle differences in abundance, we treated ESCs with the proteasome inhibitor MG132. In the presence of MG132, the difference in the phosphorylation status of cytosolic β-catenin in wild-type cells compared to *mTert*$^{-/-}$ ESC achieved statistical significance (**Figure 2D**, $P = 0.0014$). These results suggest that β-catenin is degraded less rapidly in *mTert*$^{-/-}$ ESC with short telomeres, or that there is a pool of β-catenin in cells with critically short telomeres that is immune to proteasome-dependent degradation.

As GSK3β activity is inhibited by the phosphorylation of a serine at amino acid position 9 (Sutherland et al., 1993; Desbois-Mouthon et al., 2001; Fukumoto et al., 2001), we assessed the serine 9 phosphorylation status of GSK3β. We did not detect a significant difference between wild-type and *mTert*$^{-/-}$ ESCs (**Figure 2E**). GSK3β is phosphorylated by the kinase AKT, whose activity is regulated by the phosphorylation of serine 473 (Alessi et al., 1997; Fukumoto et al., 2001). Furthermore, we did not observe a significant difference in the level of AKT phosphorylation between wild-type and *mTert*$^{-/-}$ cells (**Figure 2E**). These results suggest

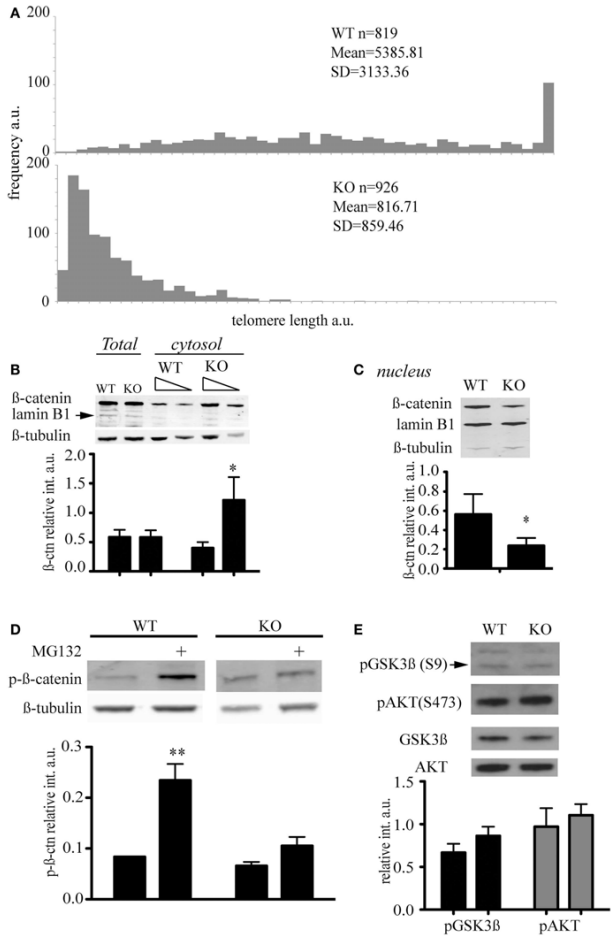

FIGURE 2 | Telomere shortening affects β-catenin cellular distribution and its degradation. **(A)** Q-FISH analysis of wild-type (WT) and *mTert*$^{-/-}$ mESC (KO) at passage 61 and 70 respectively ($P < 0.001$). **(B)** Immunoblot of total and cytosolic cell extract of WT and KO mESC at passage >60. The membrane was probed with an anti-total β-catenin antibody and anti-β-tubulin antibody. Anti-lamin B antibody was used to assess the purity of the cytosolic fractionation (10 and 5 μg loaded, respectively). The signal for cytosolic β-catenin was quantified relative to the signal for β-tubulin (IRDye® Infrared Dyes, LI-COR Biosciences). **(C)** Immunoblot of nuclear cell extract of WT and KO mESC at a passage >60. The membrane was probed with an anti-total β-catenin antibody and an anti-lamin B1 antibody. Anti-β-tubulin antibody was used to assess the purity of the nuclear fractionation. The signal for nuclear β-catenin was quantified relative to the signal for lamin B1. **(D)** Immunoblot of phosphorylated β-catenin in cytosolic cell extracts treated with (+) and without the proteasome inhibitor MG132 (10 μM) for 6 h. The signal for cytosolic phospho-β-catenin was quantified relative to the signal for β-tubulin. The histograms in **(A–C)** represent the data of the blot shown plus two other independent data sets (average ± standard deviation; Student's *t*-test: $*P < 0.05$, $**P < 0.01$). **(E)** Enhanced chemiluminescence immunoblot of total cell extract of WT and KO mESC probed with anti-phospho-GSK (S9), anti-total GSK, anti-phospho-AKT (S473), and anti-total AKT antibodies. The blot shown is representative of at least three independent experiments. The signal of p-GSK3β and p-AKT was quantified relative to the total unphosphorylated protein, GSK, and AKT respectively. The histograms represent the average of four independent analysis, $P = 0.057$ for p-GSK3β and $P = 0.39$ for p-AKT. β-ctn = β-catenin. Error bars indicate standard deviation.

that downstream effectors of Wnt signaling remain unaltered in *mTert*$^{-/-}$ cells with critically short telomeres.

COMPARISON OF WNT SIGNAL TRANSDUCTION

LiCl is an inhibitor of GSK3β that triggers phosphorylation on serine 9 through an as yet unknown mechanism (Rao et al., 2005a). Because inactivation of the kinase activity of GSK3β results in the inhibition of phosphorylation of β-catenin and its stabilization, LiCl treatment is often used to activate Wnt (Rao et al., 2005b). To assess whether the different distribution of β-catenin was associated with a difference in Wnt signaling, we treated mESC with LiCl and, as expected, observed a stabilization of β-catenin levels in both wild-type and *mTert*$^{-/-}$ ESCs (**Figure 3A**). We did not detect a significant difference in the transcription of a specific target of Wnt signaling, *Axin2*, in response to Wnt3a (**Figure 3B**). Similar to *Axin2*, a reporter system containing three consensus TCF binding sites upstream of firefly luciferase gene did not exhibit a statistically significant difference between WT and KO cells (**Figure 3C**) (Korinek et al., 1998). Thus, two independent outputs of Wnt signaling were not appreciably altered in *mTert*$^{-/-}$ ESCs with short telomeres. The transcription of the cell cycle-regulated genes *c-myc* and *cyclinD1* are also regulated by Wnt and many other signaling networks, but did not exhibit a statistically significant trend in response to Wnt3a (Burdon et al., 2002; Jho et al., 2002) (data not shown).

In order to identify factors responsible for β-catenin cytosolic accumulation in *mTert*$^{-/-}$ ESCs with short telomeres, we compared the profile of β-catenin interacting proteins using mass spectrometry. Three independent β-catenin immunoprecipitations from total lysates were performed and only proteins recovered in all three experiments were considered (152 proteins in total). We considered a protein interaction significantly different between wild-type or *mTert*$^{-/-}$ ESC if it exhibited a peptide intensity ratio of <0.667 or >1.5 with an unpaired Student's *t*-test *P* value < 0.05 (see Section Materials and Methods). Adenomatous polyposis coli (APC), was enriched by approximately twofold, ($P = 0.03$) in *mTert*$^{-/-}$ ESC relative to wild-type ESC (**Table 1**). APC interacts with β-catenin and together with Axin1, constitutes the scaffold of the destruction complex that regulates the stability of cytosolic β-catenin (Rubinfeld et al., 1993; Hart et al., 1998; Hamada and Bienz, 2004; Clevers and Nusse, 2012). Interestingly APC is also

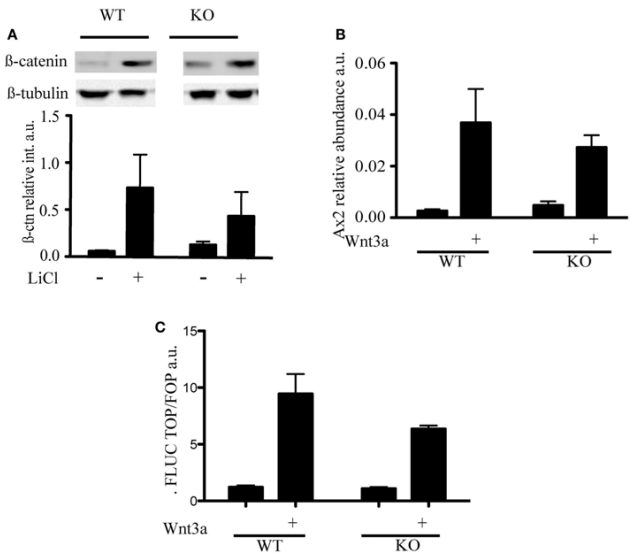

FIGURE 3 | Wnt signaling in telomerase knock-out mESC with short telomeres and β-catenin interactors. **(A)** Immunoblot and quantification of β-catenin detected in cytosolic cell extracts of mESC treated with LiCl (30 mM) for 3 h. The intensity of β-catenin was normalized to the intensity of β-tubulin. The histogram represents the average (±standard deviation) of three independent experiments. **(B)** qRT-PCR to measure the transcript of Axin2 used to quantify Wnt activation. WT and KO cells were treated with Wnt3a (100 ng/mL) for 3 days. The histogram represents the average (±standard deviation) of three independent qRT-PCR experiments, each performed with three replicates. **(C)** Transcriptional output of β-catenin activity measured using the Top-Flash Luciferase Assay. The histogram represents the average (±standard deviation) of the ratio of Renilla normalized firefly luciferase activity in Top versus Fop plasmid transfected cells of two independent experiments. Using a student's *t*-test, no difference was noted in the presence or absence of Wnt3a ($P = 0.223$).

Table 1 | Results of IP-MS of β-catenin in WT and *mTert*$^{-/-}$ mESC.

Accession ID	Description	Total peptides	Peptides quantified	Average intensity WT a.u.	Average intensity KO a.u.	*P* value	Ratio KO/WT
Gi|86262157|ref|NP_808386.2|	Hypothetical protein LOC239796	4	3	0.00343	0.00155	0.00037	0.45091
Gi|124486588|ref|NP_001074475.1|	Sickle tail protein isoform c	28	28	0.05906	0.02017	0.00154	0.34160
Gi|40254129|ref|NP_258435.2|	Armadillo repeat protein deleted in velo-cardio-facial syndrome homolog	17	17	0.06524	0.05290	0.01504	0.81088
Gi|6755368|ref|NP_035426.1|	40S Ribosomal protein S18	5	5	0.01326	0.00710	0.01607	0.53595
Gi|31982755|ref|NP_035831.2|	Vimentin	11	8	0.00262	0.00749	0.01611	2.85760
Gi|31542151|ref|NP_038827.2|	Arginyl-tRNA-protein transferase 1 isoform 1	8	8	0.03619	0.06278	0.02867	1.73447
Gi|112807186|ref|NP_766307.2|	GCN1 general control of amino acid synthesis 1-like 1	2	2	0.00068	0.00027	0.02990	0.40295
Gi|110225370|ref|NP_031488.2|	Adenomatosus polyposis coli protein (APC)	35	35	0.05596	0.09804	0.03139	1.75192
Gi|79750409|ref|NP_075025.2|	Hamartin	7	7	0.00687	0.01120	0.03649	1.63012

Nine proteins were differently represented in β-catenin immunoprecipitations of WT and mTert$^{-/-}$ *mESC. The stringency criteria used to determine hits are described in Section "Materials and Methods." Note that β-catenin was immunoprecipitated in WT and mTert*$^{-/-}$ *cells with a comparable efficiency [over 20 peptides in all IPs and peptide intensity ratio (KO/WT) of 0.97].*

implicated in the regulation of the nuclear export of β-catenin and, therefore, influence the balance between nuclear and cytoplasmic β-catenin independently of Wnt signaling (Henderson, 2000). Eight other proteins were also identified as novel interactors of β-catenin and have not yet been further characterized (**Table 1**).

RESCUE OF CYTOSOLIC β-CATENIN WITH TELOMERE LENGTHENING

To address whether the reintroduction of telomerase and extension of telomeres could restore the level of cytosolic β-catenin, we reintroduced *mTert* into *mTert*$^{-/-}$ ESCs under the control of a tetracycline-inducible promoter and, after selection of *mTert*-positive clones, cells were propagated under *mTert* induction conditions (+Dox) for 70 days (**Figures 4A,B**). The reactivation of telomerase upon addition of doxycycline was confirmed by TRAP (telomerase repeat amplification protocol, data not shown) and the extension of the telomeres verified by Q-FISH analysis (**Figure 4B**). At this point, the culture was split in two and propagated in the absence (−Dox) or presence (+Dox) of *mTert* for an additional four population doublings (**Figure 4B**). Analysis of the level of cytosolic β-catenin in ESCs with extended telomeres, irrespective of *mTert* expression, revealed a rescue of the cytosolic β-catenin to levels comparable to wild-type ESCs (**Figure 4C**, $P = 0.20$). This result suggests that the distribution of β-catenin is dependent on telomere length rather than telomerase activity. This result is similar to the finding that mice or ESCs lacking telomerase activity do not exhibit phenotypes until telomeres become critically shortened (Erdmann and Harrington, 2009; Strong et al., 2011). Instead, a loss of tissue self-renewal is evident at generations above G4, underscoring the dependence of the phenotype upon loss of telomere integrity (Vidal-Cardenas and Greider, 2010; Strong et al., 2011).

DISCUSSION

Here, we discussed the impact of telomere integrity on cell signaling. We show new data that mESC with short telomeres undergo an accumulation of cytosolic β-catenin. Although the level of nuclear β-catenin is higher in wild-type cells, this difference does not result in an induction in the transcription of Wnt target genes. This observation is in general agreement with the finding that activation of Wnt signaling leads to β-catenin nuclear import, but there is no relationship between the level of nuclear β-catenin and Wnt activation (Guger and Gumbiner, 2000). The higher cytosolic content of β-catenin in *mTert*$^{-/-}$ ESCs might be the result of an altered balance of β-catenin nuclear import/export or of β-catenin degradation/stabilization. In support of the first explanation, we observed an enrichment of APC in β-catenin immunoprecipitates from *mTert*$^{-/-}$ cells. APC shuttles between the nucleus and the cytoplasm independently from other factors of the destruction complex (Henderson, 2000). The destruction complex is not disassembled in the presence of Wnt; instead, degradation of β-catenin by the proteasome is altered upon Wnt stimulation (Hilger and Mann, 2012; Li et al., 2012). This finding may explain why an increased level of APC-β-catenin complex might not necessarily result in higher β-catenin degradation. Furthermore, our finding that the phosphorylation of β-catenin is increased in wild-type ESCs but not *mTert*$^{-/-}$ ESCs in the presence of the proteasome inhibitor MG132 supports the notion that the activity of the proteasome is altered in *mTert*$^{-/-}$ ESCs

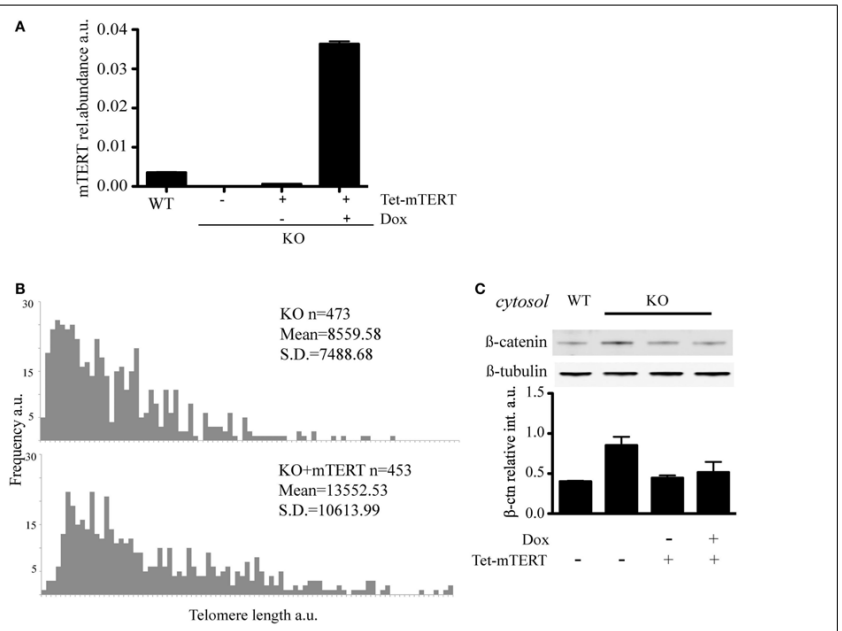

FIGURE 4 | (A) qRT-PCR to quantify mTert transcript in WT, KO, and KO cells re-transfected with inducible mTert under Doxycyclin inducible promoter (see text for details). The histogram represents the average (±standard deviation) of three qPCR replicates. **(B)** Q-FISH to evaluate telomere lengthening in KO cells re-transfected with mTERT under the induction of Doxycyclin for 70 days. The samples shown are the same samples analyzed in **Figure 2D**. **(C)** Rescue of the level of cytosolic β-catenin in KO cells stably re-transfected with mTert under the control of an inducible promoter. Doxycycline (Dox) was used to induce *mTert* transcription. The results were verified with two independent protein extractions.

with critically short telomeres. Such an effect on the proteasome may not be surprising as previous studies have demonstrated a link between cellular aging and an alteration of the ubiquitin-proteasome machinery (Grillari et al., 2006). These results support the notion that the up-regulation of β-catenin occurs as result of altered protein degradation in the presence of short telomeres. Further analysis of the complex composition, stoichiometry, and relative abundance of these complexes in the nucleus and cytoplasm in response to critically short telomeres will be informative.

It remains to be tested whether difference in β-catenin phosphorylation status in murine ESCs with critically short telomeres also impacts Wnt signaling more generally. β-catenin intersects several signaling cascades, not all of which are linked to Wnt (Valenta et al., 2012). For example, in the presence of LIF, β-catenin transcriptional activity is not required to maintain self-renewal; it is mostly its role at the cell adhesion structures that is required to allow differentiation (Lyashenko et al., 2011). On the cytoplasmic side of the plasma membrane, β-catenin interacts with cadherins and α-catenin to stabilize cell–cell adhesion structures but also to regulate cytoskeleton dynamics (Yamada et al., 2005). The majority of these interactions with its partners are regulated by phosphorylations at sites other than the S33, 37, T41 (Liu, 1999). In general, the pattern of β-catenin phosphorylation regulates the transition from a structural versus signaling role (Valenta et al., 2012). Thus, the impact of critically short telomeres upon the phophorylation of β-catenin at sites other than S33, 37, T41 should also be investigated.

In conclusion, global genomic changes driven by short telomeres have consequences on general gene expression and cell metabolism (**Figure 4**). For example, critically short telomeres in mESCs lacking *Tert* influence DNA and histone methylation at the promoters of pluripotency regulators such as *Nanog* and *Oct4*, thereby negatively affecting the stable differentiation of mESCs (Pucci et al., 2013). In the nuclear compartment, β-catenin interacts with several chromatin remodeling complexes, including the histone acetylase p300/CBP and the helicases TIP49a/Pontin52 and TIP49b/Pontin52 and Brg1, the latter of which also interacts with telomerase (Mosimann et al., 2009; Park et al., 2009). β-catenin increases H3K4 methylation at the *c-myc* promoter through its

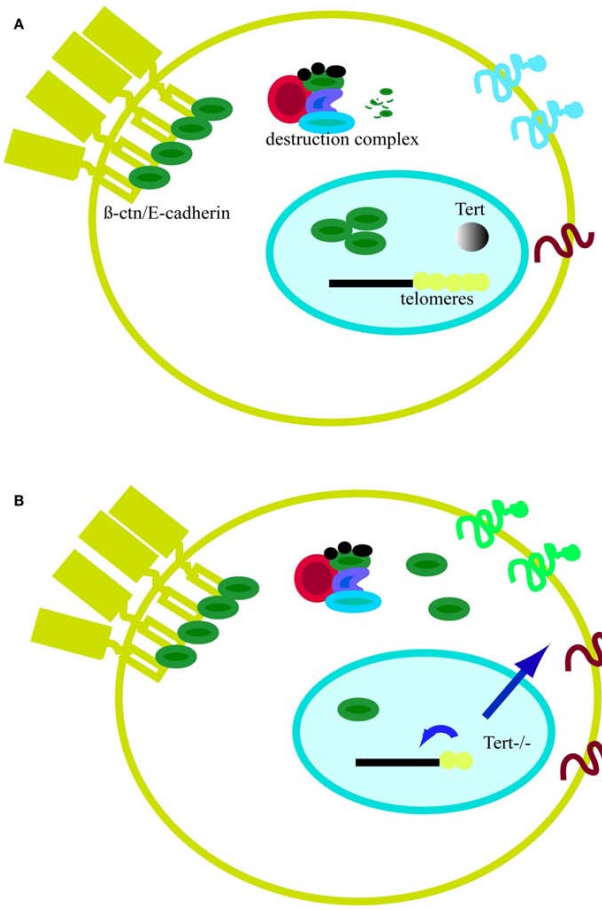

FIGURE 5 | Model of telomeres as platform for cell signaling. (A) In the presence of telomerase, telomeres remain stable. In the absence of Wnt, cytosolic β-catenin (β-ctn, green particle) associates with the APC (red particle) and the kinase GSK3β (blue particle). Free β-catenin is rapidly degraded by the proteasome. The majority of β-catenin is bound to the cell membrane in a complex with E-cadherin (yellow element at the plasma membrane). **(B)** In the absence of telomerase, telomeres shorten and the protective effect of shelterin is eventually lost (yellow dots). Telomere shortening affects epigenetics marks in sub-telomeric regions and at the global genome level (small blue arrow). Signals emanating from telomeres, directly or indirectly, can alter cell signaling. One sign of this influence is the accumulation of β-catenin in the cytosol as result of proteasome impairment or higher nuclear export by APC. Cell signaling changes may also affect proteins expressed at the cell membrane and influence cell adhesion properties (darker blue arrow).

interaction with the histone methyltransferase SET1. Interestingly, this activity is counteracted by Apc, which displaces β-catenin from the chromatin remodeling complex (Sierra et al., 2006). Furthermore, the involvement of β-catenin in the control of telomerase transcription and the previous finding of complexes containing both telomerase and β-catenin at promoter sequences show that β-catenin and telomere integrity are connected (Park et al., 2009; Hoffmeyer et al., 2012). Hence, it is

reasonable to postulate that the alteration of binding of telomeric proteins or epigenetic modifications can trigger signaling cascades that might culminate in changes at the plasma membrane and alter communication with the environment (**Figure 4**). Although the precise means by which short telomeres elicit genome-wide changes in gene expression is unknown, one candidate mechanism is RAP1, a transcription factor that binds extra-telomeric sites and in whose absence there are a number of changes in gene expression in processes related to cell metabolism, cell adhesion, and cancer (Martinez et al., 2010; Martinez and Blasco, 2011). Moreover, together with *Trf2*, *Rap1* transcription is directly regulated by β-catenin (Diala et al., 2013). Taken together, these findings reinforce the notion that β-catenin and telomere structure and function are interconnected. Clearly, the future promises to uncover additional intriguing links between the impact of critically short telomeres and cytoplasmic cell signaling.

MATERIALS AND METHODS

CELL CULTURE

Wild-type and telomerase reverse transcriptase-deficient mESC (E14) were cultured in GMEM, 15% v/v FBS (Hyclone, UK), β-mercaptoethanol, penicillin/streptomycin, and leukemia inhibitory factor (Sigma, UK), and split according to a ratio of 1:8 every 3 days, as described in Erdmann et al. (2004). The absence or presence of telomerase activity was assessed by the TRAP (telomerase repeat amplification protocol), performed following manufacturer's instructions (TRAPeze, Millipore, UK). Cells grown in 6-well plates were lysed in 50 μL of CHAPS 1 × buffer. Two microliters of cell lysate were assayed in the TRAP.

CELL FRACTIONATION AND IMMUNOBLOTTING

Cells grown in 10-cm diameter plates were washed and scraped in PBS. For cell fractionation, cells were pelleted for 5 min at 1500 × *g* and re-suspended in hypotonic lysis buffer (50 mM Tris, pH 7.8, 250 mM sucrose, 2 mM EDTA) supplemented with Roche's Complete Protease Inhibitor Cocktail and PhoSTOP Phosphatase Inhibitor Cocktail. Cells were homogenized with 20 strokes in a Dounce homogenizer and then centrifuged for 10 min at 2800 × *g* to precipitate the nuclei. The supernatant represented the cytosolic fraction. The nuclear pellet was re-suspended in buffer S1 (0.25 M sucrose, 10 mM $MgCl_2$), layered over an equal volume of buffer S3 (0.88 M sucrose, 0.5 M $MgCl_2$), and centrifuged at 2800 × *g* for 10 min. The pellet was re-suspended in RIPA buffer (50 mM Tris, pH 7.5, 150 mM NaCl, 1% v/v NP-40, 0.5% w/v deoxycholic acid) containing protease and phosphatase inhibitors. The nuclear extract was sonicated and centrifuged at maximum speed 16,000 × *g* for 10 min to obtain the nuclear extract. The protein concentrations of the cytosolic and nuclear lysates were measured using the Bradford method prior to loading onto gels for SDS-PAGE. In all experiments, 10 μg of cytosolic protein and 2 μg of nuclear protein were loaded. For total cell extracts, cells were scraped and re-suspended in RIPA buffer. Ten micrograms of total protein lysate, measured by the Bradford method, were loaded onto gels for SDS-PAGE. SDS-PAGE was performed with NuPAGE Bis–Tris 4–12% w/v gradient gels (Invitrogen, UK). After electrophoresis, the proteins were transferred onto an Immobilon-FL membrane (Millipore) at a constant 100 V for 1 h. The membrane was blocked in 5% w/v skimmed milk powder (non-fat) in TBST. Primary antibodies were incubated with the membrane overnight at 4 °C in 2.5% w/v skimmed milk powder in TBST. The primary antibodies used were as follows: rabbit polyclonal anti-β-catenin (1:4000; Bethyl Laboratories, Inc., USA); rabbit monoclonal anti-β-catenin, clone E247 (1:4000; Millipore); rabbit polyclonal anti-phospho-β-catenin (Ser33/37/Thr41) (1:2000; Cell Signaling UK); anti-E-cadherin (1:4000; BD Biosciences UK); rabbit anti-phospho-GSK3β (S9) and mouse anti-GSK3β total (both at 1:1000; Cell Signaling); rabbit anti-phospho-AKT (S473) and rabbit anti-AKT total (both at 1:2000; Cell Signaling). Mouse anti-β-tubulin (1:4000; Sigma) was used as a loading control for the total protein extracts and cytosolic fractions, whereas rabbit anti-lamin B1 (1:2000; a gift from Dr. Eric Schirmer) was used for nuclear fractions. Secondary antibodies were HRP-conjugated anti-mouse and anti-rabbit (1:10000 and 1:5000, respectively; GE Healthcare). For quantification of the immunoblot bands, secondary antibodies were donkey anti-mouse (IRDye 800) and donkey anti-rabbit (IRDye 680) (1:10000 and 1:5000, respectively; LI-COR Biosciences, UK). For Wnt3a treatment, 100 ng/mL of recombinant mouse Wnt3a (Millipore) was added to the culture medium for 3 days. For LiCl treatment, 30 mM LiCl was added to the culture medium for 4 h. For the inhibition of the proteasome, cells were treated with 10 μM of MG132 (Sigma, UK, dissolved in DMSO) for 6 h. Cells were collected by scraping and lysed as previously described for cell fractionation and western blot analysis.

WESTERN BLOT QUANTITATIVE ANALYSIS

Images of membranes probed with secondary IRDye antibody were acquired with an Odyssey scanner and analyzed with Odyssey software (Licor Biosciences). Excel and GraphPad Prism v.5 were used for statistical analysis. Briefly, two rectangles of the same size were placed over β-catenin and the relevant control (β-tubulin or lamin B1 for cytosol or nuclear extract, respectively). The intensity of β-catenin was normalized to the value of the loading control within the same lane and averaged against at least three independent replicates. The Student's *t*-test was used to evaluate the statistical significance of the comparison (Gardano et al., 2011).

QUANTITATIVE FLUORESCENCE *IN SITU* HYBRIDIZATION

The Q-FISH protocol was carried out as described (Liu et al., 2000). Metaphase spreads were captured using Metafer 4 software and analyzed using Isis software. Statistical analysis of telomere intensity distribution was performed using Welch's unpaired *t*-test.

qRT-PCR

RNA was extracted from cells grown in 6-well plates using Qiagen's RNeasy Mini Kit. The RNA was treated with DNase for 1 h prior to the reverse transcription reaction. One microgram of RNA was retrotranscribed with random primers (Invitrogen) using SMART MMLV reverse transcriptase (Clontech Laboratories, Inc., USA). The cDNA

mixture was diluted 20 times in water containing RNase before proceeding with the qPCR (Lightcycler 480, Roche, UK). The sequences of the primers used were as follows: Axin2 forward 5′-AGCGCCAACGACAGCGAGTT-3′; Axin2 reverse 5′-TCCCCATGCGGTAAGGAGGGAC-3′; GAPDH forward 5′-AGGTCGGTGTGAACGGATTTG-3′; GAPDH reverse 5′-TGTAGACCATGTAGTTGAGGTCA-3′mTERT forward 5′-TTCTAGACTTGCAGGTGAACAGCC-3′; mTERT reverse 5′-TTCCTAACACGCTGGTCAAAGGGA-3′. Data were analyzed with Excel and GraphPad Prism v.5.

TOP-FLASH EXPERIMENTS

Cells were seeded at a concentration of 2.5×10^4 mL in 12-well dishes and, 24 h later, Extreme Gene 9 (Roche, UK) was used to transfect 0.5 μg DNA (in total) consisting of Top-firefly luciferase plasmid or the negative control Fop-firefly luciferase (Millipore) and 0.05 μg of Renilla plasmid transcribed with a SV40 promoter, pRL (Promega). Cell lysis was performed 48 h after transfection with the Passive Lysis buffer supplied by the Dual luciferase assay (Promega, UK). Firefly and Renilla luciferase activities were monitored following manufacturer's instructions. Luciferase activity was recorded using an Infinite 200 instrument (Tecan group Ltd.). Wnt3a treatment was performed as previously described. Top-firefly luciferase signals were normalized to renilla luciferase values and then normalized to Fop-luciferase activity for each respective treatment, i.e., with or without Wnt3a. Graphpad Prism v.5 was used for statistical analysis.

mTERT CELL TRANSFECTION AND PLASMIDS

The plasmid pTRE-Bi-*Tert*-IRES-EGFP-Hygro was constructed by amplification of *Tert* cDNA by PCR and insertion into pTRE-Tight-Bi (Clontech) following digestion with *Eco*RI and *Sal*I. IRES-EGFP sequence was obtained from pCAGMKOSiE (kindly provided by K. Kaji) and inserted into pTRE-Tight-Bi (following digestion with *Sal*I and *Eco*RV) using *Sal*I and *Hpa*I sites and then inserted into pTRE-Bi-*Tert* using *Not*I sites. Finally, the hygromycin resistance gene was cloned by PCR into the *Xba*I restriction site of pTRE-Tight-Bi and pTRE-Bi-*Tert*-IRES-EGFP vectors to create pTRE-Bi-EGFP-Hygro and pTRE-Bi-*Tert*-IRES-EGFPHygro. The pCAG-rtTA-advanced vector was constructed by removal of the MKOS ORFs from CAGMKOSiE with *Eco*RI and *Bam*HI and replacement with the advanced tetracycline reverse transactivator sequence (Clontech) (Pucci et al., 2013).

IMMUNOPRECIPITATION AND MASS SPECTROMETRY

Wild-type and $mTert^{-/-}$ ESC were propagated in three 15-cm diameter plates for each immunoprecipitation. Three independent immunoprecipitations were performed contemporaneously on wild-type and $mTert^{-/-}$ ESC. Cells were lysed in 1 mL of lysis buffer (50 mM Tris, pH 7.5, 5 mM EDTA, 5 mM NaF, 10% v/v glycerol, 0.1% v/v NP-40, 1 mM DTT) supplemented with Roche's Complete Protease Inhibitor Cocktail. Following centrifugation at $16{,}000 \times g$ for 10 min, the amount of total protein in all the samples was assessed by the Bradford method. Ten micrograms of rabbit monoclonal anti-β-catenin antibody (clone E247, Millipore) were added to each lysate and incubated for 2 h at 4 °C with rocking. Magnetic Dynabeads Protein A (Invitrogen) was equilibrated in the lysis buffer prior to addition to cell lysates (10 μL beads added to each immunoprecipitation). The bead/lysate mixtures were then incubated for 40 min at 4 °C. Following four washes with a washing buffer (lysis buffer without glycerol), the beads were re-suspended in 20 μL washing buffer. The samples were boiled in Laemmli buffer and loaded onto a NuPAGE Bis–Tris 4–12% v/v gradient gel for SDS-PAGE. The gel was stained with SimplyBlue SafeStain (Life Technologies, UK). Each entire gel lane was sliced into six pieces, then processed according to an in-gel protocol for trypsin digestion.

Capillary-HPLC-MS/MS analysis was performed on an on-line system consisting of a micro-pump (1200 binary HPLC system, Agilent, UK) coupled to a hybrid LTQ-Orbitrap XL instrument (Thermo-Fisher, UK). MS/MS data was searched using MASCOT (Matrix Science Ltd, UK) against the *Mus musculus* subset of the NCBI protein database using a maximum missed-cut value of 2. Variable methionine oxidation, ST and Y phosphorylation, and N-term acetylation were used and fixed cysteine carbamidomethylation were used in all searches; precursor mass tolerance was set to 7 ppm and MS/MS tolerance to 0.4 amu. The significance threshold (p) was set below 0.05 (MudPIT scoring). A peptide Mascot score cut-off of 20 was used in the final analysis, which corresponds to a global false discovery rate of 3.6% using a decoy database search. LC-MS label-free quantification was performed using Progenesis (Non-linear Dynamics, UK). For label-free quantitation, the total number of Features (i.e., intensity signal at a given retention time and m/z) was reduced to MS/MS peaks with charge of 2, 3, or 4+ and only five most intense MS/MS spectra were retained per "Feature." The subset of multicharged ions (2+, 3+, 4+) was extracted from each LC-MS run. Protein quantification was performed as follows; for each protein, the associated unique peptide ions were summed to generate an abundance value and normalized by dividing the protein intensity by the bait intensity (β-catenin). The within group means were calculated to determine the fold change and a t-test was used between the two groups. Regarding quantitative cut-off, proteins were considered a hit if two or more peptides were detected with an absolute ratio of at least 1.5 (i.e., 1.5 fold increase, or 0.667 decrease) and a significance of $p < 0.05$. Nine proteins met this threshold criteria (**Table 1**).

ACKNOWLEDGMENTS

We thank Prof. Mike Tyers and his group for their scientific and technical support and Dr. Eric Schirmer for supplying the lamin B1 antibody. We gratefully acknowledge all the members of the Harrington Laboratory, Dr. Marcia Roy, Dr. Lionel Guittat, and Dr. Olivier Cordin for constructive discussions during the preparation of this manuscript. This work was supported by the Medical Research Council UK (G0800081 to Lea Harrington), the Wellcome Trust (084637 and 086580 to Lea Harrington), and the Centre for Systems Biology at Edinburgh (CSBE) which is a Centre for Integrative Systems Biology (CISB) funded by the BBSRC and EPSRC (reference BB/D019621/1 to Thierry Le Bihan).

REFERENCES

Alessi, D. R., James, S. R., Downes, C. P., Holmes, A. B., Gaffney, P. R., Reese, C. B., et al. (1997). Characterization of a 3-phosphoinositide-dependent protein kinase which phosphorylates and activates protein kinase Balpha. *Curr. Biol.* 7, 261–269. doi:10.1016/S0960-9822(06)00122-9

Azzalin, C. M., Reichenbach, P., Khoriauli, L., Giulotto, E., and Lingner, J. (2007). Telomeric repeat containing RNA and RNA surveillance factors at mammalian chromosome ends. *Science* 318, 798–801. doi:10.1126/science.1147182

Baur, J. A., Zou, Y., Shay, J. W., and Wright, W. E. (2001). Telomere position effect in human cells. *Science* 292, 2075–2077. doi:10.1126/science.1062329

Behrens, J., Von Kries, J. P., Kuhl, M., Bruhn, L., Wedlich, D., Grosschedl, R., et al. (1996). Functional interaction of beta-catenin with the transcription factor LEF-1. *Nature* 382, 638–642. doi:10.1038/382638a0

Benetti, R., Garcia-Cao, M., and Blasco, M. A. (2007a). Telomere length regulates the epigenetic status of mammalian telomeres and subtelomeres. *Nat. Genet.* 39, 243–250. doi:10.1038/ng1952

Benetti, R., Gonzalo, S., Jaco, I., Schotta, G., Klatt, P., Jenuwein, T., et al. (2007b). Suv4-20h deficiency results in telomere elongation and derepression of telomere recombination. *J. Cell Biol.* 178, 925–936. doi:10.1083/jcb.200703081

Benetti, R., Gonzalo, S., Jaco, I., Munoz, P., Gonzalez, S., Schoeftner, S., et al. (2008a). A mammalian microRNA cluster controls DNA methylation and telomere recombination via Rbl2-dependent regulation of DNA methyltransferases. *Nat. Struct. Mol. Biol.* 15, 998. doi:10.1038/nsmb.1399

Benetti, R., Schoeftner, S., Munoz, P., and Blasco, M. A. (2008b). Role of TRF2 in the assembly of telomeric chromatin. *Cell Cycle* 7, 3461–3468. doi:10.4161/cc.7.21.7013

Blackburn, E. H. (1991). Structure and function of telomeres. *Nature* 350, 569–573. doi:10.1038/350569a0

Blackburn, E. H., Greider, C. W., Henderson, E., Lee, M. S., Shampay, J., and Shippen-Lentz, D. (1989). Recognition and elongation of telomeres by telomerase. *Genome* 31, 553–560. doi:10.1139/g89-104

Blasco, M. A. (2007). The epigenetic regulation of mammalian telomeres. *Nat. Rev. Genet.* 8, 299–309. doi:10.1038/nrg2047

Burdon, T., Smith, A., and Savatier, P. (2002). Signalling, cell cycle and pluripotency in embryonic stem cells. *Trends Cell Biol.* 12, 432–438. doi:10.1016/S0962-8924(02)02352-8

Choi, J., Southworth, L. K., Sarin, K. Y., Venteicher, A. S., Ma, W., Chang, W., et al. (2008). TERT promotes epithelial proliferation through transcriptional control of a Myc- and Wnt-related developmental program. *PLoS Genet.* 4:e10. doi:10.1371/journal.pgen.0040010

Cimprich, K. A., and Cortez, D. (2008). ATR: an essential regulator of genome integrity. *Nat. Rev. Mol. Cell Biol.* 9, 616–627. doi:10.1038/nrm2450

Clevers, H., and Nusse, R. (2012). Wnt/beta-catenin signaling and disease. *Cell* 149, 1192–1205. doi:10.1016/j.cell.2012.05.012

de Lange, T. (2005). Shelterin: the protein complex that shapes and safeguards human telomeres. *Genes Dev.* 19, 2100–2110. doi:10.1101/gad.1346005

Desbois-Mouthon, C., Cadoret, A., Blivet-Van Eggelpoel, M. J., Bertrand, F., Cherqui, G., Perret, C., et al. (2001). Insulin and IGF-1 stimulate the beta-catenin pathway through two signalling cascades involving GSK-3beta inhibition and Ras activation. *Oncogene* 20, 252–259. doi:10.1038/sj.onc.1204064

Diala, I., Wagner, N., Magdinier, F., Shkreli, M., Sirakov, M., Bauwens, S., et al. (2013). Telomere protection and TRF2 expression are enhanced by the canonical Wnt signalling pathway. *EMBO Rep.* Q5 doi:10.1038/embor.2013.16

Erdmann, N., and Harrington, L. A. (2009). No attenuation of the ATM-dependent DNA damage response in murine telomerase-deficient cells. *DNA Repair (Amst.)* 8, 347–353. doi:10.1016/j.dnarep.2008.11.009

Erdmann, N., Liu, Y., and Harrington, L. (2004). Distinct dosage requirements for the maintenance of long and short telomeres in mTert heterozygous mice. *Proc. Natl. Acad. Sci. U.S.A.* 101, 6080–6085. doi:10.1073/pnas.0401580101

Fukumoto, S., Hsieh, C. M., Maemura, K., Layne, M. D., Yet, S. F., Lee, K. H., et al. (2001). Akt participation in the Wnt signaling pathway through Dishevelled. *J. Biol. Chem.* 276, 17479–17483. doi:10.1074/jbc.C000880200

Galati, A., Magdinier, F., Colasanti, V., Bauwens, S., Pinte, S., Ricordy, R., et al. (2012). TRF2 controls telomeric nucleosome organization in a cell cycle phase-dependent manner. *PLoS ONE* 7:e34386. doi:10.1371/journal.pone.0034386

Gardano, L., Holland, L., Oulton, R., Le Bihan, T., and Harrington, L. (2011). Native gel electrophoresis of human telomerase distinguishes active complexes with or without dyskerin. *Nucleic Acids Res.* 40, e36. doi:10.1093/nar/gkr1243

Gonzalo, S., Jaco, I., Fraga, M. F., Chen, T., Li, E., Esteller, M., et al. (2006). DNA methyltransferases control telomere length and telomere recombination in mammalian cells. *Nat. Cell Biol.* 8, 416–424. doi:10.1038/ncb1386

Gottschling, D. E., Aparicio, O. M., Billington, B. L., and Zakian, V. A. (1990). Position effect at *S. cerevisiae* telomeres: reversible repression of Pol II transcription. *Cell* 63, 751–762. doi:10.1016/0092-8674(90)90141-Z

Greider, C. W. (2012). Molecular biology. Wnt regulates TERT – putting the horse before the cart. *Science* 336, 1519–1520. doi:10.1126/science.1223785

Greider, C. W., and Blackburn, E. H. (1987). The telomere terminal transferase of Tetrahymena is a ribonucleoprotein enzyme with two kinds of primer specificity. *Cell* 51, 887–898. doi:10.1016/0092-8674(87)90576-9

Greider, C. W., and Blackburn, E. H. (1989). A telomeric sequence in the RNA of Tetrahymena telomerase required for telomere repeat synthesis. *Nature* 337, 331–337. doi:10.1038/337331a0

Griffith, J. D., Comeau, L., Rosenfield, S., Stansel, R. M., Bianchi, A., Moss, H., et al. (1999). Mammalian telomeres end in a large duplex loop. *Cell* 97, 503–514. doi:10.1016/S0092-8674(00)80760-6

Grillari, J., Katinger, H., and Voglauer, R. (2006). Aging and the ubiquitinome: traditional and non-traditional functions of ubiquitin in aging cells and tissues. *Exp. Gerontol.* 41, 1067–1079. doi:10.1016/j.exger.2006.07.003

Guger, K. A., and Gumbiner, B. M. (2000). A mode of regulation of beta-catenin signaling activity in Xenopus embryos independent of its levels. *Dev. Biol.* 223, 441–448. doi:10.1006/dbio.2000.9770

Hamada, F., and Bienz, M. (2004). The APC tumor suppressor binds to C-terminal binding protein to divert nuclear beta-catenin from TCF. *Dev. Cell* 7, 677–685. doi:10.1016/j.devcel.2004.08.022

Hart, M. J., De Los Santos, R., Albert, I. N., Rubinfeld, B., and Polakis, P. (1998). Downregulation of beta-catenin by human Axin and its association with the APC tumor suppressor, beta-catenin and GSK3 beta. *Curr. Biol.* 8, 573–581. doi:10.1016/S0960-9822(98)70226-X

Hemann, M. T., and Greider, C. W. (1999). G-strand overhangs on telomeres in telomerase-deficient mouse cells. *Nucleic Acids Res.* 27, 3964–3969. doi:10.1093/nar/27.20.3964

Henderson, B. R. (2000). Nuclear-cytoplasmic shuttling of APC regulates beta-catenin subcellular localization and turnover. *Nat. Cell Biol.* 2, 653–660. doi:10.1038/35046558

Hilger, M., and Mann, M. (2012). Triple SILAC to determine stimulus specific interactions in the Wnt pathway. *J. Proteome Res.* 11, 982–994. doi:10.1021/pr200740a

Hoffmeyer, K., Raggioli, A., Rudloff, S., Anton, R., Hierholzer, A., Del Valle, I., et al. (2012). Wnt/beta-catenin signaling regulates telomerase in stem cells and cancer cells. *Science* 336, 1549–1554. doi:10.1126/science.1218370

Jho, E. H., Zhang, T., Domon, C., Joo, C. K., Freund, J. N., and Costantini, F. (2002). Wnt/beta-catenin/Tcf signaling induces the transcription of Axin2, a negative regulator of the signaling pathway. *Mol. Cell. Biol.* 22, 1172–1183. doi:10.1128/MCB.22.4.1172-1183.2002

Korinek, V., Barker, N., Willert, K., Molenaar, M., Roose, J., Wagenaar, G., et al. (1998). Two members of the Tcf family implicated in Wnt/beta-catenin signaling during embryogenesis in the mouse. *Mol. Cell. Biol.* 18, 1248–1256.

Levis, R., Hazelrigg, T., and Rubin, G. M. (1985). Effects of genomic position on the expression of transduced copies of the white gene of *Drosophila*. *Science* 229, 558–561. doi:10.1126/science.2992080

Li, V. S., Ng, S. S., Boersema, P. J., Low, T. Y., Karthaus, W. R., Gerlach, J. P., et al. (2012). Wnt signaling through inhibition of beta-catenin degradation in an intact Axin1 complex. *Cell* 149, 1245–1256. doi:10.1016/j.cell.2012.05.002

Liu, C., Li, Y., Semenov, M., Han, C., Baeg, G. H., Tan, Y., et al. (2002). Control of beta-catenin phosphorylation/degradation by a dual-kinase mechanism. *Cell* 108, 837–847. doi:10.1016/S0092-8674(02)00685-2

Liu, J. P. (1999). Studies of the molecular mechanisms in the regulation of telomerase activity. *FASEB J.* 13, 2091–2104.

Liu, Y., Snow, B. E., Hande, M. P., Yeung, D., Erdmann, N. J., Wakeham, A., et al. (2000). The telomerase reverse transcriptase is limiting and necessary for telomerase function in vivo. *Curr. Biol.* 10, 1459–1462. doi:10.1016/S0960-9822(00)00805-8

Longhese, M. P. (2008). DNA damage response at functional and dysfunctional telomeres. *Genes Dev.* 22, 125–140. doi:10.1101/gad.1626908

Lyashenko, N., Winter, M., Migliorini, D., Biechele, T., Moon, R. T., and Hartmann, C. (2011). Differential requirement for the dual functions of beta-catenin in embryonic stem cell self-renewal and germ layer formation. *Nat. Cell Biol.* 13, 753–761. doi:10.1038/ncb2260

Makarov, V. L., Lejnine, S., Bedoyan, J., and Langmore, J. P. (1993). Nucleosomal organization of telomere-specific chromatin in rat. *Cell* 73, 775–787. doi:10.1016/0092-8674(93)90256-P

Martinez, P., and Blasco, M. A. (2011). Telomeric and extra-telomeric roles for telomerase and the telomere-binding proteins. *Nat. Rev. Cancer* 11, 161–176. doi:10.1038/nrc3025

Martinez, P., Thanasoula, M., Carlos, A. R., Gomez-Lopez, G., Tejera, A. M., Schoeftner, S., et al. (2010). Mammalian Rap1 controls telomere function and gene expression through binding to telomeric and extratelomeric sites. *Nat. Cell Biol.* 12, 768–780. doi:10.1038/ncb2081

Molenaar, M., Van De Wetering, M., Oosterwegel, M., Peterson-Maduro, J., Godsave, S., Korinek, V., et al. (1996). XTcf-3 transcription factor mediates beta-catenin-induced axis formation in *Xenopus* embryos. *Cell* 86, 391–399. doi:10.1016/S0092-8674(00)80112-9

Mosimann, C., Hausmann, G., and Basler, K. (2009). Beta-catenin hits chromatin: regulation of Wnt target gene activation. *Nat. Rev. Mol. Cell Biol.* 10, 276–286. doi:10.1038/nrm2654

Nimmo, E. R., Cranston, G., and Allshire, R. C. (1994). Telomere-associated chromosome breakage in fission yeast results in variegated expression of adjacent genes. *EMBO J.* 13, 3801–3811.

Ozawa, M., Baribault, H., and Kemler, R. (1989). The cytoplasmic domain of the cell adhesion molecule uvomorulin associates with three independent proteins structurally related in different species. *EMBO J.* 8, 1711–1717.

Park, J. I., Venteicher, A. S., Hong, J. Y., Choi, J., Jun, S., Shkreli, M., et al. (2009). Telomerase modulates Wnt signalling by association with target gene chromatin. *Nature* 460, 66–72. doi:10.1038/nature08137

Pucci, F., Gardano, L., and Harrington, L. (2013). Short telomeres in ESCs lead to unstable differentiation. *Cell Stem Cell* 12, 479–486. doi:10.1016/j.stem.2013.01.018

Rao, A. S., Kremenevskaja, N., Resch, J., and Brabant, G. (2005a). Lithium stimulates proliferation in cultured thyrocytes by activating Wnt/beta-catenin signalling. *Eur. J. Endocrinol.* 153, 929–938. doi:10.1530/eje.1.02038

Rao, R., Zhang, M. Z., Zhao, M., Cai, H., Harris, R. C., Breyer, M. D., et al. (2005b). Lithium treatment inhibits renal GSK-3 activity and promotes cyclooxygenase 2-dependent polyuria. *Am. J. Physiol. Renal Physiol.* 288, F642–F649. doi:10.1152/ajprenal.00287.2004

Rubinfeld, B., Souza, B., Albert, I., Muller, O., Chamberlain, S. H., Masiarz, F. R., et al. (1993). Association of the APC gene product with beta-catenin. *Science* 262, 1731–1734. doi:10.1126/science.8259518

Samper, E., Flores, J. M., and Blasco, M. A. (2001). Restoration of telomerase activity rescues chromosomal instability and premature aging in Terc$^{-/-}$ mice with short telomeres. *EMBO Rep.* 2, 800–807. doi:10.1093/embo-reports/kve174

Schoeftner, S., and Blasco, M. A. (2008). Developmentally regulated transcription of mammalian telomeres by DNA-dependent RNA polymerase II. *Nat. Cell Biol.* 10, 228–236. doi:10.1038/ncb1685

Schoeftner, S., and Blasco, M. A. (2010). Chromatin regulation and non-coding RNAs at mammalian telomeres. *Semin. Cell Dev. Biol.* 21, 186–193. doi:10.1016/j.semcdb.2009.09.015

Sfeir, A., and de Lange, T. (2012). Removal of shelterin reveals the telomere end-protection problem. *Science* 336, 593–597. doi:10.1126/science.1218498

Sfeir, A. J., Chai, W., Shay, J. W., and Wright, W. E. (2005). Telomere-end processing the terminal nucleotides of human chromosomes. *Mol. Cell* 18, 131–138. doi:10.1016/j.molcel.2005.02.035

Shippen-Lentz, D., and Blackburn, E. H. (1990). Functional evidence for an RNA template in telomerase. *Science* 247, 546–552. doi:10.1126/science.1689074

Sierra, J., Yoshida, T., Joazeiro, C. A., and Jones, K. A. (2006). The APC tumor suppressor counteracts beta-catenin activation and H3K4 methylation at Wnt target genes. *Genes Dev.* 20, 586–600. doi:10.1101/gad.1385806

Stern, J. L., and Bryan, T. M. (2008). Telomerase recruitment to telomeres. *Cytogenet. Genome Res.* 122, 243–254. doi:10.1159/000167810

Strong, M. A., Vidal-Cardenas, S. L., Karim, B., Yu, H., Guo, N., and Greider, C. W. (2011). Phenotypes in mTERT± and mTERT$^{-/-}$ mice are due to short telomeres, not telomere-independent functions of TERT. *Mol. Cell. Biol.* Q6 doi:10.1128/MCB.05312-11

Sutherland, C., Leighton, I. A., and Cohen, P. (1993). Inactivation of glycogen synthase kinase-3 beta by phosphorylation: new kinase connections in insulin and growth-factor signalling. *Biochem. J.* 296(Pt 1), 15–19.

Valenta, T., Hausmann, G., and Basler, K. (2012). The many faces and functions of beta-catenin. *EMBO J.* 31, 2714–2736. doi:10.1038/emboj.2012.150

Vidal-Cardenas, S. L., and Greider, C. W. (2010). Comparing effects of mTR and mTERT deletion on gene expression and DNA damage response: a critical examination of telomere length maintenance-independent roles of telomerase. *Nucleic Acids Res.* 38, 60–71. doi:10.1093/nar/gkp855

Wang, J., Xie, L. Y., Allan, S., Beach, D., and Hannon, G. J. (1998). Myc activates telomerase. *Genes Dev.* 12, 1769–1774. doi:10.1101/gad.12.12.1769

Wright, W. E., Tesmer, V. M., Huffman, K. E., Levene, S. D., and Shay, J. W. (1997). Normal human chromosomes have long G-rich telomeric overhangs at one end. *Genes Dev.* 11, 2801–2809. doi:10.1101/gad.11.21.2801

Wu, P., Takai, H., and De Lange, T. (2012). Telomeric 3' overhangs derive from resection by Exo1 and Apollo and fill-in by POT1b-associated CST. *Cell* 150, 39–52. doi:10.1016/j.cell.2012.05.026

Yamada, S., Pokutta, S., Drees, F., Weis, W. I., and Nelson, W. J. (2005). Deconstructing the cadherin-catenin-actin complex. *Cell* 123, 889–901. doi:10.1016/j.cell.2005.09.020

Conflict of Interest Statement: The authors declare that the research was conducted in the absence of any commercial or financial relationships that could be construed as a potential conflict of interest.

Received: 28 January 2013; accepted: 21 May 2013; published online: xx May 2013.

*Citation: Gardano L, Pucci F, Christian L, Bihan TL and Harrington L (2013) Telomeres, a busy platform for cell signaling. Front. Oncol. **3**:146. doi: 10.3389/fonc.2013.00146*

This article was submitted to Frontiers in Cancer Molecular Targets and Therapeutics, a specialty of Frontiers in Oncology.

3CAFD43793